

Crystallization Kinetics of Polypropylene Fractions*

S. HOSHINO,† E. MEINECKE,‡ J. POWERS,§ and R. S. STEIN,
Polymer Research Institute, University of Massachusetts, Amherst, Massa-
chusetts, and S. NEWMAN, Monsanto Company, Plastics Division, Spring-
field, Massachusetts

Synopsis

The overall crystallization rate of polypropylene fractions was studied dilatometrically, and the crystallization behavior was considered in relation to the stereoregularity of the samples. The study includes a photomicroscopic analysis of the nucleation, formation, and growth of spherulites, as well as an evaluation by means of rapid x-ray scanning techniques of the increase of crystallinity within the spherulites. A theory was applied to the discussion of crystallization behavior in which two stages of growth were introduced: (a) growth at the spherulite interface, and (b) secondary crystallization within the spherulite. These were described in terms of Avrami-type equations with differing parameters.

DILATOMETRIC STUDIES

Dilatometric techniques were applied to the study of crystallization kinetics of polypropylene fractions in order to describe experimentally how the overall rate of crystallization of polypropylene is influenced by the stereo-regular nature of the polymer.

The dilatometric techniques and methods of data reduction employed have been previously described.¹ Three polypropylene fractions of varying tacticity, an octane, a 2,2,4-trimethylpentane, and a hexane extract with dilatometric melting points of 172, 160, and 140°C., respectively, were studied. These polypropylene fractions, while they vary in tacticity, do not have appreciably different molecular weights; thus the intrinsic viscosities in tetralin at 130°C. are 0.817 and 0.883 for the hexane and octane fractions, respectively. (For a fuller description of these materials, see Newman.¹)

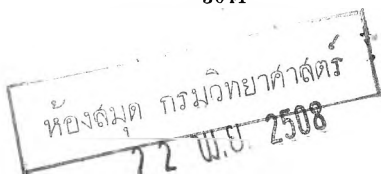
Crystallization isotherms describing the rate of crystallization as a func-

* A part of this paper was presented before the 1961 March Meeting of the Division of High Polymer Physics, American Physical Society. Supported in part by Contracts with the Office of Naval Research and with the Atomic Energy Commission.

† On leave from Ube Industries Ltd., Japan. Present address: Department of Polymer Chemistry, Kyoto University, Kyoto, Japan.

‡ Present address: Institute for Rubber Research, University of Akron, Akron, Ohio.

§ Present address: American Cyanamid Co., Stamford, Connecticut.



tion of temperature for three polypropylene samples are shown in Figures 1-3. All of the isotherms show a characteristic sigmoidal shape; moreover, all of the apparent induction times τ_i , show a similar dependence on $\Delta T = T_m - T$, the difference between the melting point and the crystalliza-

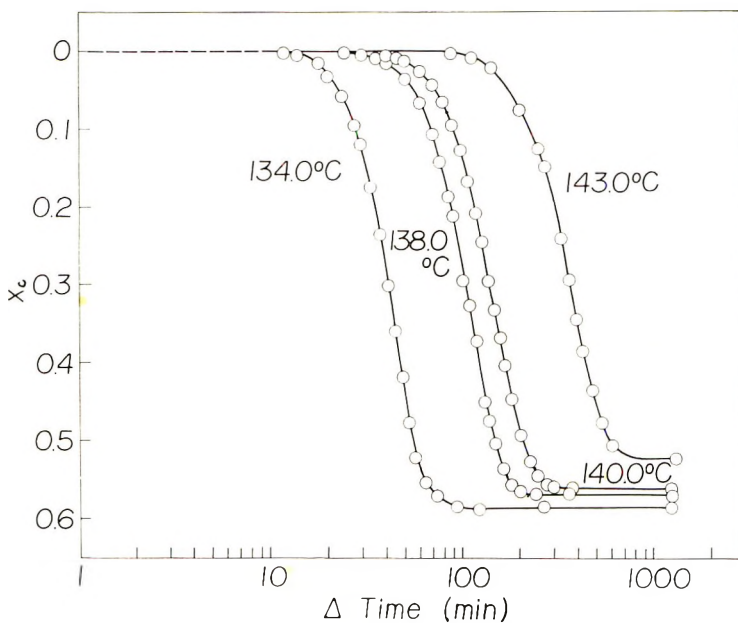


Fig. 1. Weight fraction crystallinity vs. time for an octane extract of crystalline polypropylene ($T_m = 172^\circ\text{C}$.).

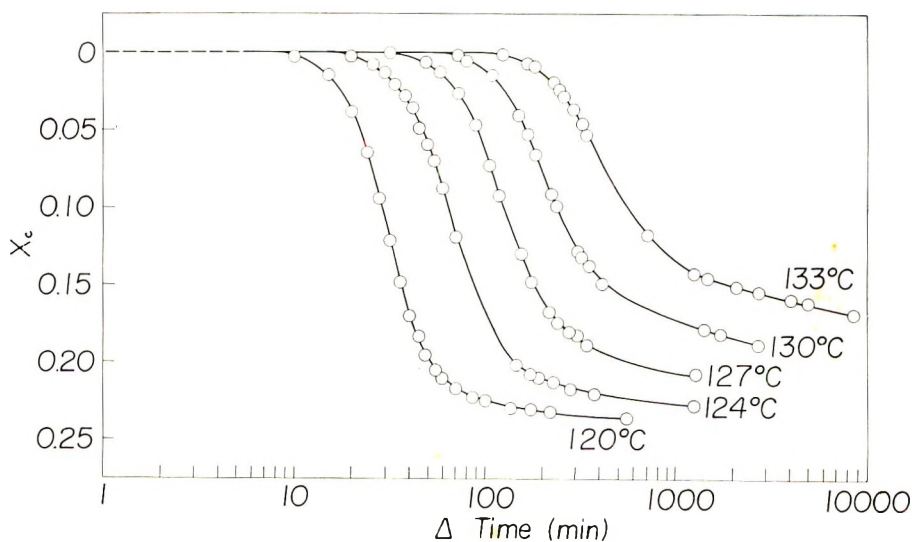


Fig. 2. Weight fraction crystallinity vs. time for a 2,2,4-trimethylpentane extract of crystalline polypropylene ($T_m = 160^\circ\text{C}$.).

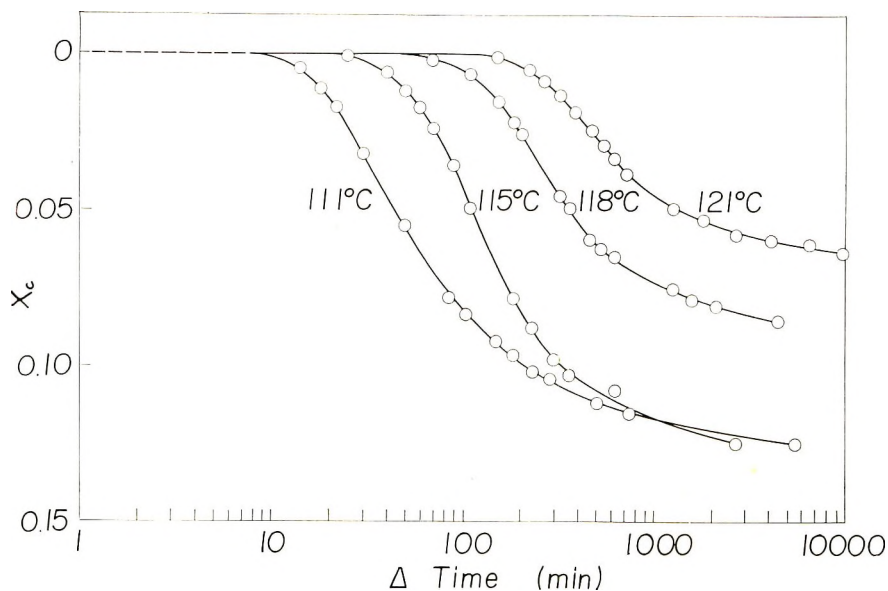


Fig. 3. Weight fraction crystallinity vs. time for a hexane extract of crystalline polypropylene ($T_m = 140^\circ\text{C}$.).

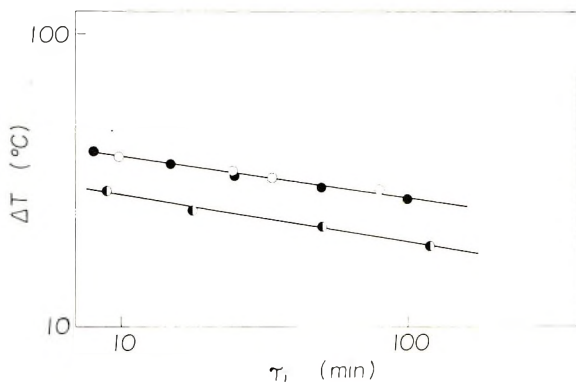


Fig. 4. Apparent induction time vs. $\Delta T = (T_m - T)$ for three fractions of crystalline polypropylene: (O) octane extract; (●) 2,2,4-trimethylpentane extract; (●) hexane extract.

tion temperature. A displacement of the $\log \tau_i$ versus $\log \Delta T$ plots (Fig. 4) may be a reflection, in part, upon the uncertainty of T_m determinations for the lowest-melting fraction. It should be noted that the degree of supercooling, ΔT , required to achieve a given value of τ_i is much larger for polypropylene than for polyethylene; this, in turn, is probably related to the fact that the polypropylene chain must transform to a helical conformation in order to crystallize.

The isotherms of the octane fraction are in one sense characteristic of linear polymers, that is, they are superposable by translation along the log

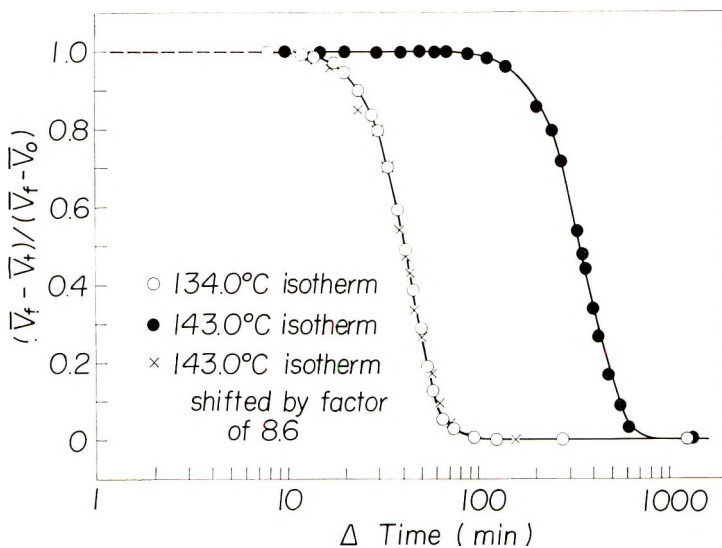


Fig. 5. Avrami plot of octane extract of crystalline polypropylene.

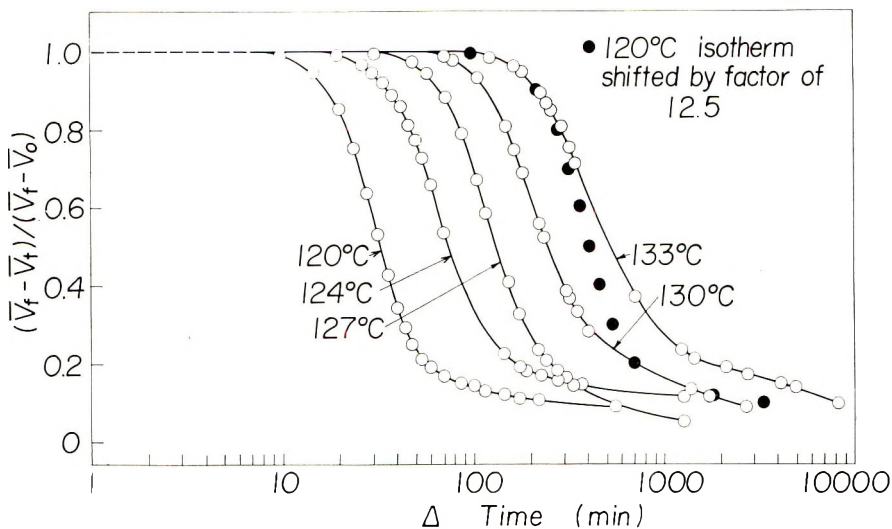


Fig. 6. Avrami plot of 2,2,4-trimethylpentane extract of crystalline polypropylene.

t axis. However, with decreasing chain regularity or tacticity, it no longer becomes possible to effect exact coincidence of the isotherms by a change in a time scale factor.

Moreover, with decreasing stereoregularity, there is a marked slowing down of the crystallization process, particularly in the later stages. This is readily illustrated by the observation that less than one cycle of log time is required for completion of an octane isotherm, whereas several are required for the hexane fraction.

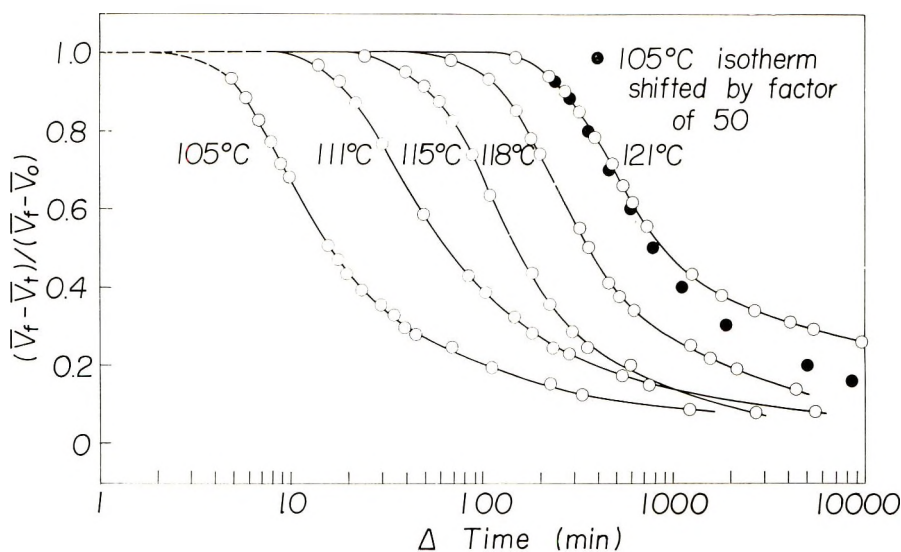


Fig. 7. Avrami plot of hexane extract of crystalline polypropylene.

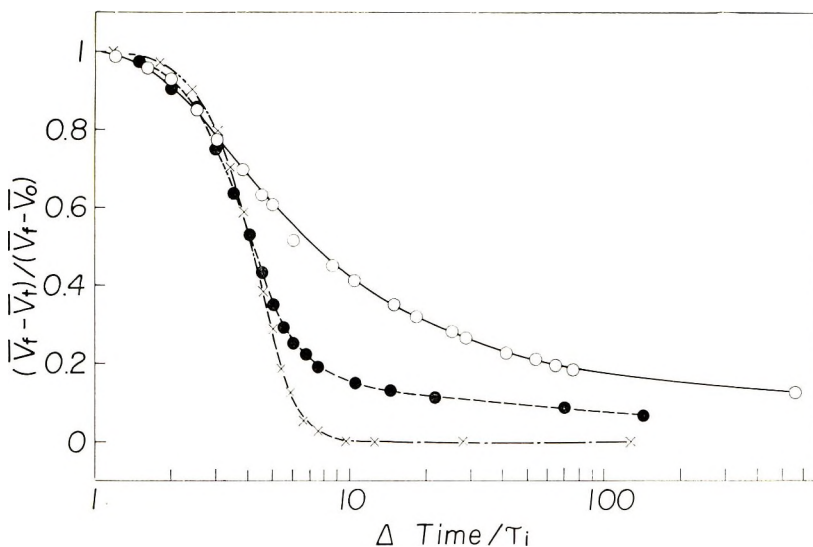


Fig. 8. Crystallization isotherms for three crystalline polypropylene fractions compared at similar induction times: (O) 111°C. isotherm for hexane extract ($\tau_i = 10$ min.); (●) 120°C. isotherm for 2,2,4-trimethylpentane extract ($\tau_i = 8$ min.); (×) 134°C. isotherm for octane extract ($\tau_i = 10$ min.).

In order to compensate for the differences in the limiting weight fraction of crystallinity, X_{cf} , attainable for the three fractions at the several temperatures, the crystallinity data have been normalized to correspond to the Avrami expression:

$$(\bar{V}_f - \bar{V}_t) / (\bar{V}_f - \bar{V}_0) = (1 - X_c / X_{cf}) = \exp \{-Kt^n / X_{cf}\} \quad (1)$$

where \bar{V}_t , \bar{V}_f , and \bar{V}_0 refer to the values of the specific volume at time t , finally, and initially, respectively. K is a rate constant, the Avrami exponent n is a number whose value depends on the type of nucleation and geometry of growth, and X_c is the weight fraction crystallinity of the sample. Since the final value of the specific volume \bar{V}_f at certain temperatures is experimentally unattainable, an estimate was made by crystallizing the samples several degrees below the temperature of the experiment to develop an excess of crystallinity, and then warming up to the original temperature to melt out the excess crystallinity.

The resulting plots (Figs. 5-7) show the following: (a) the octane isotherms can be made to coincide exactly by a shift of a time scale factor; (b) the lower-melting samples show some retardation in crystallization as the temperature of crystallization is increased; (c) there is a similar but more marked retardation (Fig. 8) when the three fractions are compared at temperatures which effect similar apparent induction times. In other words, decreasing tacticity and (to a lesser degree) increasing temperature both inhibit the crystallization in its later stages. Normalizing the data results in an irregular pattern of curve shapes as the final crystallinity is reached; this confusion is attributed to the view that the ultimate crystallinity X_{cf} and the state of organization obtained by melting out the excess crystallinity are dissimilar from the state achieved by an isothermal crystallization process.

The parameter n in eq. (1) which depends on the type of nucleation and geometry of crystal growth has been evaluated as a function of time for the octane and hexane extracts. For this purpose, Hoffman, Weeks, and Murphy² have derived the expression:

$$n = (t/X_c)(dX_c/dt)[1 + (1/2)(X_c/X_{cf}) + \dots] \quad (2)$$

In order to calculate n , the derivative (dX_c/dt) must be obtained as a function of time. This quantity was calculated for the octane extract by fitting successive portions of the crystallization isotherm with a generalized function of time (Newton's interpolation formula³) and then computing the derivative of this function. Accordingly, an IBM program has been prepared which carries out the computation of the interpolation formula, solves for (dX_c/dt) , and uses the result to obtain the desired quantities in the expression for n . It should be noted that eq. (2) is approximate, and that neglect of higher terms may result in errors of about 10% when X_c reaches values of about $1/2$.

Results of such an analysis led to an undesirable scatter in n , probably due to choice of data points that are too closely spaced. Nevertheless, n was found to vary from 3.99 at the beginning of the isotherm to 3.01 at the half-time. This variability of n is readily demonstrated by a change of shape in a plot of $\log [\ln(1 - X_c/X_{cf})]$ versus $\log t$. These observations are in disagreement with those of other workers^{4,5} who assume a fixed value of $n = 3$ as applying to the entire curve. Using a value of $n = 3$, the rate constant k_0 ($= K/X_{cf}$) is found to be $1.05 \times 10^{-5} \text{ min.}^{-3}$ at 134°C. ,

decreasing to 2.2×10^{-9} at 146°C ., in general agreement with Griffith and Rånby's⁴ data. At 138°C ., X_{c_f} is found to be 0.56; the calculation of n is insensitive to the value of this quantity.

Figure 9 shows the variation of the exponent n throughout the crystallization process. Since the bulk of the data shown in Figure 9 corresponds to values of $X_c \leq 1/2$, the general conclusions are not altered by use of the approximate eq. (2).

The isotherm of the octane fraction is much more compressed, and roughly half of the crystallization occurs within times where $3 < n < 4$, whereas the bulk of the isotherm for the hexane fraction corresponds to $0 < n < 3$. A value of $3 < n < 4$ can be interpreted as being due to a three-dimensional growth of objects born at the same time. To determine

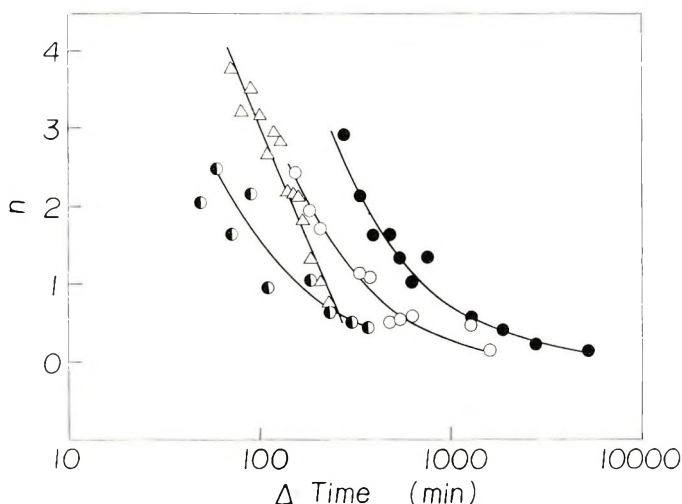


Fig. 9. Variation of the parameter n in Avrami equation with log time: (●) 115°C ., hexane extract; (○) 118°C ., hexane extract; (●) 121°C ., hexane extract; (Δ) 140°C ., octane extract.

whether nucleation occurred on incompletely melted crystallites, the following experiments were tried on the octane fraction.

To obtain the isotherms shown in Figure 1, the dilatometer was first heated to 200°C . for 60 min. and then rapidly cooled to the crystallization temperature. This method appears reproducible, as is evidenced by the close agreement of duplicate isotherms. To assess whether crystalline embryos or nuclei were still present, the sample was heated to 230°C . for 85 min. Again the isotherm at 138.0°C . was reproduced. The absence of an appreciable superheating effect indicates that crystalline embryos, if present as heterogeneities, do not persist upon heating to 200°C . for 60 min. From these data, it was not possible to conclude whether the nucleation is controlled by the presence of existing nuclei (heterogeneous) or is homogeneous with nuclei forming sporadically in time.

The time dependence of n and its variation with temperature and stereoregularity suggested that the crystallization depends on the concentration of tactic (or copolymer^{1,6,7}) sequences permitted to crystallize and on the difficulty of achieving the ideal situation, in which crystallinities form from sequences not much longer than themselves.

MICROSCOPIC STUDIES

In order to resolve the total crystallization rate into its components the dilatometric work described in the previous section was accompanied by microscopic measurements of spherulite nucleation and radial growth rates.⁸ A polypropylene whole polymer with a melting point measured by microscope of 176°C. was used,* in addition to the three polypropylene fractions used for the dilatometric measurements.

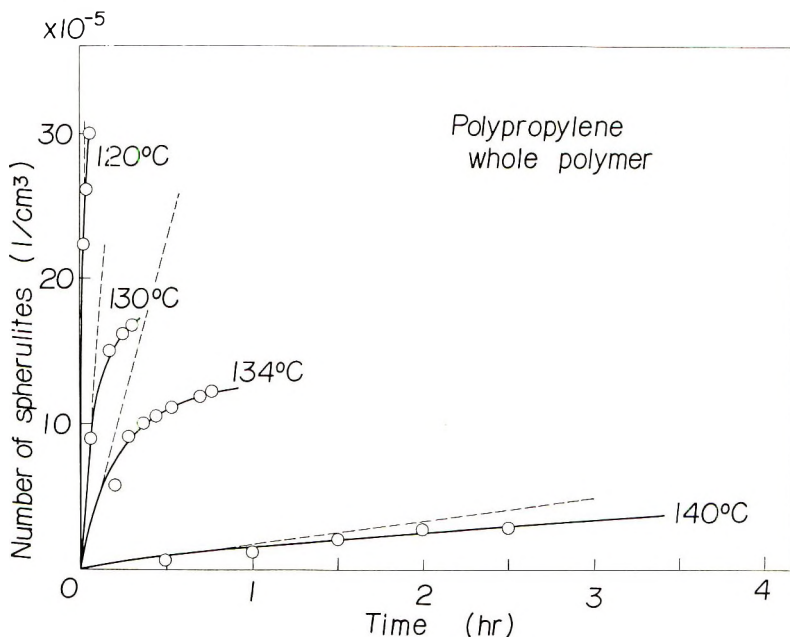


Fig. 10. Relationship between number of spherulites and time.

Measurements were made on samples held in an electrically heated oven mounted on an optical bench equipped with a horizontal polarizing microscope and an automatic 70 mm. camera. Temperature was regulated to $\pm 0.1^\circ\text{C}$. by the use of a thermocouple placed in the sample block and a proportional controller.

Samples were fused between microscope cover glasses at temperatures of 15–20°C. above their melting points and rapidly inserted into the oven

* Not the parent polymer for the fractions described in the previous section.

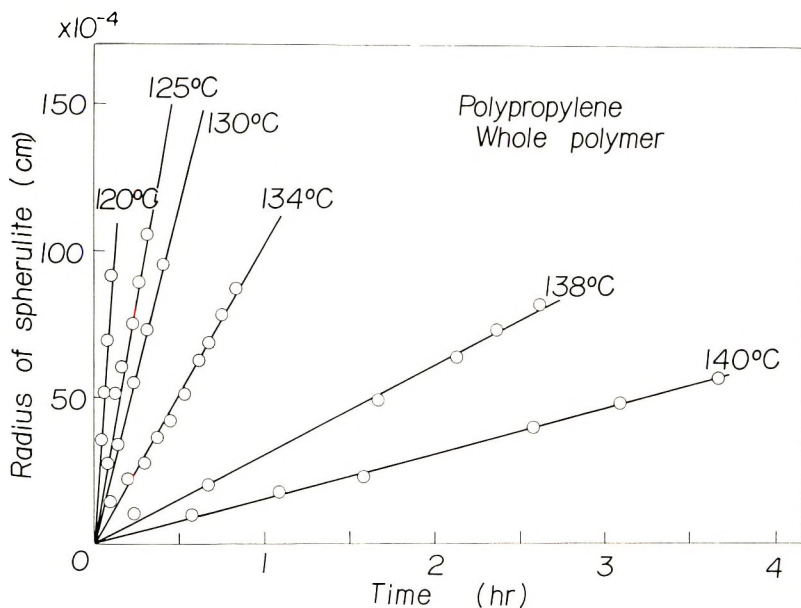


Fig. 11. Relationship between radius of spherulites and time.

preheated to the crystallization temperature. The numbers and radii of spherulites were observed as a function of time at each temperature. Typical data are plotted in Figures 10 and 11 for the whole polymer. The nucleation rate appears to decrease with time, suggesting a mechanism of sporadic nucleation on predetermined heterogeneities. Also, Figure 10 implies that the availability or activity of these nuclei increases with decreasing temperature. Spherulite radii were observed to increase linearly with time. (A more detailed report of the techniques and results of this study may be found elsewhere.⁸)

It was not possible to determine radial growth rates for the less tactic 2,2,4-trimethylpentane and hexane fractions because of their inability to develop well-formed spherulites, as seen in Figure 12. Small non-circular crystalline aggregates form which do not become volume-filling.

Logarithms of nucleation rates (calculated from the initial slope of Figure 10 and radial growth rates are plotted against $1/T(\Delta T)$ and $1/T - (\Delta T)^2$ in Figures 13 and 14. The plots are fairly linear, as expected from theory. On the basis of these plots, it is not possible to distinguish between two- and three-dimensional nucleation and growth mechanisms. A similar plot is presented for the growth rate for the octane extract in Figure 15 (using the dilatometric melting point of 172°C.). There is less curvature for the plot against $1/T(\Delta T)$, suggesting two-dimensional rather than three-dimensional secondary nucleation. The curvature may also be related to the uncertainty in T_m as well as to the microscopic observation that the spherulite morphology is dependent upon growth temperature for this polymer, being more perfect at higher temperatures.

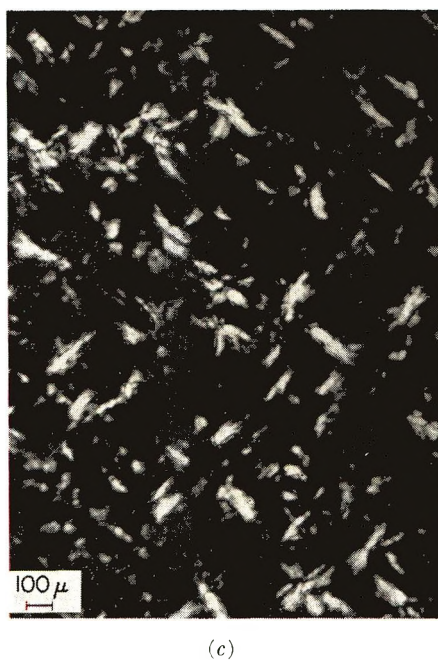
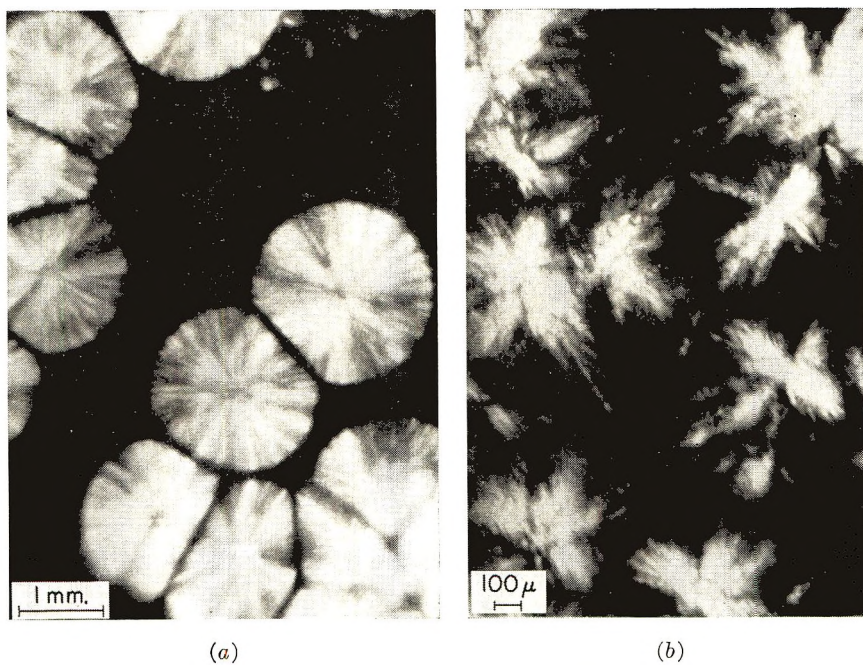


Fig. 12. Spherulites of various polypropylene fractions: (a) octane extract; (b) 2,2,4-trimethylpentane extract; (c) hexane extract.

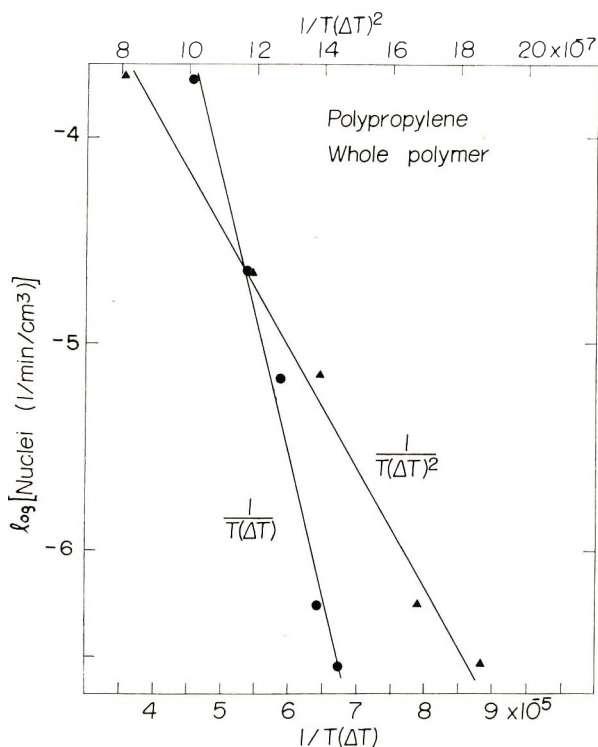


Fig. 13. Polypropylene whole polymer nucleation rate vs. $1/T(\Delta T)$ and $1/T(\Delta T)^2$.

The initial slopes and intercepts for these plots are summarized in Table I. The smaller slope for the growth than for the nucleation is in agreement with the observation by Flory and McIntyre⁹ for poly(decamethylene sebacate) and may indicate a smaller effective surface free energy for the secondary than for the primary nucleation process.

Overall degrees of crystallinity were calculated from the spherulitic nucleation and radial growth rates G by using the equation:

$$X_c = (4\pi/3) X_{cs} G^3 (\rho_c/\rho) \int_{z=0}^{z=t} [(dN(z)/dz) (t-z)^3 dz] \quad (3)$$

where X_c is the weight fraction of crystallites at time t , X_{cs} is the weight fraction crystallinity of the spherulite, $dN(z)/dz$ is the nucleation rate at time z , the time when the spherulite starts growing. ρ_c and ρ are the densities of the crystal and of the polymer, respectively. X_c was calculated by using the nucleation and growth rates plotted in Figures 10 and 11 and by assuming that X_{cs} is constant and equal to the final degree of crystallinity measured dilatometrically when the volume of the samples is completely filled with spherulites.

From the Avrami equation

$$(1 - X_c) = \exp \{-k_0 t^n\} \quad (4)$$

TABLE I
Crystallization Kinetics of Polypropylene Whole Polymer,
Octane Extract, and 2,2,4-Trimethylpentane Extract (From Figures 13, 14, and 15)

$T_m, ^\circ\text{C.}$	Crystallinity X_{cf}	Nucleation rate slope		Growth rate slope	
		Plot vs. $1/T(\Delta T),$ $T^2/\text{cm.}^3 \text{ min.}$	Plot vs. $1/T(\Delta T)^2,$ $T^3/\text{cm.}^3 \text{ min.}$	Plot vs. $1/T(\Delta T),$ $\text{cm. } T^2/\text{min.}$	Plot vs. $1/T(\Delta T)^2,$ $\text{cm. } T^3/\text{min.}$
Whole polymer	0.75	-1.4×10^5	-2.9×10^6	-7.7×10^4	-1.6×10^5
Octane extract	0.70	—	—	-3.1×10^4	-6.5×10^5
2,2,4-TMP extract	0.41	—	—	—	—

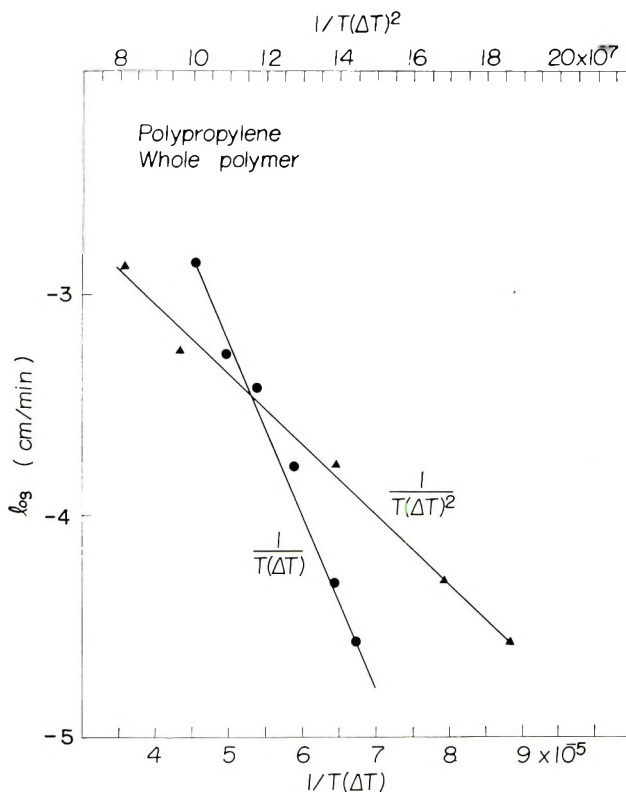


Fig. 14. Polypropylene whole polymer radial growth rate vs. $1/T(\Delta T)$ and $1/T(\Delta T)^2$.

it is apparent that

$$\ln [-\ln (1 - X_c)] = \ln k_0 + n \ln t \quad (5)$$

A plot of $\ln [-\ln (1 - X_c)]$ against $\ln t$, using the values of X_c calculated from eq. (3), is presented in Figure 16 for the whole polymer at 138°C. This gives a straight line with slope $n = 3.90$. The apparent disagreement of this observation with the observation of the variation of n during crystallization indicates that the assumption of constant X_{cs} involved in the use of eq. (3) is subject to question. Consequently, a more careful comparison of changes in degree of crystallinity with changes in volume fraction of spherulites was undertaken and is described in the next section.

X-RAY STUDIES

Experimental

A quantitative comparison of microscopic studies (necessarily made on thin film samples) with dilatometric studies on bulk samples is difficult because of the very different surface area/volume ratios which may affect nucleation rates. In such a comparison it is desirable to parallel experi-

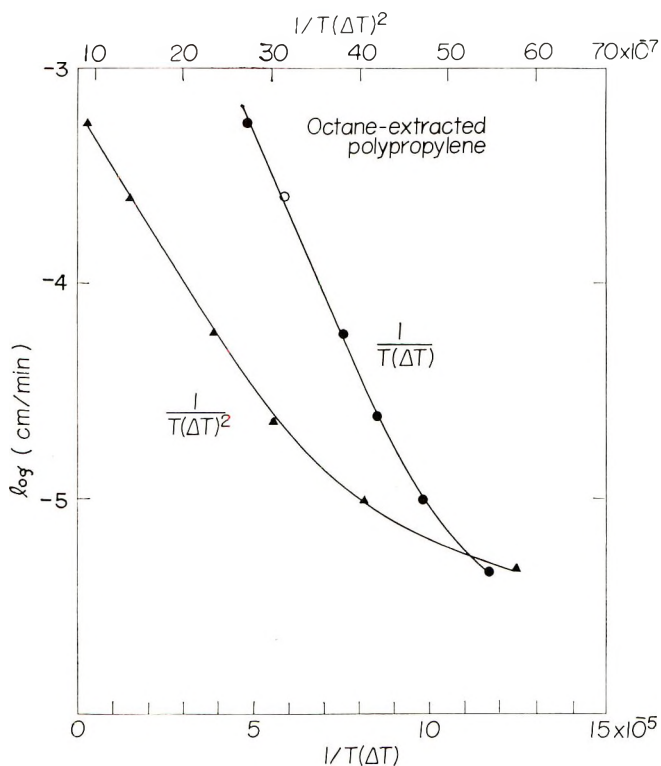


Fig. 15. Polypropylene octane extract radial growth rate vs. $1/T(\Delta T)$ and $1/T(\Delta T)^2$.

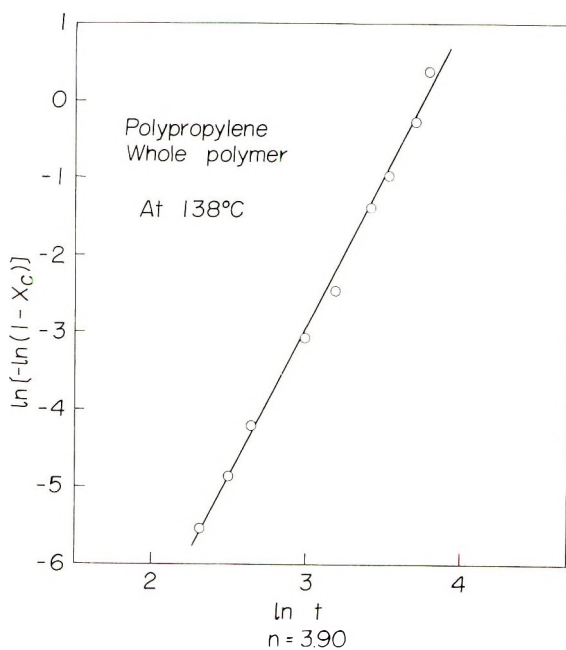


Fig. 16. Relationship between crystallinity and growth time for polypropylene whole polymer at 138°C. calculated from nucleation and growth rate.

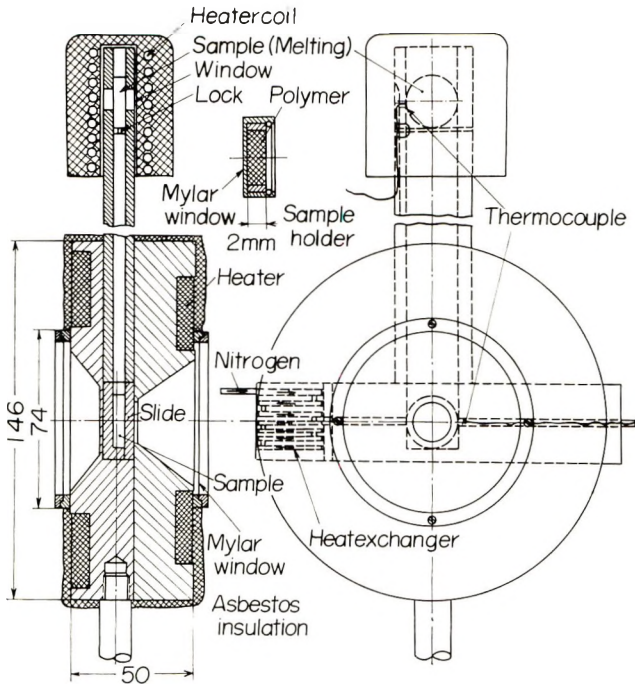


Fig. 17. Constant-temperature oven and sample holder.

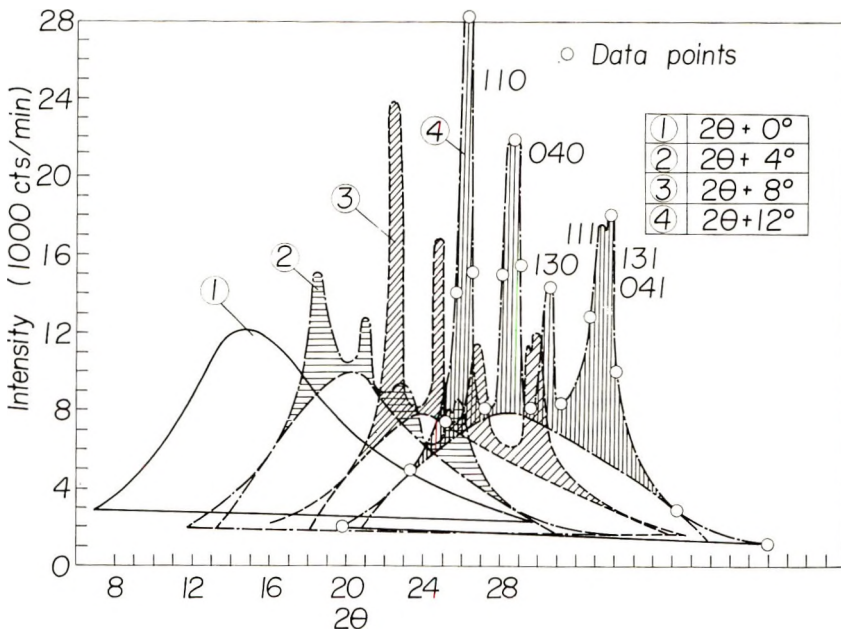


Fig. 18. Change of diffracted x-ray intensities with time during isothermal crystallization of polypropylene whole polymer.

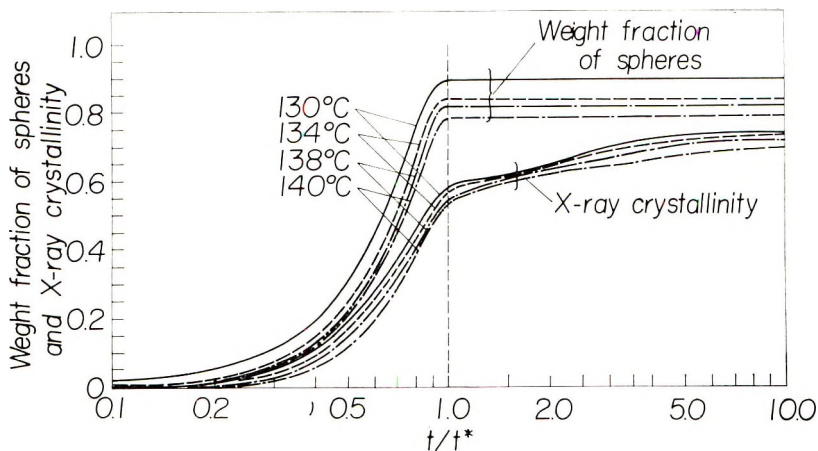


Fig. 19. Change in weight fraction of spherulites and weight fraction of crystallites with reduced time, t/t^* , during the isothermal crystallization of polypropylene whole polymer.

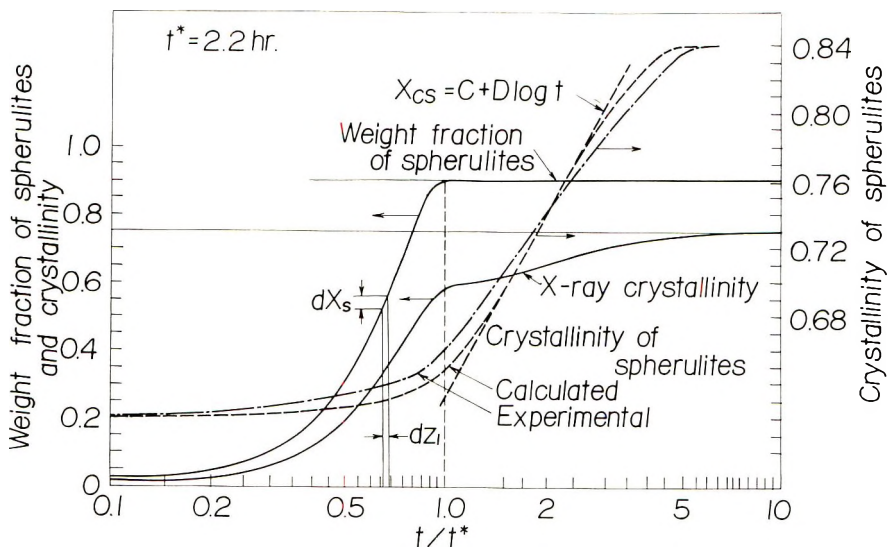


Fig. 20. Variation of weight fraction of crystals and that of spherulites and of fraction of crystallinity of spherulites with reduced time during isothermal crystallization of polypropylene whole polymer at 130°C.

mental conditions as closely as possible. In order to do this, the crystallization rates were followed by use of a rapidly scanning x-ray diffractometer.

Samples were studied in the form of films in the thickness range of 0.25–2.0 mm. and were melted between 2-mil Mylar films, held in a small sample holder, and inserted in an oven (shown in Fig. 17) somewhat similar to that used for the microscopic studies. Trial experiments indicated that results were not affected by variation of thickness within the stated interval

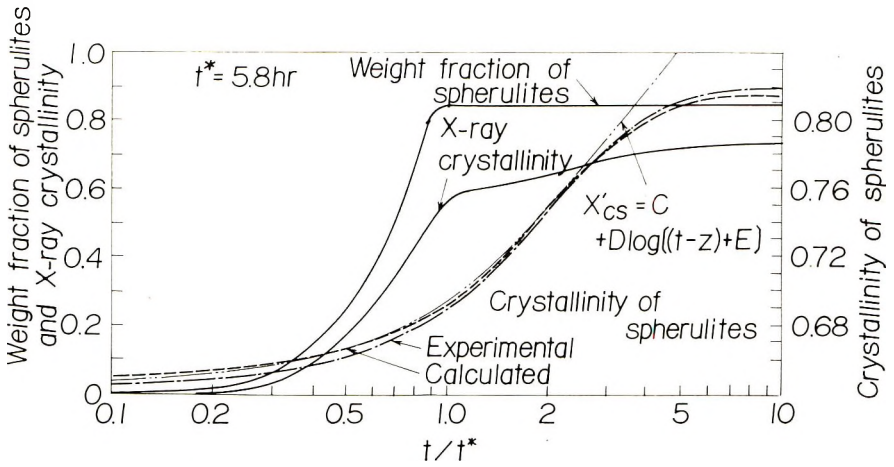


Fig. 21. Variation of weight fraction of crystals and of spherulites and of fraction of crystallinity of spherulites with reduced time during isothermal crystallization of polypropylene whole polymer at 134°C .

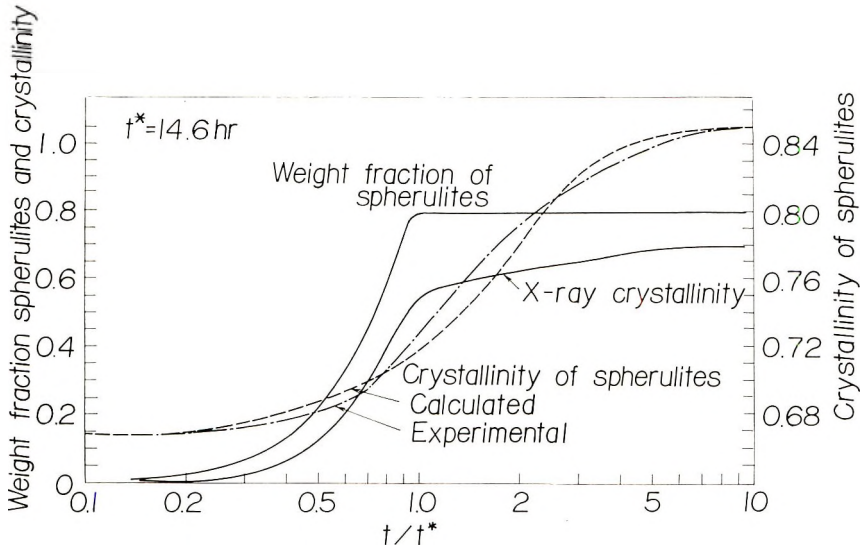


Fig. 22. Variation of weight fraction of crystals and of spherulites and of fraction of crystallinity of spherulites with reduced time during isothermal crystallization of polypropylene whole polymer at 138°C .

so long as the surfaces were clean. The oven is equipped with a preheating chamber within which the sample may be melted and then dropped into the crystallizing chamber, thermostatically controlled to within $\pm 0.3^\circ\text{C}$. of the crystallizing temperature. The oven is provided with Mylar windows and may be flushed with preheated nitrogen to reduce sample oxidation.

Samples were held at about 15°C . above their melting points for 15–20 min. before being dropped into the crystallizing chamber. Trial experi-

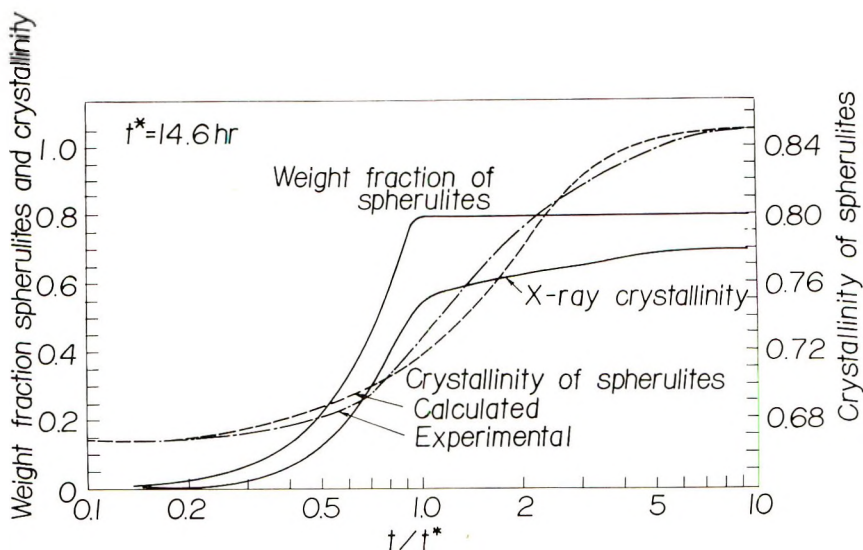


Fig. 23. Variation of weight fraction of crystals and of spherulites and of fraction of crystallinity of spherulites with reduced time during isothermal crystallization of polypropylene whole polymer at 140°C.

ments indicated that variation of this time in the range of 10–60 min. and a range in temperature of 180–230°C. did not affect the results reported. Repeated melting and recrystallization had little effect. Measurements with thermocouples embedded in the sample revealed that in the least favorable cases, the sample practically reached its crystallizing temperature essentially within 8 min. after insertion (a short enough time to prevent a contribution to error from this source for the rates investigated).

The programmed x-ray diffractometer, which has been described,¹⁰ was modified for rapid point-by-point scanning at selected points in a Bragg angle interval of 2θ between 7° and 30° which are so chosen as to characterize the crystallinity best in a minimal scanning period. Typical scanning points utilized during the crystallization of one of the samples are indicated in Figure 18.

X-ray data were corrected for polarization, incoherent scattering, and background. The Hermans and Weidinger method¹¹ was used for construction of the amorphous scattering contribution in Figure 18. The degree of crystallinity was taken as the ratio of the crystalline area to the total area under these curves, according to the Hermans-Weidinger method.

The variation of X_c with reduced time (t/t^* , where t^* is the time required for spherulites to become volume-filling) calculated in this way is presented in Figure 19 for the whole polymer at a number of crystallization temperatures. This is compared with the variation of weight fraction of spherulites calculated from the volume fraction of spherulites obtained by measuring the area fraction of the photomicrograph which is occupied by spherulites. Natta's values of the densities of crystalline ($\rho_c = 0.936 \text{ g./m.}^3$) and

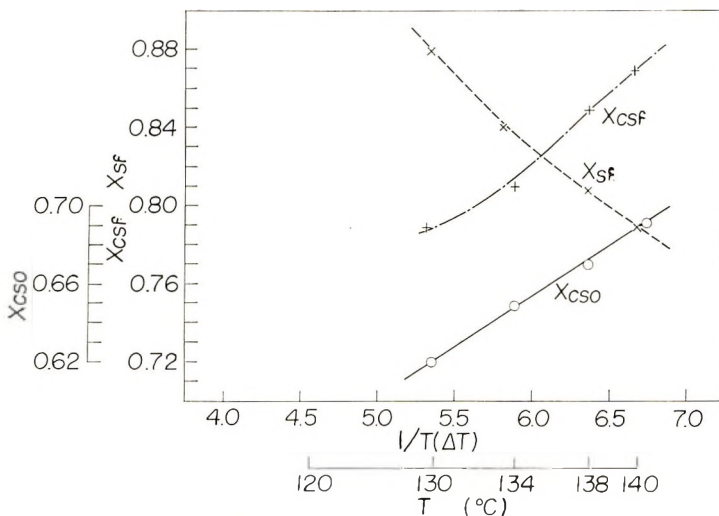


Fig. 24. Variation of the limiting weight fraction of spherulites and the initial and limiting fractional crystallinity of the spherulites, X_{cso} , X_{csf} with $1/T(\Delta T)$.

amorphous ($\rho_a = 0.86$ g./cm.³) polypropylene at 20°C. were used for this calculation.¹²

It is seen in Figure 19 that the weight fraction X_s of spherulites increases at a more rapid rate than the weight fraction of crystals X_c . Thus the degree of crystallinity of the spherulite X_{cs} defined by

$$X_{cs} = X_c/X_s \quad (6)$$

is not constant, as postulated in the preceding section, but increases with time, as seen in Figures 20–23. This indicates that a secondary crystallization process takes place within the spherulite along with the primary crystallization. A plot of the variation with temperature of the initial degree of crystallinity X_{cso} of the spherulite and the final internal crystallinity X_{csf} is given in Figure 24 and indicates that both of these are lower for crystallization at low temperature (high supercooling) where the crystallization rate is rapid. On the other hand, the ultimate weight fraction of spherulites, also shown on this plot, is greatest at the lower crystallization temperatures. At the higher crystallization temperatures, the spherulites do not become volume-filling. Examination of the samples after such crystallization reveals that the space between spherulites contains polymer (not voids).

These observations might be consistent with the occurrence of fractionation or rejection of more poorly crystallizable species during crystallization,¹³ occurring to a greater degree at the higher temperatures. At higher supercooling, more noncrystallizable material is included within the fast-growing spherulites, giving rise to a low X_{cs} , while at smaller supercooling, there is time for exclusion of the noncrystallizable material into the

interspherulitic region, resulting in a more crystalline spherulite which will not grow to fill completely the volume of the sample.

Theory

In previous treatments of secondary crystallization, it has been assumed that the primary and secondary process take place consecutively. The primary process is usually fitted by an Avrami-type equation and the secondary by an empirical equation of the form

$$X_c = C + \log t \quad (7)$$

We have attempted to apply this equation to the process of internal crystallization of the spherulite, (see Fig. 20), but find that it fits the data only over a limited range of times, $1.5 < t/t^* < 3.5$. Alternatively, we have formulated a theory for crystallization which is more compatible with our experimental evidence.*

We shall assume that the spherulite initially forms with a degree of crystallinity X_{cs0} . During the time interval dz , the increase in weight of spherulites is

$$dW_s(z) = WF(z) dz \quad (8)$$

where $F(z)$ is the slope of a plot of the weight fraction of spherulites versus time, and W is the weight of the sample. This spherulitic material formed at time z with a degree of crystallinity X_{cs0} continues to crystallize (within the growing spherulite) up to the time of measurement, approaching the limiting degree of crystallinity X_{csf} . At a time t , the weight fraction of crystalline material within the element of spherulite formed at time z is

$$X_{cs}(t,z) = X_{cs0} + (X_{csf} - X_{cs0}) f(t - z) \quad (9)$$

where $f(t - z)$ is the fraction of this secondary crystallization which has taken place up to time t . The weight of crystalline material at time t contributed by this element of weight of spherulite formed at time z is then

$$\begin{aligned} dW_{cs}(t,z) &= X_{cs}(t,z) dW_s(z) \\ &= WF(z) X_{cs}(t,z) dz \\ &= WF(z) [X_{cs0} + (X_{csf} - X_{cs0}) f(t - z)] dz \end{aligned} \quad (10)$$

This equation predicts that the degrees of crystallinity of all portions of the spherulite are not equal, but depend on how long ago they were formed ($t - z$). Thus at a given time, the center of a spherulite is more crystalline than its periphery because the center has had more time for secondary crystallization. The measured values of X_{cs} that we have reported are averages over all parts of the spherulite and are obtained by integrating

* Dr. F. Price (General Electric Research Laboratories) and Dr. I. Hillier (University of Chicago) have independently formulated theories similar or related to that described here; these contributions are to be found elsewhere in this Journal, pp. 3067-3086.

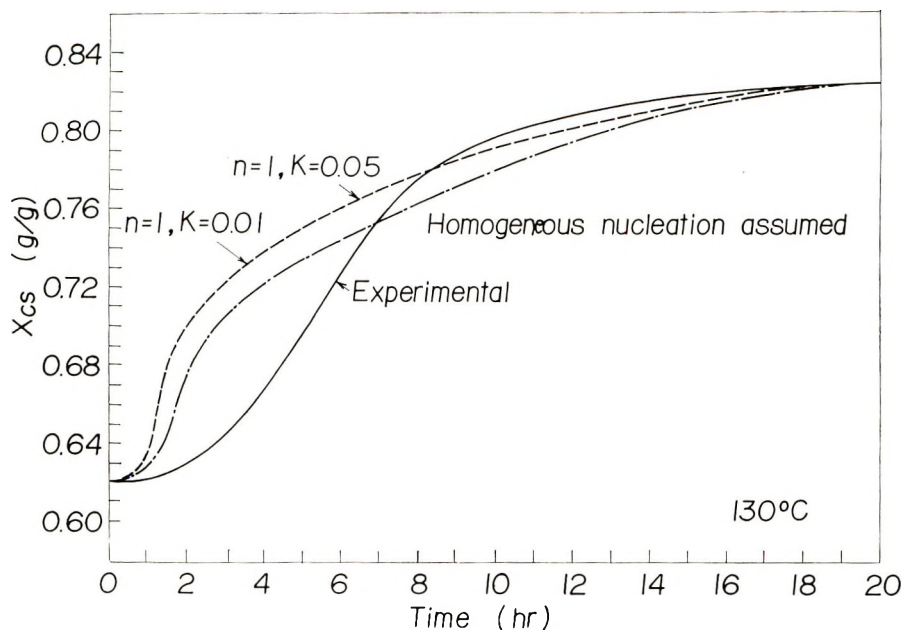


Fig. 25. Comparison of the calculated and experimental variation of the fractional crystallinities of spherulites, X_{cs} , with time.

over all values of z . Thus, the total weight of crystals within spherulites at time t is

$$W_{cs}(t) = \int_{z=0}^t dW_{cs}(t,z) \quad (11)$$

The average weight fraction of crystals within spherulites at time t is then

$$\begin{aligned} X_{cs}(t) &= W_{cs}(t)/W_s(t) \\ &= \frac{\int_{z=0}^t WF(z)[X_{cs0} + (X_{csf} - X_{cs0})f(t-z)]dz}{\int_{z=0}^t WF(z) dz} \\ &= X_{cs0} + (X_{csf} - X_{cs0}) \frac{\int_{z=0}^t F(z)f(t-z)dz}{\int_{z=0}^t F(z)dz} \end{aligned} \quad (12)$$

$F(z)$ may be calculated from values of X_s obtained from the photomicrographs. It is evident from Figure 16 that at least in the earlier part of the crystallization, this may be fitted by an Avrami equation with the Avrami exponent for spherulite nucleation $n_1 = 3.9$. Thus,

$$X_s = X_{sf}(1 - \exp\{-k_1 z^{n_1}\}) \quad (13)$$

or

$$F(z) = dX_s/dz = X_{sf}k_1n_1z^{(n_1-1)} \exp\{-k_1z^{n_1}\} \quad (14)$$

where X_{sf} is the limiting weight fraction of spherulites and k_1 is the rate constant for spherulite nucleation. The functional form of $f(t-z)$ is not known, but an Avrami-type equation has been found empirically to fit the data in spite of the fact that its geometric foundation, the growth of geometrically defined particles into the diminishing amorphous phase, is not evident. We thus assume

$$f(t-z) = [1 - \exp\{-k_2(t-z)^{n_2}\}] \quad (15)$$

where k_2 and n_2 are parameters for the local secondary process, to be determined by curve fitting. (The use of this equation for the local secondary crystallization at a particular part of the spherulite is not necessarily in conflict with the use of a logarithmic equation for the overall secondary process, since the overall process represents an average over many local processes.)

By combining eqs. (12), (14), and (15), one obtains for the average degree of crystallinity of the spherulite at time t

$$\begin{aligned} X_{cs}(t) &= X_{cs0} + (X_{csf} - X_{cs0}) \frac{\int_{z=0}^t z^{(n_1-1)} (\exp\{-k_1z^{n_1}\}) [1 - \exp\{-k_2(t-z)^{n_2}\}] dz}{\int_{z=0}^t z^{(n_1-1)} (\exp\{-k_1z^{n_1}\}) dz} \\ &= X_{cs0} + (X_{csf} - X_{cs0}) k_1n_1 \frac{\int_{z=0}^t z^{(n_1-1)} (\exp\{-k_1z^{n_1}\}) [1 - \exp\{-k_2(t-z)^{n_2}\}] dz}{1 - \exp\{-k_1t^{n_1}\}} \end{aligned} \quad (16)$$

This equation is analytically integrable over z only for special cases of the n 's and must in general be solved numerically. This was done using finite increments of z ; values of k_2 and n_2 were determined by trial and error to give the best fit to the data. The results are best fitted by $n_2 = 1.8$, as can be seen from Figures 25 and 26 for $T = 130^\circ\text{C}$. There is an appreciably better fit for this value of n_2 than for $n_2 = 2.0$. The theoretical variation of X_{cs} with time calculated in this manner is compared with the experimental results in Figures 20-23 for $n_2 = 1.8$ but different k_2 's. Values of k_2 are plotted against $1/T\Delta T$ in Figure 27, where it is seen that k_2 increases with the degree of supercooling as does k_1 . The same procedure of numerical integration using

$$X_{cs}(t,z) = C + D \log [(t-z) + E] \quad (17)$$

was tried and is also plotted in Figure 21. This fits the data over a more restricted range of time than does eq. (15).

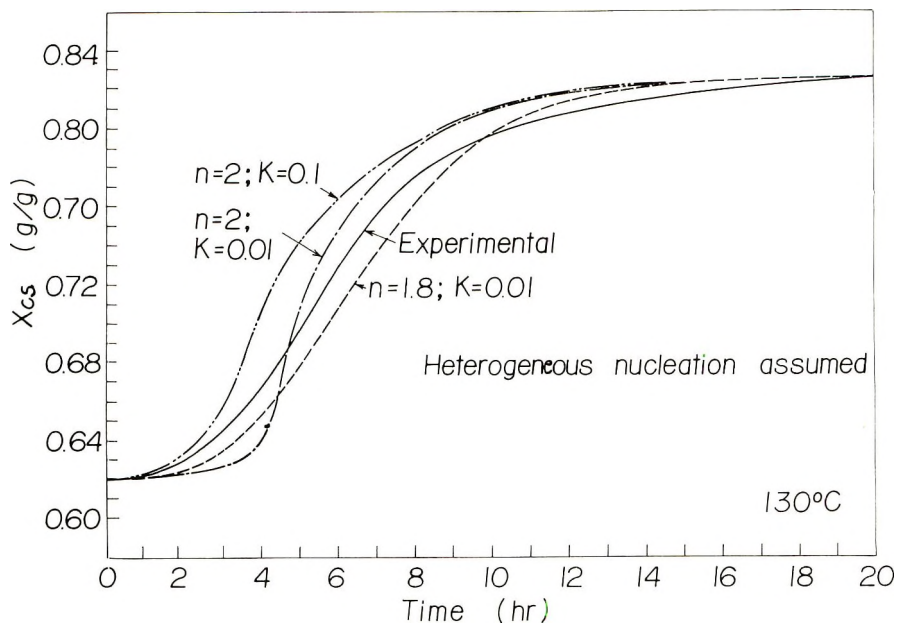


Fig. 26. Comparison of the calculated and experimental variation of the fractional crystallinities of spherulites, X_{cs} , with time.

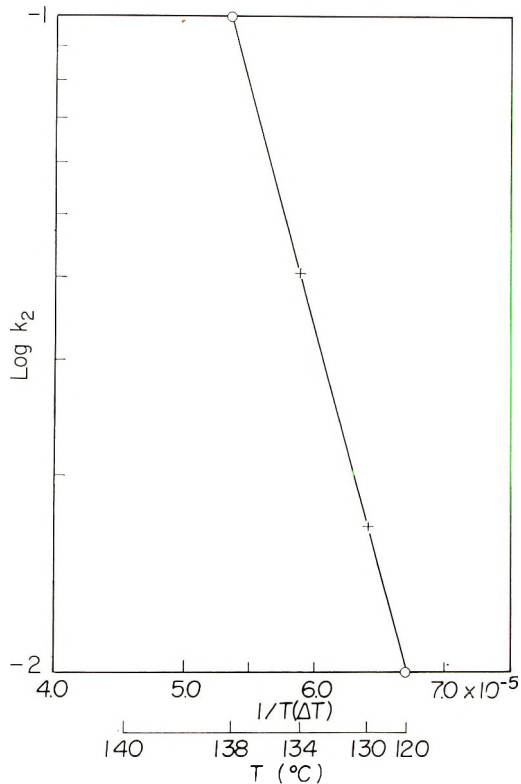


Fig. 27. Variation of $\text{log } k_2$ for the Avrami equation for secondary crystallization with $1/T(\Delta T)$.

CONCLUSIONS

The combined results of studies of the crystallization of polypropylene by optical microscopy and by x-ray diffraction are consistent with a two-stage process of crystallization, the first stage being the radial growth of spherulites on nuclei that are predetermined but which do not all start growth at once. This process is describable by an Avrami equation characterized by $n_1 = 3.9$ in its earlier stages.

The primary spherulite growth process occurs by a mechanism of the type described by Keith and Padden¹³ in which less crystallizable species are first excluded and concentrate between the more rapidly growing fibrils. Since the radial growth rate remains constant in the more tactic samples, a steady-state concentration of these rejected species is maintained behind the growth front of the spherulite, and no appreciable increase in its concentration occurs in the nonspherulitic material. The secondary crystallization then involves the slower crystallization of some of this material initially left uncrystallized within the spherulite.

The second process is a secondary crystallization within the spherulite. The local process is also describable by an Avrami equation having an exponent of 1.8 and with a rate which decreases with increasing temperature in a way similar to that for primary crystallization. The commonly observed rates of secondary crystallization are averages over these local processes.

The variation in the Avrami exponent with time determined from the dilatometric measurements reported in the first part of the paper, while not directly comparable with the latter results, are probably a consequence of this n 's being an "effective average" representing chiefly the larger n_1 for primary crystallization at the beginning and the smaller n_2 for secondary crystallization at further stages of crystallization. This explanation is consistent with the faster decrease of the overall crystallization rate for the less tactic fractions, resulting from the fact that most of the process involves secondary crystallization. In fact, for the samples of very low tacticity, spherulitic structures are "frustrated" in growth at very early stages of development, and a large part of the crystallization is of the secondary type.

In this work, we have only considered a single secondary process. In reality, there are probably several, including lamellae thickening as well as crystallization of interlamellae material. A more accurate treatment should include more than one process, but the present accuracy of the data does not warrant elaboration at the present time.

The authors are indebted to Mr. A. Bibeau (Monsanto) for his dilatometric measurements, to Mr. D. A. Keedy (University of Massachusetts) for his construction of photo-microscopic and x-ray diffraction apparatus, and to Dr. Leon Marker (General Tire and Rubber Company) for his comments on this work, and to Dr. Frasier Price (General Electric Research Laboratories) for the opportunity to see and discuss his results prior to publication.

References

1. Newman, S., *J. Polymer Sci.*, **47**, 111 (1960).
2. Hoffman, J. D., J. J. Weeks, and W. M. Murphy, *J. Res. Natl. Bur. Std.*, **63A**, 67 (1959).
3. Willers, F. T., and R. T. Beyer, *Practical Analysis*, Dover, New York, 1948.
4. Griffith, J. R., and B. G. Rånby, *J. Polymer Sci.*, **38**, 107 (1959).
5. Marker, L., P. Hay, G. Tilley, R. Early, and O. Sweeting, *J. Polymer Sci.*, **38**, 33 (1959).
6. Mandelkern, L., in *Growth and Perfection of Crystals*, R. H. Doremus, B. W. Roberts, and D. Turnbull, Eds., Wiley, New York, 1958.
7. Buchdahl, R., R. L. Miller, and S. Newman, *J. Polymer Sci.*, **36**, 215 (1959).
8. Hoshino, S., J. Powers, and R. S. Stein, ONR Technical Report No. 43, Project NR 356-378 Contract, NONR 3557(01), University of Massachusetts, Amherst, Massachusetts (1962).
9. Flory, P. J., and A. D. McIntyre, *J. Polymer Sci.*, **18**, 592 (1955).
10. Meinecke, E., and R. S. Stein, ONR Technical Report No. 58, Project NR 356-378, Contract NONR 3557(01), University of Massachusetts, Amherst, Mass. (1963).
11. Weidinger, B. A., and P. H. Hermans, *Makromol. Chem.*, **50**, A8 (1963).
12. Natta, G., et al., *Atti Accad. Nazl. Lincei Rend. Classe Sci. Fis., Mat. Nat.*, [8] **22**, 11 (1957).
13. Keith, H. D., *Bull. Am. Phys. Soc.*, **8**, 242 (1964); F. J. Padden, *Bull. Am. Phys. Soc.*, **8**, 242 (1964).

Résumé

On a étudié, par dilatométrie, la vitesse totale de cristallisation de fraction de polyéthylène, et on a suivi le processus de cristallisation en tenant compte de la stéréorégularité des échantillons. L'étude comprend une analyse photomicroscopique de la formation des germes, de la formation et de la croissance des sphérolites, ainsi que l'évaluation par des techniques rapides de diffraction aux rayons-X, de l'accroissement de la cristallinité au sein des sphérolites. Application fut faite d'une théorie pour l'interprétation du comportement à la cristallisation, théorie dans laquelle on a introduit deux étapes de croissance: (a) croissance à l'interface des sphérolites et (b) cristallisation secondaire au sein du sphérolite. Ces étapes sont décrites au moyen d'équations du type Avrami avec différents paramètres.

Zusammenfassung

Die Bruttokristallisationsgeschwindigkeit von Polypropylenfraktionen wurde dilatometrisch untersucht und das Kristallisationsverhalten in Beziehung zur Stereoregularität der Proben gebracht. Die Untersuchung bestand in einer lichtmikroskopischen Analyse von Keimbildung, Bildung und Wachstum der Sphärolithe und einer Bestimmung der Zunahme der Kristallinität in den Sphärolithen durch ein rasches Röntgenverfahren. Das Kristallisationsverhalten wurde an Hand einer Theorie diskutiert, bei welcher zwei Wachstumsstadien eingeführt werden: (a) Wachstum an der Sphärolithgrenzfläche und (b) Sekundärkristallisation innerhalb des Sphäroliths. Sie wurden durch Gleichungen vom Avrami-Typ mit verschiedenen Parametern beschrieben.

Received October 22, 1964

Prod. No. 4583A

Modified Avrami Equation for the Bulk Crystallization Kinetics of Spherulitic Polymers

I. H. HILLIER,* *Chemistry Department, Imperial College, London, England*

Synopsis

An explanation of the anomalous fractional values of the Avrami exponent found for the crystallization of a number of polymers is presented. The interpretation is based on a model which postulates the constant radial growth of spherulites, followed by an increase in crystallinity within them by a first order process. The model is supported by direct microscopic observations of other workers. Crystallization isotherms for polymethylene, poly(ethylene oxide), and poly(decamethylene terephthalate) are fitted to this model. Apart from the removal of the fractional values of the Avrami exponent, which have no physical meaning, this model gives a considerably better fit than the Avrami equation to most isotherms analyzed. The temperature dependence of the rate constants found for the two rate processes of this model is also discussed. An interpretation of the results of seeded experiments is presented in terms of this model.

INTRODUCTION

The crystallization kinetics of bulk polymers is usually interpreted,¹ although with varying degrees of success,^{2,3} in terms of the Avrami equation:

$$\chi(a,t) = \chi(a, \infty) (1 - \exp\{-zt^n\}) \quad (1)$$

where χ is the crystallinity, t the time, z a constant depending upon the nucleation and growth rates, and n an integer depending on the shape of the growing crystalline body. As spherulites are observed in most crystalline polymers and in thin films are seen to grow with a constant radial rate, a value $n = 3$ (instantaneous nucleation) or $n = 4$ (sporadic nucleation) is expected if the density of the spherulites is constant. Recent work on a number of polymers²⁻⁷ has revealed that values of n of 3 or 4 are rarely found. The results of detailed analysis of crystallization isotherms which appear in the literature are summarized in Table I on the following page. The Avrami exponent n may vary with temperature and be a noninteger less than 4 but rarely exceeds this value. Deviations of n from the integral values required by eq. (1) may be explained by postulating either (a) a nonconstant growth rate or (b) a nonconstant density of the growing spherulites.

* Present address: Institute for the Study of Metals, University of Chicago, Illinois.

TABLE I
Summary of Anomalous Avrami Exponents from the Literature

Polymer	Range of Avrami exponent	Reference
Poly(3,3-bis(chloromethyl)oxacyclobutane)	1.7 -3.3	4
Poly(decamethylene terephthalate)	2.66-3.97	2
Polyethylene	2.70-3.87	3
Polymethylene	1.81-2.55	5
Poly(ethylene oxide)	2	6
Polypropylene	2.8 -4.1	7

A model in which the crystalline bodies are considered to be single crystal lamellae growing by a chain-folding mechanism has been shown to be a possible explanation of the observed kinetics of polymethylene.⁵ This model leads to a nonconstant growth rate, the single crystal lamellae having a constant density.

A number of authors have independently proposed⁸⁻¹⁰ that the "primary" (Avrami) and "secondary" (post-Avrami) crystallization processes occurring in polyethylene may be described by the growth and subsequent relaxation of the crystalline regions, leading to a variable density within the sample. Gordon and Hillier⁸ have shown that such a scheme, in which the secondary relaxation is described by a general rate equation due to Hirai and Eyring¹¹ successfully describes the overall crystallization rate in bulk polymethylene.

In this paper, it is shown that the fractional values of the Avrami exponent may be explained by the constant radial growth of spherulites (termed the primary crystallization in this work) followed by further crystallization within the spherulite which obeys a first-order law. This model is fitted to crystallization isotherms of polymethylene, poly(ethylene oxide) and poly(decamethylene terephthalate). It must be stressed that this postulated subsequent crystallization is distinct from the secondary crystallization which varies linearly with \ln (time), observed in polyethylene and other polymers. The mechanism of this secondary or post-Avrami crystallization has been fully discussed elsewhere,⁸ and is interpreted in terms of an increase in lamellar thickness. The first-order process proposed in this paper differs from this post-Avrami crystallization both kinetically and in the morphological interpretation of the kinetics.

The slow secondary crystallization is absent in the samples analyzed here.

DESCRIPTION OF THE MODEL

Price¹⁰ has proposed this model to account for the slow secondary crystallization observed in polymethylene. In this model, spherulites grow with a constant radial rate from random centers. The crystallinity at time t [$\chi(a, t)$] due to this process is given by the Avrami equation, eq. (1), with $n = 3$ or 4. Once a volume element has been included in the spherulite its

crystallinity jumps from zero to $\chi(a, \infty)$. A first-order process then occurs within the volume element whereby its crystallinity increases by an amount $\chi(s, t - \theta)$, where

$$\chi(s, t - \theta) = \chi(s, \infty) [1 - \exp\{-z_2(t - \theta)\}] \quad (2)$$

This eq. (2) gives the additional crystallinity at time t , of an element which was included in the spherulite at time θ . The total crystallinity at time t [$\chi(c, t)$] arising from these two consecutive crystallization processes becomes⁸

$$\chi(c, t) = \chi(a, t) - \int_0^t \frac{\chi(a, \theta)}{\chi(a, \infty)} \frac{d}{d\theta} [\chi(s, t - \theta)] d\theta \quad (3)$$

From eqs. (1) and (2), eq. (3) becomes

$$\begin{aligned} \chi(c, t) = \chi(a, \infty) [1 - \exp\{-z_1 t^n\}] + \chi(s, \infty) z_2 \\ \times \int_0^t (1 - \exp\{-z_1 \theta^n\}) [\exp\{-z_2(t - \theta)\}] d\theta \end{aligned} \quad (4)$$

Price¹⁰ has shown that if the first-order process is sufficiently slower than the primary crystallization, then this rate eq. (4) gives crystallization isotherms which resemble those found when both primary and secondary crystallization are present. It is here shown that if the two processes have comparable half-lives, then crystallization isotherms are obtained which resemble those found experimentally when the secondary crystallization is absent, and which further lead to fractional values of the Avrami exponent, when analyzed according to eq. (1). Equation (4) shows that the isotherms obtained from this model lead to an exponent which is initially equal to n (3 or 4) and falls towards unity as the crystallization proceeds. A progressively decreasing exponent is found for both polymethylene⁵ and poly(ethylene oxide).¹² On the other hand, a number of Avrami processes with different but integral values of n , occurring simultaneously, lead to an apparent n value which increases as crystallization proceeds. This has been rejected as a possible explanation of the anomalous fractional values of the Avrami exponent.¹³

FIT OF CONVOLUTED RATE EQUATION (4) TO AVRAMI EQUATION (1)

From eq. (4), isotherms were calculated for a number of values of the parameters z_1 , z_2 , $\chi(a, \infty)$, and $\chi(s, \infty)$, for both $n = 3$ and $n = 4$. The integral in this equation could not be evaluated analytically and was approximated by the 20-point Gauss formula, giving an accuracy of greater than 0.1%. A typical isotherm is shown in Figure 1, where the contributions to the total crystallinity of both processes are individually shown. The isotherms thus obtained were then fitted by a least-squares procedure, by using a modified steepest descent program to the simple Avrami eq. (1), having the two adjustable parameters n and z . Table II summarizes the

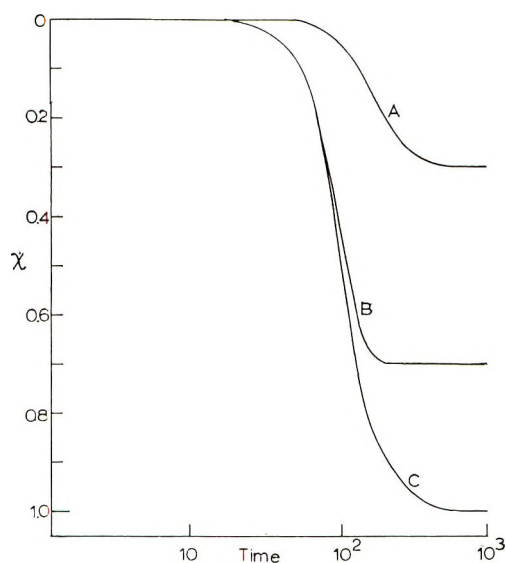


Fig. 1. Isotherms constructed from eq. (4) with $z_1 = 1 \times 10^{-6}$, $z_2 = 1 \times 10^{-2}$, $\chi(a, \infty) = 0.7$, $\chi(s, \infty) = 0.3$, $n = 3$: (A) crystallinity due to first-order process, $\chi(c, t) - \chi(a, t)$; (B) crystallinity due to primary crystallization, $\chi(a, t)$; (C) total crystallinity, $\chi(c, t)$.

results obtained. The value of the Avrami exponent is reduced from 4 and 3 [eq. (4)] to an optimum value between 3.5 and 2. The standard deviation may be up to 5%, the larger values being found when the first order process is relatively slow. When experimental isotherms are fitted to the Avrami eq. (1), standard deviations of this magnitude are commonly found.⁵ If the primary process contributes more to the total crystallinity than the first-order process, then the very good fit to the simple Avrami eq.

TABLE II
Fit of Isotherms, Constructed from Convolved Rate Equation (4),
to Avrami Equation (1)

Parameters of eq. (4)					Parameters from optimum fit of eq. (1)		
n	z_1	z_2	$\chi(a, \infty)$	$\chi(s, \infty)$	n	z	$\sigma, \%$
3	1×10^{-6}	1×10^{-2}	0.7	0.3	2.32	1.46×10^{-5}	2.71
3	1×10^{-6}	1×10^{-2}	0.5	0.5	2.16	2.29×10^{-5}	2.79
3	1×10^{-6}	1×10^{-2}	0.9	0.1	2.73	3.00×10^{-6}	1.43
3	1×10^{-6}	1×10^{-1}	0.7	0.3	3.04	7.47×10^{-7}	0.08
3	1×10^{-6}	1×10^{-3}	0.7	0.3	2.18	3.04×10^{-5}	4.62
4	5×10^{-9}	1×10^{-2}	0.7	0.3	3.06	2.83×10^{-7}	2.90
4	5×10^{-9}	1×10^{-2}	0.5	0.5	3.39	3.74×10^{-8}	4.20
4	5×10^{-9}	1×10^{-2}	0.9	0.1	3.50	4.70×10^{-8}	1.56
4	5×10^{-9}	1×10^{-1}	0.7	0.3	3.50	5.01×10^{-8}	1.84
4	5×10^{-9}	1×10^{-3}	0.7	0.3	2.99	4.26×10^{-7}	4.83

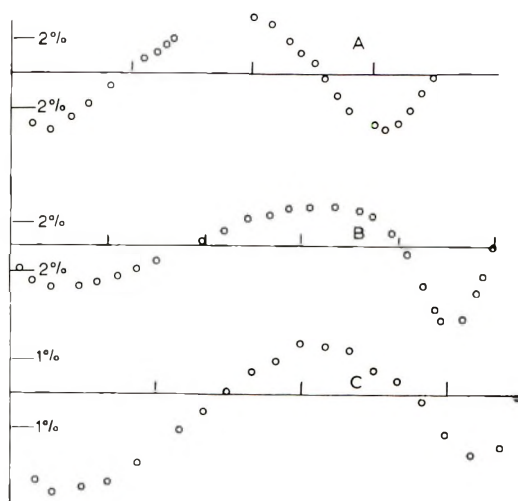


Fig. 2. Difference plot showing fit of isotherms to simple Avrami eq. (1): (A) polymethylene, run D, $T = 127.61^{\circ}\text{C}$. ($\sigma = 2.1\%$); (B) isotherm construction from eq. (4) ($\sigma = 2.7\%$), parameters as for Fig. 1; (C) poly(ethylene oxide), $T = 53.77^{\circ}\text{C}$. ($\sigma = 1.5\%$). The vertical scale is experimental contraction - calculated contraction, as a percentage of total contraction. The horizontal scale is experimental shrinkage.

(1) (Table II) shows that isotherms are obtained which would give apparent constant fractional n values when analyzed by conventional double logarithmic plots.⁷ The residual deviations remaining after the fit of the Avrami equation to the constructed isotherms [eq. (4)] are systematic, and follow the same pattern in all cases. A representative difference plot (i.e., percentage difference calculated on the total crystallinity between the calculated and observed crystallinity at time t) is shown in Figure 2 and compared to ones for polymethylene⁵ and poly(ethylene oxide).¹⁴ The residual deviations follow very closely the same pattern in all three cases. This strongly indicates that the experimental isotherms for polymethylene and poly(ethylene oxide) may be well fitted by the rate eq. (4).

ANALYSIS OF CRYSTALLIZATION ISOTHERMS IN TERMS OF THE CONVOLUTED RATE EQUATION

For application to dilatometry, eq. (4) is written in terms of the experimentally measured dilatometric heights $[h(0) - h(t)]$ at time t as

$$h(0) - h(t) = [h(0) - h(\infty)]_a(1 - \exp\{-z_1 t^n\}) + [h(0) - h(\infty)]_s z_2 \times \int_0^t [(1 - \exp\{-z_1 \theta^n\}) \exp\{-z_2(t - \theta)\}] d\theta \quad (5)$$

where $[h(0) - h(\infty)]_a$ and $[h(0) - h(\infty)]_s$ are proportional to the total crystallinity due to the primary and first-order processes, respectively. The total experimental contraction is taken to be equal to the sum of these contributions, leading to three adjustable parameters in fitting eq. (5)

to experimental data; the two rate constants z_1 and z_2 and the ratio of the two limiting crystallinities. A fit of an experimental run of about 50 points to eq. (5) takes approximately 1 min. on the Atlas computer.

Polymethylene

The data analyzed here are those reported previously³ for polymethylene ($P_r = 26,000$) deprived of its slow secondary crystallization. The isolated Avrami process shows an exponent which decreases to unity towards the end of the crystallization. A decrease of n from 3 to 2 has also been reported for a sample of polyethylene exhibiting secondary crystallization.¹⁵ In fitting our data, the value of the Avrami exponent [n , eq. (5)] was taken as 3 corresponding to instantaneous nucleation of spherulites. In many polyethylene samples, including the one studied here, spherulites cannot be resolved optically. However, drastic heat treatment is found to result in observable spherulites, which are formed almost instantaneously and which grow with a constant radial rate until impingement is near.¹⁵ In fitting eq. (5) it is assumed that in the untreated sample, spherulites are present, although they are too small to be observed optically. The fit of eq. (5) to runs at six temperatures giving standard deviations in the range 0.4–1.2% is shown in Table III where the fit of the two-parameter Avrami eq. (1) is also shown (see Table III, ref. 5) ($\sigma = 1.7$ –3.5%). The fit achieved by the three-parameter equation is surprisingly good, considering that fitting run *C* to an empirical 16-parameter equation leads to a standard deviation of 0.25%,³ which is regarded as the magnitude of the experimental scatter. The substantial decrease in the standard deviation on the addition of only one further adjustable parameter gives encouraging support for the model, particularly as the simple Avrami eq. (1) has no physical meaning for the optimum fractional values of the Avrami exponent.

Poly(ethylene Oxide)

Price et al.¹² have found that the value of the Avrami exponent decreases during crystallization and that spherulites grow with a constant radial rate in thin films of the polymer. Banks and Sharples⁶ observed spherulites of the same size in bulk samples, indicating instantaneous nucleation. When they analyzed dilatometric data for the spherulitic sample, the value of the Avrami exponent was found to be 2,⁶ a value incompatible with the observation of spherulites. Data analyzed here are for a similar sample as that used by Banks and Sharples (Polyox WSR 35, provided by Union Carbide Ltd.). Table IV shows the fit of both the simple Avrami eq. (1) ($\sigma = 1.1$ –3.4%) and the modified Avrami eq. (5) with $n = 3$ ($\sigma = 0.8$ –1.7%). The optimum value of n for the fit of the simple Avrami equation is near 2 at the lower temperatures (confirming the results of Banks and Sharples)⁶ and falls to near 1.5 at high temperatures. In all but one run, the standard deviation is decreased by the fit of the modified Avrami equation, although this improvement is not as marked as in the case of polymethylene.

TABLE III
Fit of Convoluted Rate Equation (5) and Avrami Equation (1) to Polymethylene

Fit of eq. (1)		Fit of eq. (5)							
Run	Temp., °C.	n	z	$\sigma, \%$	z_1	z_2	$ h(0) - h(\infty) _{av}$, cm.	Total experimental contraction, cm.	$\sigma, \%$
A	125.79	1.81	1.04×10^{-3}	2.73	5.99×10^{-5}	3.21×10^{-2}	1.28	3.67	0.69
B	125.92	1.81	8.27×10^{-4}	3.48	3.29×10^{-5}	1.96×10^{-2}	1.67	4.07	0.73
C	127.18	1.99	5.34×10^{-5}	2.64	2.02×10^{-6}	1.16×10^{-2}	0.79	3.74	0.44
D	127.61	2.28	6.28×10^{-6}	2.06	6.77×10^{-7}	1.13×10^{-2}	0.51	3.50	1.08
E	128.26	2.29	1.37×10^{-6}	1.75	7.40×10^{-8}	6.35×10^{-3}	0.80	3.49	1.17
F	129.12	2.55	2.85×10^{-8}	1.72	4.03×10^{-9}	2.41×10^{-3}	0.89	3.55	0.47

TABLE IV
Fit of Convoluted Rate Equation (5) and Avrami Equation (1) to Poly(ethylene oxide)

Fit of eq. (1)		Fit of eq. (5)						
Temp., °C.	n	z	$\sigma, \%$	z_1	z_2	$ h(0) - h(\infty) _{av}$, cm.	Total experimental contraction, cm.	$\sigma, \%$
51.14	1.91	9.82×10^{-4}	1.13	1.40×10^{-4}	4.69×10^{-2}	0.91	7.05	1.67
53.77	1.99	1.39×10^{-4}	1.51	7.81×10^{-6}	2.21×10^{-2}	1.43	6.96	1.32
54.59	1.59	5.31×10^{-4}	3.36	6.11×10^{-6}	1.21×10^{-2}	1.63	6.91	1.03
55.63	1.51	2.32×10^{-4}	2.92	8.28×10^{-7}	5.39×10^{-3}	1.11	6.87	0.83

Poly(decamethylene Terephthalate)

Data at one temperature (122.95°C.) kindly provided by Drs. Sharples and Swinton, and previously reported by them² have been analyzed. The fit of the simple Avrami eq. (1) gave $n = 3.60$, $z = 1.30 \times 10^{-8}$ with $\sigma = 0.36\%$, and that of the modified Avrami eq. (5) with $n = 4$ gave $z_1 = 2.00 \times 10^{-9}$, $z_2 = 2.99 \times 10^{-2}$, $[h(0) - h(\infty)]a = 11.41$ cm. with $\sigma = 1.43\%$. (The total experimental contraction was 14.19 cm.) The standard deviation is not improved by the addition of the further parameter although the embarrassment of the fractional n value has been removed.

DISCUSSION

The model described here attempts to account for the anomalous values of the Avrami exponent found when crystallization data are analyzed in terms of the simple Avrami eq. (1), by incorporating only features which are observed microscopically. Thus, spherulites growing with a constant radial rate are observed in thin films of the majority of polymers. It has been questioned how justifiable is the practice of using observations pertinent to thin films to interpret bulk kinetics.¹⁵ This question remains unanswered until the growth rates of spherulites in the bulk are directly measured and compared to those found in thin films. The two rate processes combined in the overall rate eq. (4) receive support from the microscopic observations of Keith and Padden.^{16, 17} These authors postulate that during spherulitic growth, low molecular weight material is ejected and is trapped in interfibrillar layers. Their results suggest that growth takes place in two stages. First, there is a growth of spherulites consisting of radial fibers fairly well separated from one another by melt in which low molecular weight or stereoirregular species are concentrated. This is then followed by the solidification of impure interfibrillar melt. (See their Fig. 13.) These authors also suggest that the subsequent crystallization of impure interfibrillar melt leads to an Avrami exponent approximately equal to unity.

TABLE V
Temperature Dependence of Rate Constants z_1, z_2 [Eq. (5)] Analyzed According to Equation (6)

Polymer	Rate Constant [eq. (5)]	N	A	B	$\sigma, \%$
Polymethylene	z_1	1	17.14	1.35×10^5	1.2
		2	1.54	2.88×10^3	2.0
	z_2	1	2.94	3.26×10^4	6.4
		2	-0.82	6.99×10^7	5.9
Poly(ethylene oxide)	z_1	1	2.85	5.60×10^4	4.6
		2	-4.15	1.10×10^8	5.0
	z_2	1	2.16	2.43×10^4	6.0
		2	-0.85	4.81×10^7	4.2

As unfractionated commercial samples of polymethylene and poly(ethylene oxide) have been used in the dilatometric experiments, it is reasonable to suppose that low molecular weight material is present, so that this mechanism may be operative. In fact, Keith and Padden have used poly(ethylene oxide) of the same designation (Polyox WSR 35) in arriving at their conclusions.

Further support for the model may be sought by examining the temperature dependence of the parameters z_1 and z_2 [eq. (4)]. If it is assumed that the number of primary nuclei is temperature-independent, the temperature dependence of z_1 may be directly compared to that of the radial growth rate observed microscopically. The temperature dependence of the growth rate has been interpreted¹ in terms of two or three dimensional secondary nucleation leading to a linear dependence of $\ln(z)$ upon $1/T\Delta T$ and $1/(T\Delta T)^2$, respectively, i.e.,

$$\ln(z) = A - B/(T\Delta T)^N \quad (6)$$

A least-squares fit of the two rate constants (z_1 , z_2) for polymethylene and poly(ethylene oxide) (Table V) shows that for both polymers, the rate constant z_1 corresponding to the radial spherulitic growth is best fitted by the $1/T\Delta T$ law. However, for poly(ethylene oxide) the distinction between the two possibilities is not as definite as for polymethylene. Hoffman and Lauritzen¹⁸ have shown that growth by coherent nucleation leading to the $1/T\Delta T$ law is necessary in the formation of the lamellar spherulites found in bulk polymethylene^{19,20} and poly(ethylene oxide).²¹ The magnitude of the slope of these plots is in reasonable agreement with the values reported from microscopic observations. For polyethylene of varying molecular weight the slope is in the range 3×10^4 – 6×10^4 ,²² the value obtained from this model being 4.5×10^4 (Table V). (The slopes in Table V must be divided by 3 to correspond to the radial growth rate.) For poly(ethylene oxide), Price et al.¹² report a microscopic value of 2.9×10^4 compared to our value of 1.9×10^4 . The agreement is encouraging, considering that the microscopic and bulk values refer to different samples. The values of z_2 do not conclusively distinguish between a two- or three-dimensional secondary nucleation mechanism for the first-order process. This analysis is complicated by an uncertainty in the melting temperature to be used here. The model postulates that z_2 refers to the crystallization of interfibrillar low molecular weight material. This will have a lower melting point than the higher molecular weight material which is initially incorporated in the spherulite. The melting points [polymethylene, 138.3°C.; poly(ethylene oxide), 65.8°C.] were taken as the temperature at which the final trace of crystallinity disappeared³ and thus refer to the higher molecular weight material. However, the rate eq. (5) does not depend upon an explicit formulation of this process. It may, as proposed by Keith and Padden, be due to interlamellar crystallization of low molecular weight material, and, in the case of tactic polymers, of stereoirregular species. Other possible mechanisms of this first-order process can also be envisaged. These include re-

laxation processes within the lamellae, leading to an increase in crystal perfection, and crystallization of lower stereoregularity segments in tactic polymers. In view of these possible mechanisms, the first-order process postulated here may be an oversimplification. The residual deviations which remain after the fitting of this model are in the majority of the runs still systematic, although for the runs fitted to less than 1% the deviations become more random. (For the fit of polymethylene, run C, $\sigma = 0.44\%$, the deviations change sign 16 times.) In the runs in which the deviations are still systematic, including all those of poly(ethylene oxide) and the one poly(decamethylene terephthalate) run, the deviations follow the same

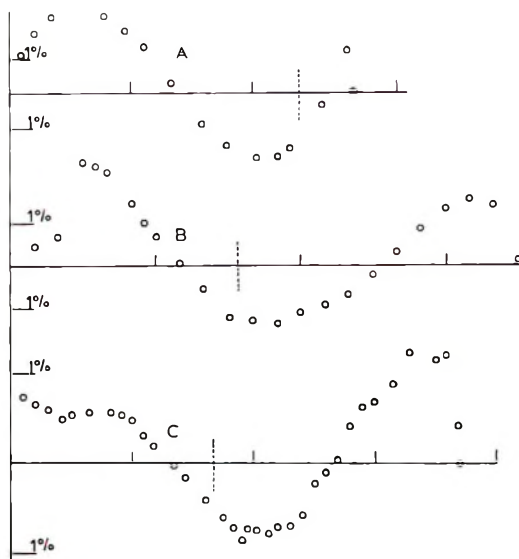


Fig. 3. Difference plots showing fit of combined rate eq. (5) to: (A) poly(decamethylene terephthalate), $T = 122.95^{\circ}\text{C}$. ($\sigma = 1.4\%$); (B) poly(ethylene oxide), $T = 53.77^{\circ}\text{C}$. ($\sigma = 1.3\%$); (C) polymethylene, run A, $T = 125.79^{\circ}\text{C}$. ($\sigma = 0.7\%$). The scales are as in Fig. 2. The vertical dotted lines indicate where the primary crystallization is 90% completed.

pattern, indicating that in all three polymers, a common deviation from the model occurs. Figure 3 shows a representative difference plot for each polymer. It is seen that towards the end of the primary process the calculated crystallinity is in excess of the experimental value. This may be due to a decrease in the radial growth rate of the spherulites when abutment is near. Such a decrease has been observed microscopically for both polyethylene¹⁵ and poly(ethylene oxide).^{12,17}

This model also leads to a possible explanation of the results of seeded⁵ experiments on polyethylene and poly(ethylene oxide) (crystallization after partial melting). An Avrami exponent slightly greater than unity is found dilatometrically,^{23,14} and the final linear growth rate is approximately the

same in the seeded and unseeded experiments.⁵ Microscopically, the birefringence disappears uniformly on melting and returns uniformly on recrystallization.^{15,23} This suggests that the crystallization observed after partial melting is mainly the first-order process which occurs within the spherulite during crystallization from the melt. Although there are a number of possible mechanisms for this process, the observations are most readily interpreted if it is assumed that it is due to the crystallization of low molecular weight interfibrillar material. This leads to the following picture in terms of the model discussed. On partial melting, crystallinity due to the first-order process is lost first, owing to its lower molecular weight and hence melting point, resulting in a uniform disappearance of the birefringence. Tables III and IV show that this crystallinity is about 60–70% of the total, so that when the seed crystallinity is 30–40% and above, subsequent crystallization will be solely due to the first-order process leading ideally to an Avrami exponent of unity. The final growth rates will be the same in the seeded and unseeded cases as they both refer to the first order process. Values of n slightly greater than unity, which are found to occur for lower degrees of seed, may be the result of the loss on partial melting of some of the crystallinity added during the primary radial growth.

Thanks are due to Professor M. Gordon for many helpful discussions.

These calculations were performed on the Atlas Computer at the Institute of Computer Science of London University. Thanks are due to the Director for use of these facilities.

References

1. Mandelkern, L., *Growth and Perfection of Crystals*, Chapman and Hall, London, 1958, pp. 467–497.
2. Sharples, A., and F. L. Swinton, *Polymer*, **4**, 119 (1963).
3. Banks, W., M. Gordon, R. J. Roe, and A. Sharples, *Polymer*, **4**, 61 (1963).
4. Hatano, M., and S. Kambara, *Polymer*, **2**, 1 (1961).
5. Gordon, M., and I. H. Hillier, *Trans. Faraday Soc.*, **60**, 763 (1964).
6. Banks, W., and A. Sharples, *Makromol. Chem.*, **59**, 233 (1963).
7. Parrini, P., and G. Corrieri, *Makromol. Chem.*, **62**, 83 (1963).
8. Gordon, M., and I. H. Hillier, *Phil. Mag.*, **11**, 31 (1965).
9. Peterlin, A., *J. Appl. Phys.*, **35**, 75 (1964).
10. Price, F. P., private communication.
11. Hirai, N., and H. Eyring, *J. Appl. Phys.*, **29**, 810 (1958).
12. Barnes, W. J., W. G. Leutzen, and F. P. Price, *J. Phys. Chem.*, **65**, 1742 (1961).
13. Banks, W., A. Sharples, and J. N. Hay, *J. Polymer Sci.*, **A2**, 4059 (1964).
14. Gordon, M., and I. H. Hillier, unpublished results.
15. Banks, W., J. N. Hay, A. Sharples, and G. Thompson, *Polymer*, **5**, 163 (1964).
16. Keith, H. D., and F. J. Padden, *J. Appl. Phys.*, **35**, 1270 (1964).
17. Keith, H. D., and F. J. Padden, *J. Appl. Phys.*, **35**, 1286 (1964).
18. Hoffman, J. D., and J. I. Lauritzen, *J. Res. Natl. Bur. Std.*, **65A**, 297 (1961).
19. Keller, A., and S. Sawada, *Makromol. Chem.*, **74**, 191 (1964).
20. Palmer, R. P., and A. J. Cobbold, *Makromol. Chem.*, **74**, 174 (1964).
21. Barnes, W. J., and F. P. Price, *Polymer*, **5**, 283 (1964).
22. Lindenmeyer, P. H., and V. F. Holland, *J. Appl. Phys.*, **35**, 55 (1964).
23. Banks, W., M. Gordon, and A. Sharples, *Polymer*, **4**, 289 (1963).

Résumé

On présente une explication pour les valeurs fractionnaires anormales de l'exposant d'Avrami trouvées lors de la cristallisation d'un certain nombre de polymères. L'interprétation se base sur un modèle qui postule la croissance radiale constante des sphérulites, suivie d'une augmentation de la cristallinité à l'intérieur de ceux-ci par un processus du premier ordre. Le choix du modèle est étayé par des observations microscopiques directes d'autres auteurs. Les isothermes de cristallisation pour le polyméthylène, l'oxyde de polyéthylène et le téréphtalate de polydécaméthylène sont en accord avec ce modèle. Indépendamment de la suppression des valeurs fractionnaires de l'exposant d'Avrami, qui n'a pas de signification physique, ce modèle fournit un accord bien meilleur que l'équation d'Avrami avec la plupart des isothermes analysés. On discute également de la dépendance vis-à-vis de la température des constantes de vitesse trouvées pour les processus à deux vitesses de ce modèle. Sur la base de ce modèle, on présente une interprétation des résultats des expériences ensemencées.

Zusammenfassung

Eine Erklärung der anomalen, bei der Kristallisation einer Anzahl von Polymeren auftretenden gebrochenen Werte des Avrami-Exponenten wird gegeben. Die Interpretation beruht auf einem Modell, in welchem ein konstantes Radialwachstum der Sphärolithe, gefolgt von einer Kristallinitätszunahme innerhalb derselben nach einem Prozess erster Ordnung angenommen wird. Dieses Modell wird durch direkte mikroskopische Beobachtungen anderer Autoren gestützt. Die Kristallisationsisothermen für Polymethylen, Poly(äthylenoxyd), und Poly(decamethylenterephthalat) werden diesem Modell angepasst. Neben der Beseitigung der gebrochenen Werte des Avrami-Exponenten, welche keine physikalische Bedeutung haben, liefert dieses Modell auch eine beträchtlich bessere Übereinstimmung mit den meisten untersuchten Isothermen wie die Avrami-Gleichung. Weiters wird die Temperaturabhängigkeit der Geschwindigkeitskonstanten der beiden Geschwindigkeitsprozesse dieses Modells diskutiert. Eine Interpretation der Ergebnisse aus Keim-Experimenten wird an Hand dieses Modells gegeben.

Received October 20, 1964

Prod. No. 4632A

A Phenomenological Theory of Spherulitic Crystallization: Primary and Secondary Crystallization Processes

FRASER P. PRICE, *General Electric Research Laboratory, Schenectady,
New York*

Synopsis

A theory is presented that takes into account the two stages occurring during the crystallization of bulk polymers. The theory assumes that all the crystallization occurs within the spherulites but that the amount of crystallinity at any particular point within a spherulite depends upon the age of that particular point. It is shown that these assumptions lead to transformation curves that look like those in actual polymer crystallizations.

The course of isothermal crystallization of high polymers frequently can be divided into two relatively distinct régimes.¹ In the first of these the transformation follows the usual Avrami² kinetics of nucleation and growth of spheres. In the second the crystallization rate is much decreased and the volume fraction transformed seems to increase approximately as the logarithm of the time. It has been noted that the second régime frequently starts about at the time when the specimen is completely filled with spherulites. The essence of the theory presented in this paper is that all the transformed material resides within growing spherulites and that the extent of transformation of any intraspherulitic region depends upon the length of time that region has been inside a spherulite.

Theory

It has been shown that for an assembly of spheres* developing with a constant radial growth rate G in a volume V that the volume fraction transformed into spheres is

$$Y = 1 - e^{-(Kst)^m} \quad (1)$$

* The best expositions of this problem of which the author knows are presented by Evans³ and Fry.⁴ All these developments rest upon Poisson's theory of expectations.⁵ They all give as the volume fraction occupied by the developing objects

$$Y = 1 - e^{-\Sigma n_i v_i / V}$$

where $\Sigma n_i v_i$ is the total volume the developing objects would have occupied had no impingement occurred and V is the volume which the Σn_i objects occupy with impingement. It is also assumed that n_i is large and $v_i \ll V$.

where t is the real time; $K_s = (4\pi G^3)/(3V)$ and $n = 3$ for a fixed number of spheres; and $K_s = (\pi G^3 N_0)/(3V)$ and $n = 4$ for a constant rate of injection of new spheres, N_0 . For convenience we change to reduced variables by letting $\tau = K_s t$ and consider the system at $\tau = X$. At some time, τ , prior to X the volume fraction of the system that has just been engulfed by the spheres is

$$dY = (\partial Y / \partial \tau) d\tau = m\tau^{m-1} e^{-\tau^m} d\tau \quad (2)$$

At time X this volume of material has been in existence $(X - \tau)$ time units. We assume that once inside a sphere the transformation from liquid to crystal is again defined by Avrami-type kinetics and thus the volume fraction transformed to crystal is

$$Q = 1 - ce^{-\beta^n (X - \tau)^n} \quad (3)$$

where $\beta = K_i/K_s$, $K_i =$ constant characterizing rate of the intrasphere crystallization in terms of real time, i.e. $\beta\tau = K_i t$, $c =$ volume fraction of liquid just inside the sphere boundary, and $n =$ constant = 1,2,3. Then at reduced time X , the volume fraction of material that is inside spheres and has transformed to crystals is

$$F = \int_0^X [1 - ce^{-\beta^n (X - \tau)^n}] m\tau^{m-1} e^{-\tau^m} d\tau \quad (4)$$

Upon integration, where possible, this yields for the volume fraction untransformed,

$$\phi = 1 - F = e^{-X^m} + mc \int_0^X \tau^{m-1} e^{-[\tau^m + \beta^n (X - \tau)^n]} d\tau \quad (5)$$

Thus for selected values of c , m , n , and β , in principle ϕ can be calculated as a function of X . Plots of volume fraction untransformed versus reduced time can then be constructed and compared to experiment. It is worth noting that the course of the intraspherical crystallization might be described by some function other than that given in eq. (3). The effect of this would be to replace the factor, $\exp \{-\beta^n (X - t)^n\}$ in the integral by the other expression.

In principle the integral on the right-hand side of eq. (5) can be reduced to a sum of incomplete gamma functions of fractional order, which can be evaluated from existing tables. This reduction can be accomplished by letting $\tau^m + \beta^n (X - \tau)^n = Z$, solving for τ in terms of Z , and making the appropriate substitutions. However, the solution of third- or fourth-order equations is so cumbersome that usually it is preferable to evaluate the integrals numerically for selected values of m , n , and β .

There is one case of apparent experimental interest where the reductions are simple enough to make the above procedure feasible. This is when $n = 1$ and β is small enough so that the approximation

$$e^{\beta\tau} = 1 + \beta\tau + (\beta\tau)^2/2 \quad (6)$$

is valid. Here eq. (5) reduces to

$$\phi = e^{-X^m} + ce^{-\beta X} [1 - e^{-X^m}] + c\beta e^{-\beta X} \int_0^{X^m} y^{1/m} e^{-y} dy + (c\beta^2 e^{-\beta X} / 2) \int_0^{X^m} y^{2/m} e^{-y} dy \quad (7)$$

where the first and second integrals on the right-hand side are incomplete gamma functions of order $1 + (1/m)$ and $1 + (2/m)$, respectively.

Results

The results of computer calculations of ϕ versus X for $m = 3$ (constant number of spheres) are plotted in Figures 1-6. Also plotted, as the dashed lines in the same figures, against X are values of $I = \phi - e^{-X^3}$, the volume fraction of liquid within the spheres. Figures 1, 2, and 3 present the curves for $c = 1$, the situation with no crystals at spherulite boundary. This case clearly is physically absurd. However the liquid fraction is made up of that outside the spheres plus that inside the spheres, and that outside the spheres is fixed at e^{-X^3} . Thus the dashed curves of I versus X , when multiplied by physically reasonable values of c , can be used to calculate the ϕ - X relationships for any situation. This has been done in Figures 4, 5, and 6 for $c = 0.5$. These will be discussed below. First it will be noted in Figures 1-3 that as β becomes smaller the separation into two distinct regimes becomes more marked. This is intuitively reasonable, as β represents the rate of intrasphere crystallization relative to the rate of sphere growth. If the ratio is small, the system will fill with spheres before they become appreciably crystallized and two distinct stages will ensue. Figures 1-3 also show that as β becomes larger the maximum fraction of non-

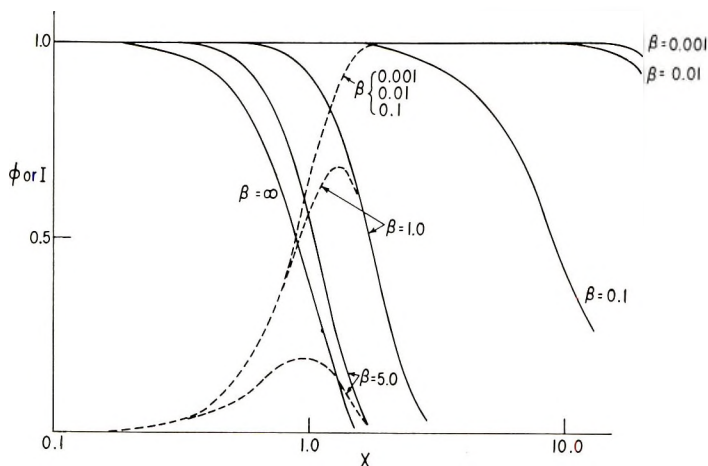


Fig. 1. Plots of (—) ϕ and (---) I vs. X for various values of β with $c = 1.0$, $m = 3.0$, $n = 3.0$.

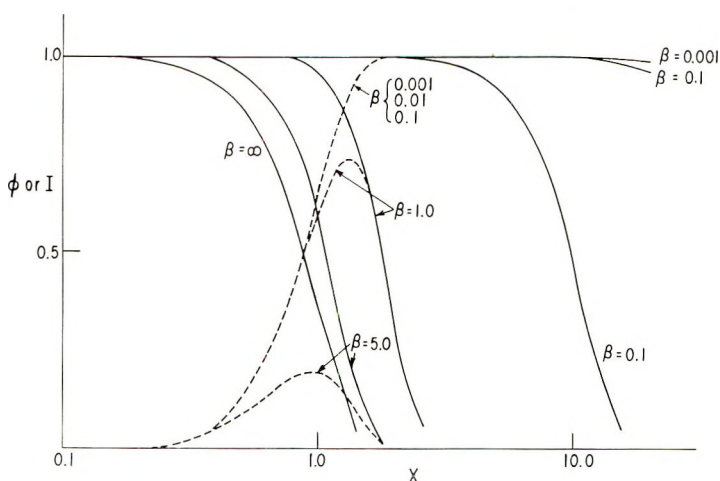


Fig. 2. Plots of (—) ϕ and (---) I vs. X for various values of β with $c = 1.0$, $m = 3.0$, $n = 2.0$.

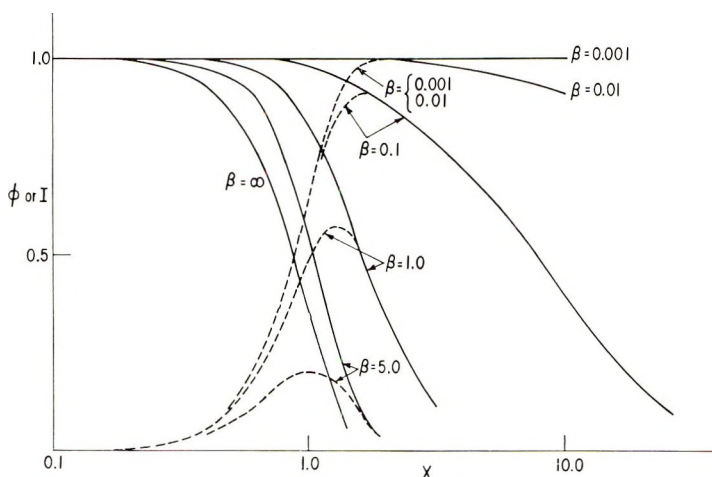


Fig. 3. Plots of (—) ϕ and (---) I vs. X for various values of β with $c = 1.0$, $m = 3.0$, $n = 1.0$.

crystallized intrasphere material both decreases and moves to shorter times. This also is to be expected, for as the rate of intrasphere crystallization increases with respect to sphere growth, the spheres become relatively more crystalline. The limit of this situation occurs when $\beta = \infty$, there is never any liquid within the spheres, and $\phi = e^{-X^3}$. Comparison of the I versus X curves at fixed values of β in Figures 1–3 shows that as n is decreased the value of X at the maximum is unaltered but the value of I decreases.

In Figures 4, 5, and 6 are displayed the curves of ϕ and I versus X for various values of n and β , with $c = 0.5$. Here the increasing separation of

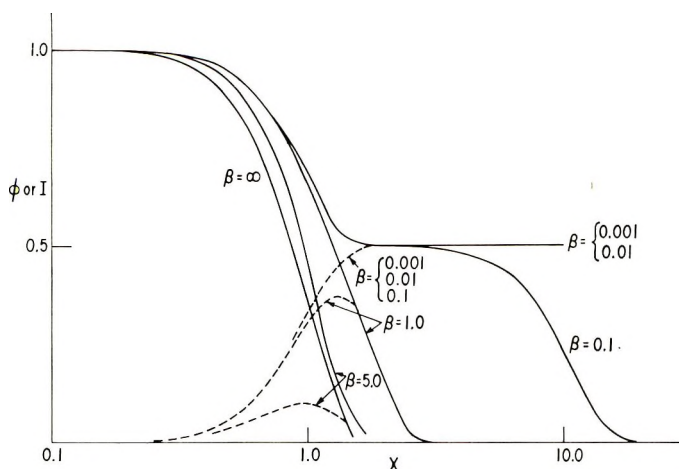


Fig. 4. Plots of (—) ϕ and (---) I vs. X for various values of β with $c = 0.5$, $m = 3.0$, $n = 3.0$.

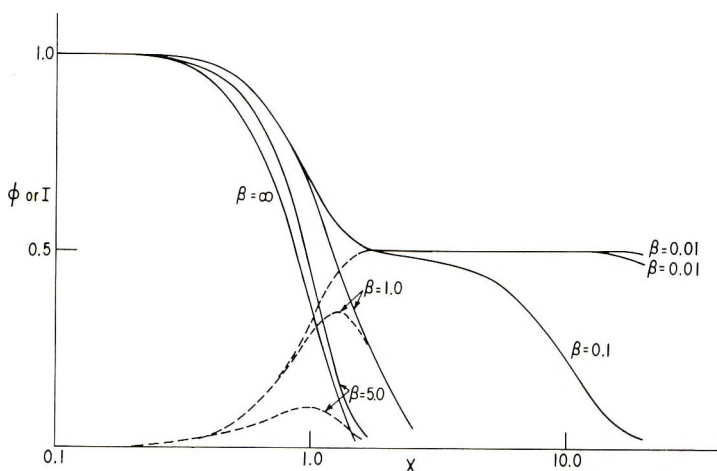


Fig. 5. Plots of (—) ϕ and (---) I vs. X for various values of β with $c = 0.5$, $m = 3.0$, $n = 2.0$.

the ϕ - X curves into two stages with decreasing values of β is very marked. In fact, in Figures 4 and 5 where $n = 3$ and 2, respectively, the transition from an apparent one-stage process to a two-stage one occurs over a relatively short range of β . Only in the case presented in Figure 6 where $n = 1$ is the transition between the stages sufficiently broad to make the curves look like those encountered experimentally. Accordingly, we henceforth will fix our attention on the case where $n = 1$. This is fortunate, as it permits easy expansion of the integral in eq. (5) by the methods indicated in eqs. (6) and (7). Values of ϕ were calculated by using eq. (7), by neglecting the last integral, the $\Gamma(5/3, X)$ one, and evaluating the first integral,

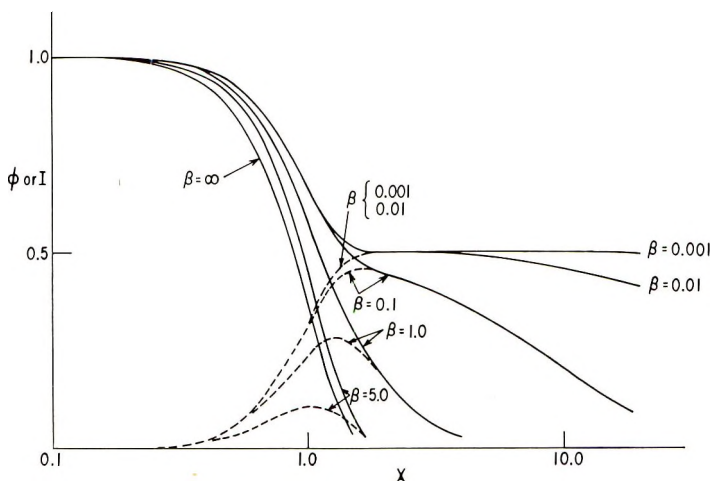


Fig. 6. Plots of (—) ϕ and (---) I vs. X for various values of β with $c = 0.5$, $m = 3.0$, $n = 1.0$.

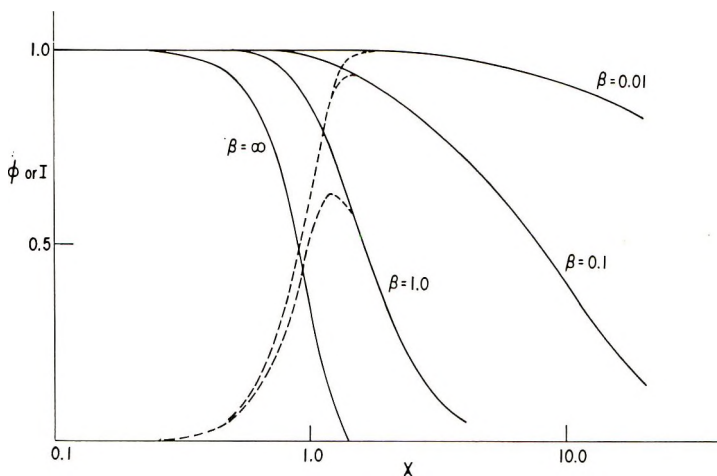


Fig. 7. Plots of (—) ϕ and (---) I vs. X for various values of β with $c = 1.0$, $m = 4.0$, $n = 1.0$.

the $\Gamma(4/3, X)$ one, by use of Pearson's tables of incomplete Γ -functions.⁶ The curves of ϕ versus X thus calculated everywhere fitted the computer calculated ones displayed in Figure 6 to within ± 0.005 in ϕ when $\beta \leq 1.0$. It thus appears that the approximations involved in obtaining an even somewhat abridged form of eq. (7) are not too drastic and that use of Pearson's tables is feasible. This is fortunate, as it permits evaluation of the necessary integrals without recourse to a digital computer.

In Figures 7 and 8 are displayed the curves of ϕ and I versus X for the case where $m = 4$ (constant nucleation rate of spheres) and $n = 1$ (disklike crystal growth within spheres). The results are not extremely different

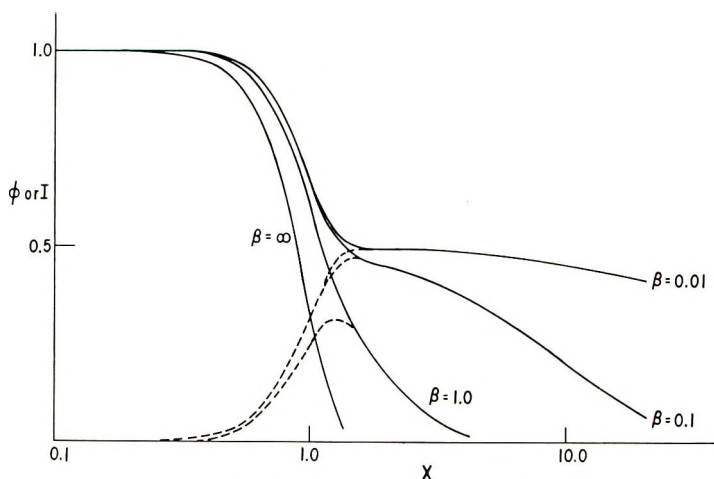


Fig. 8. Plots of (—) ϕ and (---) I vs. X for various values of β with $c = 0.5$, $m = 4.0$, $n = 1.0$.

from those for the $m = 3$ case. It is worth noting from a comparison of the ϕ - X curves in Figure 6 with those in Figure 8 that only near the beginning of crystallization is there any significant differences. This is due to the fact that only in this region do the kinetics of sphere nucleation and growth differ appreciably. After the system is essentially full of spheres it is the intrasphere crystallization which is important and this has been assumed identical in the two systems. The ϕ - X curves in Figure 8 were calculated by using the abridged form of eq. (7) discussed above in conjunction with Pearson's tables. Here the fit in ϕ was to within ± 0.008 .

In conclusion it should be noted that workers at the University of Massachusetts and the Plastics Division, Monsanto Chemical Company, have used essentially the same concepts to develop a theory similar to the one presented here.⁷ They included the concept of a limiting fraction of crystallinity, while the theory in this paper allows the crystallization to go to completion. They fitted the theory to the crystallization of polypropylene and found that, in the terminology of this paper, $m = 3.9$, $n = 1.8$. If this relatively large value of n is found to obtain in many polymer crystallizations, the simplified eq. (7) unfortunately may not be as useful as originally was hoped.

The author wishes to express his gratitude to Dr. C. Muckenfass for much helpful discussion during the course of this work and Miss A. D. Warner for setting up the computer program.

References

1. Mandelkern, L., *Chem. Revs.*, **56**, 903 (1956); L. Mandelkern, F. A. Quinn, and P. J. Flory, *J. Appl. Phys.*, **25**, 830 (1954).
2. Avrami, M., *J. Chem. Phys.*, **7**, 1103 (1939); *ibid.*, **8**, 212 (1940).
3. Evans, U. R., *Trans. Faraday Soc.*, **41**, 365 (1945).

4. Fry, T. C., *Probability and Its Engineering Uses*, Van Nostrand, New York, 1928, pp. 220-227.
5. Poisson, S. D., *Probabilité des Jugements en Matière criminelle et en Matière civile*, Paris, Bachlier, 1837, p. 206.
6. Pearson, K., *Tables of Incomplete Γ -Functions*, Office of Biometrika, London, 1934.
7. Hoshino, S., E. Meinecke, J. Powers, S. Newman, and R. S. Stein, *J. Polymer Sci.*, in press.

Résumé

On présente une théorie qui tient compte de deux étapes qui ont lieu pendant la cristallisation des polymères en bloc. La théorie admet que toute la cristallisation a lieu à l'intérieur des sphérulites mais que le taux de cristallinité à un point particulier à l'intérieur d'un sphérulite dépend du vieillissement de ce point particulier. On montre que ces hypothèses conduisent à des courbes de transformation qui ressemblent à celles des cristallisations de polymères.

Zusammenfassung

Eine Theorie, welche die beiden bei der Kristallisation von Polymeren in Substanz auftretenden Stufen berücksichtigt, wird vorgelegt. In der Theorie wird angenommen, dass die gesamte Kristallisation innerhalb der Sphärolithe verläuft und dass der Betrag an Kristallinität an einem bestimmten Punkt innerhalb des Sphärolithen vom Alter dieses Punkts abhängt. Es wird gezeigt, dass diese Annahmen zu Umwandlungskurven führen, welche den bei der Polymerkristallisation tatsächlich auftretenden gleich sind.

Received November 23, 1964

Prod. No. 4654A

Surface Energetics, Adhesion, and Adhesive Joints.

IV. Joints between Epoxy Adhesives and Chlorotrifluoroethylene Copolymer and Terpolymer (Aclar)

H. SCHONHORN and L. H. SHARPE, *Bell Telephone Laboratories Incorporated, Murray Hill, New Jersey*

Synopsis

It is shown that structural joints can be formed between conventional epoxy adhesives and copolymer and terpolymer of chlorotrifluoroethylene, at temperatures well below the softening points of these polymers, without their prior surface treatment. An explanation of this low temperature behavior is given in terms of the surface tension of the adhesive, surface roughness, and the micro-Brownian motion of the polymers associated with the glass transition.

Recently, Schonhorn and Sharpe¹ demonstrated the feasibility of forming strong adhesive joints between a conventional epoxy adhesive and a fluorocarbon polymer well below the melting point of the fluorocarbon polymer without expensive and hazardous pretreatment of the polymer surface. This previously unreported low temperature behavior was dependent upon the surface tension of the epoxy adhesive and the micro-Brownian motion of the polymer associated with its glass transition.

This study, which deals with the formation of strong joints between chlorotrifluoroethylene copolymers and terpolymers and epoxy adhesives, is an extension of our previous work.^{1,2} A brief outline of the scope of the present paper is as follows.

The surface tensions of the epoxy adhesives used in preparing tensile shear specimens were varied by choosing two different curing agents, diethylaminopropylamine (DEAPA) and diethylenetriamine (DETA). The former imparts to the epoxy adhesive a surface tension of 32.9 dynes/cm. and the latter 44.0 dynes/cm. The effect on joint strength of lowering the surface tension of the epoxy adhesive containing the latter curing agent by addition of a fluorocarbon surfactant was also investigated. Further, joints in which the adhesive was allowed to set at room temperature were subsequently subjected to higher temperature cures to observe the effect of this procedure on strength. In addition, joints were prepared with polymer films which had previously been annealed, to study the effect of this variable on joint strength. Finally, the effect of gross surface roughness of the polymer on joint strength was investigated.

Experimental

The metal tensile-shear adherends were of 2024-T3 aluminum (Aluminum Co. of America). Their dimensions were $5 \times 1 \times 1/16$ in. The surface of the aluminum was prepared by first vapor-degreasing in trichloroethylene and then etching for 7 min. at 65°C. in the following solution: sodium dichromate ($\text{Na}_2\text{Cr}_2\text{O}_7 \cdot 2\text{H}_2\text{O}$), 1 part (by weight); water, 30 parts; sulfuric acid (95%), 10 parts.

After etching, the specimens were rinsed for 5 min. in running tap water and for 1 min. in running distilled water, and then dried in a forced air oven at 60°C. Specimens were stored in desiccators over Ascarite and removed just prior to use. For the measurement of tensile shear strengths, standard composite test pieces consisting of aluminum-epoxy adhesive-polymer sheet-epoxy adhesive-aluminum were prepared for bonding in a special device designed to maintain a $1/2$ -in. overlap. The thickness of the epoxy adhesive was maintained constant by insertion of a piece of 0.003-in. diameter gold wire in each glue line between the aluminum and the polymer. Clean gloves and tweezers were used in all specimen preparations to avoid possible contamination. Bonding was accomplished, at approximately 20 psi pressure, by placing stacks of composites in forced air ovens at specified temperatures for 16 hr. The bonded specimens were tested in tensile shear in accordance with ASTM D1002-53T, except that the strain rate was 0.1 in./min.

A DuNouy tensiometer was used to measure the surface tension of the epoxy resin and curing agent. The instrument was calibrated with water and benzene. Prior to each determination, the surface tension of water was measured. Mixtures of the epoxy resin and curing agent were equilibrated for a few minutes after mixing before the surface tension was determined. Since the mixtures had high viscosities, the DuNouy ring was equilibrated in the surface of the liquid for a few minutes at a stress several tenths of a dyne below the point of maximum stress, to permit the material to relax. The break point was approached slowly until rupture occurred. Three readings were taken for each mixture. Deviations of the order of ± 0.2 dyne/cm. or less were obtainable by this procedure. The surface tensions were calculated by using the appropriate correction parameter of Harkins and Jordan.³

The polymers employed in the present investigation were Aclar 22A and 22C and Aclar 33A* and 33C supplied in 0.005 in. thickness by the General Chemical Division, Allied Chemical Corporation, Morristown, New Jersey. Prior to adhesive bonding these materials were solvent-wiped with trichloroethylene to remove surface dust and any obvious contamination. The Aclar 22 material is a copolymer of chlorotrifluoroethylene and vinylidene fluoride. The composition of this copolymer is somewhat different from the Kel-F 82 which was investigated earlier.¹ The Aclar 33 material is a terpolymer of chlorotrifluoroethylene, vinylidene fluoride, and tetra-

* Not a standard product.

fluoroethylene. Both the copolymers and the terpolymers contained about 95% chlorotrifluoroethylene. The designations A and C refer to primarily amorphous and primarily crystalline forms of the polymers. The amorphous materials were about 25% crystalline and were clear. The crystalline materials were about 60% crystalline and slightly hazy.

The adhesive joints were prepared at elevated temperatures (ultimate temperature) for 16 hr. and tested at room temperature. The room temperature specimens were cured for one week to allow the epoxy adhesive to reach a reasonable degree of cure. Reproducibility of joint strengths was approximately $\pm 15\%$.

Results and Discussion

Figures 1 and 2 present data for the joint strength of composites consisting of aluminum-epoxy adhesive-fluorocarbon polymer-epoxy adhesive-aluminum. The epoxy resin was a pure diglycidyl ether of bisphenol A which had been used previously.^{1,2} This resin was cured with DEAPA in a ratio of 100 parts by weight resin to 7 parts by weight of curing agent. Maxima lower in value and broader than those obtained with the Kel-F materials are noted. The initial rise in joint strength is due to the onset of micro-Brownian motion in the polymers which is associated with their glass transition. Increased motion in the polymers aids in achieving ex-

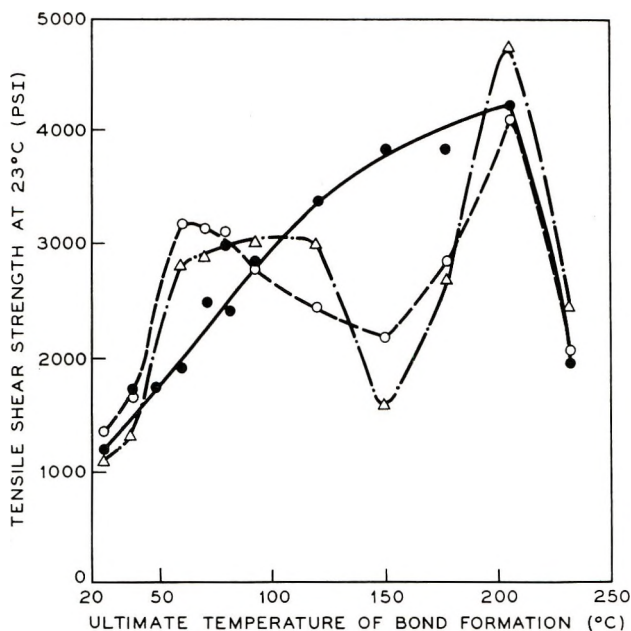


Fig. 1. Tensile shear strength of lap shear composites consisting of aluminum-(epoxy resin + DEAPA)-fluorocarbon polymer-(epoxy resin + DEAPA)-aluminum, plotted as a function of the ultimate temperature of joint formation: (●) aluminum-epoxy adhesive-aluminum composite; (O) Aclar 22A in the composite; (Δ) Aclar 22C in the composite.

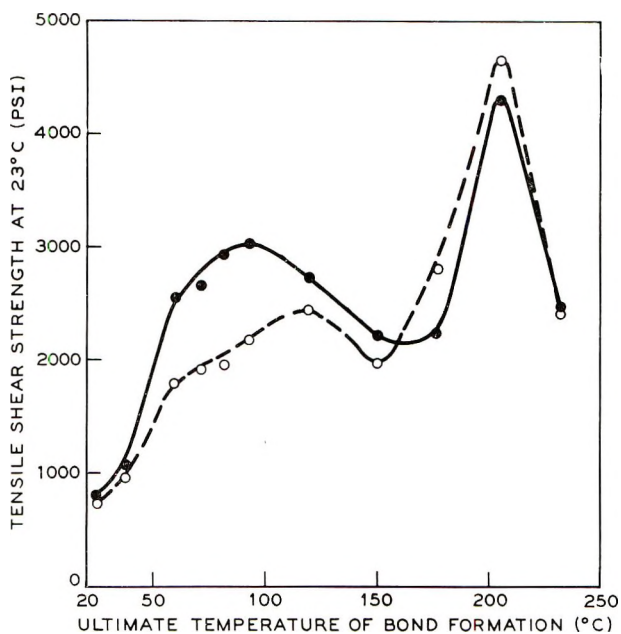


Fig. 2. Tensile shear strength of lap shear composites consisting of aluminum-(epoxy resin + DEAPA)-fluorocarbon polymer-(epoxy resin + DEAPA)-aluminum, plotted as a function of the ultimate temperature of joint formation: (●) Aclar 33A in the composite; (○) Aclar 33C in the composite.

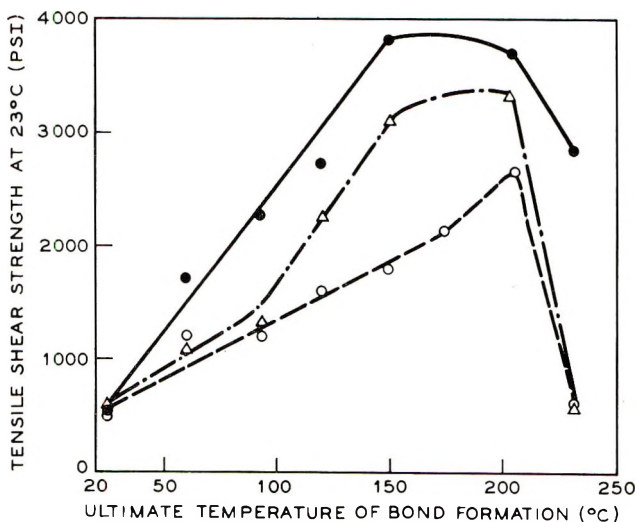


Fig. 3. Tensile shear strength of lap shear composites consisting of aluminum-(epoxy resin + DETA)-fluorocarbon polymer-(epoxy resin + DETA)-aluminum, plotted as a function of the ultimate temperature of joint formation: (●) aluminum-epoxy adhesive-aluminum composite; (Δ) Aclar 22A in the composite; (○) Aclar 22C in the composite.

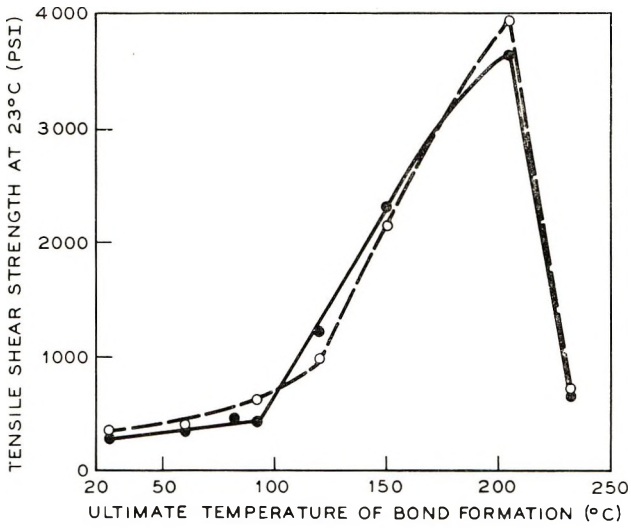


Fig. 4. Tensile shear strength of lap shear composites consisting of aluminum-(epoxy resin + DETA)-fluorocarbon polymer-(epoxy resin + DETA)-aluminum plotted as a function of the ultimate temperature of joint formation: (●) Aclar 33A in the composite; (○) Aclar 33C in the composite.

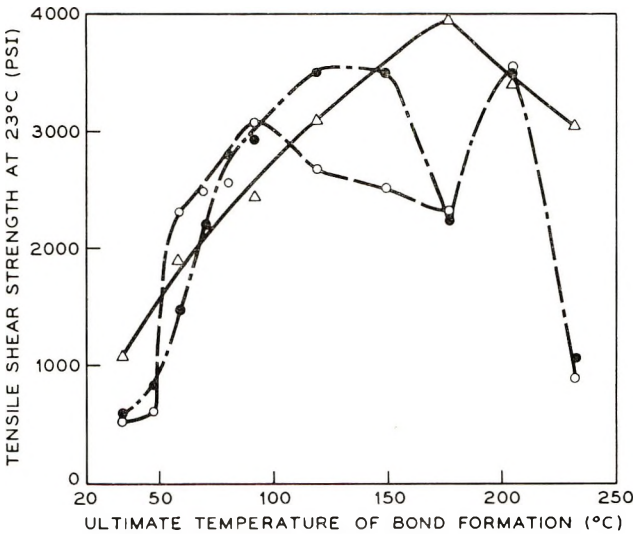


Fig. 5. Tensile shear strength of lap shear composites consisting of aluminum-(epoxy resin + DETA + 0.1% L-1074 fluorocarbon surfactant)-fluorocarbon polymer-(epoxy resin + DETA + 0.1% L-1074 fluorocarbon surfactant)-aluminum plotted as a function of the ultimate temperature of joint formation: (Δ) aluminum-(epoxy resin + DETA + 0.1% L-1074 fluorocarbon surfactant)-aluminum composite; (○) Aclar 22A in the composite; (●) Aclar 22C in the composite.

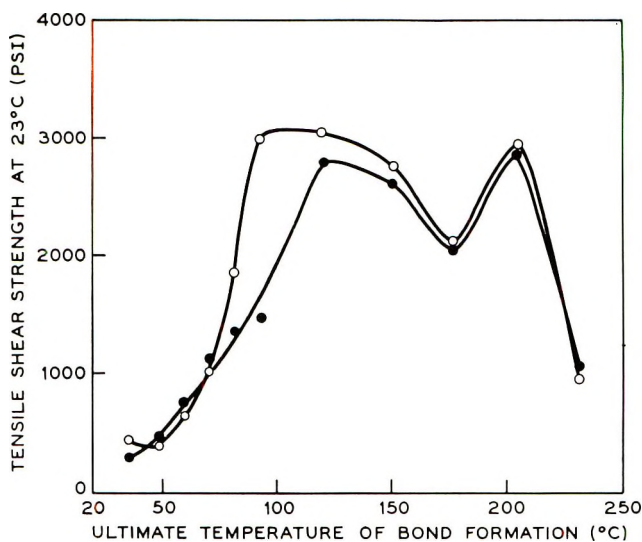


Fig. 6. Tensile shear strength of lap shear composites consisting of aluminum-(epoxy resin + DETA + 0.1% L-1074 fluorocarbon surfactant)-fluorocarbon polymer-(epoxy resin + DETA + 0.1% L-1074 fluorocarbon surfactant)-aluminum plotted as a function of the ultimate temperature of joint formation: (O) Aclar 33A in the composite; (●) Aclar 33C in the composite.

tensive and proper interfacial contact resulting in stronger adhesive joints. The kinetics of this process will be deferred to a subsequent publication.⁴

The importance of the surface tension of the liquid epoxy adhesive is demonstrated in Figures 3 and 4, where the same epoxy resin but a different curing agent, DETA, was used. As we stated earlier, the surface tension of the DETA adhesive is considerably higher than the DEAPA adhesive. Because of this, the DETA adhesive wets the polymer surface less extensively than the other, and the micro-Brownian motion of the fluorocarbon polymer is insufficient to heal the interface. The low temperature maximum, therefore, is absent, and a low joint strength is observed until the melting region of the polymer is approached. Then the macromotion of the thermoplastic polymers causes them to achieve the extensive and proper interfacial contact with the cured epoxy which results in strong adhesive joints.^{1,2} The micro-Brownian motion associated with the glass transition should aid in the formation of strong joints with all thermoplastic polymers that have their T_g in a favorable region. That the surface tension of the epoxy adhesive is an important factor is evident from the comparison of data when the resin is cured with DEAPA and DETA. The low surface tension of the epoxy resin-DEAPA adhesive enables it to approximate better the microscopic surface roughness of the thermoplastic polymers. The contact angles of this epoxy adhesive on the as-received surfaces of the fluorocarbon polymers are about 25° at 25°C . as measured with a Gaertner contact angle goniometer. When the epoxy resin is mixed with DETA,

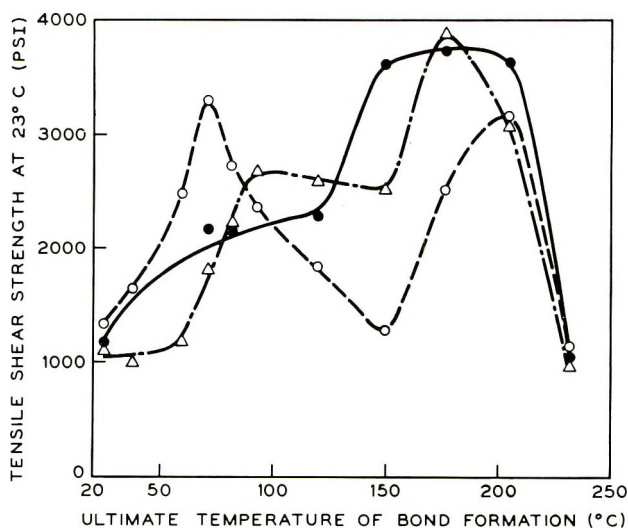


Fig. 7. Tensile shear strength of lap shear composites consisting of aluminum-(epoxy resin + DEAPA)-fluorocarbon polymer-(epoxy resin + DEAPA)-aluminum plotted as a function of the ultimate temperature of joint formation: (●) aluminum-(epoxy resin + DEAPA)-aluminum composite; (O) Aclar 22A in the composite; (Δ) Aclar 22C in the composite. The joints were cured at room temperature for 7 days prior to being subjected to elevated temperatures.

the contact angles rise to about 50° , indicating that this adhesive has a tendency to less conformity to the polymer surface than the DEAPA-cured adhesive. The increase in the mobility of the fluorocarbon polymers at and above their glass transition temperatures is apparently not sufficient to bridge the gaps in enough areas to result in strong joints. As we reported previously,¹ a fluorocarbon surfactant (L-1074, Minn. Mining and Mfg. Co.) was added in the amount of 0.1% by weight to the mixture of epoxy resin-DETA to reduce the surface tension to 28 dynes/cm. This epoxy adhesive spreads on the Aclar films. Figures 5 and 6 depict the effect of this additive on the joint strengths of the lap shear composites. A low temperature maximum is in evidence where none existed before. The lowering of the surface tension of the DETA system causes it to behave in a manner similar to the DEAPA system. It should be repeated that nowhere in these investigations were the surfaces of the fluorocarbon polymers altered chemically in any manner prior to the forming of the joint.

As we noted in a previous publication,¹ the low temperature maximum is followed by a decrease in joint strength which was postulated to be a consequence of setting of the epoxy adhesive before sufficiently extensive interfacial contact had occurred. Subsequently we observed a marked decrease in the mechanical strength of the free fluorocarbon films when they were subjected to temperatures in the neighborhood of 150°C . This prompted a re-examination of the nature of the minima in the tensile shear strength at these intermediate temperatures. Accordingly, a series of

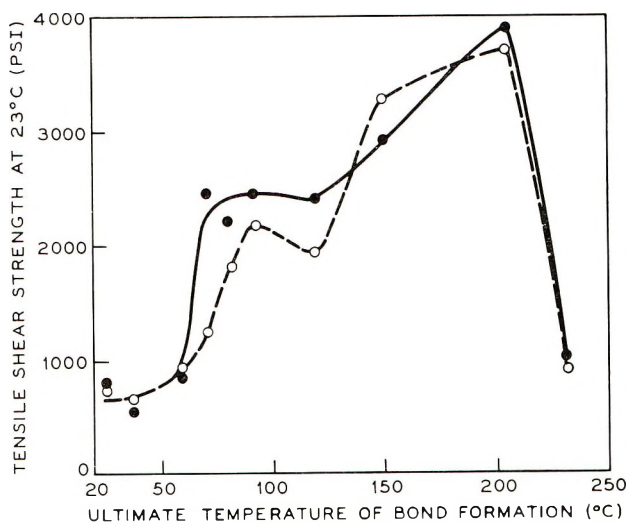


Fig. 8. Tensile shear strength of lap shear composites consisting of aluminum-(epoxy resin + DEAPA)-fluorocarbon polymer-(epoxy resin + DEAPA)-aluminum plotted as a function of the ultimate temperature of joint formation. (●) Aclar 33A in the composite; (○) Aclar 33C in the composite. The joints were cured at room temperature for 7 days prior to being subjected to elevated temperatures.

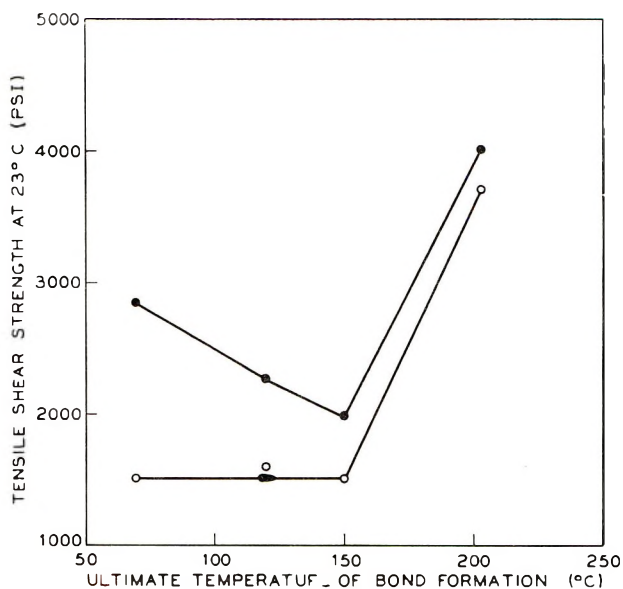


Fig. 9. Tensile shear strength of lap shear composites consisting of aluminum-(epoxy resin + DEAPA)-fluorocarbon polymer-(epoxy resin + DEAPA)-aluminum plotted as a function of the ultimate temperature of joint formation: (○) Aclar 22A in the composite; (●) Aclar 22C in the composite. The fluorocarbon polymer films were annealed at 150°C. for 1 hour prior to adhesive bonding.

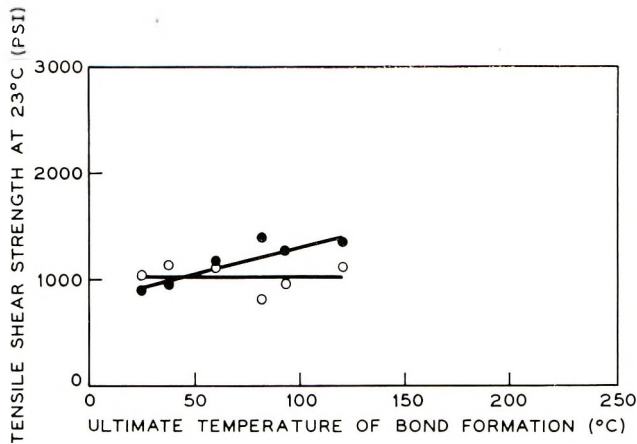


Fig. 10. Tensile shear strengths of lap shear composites consisting of aluminum (epoxy resin + DEAPA)-abraded fluorocarbon polymer-(epoxy resin + DEAPA)-aluminum plotted as a function of the ultimate temperature of joint formation: (O) Aclar 22A in the composite; (●) Aclar 22C in the composite. The fluorocarbon polymers were scraped with a razor blade to produce a roughened surface prior to adhesive bonding.

Aclar 22A and C and Aclar 33A and C specimens were bonded with the epoxy-DEAPA adhesive and allowed to cure at room temperature for one week. They were then subjected to elevated temperatures for 16 hr., brought back to room temperature, and their strengths measured. The results of this experiment are presented in Figures 7 and 8. The minimum still is evident though, in certain cases, it is not as pronounced. Further, joints formed at the temperature of the first maximum for 16 hr. and then subjected to 150°C. for 16 hr. show only a relatively small (< 10%) decrease in strength from that at the maximum. In addition, joints formed with 22A films which are first heated at 150°C. for 30 min. prior to adhesive bonding (Fig. 9) do not show a low temperature maximum but, rather, a plateau, at relatively low strengths, which changes into the normal maximum in the melting region of the fluorocarbon polymers.

The manufacturers's information indicates that the A form of these films, in particular, tends to expand significantly in one dimension and shrink in the orthogonal dimension quite rapidly at 150°C. The severe wrinkling of such films when they are heat treated reveals this dimensional instability. The C form of these films is far more dimensionally stable than the A form. This is revealed by lack of wrinkling of heat-treated, C-type films and, in addition, by the much shallower minima in the curves for these films (except in the case of Figure 1, for which we have no explanation).

It appears, then, that what is lowering the joint strength in the intermediate temperature region is the recrystallization of the fluorocarbon polymer, causing both dimensional changes in the polymer film which induce internal stresses in the joint, and a lowering of the mechanical strength of the polymer film itself.

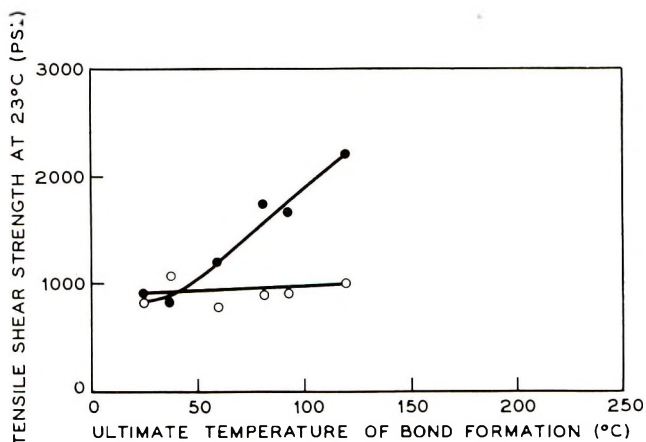


Fig. 11. Tensile shear strength of lap shear composites consisting of aluminum-(epoxy resin + DEAPA)-abraded fluorocarbon-(epoxy resin + DEAPA)-aluminum plotted as a function of the ultimate temperature of joint formation: (O) Aclar 33A in the composite; (●) Aclar 33C in the composite. The fluorocarbon polymers were scraped with a razor blade to produce a roughened surface prior to adhesive bonding.

An attempt was made to moderate these effects by employing a less rigid adhesive. For this purpose a formulated commercial resin, containing a conventional bisphenol A-epichlorohydrin resin, allyl glycidyl ether, poly(vinyl acetate), and Asbestine as a filler and cured with DETA was employed. The surface tension of this mixture could not be measured accurately because of its extremely high viscosity. Our results show a rise in joint strength as the temperature increases, the rise beginning at a significantly higher temperature than for the pure epoxy resin-DEAPA system, then becoming a plateau. No minimum is observed. A more comprehensive study of this and another adhesive system is given elsewhere.⁴

To test the effect of surface roughness on the formation of strong adhesive joints with these fluorocarbon polymers, specimens of the copolymers and terpolymers were scraped with a razor blade to produce a roughened surface. They were then joined with the epoxy resin-DEAPA adhesive system in the form of lap shear composites. The results (Figs. 10 and 11) show very low joint strengths and no low temperature maximum. Therefore, although both the micromotion of the polymers and the low surface tension of the adhesive are operative, the roughness of the polymers evidently is sufficient to prevent the formation of joints equivalent in strength to those formed with the unroughened polymers. The roughened surface apparently, in these experiments, precludes the achievement of extensive and proper interfacial contact.

Conclusions

The results presented here quite dramatically demonstrate the influence of bulk properties of a polymeric substrate upon the making of an adhesive

joint, and particularly upon the achievement of the intrinsic load-bearing capability of that joint. The results further indicate the importance of studying the formation of an adhesive joint over a range of temperature. Quite erroneous conclusions regarding the bondability of the systems here described could have resulted from a study of joint formation at a single temperature.

Specifically, the importance of the effect of the motion associated with the glass transition is readily apparent from the joint strengths at the low temperature maxima. This effect, moreover, is not limited to this system. We have observed similar behavior in systems involving poly(vinyl acetate), poly(vinyl butyral), and poly(vinyl formal).⁴ That the adhesive should form a very small or zero contact angle with the adherend is also quite evident from the results presented in this paper. It is also quite evident that deliberate roughening of the polymer substrate can overshadow wettability and glass transition effects and result in a weak joint.

The authors gratefully acknowledge the assistance of Messrs. D. Maccia and F. W. Ryan in the experimental phase of this work.

References

1. Schonhorn, H., and L. H. Sharpe, *J. Polymer Sci.*, **B2**, 719 (1964).
2. Sharpe, L. H., and H. Schonhorn, *Advan. Chem. Ser.*, **43**, 189 (1964).
3. Harkins, W. D., and H. F. Jordan, *J. Am. Chem. Soc.*, **52**, 1751 (1930).
4. Schonhorn, H., and L. H. Sharpe, to be published.

Résumé

On montre que des joints de structure peuvent se former entre les adhésifs conventionnels du type époxy et le copolymère et le terpolymère du chlorotrifluoroéthylène, à des températures bien inférieures aux points de ramolissement de ces polymères, sans traitement préalable de leur surface. Une explication de ce comportement à basse température est donnée en termes de tension superficielle de l'adhésif, de rugosité de la surface et du mouvement micro-Brownien des polymères associés à la transition vitreuse.

Zusammenfassung

Es wird gezeigt, dass zwischen konventionellen Epoxyadhäsiven und Chlortrifluoräthylenco- sowie-terpolymeren bei Temperaturen weit unterhalb des Erweichungspunkts dieser Polymeren ohne vorhergehenden Oberflächenbehandlung strukturelle Verbindungen gebildet werden können. Eine Erklärung dieses Tieftemperaturverhaltens wird anhand der Oberflächenspannung des Adhäsivs, der Oberflächenrauigkeit und der mit der Glasumwandlung verknüpften Mikro-Brown'schen Bewegung gegeben.

Received November 16, 1964

Revised March 2, 1965

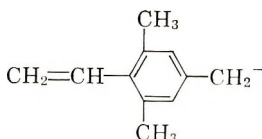
Prod. No. 4686A

Anionic Polymerization of Vinylmesitylene

D. N. BHATTACHARYYA, J. SMID, and M. SZWARC,
*Department of Chemistry, State University College of Forestry
 at Syracuse University, Syracuse, New York*

Synopsis

Anionic polymerization of vinylmesitylene was investigated in THF (counterion Na^+) at temperatures ranging from $+25^\circ$ to -70°C . The homopropagation is slow ($k_p \sim 1$ l./mole-sec. at 25°C .), indicating the basically low reactivity of the monomer. Studies of conductivity and the retardation of the polymerization by the addition of $\text{Na}^+\text{BPh}_4^-$ demonstrate that free ions and ion pairs participate in the process. At 25°C . the k_p of the free ion appears to be about 1000 times greater than that of ion pair. The outstanding feature of the polymerization is the proton transfer from the monomer to living end, producing an inert ion



(or its isomer) which does not propagate. This reaction leads to retardation of the polymerization. Its contribution decreases on lowering the temperature, and the effect of $\text{Na}^+\text{BPh}_4^-$ indicates that the free ion, and not the ion-pair, acts as a base in the proton transfer.

Anionic homopolymerization of vinylmesitylene (VM) exhibits some interesting features deserving discussion. The "living" polyvinylmesitylene is prepared by adding a THF solution of the monomer to a THF solution of low molecular weight "living" polystyrene (Na^+ counterion), and usually about 20 units of monomer are polymerized on each living end. It is essential to carry out the reaction at about -25°C ., the process being performed on a high vacuum line, with continuous magnetic stirring of the reagents.

The resulting solution is yellow, its absorption spectrum shows one fairly sharp peak at $\lambda_{\text{max}} = 360 \text{ m}\mu$ with a small inflection at $435 \text{ m}\mu$. At room temperature the solution is relatively stable, although a slight increase of optical density at $435 \text{ m}\mu$ is noticed after 24 hr. Therefore, the preparation should be kept in a freezer if stored for several days.

The initiation with living α -methylstyrene oligomer is not recommended because the reaction is extremely slow. The reaction with metallic sodium

is even slower, whereas the initiation with metallic potassium leads to some unknown side reactions resulting in partial precipitation.

The solution of living polyvinylmesitylene conducts and the equivalent conductivity was determined for $5 \times 10^{-3}M$ solution at temperatures ranging from $+30$ to -98°C . The results are given in Figure 1. The shape of the curve is not unusual—the degree of dissociation increases with decreasing temperature, but so does the viscosity of the solvent (Fig. 2); and therefore, the equivalent conductivity passes through a maximum.

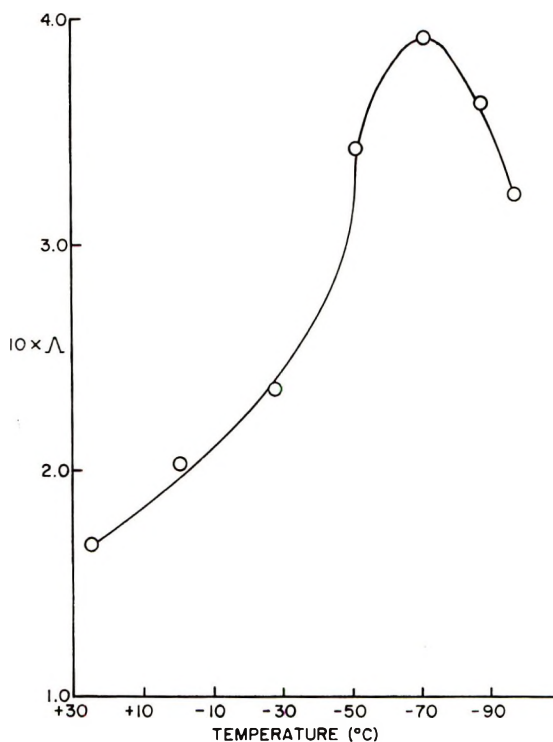


Fig. 1. Dependence of the equivalent conductance of living polyvinylmesitylene on temperature THF.

The above results demonstrate that free $\sim\text{VM}^-$ ions, as well as ion pairs, are present in solution. Since the equivalent conductivity of polyvinylmesitylene at 25°C . is 2.2 times lower than that of living polystyrene,^{1,2} ($K_{\text{Diss}} = 1.5 \times 10^{-7}$ mole/l.) the dissociation constant of $\sim\text{VM}^-$, Na^+ is about 5 times smaller than that of living polystyrene.

The kinetics of homopolymerization of living polyvinylmesitylene was investigated by removing aliquots from a polymerizing solution and determining by vapor-phase chromatography the concentration of the residual monomer after quenching of the reaction. A typical plot of $\log(C_0/C_t)$ versus time is shown in Figure 3. The observed curve shows that the re-

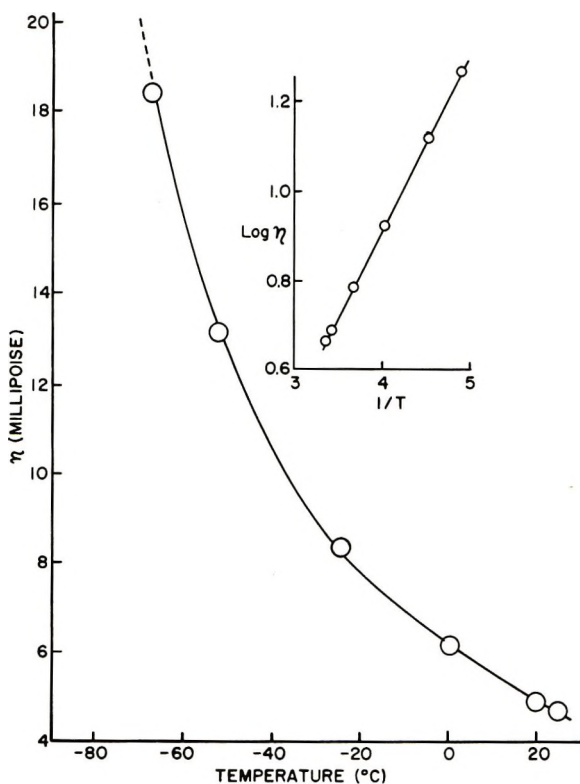
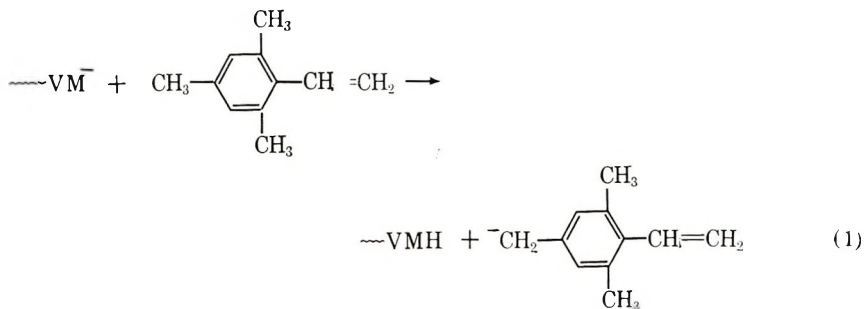


Fig. 2. Temperature dependence of THF viscosity.

action becomes increasingly retarded as the conversion proceeds. This phenomenon seems to be due to a proton transfer from the monomer to a living end (LE) as shown by eq. (1).



The resulting anion appears to be inert, and apparently it does not propagate the polymerization. This suggestion is supported by the appearance in the polymerized solution of a new absorption peak at 435 μ and remains

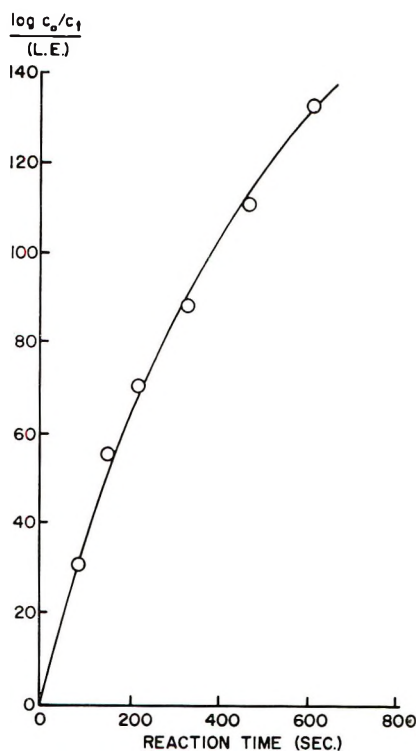
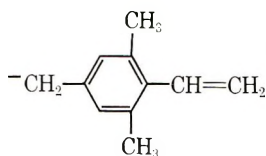


Fig. 3. Polymerization of living polyvinylmesitylene at 25°C. in THF (Na⁺).

constant after completion of the reaction. We are inclined to attribute this peak to ions of the type



The kinetic results are given in Table I. The retardation of the poly-

TABLE I
Homopolymerizations of Vinylmesitylene in THF
($T = 25^\circ\text{C}.$; Counterion Na⁺)

[LE] × 10 ³ mole/l.	[Monomer] × 10 ³ , mole/l.	Conversion, %	k_p , l./mole-sec.
1.0	1.8	7-32	1.03
3.0	60.4	24-73	0.85
3.0	6.3	28-67	0.91
4.2	5.4	24-67	0.84
4.4	69.4	29-75	0.85

merization hampers the determination of the correct values of the individual k_p 's, and this difficulty may account for their apparent constancy at different concentration of living ends.

On addition of a threefold excess of Na^+ , BPh_4^- , which is about 100 times more dissociated³ than the living ends, the rate constant of propagation decreases to 0.15 l./mole-sec., i.e., by a factor of about 6 (see Table II). Accepting K_{Diss} of $\sim\text{VM}^-$, Na^+ to be 3×10^{-8} mole/l. and con-

TABLE II
Effect of NaB(Ph)_4 on Homopropagation of Vinylmesitylene at Different Temperatures

Temp., °C.	NaB(Ph)_4 added, mole/l.	$[\text{LE}] \times 10^3$, mole/l.	$[\text{Monomer}] \times$ 10^3 , mole/l.	Conversion, %	k_p , l./mole-sec.
25	0	4.02	10.40	31-62	0.84
25	10^{-2}	3.5	10.3	2-33	0.15
0	10^{-2}	3.5	10.2	9-49	0.15 ^a
-25	10^{-2}	3.3	10.5	11-59	0.15 ^a
-65	10^{-2}	3.8	10.8	12-77	0.23 ^a

^a The contribution of free ions at lower temperatures is probably considerable. Hence, k_p of ion pairs is lower than indicated by the data of Table II.

sidering the value 0.15 l./mole-sec., given in Table II, as the propagation constant of ion pairs at 25°C., we calculate the propagation constant of the free $\sim\text{VM}^-$ ion to be about 250 l./mole-sec. It seems that the free ion is about 1000 times more reactive than the $\sim\text{VM}^-$, Na^+ ion pair—a result resembling that observed for the living polystyrene system (at 25°C. the free ion is 800 times more reactive than $\sim\text{S}^-$, Na^+ ion pair^{2,4,5}).

The temperature dependence of the overall k_p is given in Table III.

TABLE III
Effect of Temperature on k_p of Homopropagation of Vinylmesitylene in THF

Temp., °C.	$[\text{LE}] \times 10^3$, mole/l.	$[\text{Monomer}] \times$ 10^3 , mole/l.	Conversion, %	k_p , l./mole-sec.
25	3.0	6.3	28-67	0.91
0	3.1	14.6	25-62	0.91
-35	3.3	14.1	38-78	0.92
-70	3.4	13.9	29-84	0.93

The apparent activation energy is zero; however, since the degree of dissociation increases on lowering the temperature such a result is not surprising. In fact, by applying the Walden rule, we calculate Λ_0 at -70°C. to be 15 cm.²/ohm-equiv. (at 25°C., $\Lambda_0 = 64$ cm.²/ohm-equiv.), and therefore the dissociation constant increases to $\sim 3 \times 10^{-6}$ mole/l. compared to 3×10^{-8} mole/l. at 25°C. The increase in the concentration of free ions is balanced by the decrease in their reactivity, and therefore k_p of the free ion apparently decreases by about one power of ten as the tem-

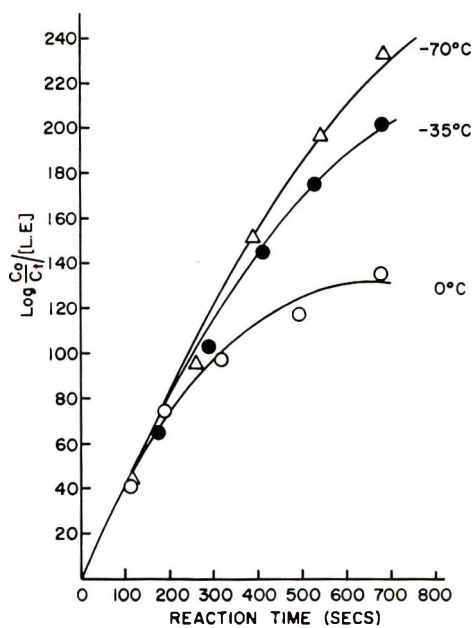


Fig. 4. Temperature effect on the propagation of living polyvinylmesitylene in THF (Na^+).

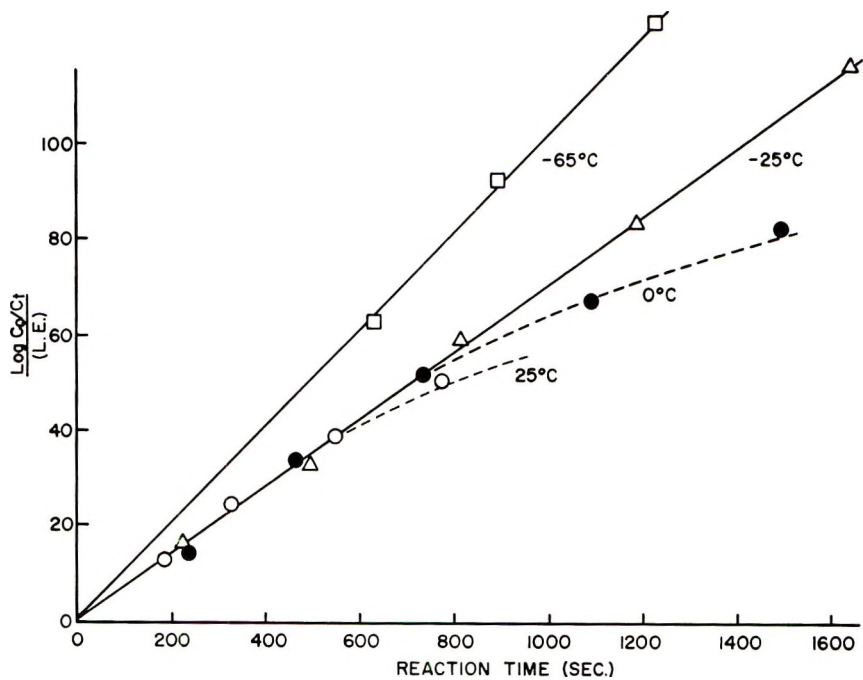
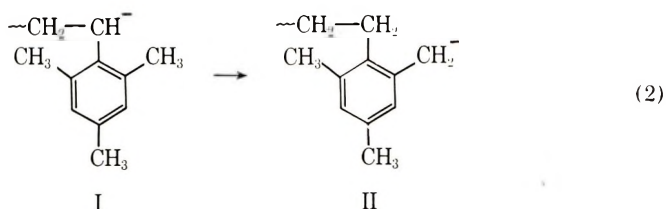


Fig. 5 Polymerization of living polyvinylmesitylene in THF in the presence of $\text{Na}^+ \text{BPh}_4^-$.

perature is lowered from +25 to -70°C . On this basis, the activation energy of propagation by the free $\sim\text{VM}^-$ ions is calculated to be about 3 kcal./mole. This value appears to be too low, i.e., the activation energy of propagation of a free $\sim\text{styryl}^-$ ion was found to be about 4–5 kcal./mole.⁶ At this stage we cannot offer any explanation for this behavior (see, however, the last paragraph of this paper).

The retardation of vinylmesitylene polymerization was attributed to a proton transfer from the monomer to the growing end [eq. (1)]. As may be seen from Figures 4 and 5, reaction (1) must have a higher activation energy than the overall propagation, since the degree of retardation diminishes at lower temperatures. Because the significance of reaction (1) diminishes as the temperature is lowered, the preparation of the polymer also has to be performed at low temperatures, as recommended earlier. Notice in Figure 5 that the retardation seems to disappear on addition of $\text{Na}^+\text{BPh}_4^-$. This indicates that only the free ions may abstract the protons.

An intramolecular proton-transfer reaction (2) is also possible. It seems



that the less stable ion (I) formed in propagation isomerizes into a more stable primary carbanion (II). Two observations support this suggestion: (1) a slight shift in the absorption spectrum of living polymer ($\lambda_{\text{max}} = 360 \text{ m}\mu$ changes into $\lambda_{\text{max}} = 350 \text{ m}\mu$) is observed when its solution is left at room temperature for about 12 hr.; (2) the conductivity of an aged solution of living polyvinylmesitylene decreases slightly on addition of monomer and thereafter the conductivity increases slowly over a period of a few hours, long after completion of the polymerization. It seems that the ion pair derived from carbanion (II), present in the aged solution, is more ionized than the ion pair derived from (I). Since the latter is formed on the addition of the monomer, the conductivity is expected to decrease at the beginning of polymerization. A slow proton transfer [reaction (2)] reforms the original species, therefore increasing the conductivity.

Existence of various ions could distort our determination of the ionization constant and this could contribute to the apparently low activation energy of propagation by the free ion.

We acknowledge the financial support of this study by the National Science Foundation.

References

1. Worsfold, D. J., and S. Bywater, *J. Chem. Soc.*, **1960**, 5234.
2. Bhattacharyya, D. N., C. L. Lee, J. Smid, and M. Szwarc, *J. Phys. Chem.*, **69**, 612 (1965).
3. Bhattacharyya, D. N., C. L. Lee, J. Smid, and M. Szwarc, *J. Phys. Chem.*, **69**, 608 (1965).
4. Bhattacharyya, D. N., C. L. Lee, J. Smid, and M. Szwarc, *Polymer*, **5**, 54 (1964).
5. Figini, R. V., H. Hostalka, and G. V. Schulz, *Makromol. Chem.*, **71**, 188 (1964).
6. Toelle, K. J., J. Smid, and M. Szwarc, unpublished results.

Résumé

On a étudié la polymérisation anionique di vinyl-mésitylène dans le THF (contre-ion Na^+) dans un domaine de températures situé entre $+25^\circ\text{C}$ et -70°C . L'homopropagation est lente ($k_p \sim 1$ l./mol. sec. à 25°C), ce qui montre la faible réactivité fondamentale du monomère. Des études de conductivité et de ralentissement de la polymérisation par l'addition de $\text{Na}^+\text{BPh}_4^-$ démontrent que des ions libres et des paires d'ions participent au processus. À 25°C , le k_p de l'ion libre semble être environ 1000 fois plus grand que celui de la paire d'ion. Le caractère dominant de la polymérisation est le transfert du proton du monomère sur l'extrémité vivante, ce qui fournit un ion inerte (Voir resume en anglais.) (ou son isomère) qui ne propage pas. Cette réaction conduit au ralentissement de la polymérisation. Sa contribution diminue par abaissement de la température et l'influence de $\text{Na}^+\text{BPh}_4^-$ indique que l'ion libre, et non la paire d'ion, agit comme une base dans le transfert protonique.

Zusammenfassung

Die anionische Polymerisation von Vinylmesitylen wurde in THF (Gegenion Na^+) bei Temperaturen von $+25^\circ\text{C}$ bis -70°C untersucht. Die Wachstumsreaktion verläuft langsam ($k_p \sim 1$ l Mol $^{-1}$ sec $^{-1}$ bei 25°C), was für eine grundsätzlichiuedripe Reaktivität des Polymeren spricht. Die Untersuchung der Leitfähigkeit und der Verzögerung der Polymerisation durch Zusatz von $\text{Na}^+\text{BPh}_4^-$ zeigt, dass an dem Prozess freie Ionen and Ionenpaare teilnehmen. Bei 25°C scheint k_p für das freie Ion etwa 1000 mal grösser zu sein als für das Ionenpaar. Die Besonderheit der Polymerisation ist der Protonentransfer vom Monomeren an das wachsende Ende, wobei ein inertes (oder sein someres)—Ion entsteht (Siehe englische Zusammenfassung.), welches nicht mehr wächst. Diese Reaktion führt zur Polymerisationsverzögerung. Ihre Bedeutung nimmt mit fallender Temperatur ab, und der Einfluss von $\text{Na}^+\text{BPh}_4^-$ zeigt, dass das freie Ion und nicht das Ionenpaar beim Protonentransfer als Base wirksam ist.

Received January 22, 1965

Prod. No. 4675A

Reaction of α, α -Diphenyl- β -Picrylhydrazyl with Acids

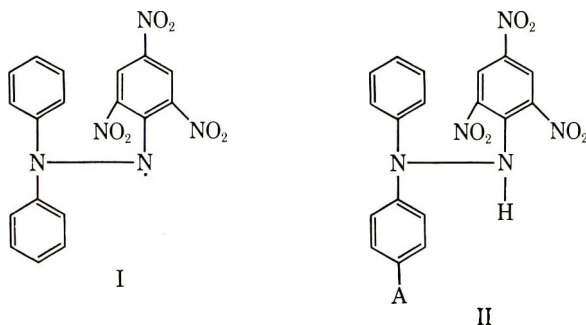
D. H. SOLOMON and JEAN D. SWIFT, *Division of Applied Mineralogy, C.S.I.R.O., Melbourne, Australia*

Synopsis

The action of dilute aqueous mineral acids on α, α -diphenyl- β -picryl hydrazyl (DPPH) has been studied and shown to result in the rapid loss of the characteristic color of the radical. Hydrobromic and hydrochloric acids yield α, α -diphenyl- β -picryl hydrazine (DPPH-H) and the corresponding halogen-substituted α, α -diphenyl- β -picryl hydrazine. Hydroiodic acid gives DPPH-H, iodine, and a small quantity of DPPH. A number of organic acids cause similar reactions. Kinetic studies on the hydrobromic acid system indicate that the reaction is first-order with respect to: hydrogen ion concentration, DPPH concentration, and anion concentration. The ability of the anion to undergo one-electron transfer and to dimerize are also important, and the strongest nucleophile gives the fastest reaction. A mechanism which involves ionic attack is proposed to account for the reaction of DPPH with acid. The limitations of DPPH in studying reaction mechanisms are then discussed in relation to the proposed ionic mechanism.

INTRODUCTION

The inhibiting action of the "stable" free radical α, α -diphenyl- β -picryl-hydrazyl (DPPH) (I) on a reaction or polymerization is generally taken as evidence supporting a free-radical mechanism.¹ Although DPPH is itself a radical, it is not sufficiently active to initiate most free-radical reactions or polymerizations but nevertheless reacts rapidly with radical intermediates.² As a tool for studying radical reactions DPPH is often preferred to the more conventional inhibitors such as phenols, quinones, and amines for a number of reasons. First, reaction of DPPH can be readily observed by loss of the characteristic violet color, and second, it reacts quantitatively with many radical intermediates and can, therefore, be used to count the radicals present,² and in some cases to measure the rate of formation of radical intermediates from, for example, polymerization initiators.



Reactions of DPPH with phenols,³⁻⁶ amines,^{3,7-8} hydroaromatic compounds,⁹ and mercaptans^{10,11} have also been reported, and such reactions generally lead to the formation of diphenylpicryl hydrazine (DPPH-H) (II, A = H).

In general, radical mechanisms involving hydrogen abstraction by DPPH have been invoked to explain such reactions, although McGowan et al.³ proposed an ionic mechanism involving hydride ions to explain certain phenol reactions. Hogg et al.,⁴ however, maintain that the phenol reaction is equally well explained by a radical mechanism.

During studies on the mechanism of polymerization of styrene on clay minerals, we noted that certain thermally activated "neutral" clays decolorize solutions of DPPH in organic solvents.¹² Details of this reaction will be reported later. However, certain structural features of the clays used suggested that "acidity" may be related to the reaction with DPPH. These observations led to the present study of the reaction of DPPH with acids.

EXPERIMENTAL

Melting points are uncorrected. Microanalyses were carried out by the C.S.I.R.O Microanalytical section. Cellulose columns were prepared from Whatman cellulose powder, standard grade. No. 1 Whatman paper was used for paper chromatography with *n*-hexane as solvent, while silica gel G (made according to Stahl by Merk) was used as the adsorbent for thin layer chromatography, with benzene-petroleum ether, b.p. 60-80°C. (17:5), as solvent.

Action of Bromine on DPPH

A solution of Br₂ in CHCl₃ was added to DPPH (0.400 g.) in CHCl₃ until a color change to red took place. The solution was washed with water and dried (anhydrous Na₂SO₄). The chloroform was removed by distillation under reduced pressure and the crude product (0.69 g.) dissolved in benzene and chromatographed on an alumina column. Elution with benzene gave α -(*p*-bromophenyl)- α -phenyl- β -picryl hydrazine (0.240 g.), m.p. 190-191°C., orange needles from chloroform.

Calculated for C₁₈H₁₂N₆O₆Br: C, 45.58%; H, 2.55%; N, 14.77%; Br, 16.86%. Found: C, 45.34%; H, 2.64%; N, 14.55%; Br, 16.7%.

Goldschmidt and Renn¹³ and other workers¹⁴ report m.p. 179-180°C.

The NMR spectrum is shown in Figure 1 and is that expected for a compound with this structure. It should be noted that this provides definite evidence for bromine in the *para* position. To obtain a satisfactory NMR spectrum it was necessary to use acetone as the solvent, and this has resulted in a displacement of the picryl group signal, (compare Fig. 2). Oxidation by PbO₂/Na₂SO₄ in benzene as described by Goldschmidt and Renn¹³ gave a typical violet color of a hydrazyl radical to the solution which gave an ESR signal similar to but not identical with that of DPPH.

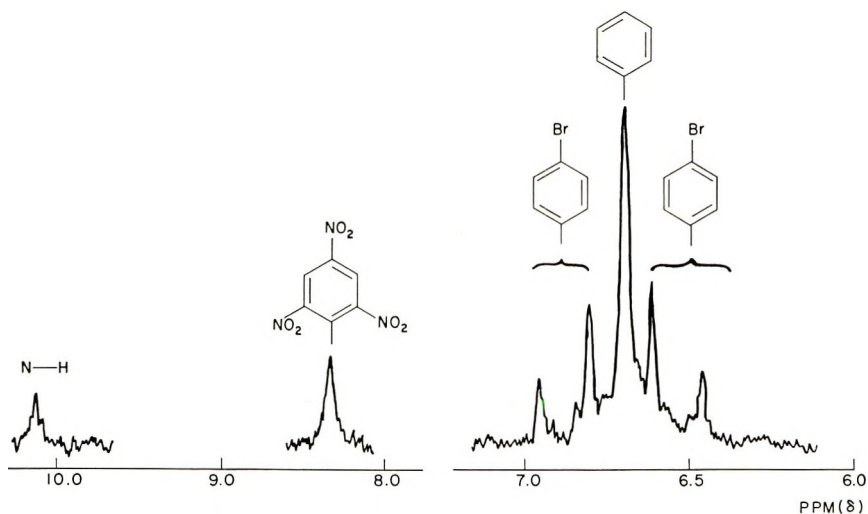


Fig. 1. NMR spectrum of α -(*p*-bromophenyl)- α -phenyl- β -picryl hydrazine in acetone, run at 60 Mcycles/sec. No other peaks were observed.

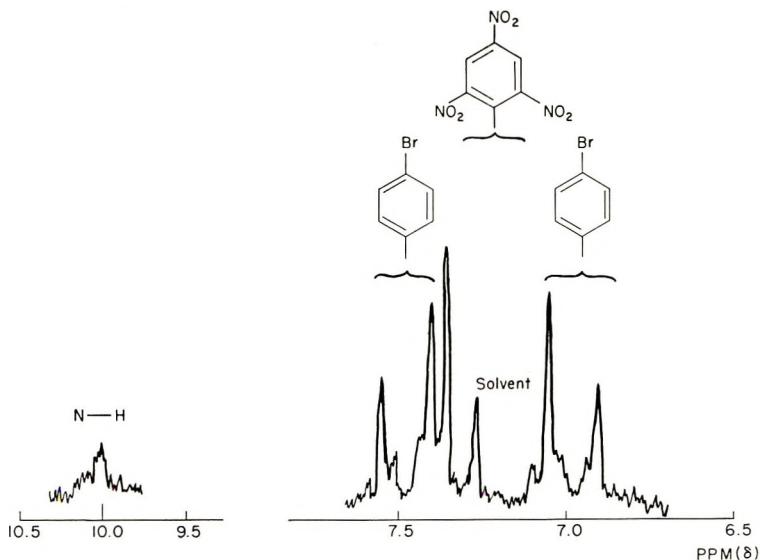


Fig. 2. NMR spectrum of α -bis(*p*-bromophenyl)- β -picryl hydrazine in deuteriochloroform, run at 60 Mcycles/sec. No other peaks were observed.

Further elution of the column with benzene gave a second product (0.120 g.) which after repeated recrystallization from chloroform-ethanol gave red plates, m.p. 107–109°C. The compound gave a positive test for bromine, and the NMR spectrum is shown in Figure 2.

Oxidation as above gave a violet color of a hydrazyl radical to the solution. The ESR signal was similar to but not identical with that of DPPH or the *p*-bromo radical. On this evidence we conclude the compound is α -bis(*p*-bromophenyl)- β -picryl hydrazine.

Action of HBr on DPPH

To a solution of DPPH (0.325 g., 8.25×10^{-4} mole) in benzene (100 ml.) was added dilute aqueous HBr. The violet color changed to yellow. After standing (1 hr.) the solution was washed with water (3×10 ml.), then with NaHCO_3 (2×10 ml.) and finally, with water (3×10 ml.). The benzene solution was dried (Na_2SO_4), filtered, and evaporated to dryness (0.364 g.).

The crude product was dissolved in benzene-petrol, b.p. 40–60°C. (20:80) and chromatographed on an alumina column. Elution with benzene gave DPPH-H (0.160 g., 4.06×10^{-4} mole), m.p. and mixed m.p. 172–173°C. from chloroform-ethanol. Infrared and NMR spectra were identical with those of an authentic specimen of DPPH-H.

Further elution with benzene gave α -(*p*-bromophenyl)- α -phenyl- β -picryl hydrazine (0.071 g., 1.5×10^{-4} mole) m.p. and mixed m.p. 190–191°C. from chloroform.

Paper and thin layer chromatography on the crude reaction mixture revealed only two products with R_f values corresponding to DPPH-H and (*p*-bromophenyl)phenylpicryl hydrazine. Therefore, no change had taken place during the separation on alumina. Quantitative separation by chromatography was exceedingly difficult, and an intermediate fraction eluted with benzene was shown to contain (*p*-bromophenyl)phenylpicryl hydrazine with some DPPH-H by paper chromatography.

Action of HCl on DPPH

Treatment of DPPH (0.250 g., 6.35×10^{-4} mole) with dilute aqueous HCl in a similar manner to that described above for HBr gave a crude reaction product (0.290 g.). Chromatography on an alumina column did not separate the mixture and caused the formation of additional products. This was demonstrated by comparative paper and thin layer chromatography. Paper and thin layer chromatography showed the main products to be DPPH-H and a number of compounds which correspond to those obtained by the action of Cl_2 on DPPH-H (see below). Chlorine analysis of the crude product was 3.98%, and this corresponds to a mixture of DPPH-H (54%) and monochlorodiphenylpicryl hydrazine (46%).

Action of HI on DPPH

DPPH (0.187 g., 4.75×10^{-4} mole) was treated with dilute aqueous HI as described above. The benzene solution was washed with water, NaHCO_3 , and water, and dried (Na_2SO_4). The aqueous washing gave a characteristic blue color when added to starch solution, indicating iodine. Titration of these washings with sodium thiosulfate (standardized with KIO_3) in the presence of excess KI with the use of starch solution as indicator showed them to contain iodine (0.0495 g. I_2). The benzene solution was shown to contain DPPH and DPPH-H by paper and thin layer chromatography. The DPPH was estimated colorimetrically (see below) and by ESR (0.004 g., 1.01×10^{-5} mole). Chromatography of the benzene

solution on an alumina column gave DPPH, m.p. and mixed m.p. 129–131°C. from chloroform–ether, after drying under vacuum. Further elution gave DPPH-H (0.155 g., 3.9×10^{-4} mole), m.p. and mixed m.p. 172–173°C. from chloroform–ethanol.

Calculated for $C_{18}H_{13}N_5O_6$: C, 54.7%; H, 3.3%; N, 17.5%. Found: C, 54.70%; H, 3.42%; N, 17.39%.

The yield of DPPH given by chromatography was low and can be related to reaction on the alumina, as shown by the formation of a number of colored bands and as previously observed by other workers.¹⁶

That DPPH results from and depends on the working-up procedure of the reaction mixture can be shown by paper and thin layer chromatography. No DPPH was detected before washing. The figures quoted above are those obtained from a typical reaction and working-up procedure. Variation in the working-up procedure can result in altered yields, particularly of DPPH.

Action of Other Acids on DPPH

Treatment of benzene solutions of DPPH (0.5 mg./ml.) with a few drops of the following acid: H_2SO_4 (2*M*), glacial acetic acid, acetic acid (2*M*), H_3PO_4 (concentrated), H_3PO_4 (dilute), formic acid, and oxalic acid caused decolorization to occur. Paper and thin layer chromatography showed that one of the products of each reaction had R_F values corresponding to those of DPPH-H.

Kinetic Studies

Preliminary measurements under an inert atmosphere gave substantially the same results as those obtained in the presence of oxygen, an observation previously noted by other workers.^{4,16–18} All subsequent experiments were conducted in the presence of air.

All optical density measurements were made on a Beckman DU spectrophotometer at a slit width of 0.05 mm. and a wavelength of 564 $m\mu$ at which it was shown that the products of the reaction had negligible absorption. The experiments were conducted at 20°C.

A number of solvent systems, varying from 50% aqueous acetone to acetone and alcohol, were evaluated to find a single-phase solvent system for both DPPH and the reaction products with acids. All of these systems were shown, by paper and thin layer chromatography, to give the same reaction products as in benzene. In order to have suitable reaction times, aqueous acetone–alcohol was eventually chosen.

The DPPH solution was added to the aqueous acid and optical density measured with respect to time. The effect of the concentration of DPPH, hydrogen ion, and anion with HBr is shown in Table I. Comparison of the reaction rates for HI, HBr, HCl, and H_2SO_4 and the effect of added salts is shown in Table II.

TABLE I
Effect of H⁺ Ion Concentration (with HBr) on Rate of Decolorization of DPPH^a

Time, min.	Concentration of DPPH × 10 ² , mg./ml. ^b	
	0.005 <i>N</i> HBr with large excess NaBr	0.010 <i>N</i> HBr with large excess NaBr
0	3.60	3.60
1	3.55	3.50
2	3.50	3.40
3	3.43	3.30
4	3.39	3.20
5	3.33	3.12
6	3.29	3.03
7	3.23	2.94
8	3.19	2.86
9	3.14	2.77
10	3.09	2.69
11	3.03	2.61
12	3.00	2.54
13	2.95	2.47
14	2.91	2.40
15	2.87	2.32
16	2.81	2.27
17	2.78	2.19
18	2.73	2.13
19	2.69	2.07
20	2.65	2.01

^a Plotting log [DPPH] against time gives a straight line for both concentrations; $d \log [\text{DPPH}]/dt = -0.0065$ in 0.005*N* HBr, -0.0129 in 0.010*N*/HBr; $d \log (\text{DPPH})/dt)/(\text{H}^+) = -1.3$ in 0.005*N*/HBr; -1.29 in 0.010*N*/HBr.

^b Solvent composition: acetone:alcohol:aqueous acid = 15:15:1.

Action of Halogens on DPPH-H

The reactions were studied under mildly acid conditions in the presence of the corresponding halogen acids. It was shown that no reaction took place between DPPH-H and the acids.

Action of I₂. To DPPH-H in benzene, a benzene solution of iodine was added. By paper and thin layer chromatography it was shown that DPPH is formed when this mixture is washed with water. No other product was found.

Action of Br₂. To DPPH-H in benzene a solution of Br₂ in benzene was added. Paper and thin layer chromatography showed the formation of α -(*p*-bromophenyl)- α -phenyl- β -picryl hydrazine and as reaction proceeded, a small amount of a hydrazyl or a substituted hydrazyl compound with a characteristic violet color.

It should be noted that this is a much preferred method for the preparation of α -(*p*-bromophenyl)- α -phenyl- β -picryl hydrazine than that used previously.^{13,14}

TABLE II
Effect of Type and Concentration of Anion on Rate of Reaction

Time, min.	Concentration of DPPH, $10^2 \times$ mg./ml. ^{a,b,c}						
	HI	HBr	HCl	HI ^d	HI/NaI ^{d,e}	HBr/ NaBr	HCl/ NaCl ^e
0	3.02	3.02	3.02	3.02	3.02	3.02	3.02
1	0.02	2.90		2.07	1.69	2.70	2.76
2		2.77	2.68	1.41	0.928	2.40	2.53
3		2.64	2.44	0.965	0.520	2.14	2.14
4		2.53	2.24	0.665	0.281	1.90	1.91
5		2.42	2.09	0.456	0.156	1.70	1.73
6		2.32	1.92	0.310		1.51	1.54
7		2.23	1.80	0.209		1.34	1.42
8		2.14	1.71			1.20	1.31
9		2.05	1.61			1.07	1.21
10		1.97	1.50			0.95	1.10
11		1.88	1.39			0.84	1.01
12		1.80	1.31			0.75	0.98
13		1.71	1.30			0.67	0.90
14		1.67	1.29			0.595	0.84
15		1.58	1.28			0.53	0.80
16		1.50				0.47	
17		1.46				0.42	
18		1.38				0.35	
19		1.33				0.33	
20		1.28				0.29	

^a H₂SO₄ (0.200*N*) reduced the DPPH concentration to 1.22×10^{-2} mg./ml. in 18 hr.; H₂SO₄/Na₂SO₄ reduced the DPPH concentration to 1.00×10^{-2} mg./ml. in 18 hr.

^b Solvent composition: acetone:alcohol:aqueous acid = 5:5:2.

^c The HI and HBr systems gave straight lines when $\log [\text{DPPH}]$ was plotted against time. HCl deviated from first-order. $d \log [\text{DPPH}]/dt$ for the HBr system was -0.018 , and with bromide ion at three times this concentration $d \log [\text{DPPH}]/dt$ was -0.051 , first-order with respect to bromide ion.

^d In order to obtain sufficiently slow rates of reaction, 0.004*N* HI was used.

^e The HI, HCl and H₂SO₄ systems with added salt had approximately twice the anion concentration.

Action of Chlorine. Chlorine was bubbled through a carbon tetrachloride solution of DPPH-H containing a little HCl. Paper and thin layer chromatography gave at least three spots. A small amount of a violet-colored product developed as the reaction proceeded.

Action of Sodium Salts on DPPH

NaI (approx. 0.1 g.) was added to an acetone-water (1:1) solution of DPPH (10 ml., approx. 0.25 mg./ml.). After 2 hr. the color had changed to an orange-red. ESR showed no DPPH remained. After precipitation of the iodide with AgNO₃, DPPH was present as shown by ESR on the solution.

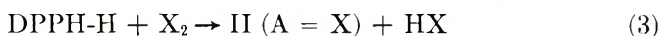
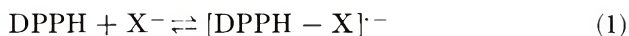
DPPH treated with NaBr as above showed only a small change, even after 24 hr., while with NaCl no reaction took place after 24 hr.

DISCUSSION

The reaction of DPPH with dilute aqueous mineral acids and with organic acids is of special significance to the use of DPPH in assigning reaction mechanisms. To gain further information on the reactions with acids, preliminary kinetic studies were undertaken. In order to have a single-phase reaction mixture, acetone-alcohol-water was used as the solvent for kinetic studies. With hydrobromic acid the reaction was shown to be first-order with respect to the concentration of DPPH, hydrogen ions, and bromide ions (Tables I and II).

The anion also greatly influences the reaction rate which decreases in the series HI, HBr, H₂SO₄. As with hydrobromic acid, the hydroiodic and sulfuric acid systems are accelerated by increasing the anion concentration by salt addition (Table II). Reaction with hydrochloric acid is discussed below.

The reaction products and kinetics of the reaction of DPPH with aqueous mineral acids can equally well be explained by a number of mechanisms. Reaction of DPPH with molecular hydrogen halide followed by hydrogen atom abstraction and the formation of the halogen is compatible with the observed results, as also is attack on the DPPH by ionic species such as a proton or halide ion. While the molecular hydrogen halide mechanism cannot be eliminated, an ionic mechanism is supported by the accelerating effect of water on organic acids and the very much faster reaction of trifluoroacetic acid when compared to acetic acid.¹⁸ At this stage the mechanism shown in eqs. (1)–(3) is suggested.



The initial attack of DPPH [reaction (1)] could be by either a proton or an anion, but we have preferred anionic attack, since sodium iodide has been shown reversibly to decolorize DPPH. Also the nitrogen carrying the odd electron in DPPH would be expected to be relatively positive because of the electron-withdrawing effect of the picryl group.

Further support for the above mechanism comes from a study of the action of the halogens on DPPH-H [reaction (3)]. Bromine gives the *p*-bromo (II, A = Br) while chlorine gives a number of compounds shown by paper chromatography to be qualitatively similar to the products from hydrochloric acid on DPPH. On the other hand, with iodine no ring-substituted iodo compound could be detected, and this is to be expected since the iodination of aromatic compounds is an equilibrium reaction where it is necessary to remove hydroiodic acid in order to get significant reaction. However, when an acidified mixture of iodine and DPPH-H is washed, small amounts of DPPH are formed, presumably by oxidation as shown in eq. (4).



This observation again supports the mechanism and products for the action of hydroiodic acid on DPPH.

With hydrochloric acid the rate of reaction is faster than with hydrobromic acid, and this does not conform to the order expected from the nucleophilic strength of the anion. However, the kinetics show a deviation from first order, and it would appear that other reactions with DPPH are involved. It is suggested that chlorine is attacking DPPH and that this reaction proceeds at a comparable rate to the chlorination of DPPH-H and to the attack of hydrochloric acid on DPPH. Attempts to support this hypothesis by studies of the chlorination of DPPH, DPPH-H, and mixtures of these compounds have, however, been inconclusive.

A number of aspects of the proposed mechanism are of special significance in relation to the use of DPPH in studying the mechanism of reactions. First, decolorization of DPPH is not necessarily an indication of a radical mechanism. Second, the formation of DPPH-H is not conclusive evidence for hydrogen atom abstraction as suggested by some workers.⁴ Third, in polymerization systems with, for example, Friedel-Craft type catalysts with mineral acid cocatalysts or in the presence of suitable organic anions and cations, decolorization of DPPH would appear likely.

CONCLUSIONS

The reaction products and kinetics resulting from the attack of aqueous acids on DPPH have been studied. A mechanism is proposed involving ionic attack on the DPPH.

In view of the proposed mechanism, the use of DPPH in assigning a reaction mechanism is limited.

Mr. F. D. Looney is thanked for assistance with the ESR spectra.

References

1. Flory, P. J., *Principles of Polymer Chemistry*, Cornell Univ., Ithaca, New York, 1953, p. 162.
2. Bartlett, P. D., and H. Kwart, *J. Am. Chem. Soc.*, **72**, 1051 (1950).
3. McGowan, J. C., T. Powell, and R. Row, *J. Chem. Soc.*, **1959**, 3103.
4. Hogg, J. S., D. H. Lohmann, and K. E. Russell, *Can. J. Chem.*, **39**, 1588 (1961).
5. Godsay, M. P., D. H. Lohmann, and K. E. Russell, *Chem. Ind. (London)*, **1959**, 1603.
6. Bickel, A. F., and E. C. Kooyman, *J. Chem. Soc.*, **1957**, 2415.
7. Brook, A. G., R. J. Anderson, and J. Tissot Van Patot, *Can. J. Chem.*, **36**, 150 (1958).
8. Hazell, J. E., and K. E. Russell, *Can. J. Chem.*, **36**, 1729 (1958).
9. Braude, E. A., A. G. Brook, and R. P. Linstead, *J. Chem. Soc.*, **1954**, 3574.
10. Russell, K. E., *J. Phys. Chem.*, **58**, 437 (1954).
11. Ewald, A. H., *Trans. Faraday Soc.*, **55**, 792 (1959).
12. Solomon, D. H., and M. J. Rosser, *J. Appl. Polymer Sci.*, **9**, 1261 (1965).
13. Goldschmidt, S., and K. Renn, *Ber.*, **55**, 628 (1922).
14. Matevosyan, R. O., I. Ya. Postovskii, and A. K. Chirkov, *Zh. Obshch. Khim.*, **29**, 858 (1959).
15. Chen, M. M., A. F. D'Adamo, Jr., and R. I. Walter, *J. Org. Chem.*, **26**, 2721 (1961).

16. Poirier, R. H., and F. Benington, *J. Org. Chem.*, **19**, 1847 (1954).
17. Poirier, R. H., E. J. Kahler, and F. Benington, *J. Org. Chem.*, **17**, 1437 (1952).
18. Proll, P. J., and L. H. Sutcliffe, *Trans. Faraday Soc.*, **59**, 2090 (1963).

Résumé

On a étudié l'influence des acides minéraux en solution aqueuse diluée sur l' α,α -diphényl- β -picrylhydrazyl (DPPH) et on montre le résultat par la perte rapide de la couleur caractéristique du radical. Les acides bromhydrique et chlorhydrique donnent l' α,α -diphényl- β -picrylhydrazine (DPH-H) et le dérivé halogéné substitué correspondant de l' α,α -diphényl- β -pidrylhydrazine. L'acide iodhydrique donne DPPH-H; de l'iode et une petite quantité de DPPH. Un certain nombre d'acides organiques provoquent des réactions semblables. Des études cinétiques effectuées avec l'acide bromhydrique montrent que la réaction est du premier ordre par rapport à: (1) la concentration en ion hydrogène; (2) la concentration en DPPH; (3) la concentration en anion. L'aptitude de l'anion à subir un transfert d'électron et à dimériser est également importante et le nucléophile le plus puissant donne la réaction la plus rapide. Un mécanisme qui implique une attaque ionique est proposé pour expliquer la réaction du DPPH avec l'acide. Les limites de l'emploi du DPPH dans l'étude des mécanismes de réaction sont discutés en relation avec le mécanisme ionique proposé.

Zusammenfassung

Die Einwirkung von verdünnten wässrigen Mineralsäuren auf α,α -Diphenyl- β -picrylhydrazyl (DPPH) wurde untersucht; sie führt zum raschen Verlust der charakteristischen Farbe des Radikals. Bromwasserstoff- und Chlorwasserstoffsäure liefern α,α -Diphenyl- β -picrylhydrazin (DPPH-H) und das entsprechende Halogensubstituierte α,α -Diphenyl- β -picrylhydrazin. Jodwasserstoffsäure liefert DPPH-H, Jod sowie eine kleine Menge an DPPH. Eine Anzahl organischer Säuren verursacht ähnliche Reaktionen. Die kinetische Untersuchung des Bromwasserstoffsäuresystems zeigt, dass die Reaktion von erster Ordnung in bezug auf (1) die Wasserstoffionenkonzentration, (2) die DPPH-Konzentration und (3) die Anionenkonzentration ist. Die Fähigkeit des Anions zum Elektronentransfer und zur Dimerisierung ist ebenfalls von Bedeutung, und das am stärksten nukleophile liefert die rascheste Reaktion. Ein Mechanismus über einen ionischen Angriff wird zur Erklärung der Reaktion von DPPH mit Säure vorgeschlagen. Die durch den vorgeschlagenen Mechanismus gegebene Beschränkung bei der Verwendung von DPPH zur Untersuchung von Reaktionsmechanismen wird diskutiert.

Received August 24, 1964

Revised January 27, 1965

Prod No. 4667A

Heteroaromatic Polymers. The Polybithiazoles*

DANIEL T. LONGONE and HOWARD H. UN, *Department of Chemistry, University of Michigan, Ann Arbor, Michigan*

Synopsis

The polycondensation of dithioöxamide with bifunctional aromatic bromomethyl ketones affords a series of poly-4,4'-diaryl-2,2'-bithiazoles. These polymers exhibit outstanding thermal stability. They are characteristically insoluble, infusible, highly crystalline, and of high molecular weight. Controlled structural variations within the polymer recurring unit allow for modifications of gross polymer properties. Structural characterization and thermal stability measurements are discussed.

INTRODUCTION

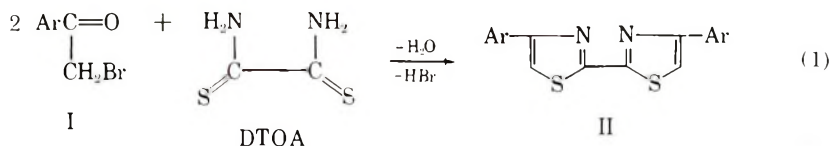
The very many polymer-forming reactions known utilize a relatively small number of different functional linkages and are sufficiently similar in nature to be classified as either condensation or addition reactions. Similarities in polymerization reactions necessarily result in similarities of gross polymer structures derivable from such reactions. One approach to obtaining new polymeric species lies in the development of polymer-forming reactions which by their very nature yield structures inaccessible through conventional condensation or addition methods. The development of novel polycondensations, especially those affording recurring heterocyclic units, has revealed an area of unusual potential and diversity. Polymers resulting from more recent work in this area include polybenzimidazoles,² polybenzoxazoles,³ polypyrimidonequinazolones,⁴ and polyquinoxalines.^{5,6} Due to their anticipated thermal stability, polymerizates containing solely heteroaromatic or mixed aromatic-heteroaromatic nuclei are of particular interest. The notable contributions of Marvel and his colleagues, which include fully aromatic polythiazoles,⁷ polybenzimidazoles,⁸ polybenzoprimidazolines,⁹ polyoxadiazoles,¹⁰ and polytriazoles,¹ have stimulated further work in this area.

We have evaluated several diverse condensations as potential polymer-forming reactions with the aim of generating thermally stable heteroaromatic polymerizates. In addition to the usual criteria, we sought reactions of such a nature that requisite monomers of great structural diversity would be synthetically accessible. The latter would allow correlation of gross polymer properties with controlled structural variations, e.g., extent

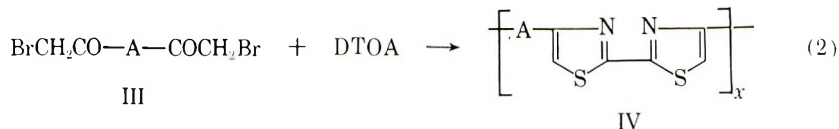
* Presented in part at the Symposium on Novel Polymer Structures, 145th National Meeting, American Chemical Society, New York, September 1963.¹

of conjugation, presence of flexible and heteroatom linkages, symmetry, etc. One reaction which proves to be extremely useful is the condensation of the commercially available dithiooxamide (DTOA) with halomethyl ketones.¹¹

Aryl bromomethyl ketones (I) and DTOA afford 4,4'-diaryl-2,2'-bithiazoles (II) in useful yields (>80%) and of high melting points: (II, Ar = phenyl,¹² β -naphthyl,¹³ and *p*-biphenyl; m.p. 222, 278, and 347°C., respectively). The use of 1,4-dibromobiacyetyl¹⁴ and 1,3,5-tris-(bromoacetyl) benzene¹⁵ in the condensation have been reported; however, the



resulting polymers were not characterized. For polymerization purposes, the requisite bifunctional aryl bromomethyl ketones would in general be accessible via Friedel-Crafts acylations of the corresponding aryl compounds. This approach allows desired structural variations of the type shown in eq. (2) where A is Ar, (Ar)_n, Ar-R-Ar, Ar-O-Ar, heteroaromatic, etc.



RESULTS AND DISCUSSION

Polybithiazoles

Bifunctional aryl bromomethyl ketones (III) were prepared from the appropriate aromatic substrates by diacetylation and bromination or, directly, by dibromoacetylation. Polycondensations of DTOA with III were carried out in dimethylformamide at the reflux temperature (153°C.). In each case the reaction was quite rapid, affording, within 15 min., a finely divided polymer precipitate.

The use of *p*-bis(bromoacetyl)benzene as comonomer generated poly-4,4'-(*p*-phenylene)-2,2'-bithiazole (V) which was isolated in 88% yield, after a standardized purification (extraction) procedure. As the prototype in the series, this polymer was examined most extensively. It is insoluble in a variety of organic solvents (at 90°C.), including dimethyl sulfoxide, dimethylacetamide, formic acid, phenyl ether, diphenylmethane, and quinoline; however, it readily dissolves in cold concentrated sulfuric acid, as do all polymers in this series. The polymer is highly refractory, showing no melt when heated to 520°C.; a 5-mg. sample heated with the full flame of a grid burner and in an open crucible requires 3 min. for complete com-

bustion, showing no melt and leaving no residue. The combination of insolubility and infusibility suggested the formation of an extensively cross-linked polymerizate. However, all subsequent chemical and structural work negated this possibility. X-ray powder patterns reveal that V is highly crystalline. Elemental analyses (see Table I) are quite good for the anticipated repeating unit and imply both structural integrity and high molecular weights. The polymer has a number-average molecular weight \bar{M}_n of about 12,000 or approximately 50 recurring units, based on bromine analysis and the assumption of an average of one bromine endgroup per polymer chain.*

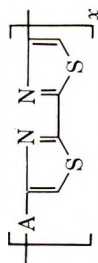
With these encouraging results we extended our studies to the preparation and characterization of polybithiazoles based on biphenyl, diphenylmethane, and phenyl ether substrates (polymers VI, VII, and VIII, respectively). The properties of these polymers closely resemble those of V (see Table I). They are characteristically insoluble, infusible, highly crystalline, and of high molecular weight. In view of the crystalline character of the polymers it appeared highly unlikely that insolubility and infusibility were due to the formation of extensively crosslinked polymerizates; however, we explored this possibility. If the polycondensation reaction utilized here does indeed afford linear polymerizates, the introduction of flexible polymethylene linkages into the recurring unit should markedly alter the physical properties of the resulting polymer. The utilization of the bisbromoacetyl derivative of 1,6-diphenylhexane as monomer provided such evidence. Polymer IX (Table I) was obtained in three fractions (total yield 89%) based on solubility in dimethylformamide. The fractions exhibit successively decreasing crystallinity, number-average molecular weight, and melting point with attendant increasing solubility. The major portion of the polymer (fraction A) is insoluble in hot dimethylformamide; it has a relatively sharp melting point and is highly crystalline. Fraction B, soluble in hot but insoluble in cold dimethylformamide, and fraction C, soluble in cold dimethylformamide, are quite similar to one another. Both display lower and wider melting point ranges along with decreased crystallinity.

Structural Characterization

While the polymer analytical data support the assignment of bithiazole-containing recurring units, confirmatory evidence for these structures was obtained by spectral characterization. For use as models, several substituted 2,2'-bithiazoles were prepared via the condensation of monobromomethyl ketones with DTOA. Ultraviolet spectra of the models were obtained by using potassium bromide disks, a medium useful for the

* It is difficult to assess the validity of this assumption; however, the complete analytical data on all polymers indicate that the molecular weights are indeed high. In addition, the relative molecular weights of all polymers in this series, based on bromine contents, are internally consistent with the physical data, indicating some degree of accuracy.

TABLE I
Polythiazoles



Polymer	Unit A	Yield, % ^a	[η] ^b	\bar{M}_n^c	Melting point, °C. ^d	Analyses, calcd. (and found)				
						C, %	H, %	N, %	S, %	Br, %
V		88	0.23	12,000	>520	59.48 (59.23)	2.49 (2.87)	11.56 (11.41)	26.47 (25.20)	0.00 (0.54, 0.76)
VI		79	0.24	84,000	>520	67.89 (67.36)	3.17 (3.53)	8.80 (8.00)	20.14 (18.85)	0.00 (0.00, 0.19)
VII		78	0.47	11,000	>520	68.64 (68.79)	3.64 (3.70)	8.43 (8.44)	19.29 (19.05)	0.00 (0.70)
VIII		79	0.38	80,000 ^e	>520	64.65 (64.24)	3.01 (3.47)	8.38 (8.36)	19.18 (18.81)	0.00 (0.0, 0.0)
IX		56	0.40	80,000 ^e	440-448	71.60 (71.60)	5.51 (5.69)	6.96 (6.85)	15.93 (16.19)	0.00 (0.0)
Fraction A		15	0.1	12,000	238-252	71.02 (69.31)	5.71 (5.49)	6.85 (6.42)	16.19 (16.19)	0.66 (0.71)
Fraction B		18	<0.1	11,000	218-235					

^a Yield of purified polymer (see Experimental).

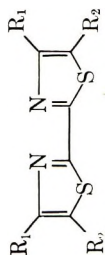
^b Inherent viscosity at 25.0°C. and at a concentration of 0.25 g./100 ml. in concentrated sulfuric acid.

^c Number-average molecular weight based on bromine content.

^d Capillary melting point.

^e Based on 0.1% Br; Beilstein test indicates less than 0.1% Br.

TABLE II
Ultraviolet Spectra of 2,2'-Bithiazoles



Compound	R ₁	R ₂	Medium	λ _{max} , mμ ^a	
				Low λ band	High λ band
X	CH ₃	H	KBr	230 (m)	332 (s), 337 (s), 344 (sh), 355 (sh), 364 (sh)
XI	CH ₃	CH ₃	C ₂ H ₅ OH	228 (3.81)	330 (4.34), 341 (sh) (4.25)
XII	CH ₃	CO ₂ C ₂ H ₅	KBr	239 (m)	350 (s), 367 (sh)
			KBr	252 (m)	345 (s)
XIII ^b	CH ₃	CH ₂ CH ₂ OH	C ₂ H ₅ OH	248 (3.73)	340 (sh) (4.32), 348 (4.37), 351 (4.38), 361 (sh) (4.25)
XIV ^d	C ₆ H ₅	C ₆ H ₅	?	<240 ^c	360 (4.25)
XV	C ₆ H ₅	H	CHCl ₃	<260 (s) ^e	376 (m) (4.26)
			KBr	248 (s), 268 (sh)	360 (m)
			C ₂ H ₅ OH	248 (4.59), 258 (sh) (4.45)	350 (4.10), 358 (sh) (4.04)
XVI	<i>p</i> -C ₆ H ₄ CH ₂ C ₆ H ₄	H	KBr	249 (s), 269 (sh)	359 (m)
XVII	<i>p</i> -C ₆ H ₄ C ₆ H ₄	H	KBr	294 (s)	364 (m)
XVIII	<i>p</i> -C ₆ H ₄ OC ₆ H ₄	H	KBr	266 (s)	355 (m)

^a s = strong absorption, m = medium absorption, sh = inflection point; log ε values in parentheses.

^b Data of Karrer and Sanz.²¹

^c Spectrum not recorded below 240 mμ.

^d Data of Karrer and Forster.²²

^e Spectrum not recorded below 260 mμ.

examination of the insoluble polymerizates described above. Simple thiazoles generally exhibit a maximum absorption in the region 240–260 $m\mu$ with $\log \epsilon$ above 3.6.^{16–20} There are few data available on the 2,2'-bithiazole system; however, based on the relatively small number of examples listed in Table II certain characteristics are discernible. The 2,2'-bithiazole system lacking aromatic substituents displays a low wavelength band (ca. 230–250 $m\mu$) of medium intensity and a high wavelength band (ca. 340–360 $m\mu$) of strong intensity. The presence of aryl substituents causes a reversal of relative intensities, the low wavelength band being stronger (compounds XIV–XVIII). Also, the position of the low wavelength band is sensitive to the nature of the aromatic moiety, while the long wavelength band appears close to 360 $m\mu$ (compare XVI, XVII, and XVIII). Spectra obtained both in potassium bromide disks and in a solution are comparable; minor differences in extent of fine structure and exact location of maxima do occur.

The ultraviolet spectra of the poly-4,4'-diaryl-2,2'-bithiazoles are summarized in Table III. The polymers exhibit the anticipated low wavelength band of strong intensity and variable position and the high wavelength band of medium intensity close to 360 $m\mu$.* The closest chromophore match between models and polymers exists in model XVI and polymers VII and IX. Significantly, the spectra of these three species are quite similar. The spectra of all fractions of polymer IX are similar; fraction C is sufficiently soluble in ethanol to yield a solution spectrum. The close correspondence of its solution and potassium bromide spectra (Table III) indicates the usefulness of the latter medium for the examination of completely insoluble polymers.

TABLE III
Ultraviolet Spectra of Polybithiazoles

Polymer	Medium	λ_{\max}	$m\mu$ and intensity
V	KBr	311 (s), 360 (m)	
VI	KBr	321 (s), 375 (m)	
VII	KBr	265 (s), 365 (m)	
VIII	KBr	286 (s), 359 (m)	
IX ^a	KBr	258 (s), 362 (m)	
	C ₂ H ₅ OH	255 (s), 355 (m)	

^a Fraction C.

Absorption in the infrared region also proved helpful in characterizing the polymers. The spectra of the 4,4'-diaryl-2,2'-bithiazoles XV–XVIII (Table II) exhibit three strong sharp bands in the region 740–940 cm.^{-1} . These bands, distinguishable from the aromatic carbon–hydrogen out-of-

* Polymer VI is exceptional, exhibiting a marked bathochromic shift at both low and high wavelengths.

plane deformations in this region, appear very close to 749, 884, and 942 cm.^{-1} . The spectra of model bithiazoles without aryl substituents (X, XI, and XII) lack one or more of these absorption bands.* Examination of the spectra of polymers V-IX reveals that each displays the above three bands. In all nine model and polymeric 4,4'-diaryl-2,2'-bithiazoles these bands occur within the remarkably narrow ranges 940-944, 882-887, and 743-755 cm.^{-1} . The examination of additional examples of structures II and IV will establish the diagnostic value of these bands for these systems.

Polymer Stabilities

The polybithiazoles exhibit unusual thermal stability. A thermogravimetric analysis (nitrogen atmosphere, heating rate of 150°C./hr.)† of polymer V reveals that major weight loss occurs between 500 and 700°C., with weight residues of 80% at 585°C. and above 50% at 900°C. A standardized static weight-loss technique was utilized in order to assess the relative thermal stabilities of the polybithiazoles. This method involved heating a polymer sample, under nitrogen, for 1-hr. periods at successively increasing temperatures. By this procedure, polymer V suffered a total weight loss of 20% after heating at 500°C. Subsequent sample heating at 600°C. resulted in an additional 20% weight loss and left a black powdery residue of low nitrogen and sulfur content (relative to carbon).‡ Examination of the infrared spectra and x-ray powder patterns of the sample during the course of the test procedure confirmed that gross structural changes occurred between 500 and 600°C.

In like manner, polymers VI, VII, and VIII exhibited total weight losses of 20% at temperatures of 400, 400, and 525°C., respectively. Although the mechanism of thermal decomposition of the polybithiazoles is unknown, the observed differences in polymer stabilities are presumably due to the nature of the aryl substituents in the recurring units. The greater stabilities of polymers V and VIII are in qualitative agreement with conclusions drawn from a study of the thermal stabilities of a variety of organic structures.²⁵

On prolonged exposure to light the surfaces of polymer samples, initially yellow-brown in color, assume a pink hue. This behavior is exhibited, in varying degrees, by all model and polymeric bithiazoles described here. In one instance an analytical sample (polymer VIII) was reanalyzed after a 3-month exposure. The carbon content had decreased from 64.2 to 62.7% implying that a photooxidation process was involved.

* The lack of correlation between the number and position of the bands in the 930-650 cm.^{-1} region and the pattern of substitution in the simpler monothiazoles has been discussed.^{23,24}

† We are indebted to Dr. G. F. L. Ehlers, Wright Air Development Division, Wright-Patterson Air Force Base, Ohio for this determination.

‡ We have not examined the volatile decomposition products. The low residual sulfur content is in accord with the observation that both thiazole and benzothiazole afford hydrogen sulfide on vapor phase pyrolysis.²⁵

EXPERIMENTAL

Materials

All melting points are uncorrected. The infrared spectra were obtained with a Perkin-Elmer Infracord or a Perkin-Elmer spectrophotometer, Model 21; the ultraviolet spectra with a Cary spectrophotometer, Model 11; the NMR spectra with a Varian A-60 instrument.*

Unless otherwise indicated, commercially available solvents and reagents were redistilled or recrystallized prior to use. Dimethylformamide was distilled over barium oxide; dithiooxamide (DTOA)† recrystallized from ethanol to give material which decomposes without melting at about 140°C. Mallinckrodt's analytical reagent grade aluminum chloride was used in the Friedel-Crafts reactions.

Preparation of Model Bithiazoles

4,4'-Dimethyl-2,2'-bithiazole (X). The reaction of chloroacetone and DTOA was utilized following essentially the described procedure.¹⁴ The product, after sublimation at 75°C. and 0.2 mm. (44% yield), is off-white in color and has a melting point at 138–139°C. (lit.¹⁴ m.p. 136°C.). The NMR spectrum (CCl₄) has singlets at τ 3.12 (vinyl hydrogen) and 7.53 (methyl); the infrared spectrum (KBr disk) has bands at 3080 (m), 2915 (m), 1511 (s), 1444 (s), 1436 (s), 1403 (s), 1366 (m), 1165 (m), 1000 (s), 984 (s), 876 (s), 770 (s), and 675 (m) cm.⁻¹.

4,4',5,5'-Tetramethyl-2,2'-bithiazole (XI). A solution of 2.1 g. (0.018 mole) of DTOA and 5.0 g. (0.033 mole) of technical grade 3-bromo-2-butanone in 100 ml. of absolute ethanol was refluxed for 7 hr. At the end of this time solvent was removed under diminished pressure and the residue taken up in benzene. The solution was filtered through a short column of alumina and the solvent then removed to give 2.9 g. (74%) of crude product, m.p. 130–170°C. Unidentified impurities were removed by sublimation at 70°C. and 0.2 mm., the residue recrystallized three times from acetonitrile to afford an analytical sample, m.p. 196.5–197.5°C.

ANAL. Calcd. for C₁₀H₁₂N₂S₂: C, 53.53%; H, 5.39%; N, 12.49%. Found: C, 53.75%; H, 5.56%; N, 12.78%.

The NMR spectrum (CDCl₃) displays a lone singlet at τ 7.60. The infrared spectrum (KBr disk) has peaks at: 2918 (m), 2850 (w), 1533 (s), 1404 (s), 1373 (m), 1108 (w), 974 (w), 922 (s), 842 (w), and 699 (m) cm.⁻¹.

4,4'-Dimethyl-5,5'-dicarbethoxy-2,2'-bithiazole (XII). The literature¹⁴ procedure of condensation of crude ethyl α -chloroacetoacetate²⁶ and DTOA afforded a very low yield (ca. 5%) of XII. The product, after two recrystal-

* We are indebted to Mr. B. E. Wenzel and Mr. F. Parker, for much of the spectral work. Analyses by Spang Microanalytical Laboratory, Ann Arbor, Michigan and Schwarzkopf Microanalytical Laboratory, New York, N. Y.

† We are indebted to the Mallinckrodt Chemical Works for a generous supply of this material.

lizations from 95% ethanol, was obtained as colorless needles, m.p. 191–192°C. (lit.¹⁴ m.p. 186°C.).

The NMR spectrum (CDCl₃) displays a quadruplet at τ 5.63 (methylene), a singlet at 7.25 (methyl), and a triplet at 8.62 (ester methyl). The infrared spectrum (KBr disk) exhibits ester bands at 1716 (s) and 1261 (s) cm.⁻¹. Additional bands occur at 2973 (m), 2918 (w), 1520 (m), 1394 (m), 1371 (s), 1314 (s), 1115 (s), 1095 (s), 850 (m), 820 (w), and 760 (s) cm.⁻¹.

4,4'-Diphenyl-2,2'-bithiazole (XV).* This model was prepared as previously described¹² from phenacyl bromide and DTOA. After recrystallization from absolute ethanol it melts at 220.0–221.5°C. (lit.¹² m.p. 220–222°C.). The infrared spectrum (Nujol) has bands at 3130 (w), 1605 (w), 1585 (w), 1420 (m), 1300 (m), 1075 (m), 1055 (m), 1025 (m), 940 (s), 885 (s), 778 (m), 740 (s), 690 (s), 678 (m), and 668 (m) cm.⁻¹.

4,4'-Bis(*p*-benzylphenyl)-2,2'-bithiazole (XVI). Acetylation of diphenylmethane was carried out essentially as described below in the preparation of *p*-phenoxyacetophenone. From 16.8 g. (0.100 mole) of diphenylmethane, 26.6 g. (0.200 mole) of aluminum chloride, and 10.2 g. (0.100 mole) acetic anhydride, there was obtained by distillation 4.95 g. diphenylmethane and 5.95 g. (40%) of *p*-benzylacetophenone, b.p. 139–165°C./0.6 mm. The major portion of the product had b.p. 139–144°C./0.6 mm. (lit.²⁷ b.p. 188–190°C./5 mm.) and n_D^{28} 1.5845. The NMR spectrum (CCl₄) displays an A₂B₂ multiplet (J 8 cycle/sec.) at τ 2.25 and 2.88 (C₆H₄), and singlets at 2.87 (C₆H₅), 6.13 (CH₂), and 7.66 (CH₃).

Bromination²⁷ of *p*-benzylacetophenone afforded crude *p*-benzylphenacyl bromide as an oil; condensation of the oil with DTOA in absolute ethanol gave crude XVI, m.p. 199–202°C., in a yield of 33% based on *p*-benzylacetophenone. Recrystallization from acetonitrile gave golden plates, m.p. 211–212°C.

ANAL. Calcd. for C₃₂H₂₄N₂S₂: C, 76.76%; H, 4.83%; N, 5.60%. Found: C, 76.91%; H, 5.15%; N, 5.67%.

The infrared spectrum (KBr disk) has bands at 3097 (w), 2022 (w), 2895 (w), 1600 (w), 1494 (m), 1480 (s), 1454 (m), 1430 (m), 1418 (m), 1056 (m), 943 (s), 885 (s), 882 (m), 753 (s), 741 (s), and 697 (s) cm.⁻¹.

4,4'-Bis(*p*-biphenyl)-2,2'-bithiazole (XVII). A solution of 5.7 g. (0.021 mole) *p*-phenylphenacyl bromide and 1.3 g. (0.011 mole) DTOA in 100 ml. dimethylformamide was refluxed for 1.5 hr., during which time a yellow solid was deposited. The reaction mixture was cooled and filtered, the solid washed with water, dried, and then recrystallized from cyclohexanone to give 4.0 g. (81%) of product as light yellow needles, m.p. 346–348°C.

ANAL. Calcd. for C₃₀H₂₀N₂S₂: C, 76.26%; H, 4.24%; N, 5.93%. Found: C, 76.41%; H, 4.08%; N, 5.82%.

The infrared spectrum (KBr disk) has bands at 3095 (w), 3043 (w), 1595 (w), 1478 (s), 1448 (m), 1412 (m), 1058 (m), 1008 (m), 941 (s), 887 (s), 849 (s), 772 (m), 750 (s), and 693 (s) cm.⁻¹.

* We are indebted to Mr. G. Nobel for the preparation of this compound.

4,4'-Bis(*p*-phenoxyphenyl)-2,2'-bithiazole (XVIII). *p*-Phenoxyacetophenone was prepared as follows. To a mixture of 17.0 g. (0.100 mole) phenyl ether and 40 g. (0.30 mole) aluminum chloride in 100 ml. of carbon disulfide was added dropwise and with vigorous stirring, 10.2 g. (0.100 mole) of acetic anhydride. During the addition the reaction vessel was cooled intermittently. After total addition, the mixture was heated over steam for 1 hr., allowed to stand at room temperature for an additional 1.5 hr., and then cautiously poured into a liter of ice containing 50 ml. of concentrated hydrochloric acid. The mixture was warmed over steam and then extracted with benzene. Removal of solvent from the dried benzene solution afforded 19 g. (90%) crude *p*-phenoxyacetophenone. Recrystallization from ethanol-water resulted in little loss and gave material with m.p. 47–48°C. (lit.²⁸ m.p. 45°C.). The infrared spectrum (Nujol) is characterized by strong bands at 1682 (carbonyl), 1250 (ether), and 845, 760, and 690 cm.⁻¹ (all aromatic out-of-plane deformations).

Bromination of the above product by the literature²⁹ procedure, gave *p*-phenoxyphenacyl bromide (43% yield) as an oil, b.p. 168–178°C./0.5 mm. (lit.²⁹ b.p. 190–192°C./3 mm.).* The infrared spectrum (neat) is characterized by strong bands at 1704 (carbonyl), 1259 (ether), 1215 (CH₂Br),† and 853, 769, and 700 cm.⁻¹ (all aromatic out-of-plane deformations).

A solution of 1.4 g. (4.8 mmole) of *p*-phenoxyphenacyl bromide and 0.29 g. (2.4 mmole) of DTOA in 60 ml. of absolute ethanol was refluxed for 1 hr., during which time a yellow-orange solid was deposited. The mixture was filtered while hot to give 0.6 g. (50%) crude XVIII, m.p. 222–226°C. Four recrystallizations from carbon tetrachloride followed by an additional two from benzene gave analytically pure material, m.p. 240.0–241.5°C.

ANAL. Calcd. for C₃₀H₂₀N₂S₂O₂: C, 71.42%; H, 3.97%; N, 5.55%. Found: C, 71.42%; H, 4.14%; N, 5.48%.

The infrared spectrum (KBr disk) includes bands at 3130 (w), 3070 (w), 1600 (vs), 1530 (s), 1500 (vs), 1480 (vs), 1415 (m), 1293 (s), 1255 (vs) (ether), 1170 (s), 942 (s), 886 (s), 870 (s), 847 (s), 778 (m), 748 (vs), and 690 (s) cm.⁻¹.

Preparation of Monomers

***p*-Bromoacetylphenacyl Bromide.**‡ Bromination³¹ of *p*-acetylacetophenone affords crude monomer in near quantitative yield, m.p. 169–172°C.; recrystallization from 95% ethanol gives a material melting at 173–174°C.

* The abstract [*Chem. Abstr.*, **49**, 9623 (1955)] describes the bromination of 4,4'-diacetyldiphenyl ether; examination of the original publication reveals that *p*-phenoxyacetophenone was the compound utilized and to which the abstracted data apply.

† This band appears to be characteristic of bromomethyl groups. We have examined a large number of aliphatic and aromatic bromomethyl compounds and find this band, usually the strongest in the spectrum, in the region 1205–1230 cm.⁻¹. We have noted a similar absorption (1150–1200 cm.⁻¹) in the case of iodomethyl compounds.³⁰

‡ We are indebted to Mr. G. Nobel for the preparation of this compound.

(lit.³¹ m.p. 177–178°C.). The infrared spectrum (Nujol) is characterized by strong bands at 1705 (carbonyl), 1205 (CH₂Br), and 810 cm.⁻¹ (aromatic out-of-plane deformation).

4,4'-Bis(bromoacetyl)biphenyl. To a solution of 9.6 g. (0.040 mole) of 4,4'-diacetylbiphenyl³² in 400 ml. glacial acetic acid was added dropwise 16 g. (0.10 mole) bromine. A red-brown precipitate developed during the later stage of addition. After total addition the mixture was stirred for an additional 15 min. The precipitate (11.2 g.) had a melting point of 214–216°C. After standing overnight the reaction filtrate had deposited an additional 3.0 g. of crude product, m.p. 206–211°C. The combined solids were recrystallized from ethyl acetate to afford, in two crops, 8.4 g. (53%) of colorless product, m.p. 219–221°C. (dec.) (sealed tube; lit.³³ m.p. 226–227°C.).

ANAL. Calcd. for C₁₆H₁₂O₂Br₂: C, 48.51%; H, 3.05%; Br, 40.35%. Found: C, 48.44%; H, 3.31%; Br, 40.38%.

The infrared spectrum (Nujol) is characterized by very strong bands at 1700 (carbonyl) and 1205 cm.⁻¹ (CH₂Br).

4,4'-Bis(bromoacetyl)diphenylmethane. The general bromination procedure³⁴ of Lutz et al. was unsatisfactory in our hands. To a solution of 7.6 g. (0.030 mole) of 4,4'-diacetyl-diphenylmethane³² in 150 ml. of glacial acetic acid was added, dropwise and with vigorous stirring, a solution of 9.6 g. (0.060 mole) bromine in 50 ml. of glacial acetic acid. After total addition the mixture was heated at the reflux temperature for 2 hr., at the end of which time the evolution of hydrogen bromide had ceased and the bromine color discharged. The reaction mixture was cooled and poured onto ice and the yellow precipitate removed, washed with 5% sodium bicarbonate solution and water, and then dried. The crude product was dissolved in benzene and chromatographed (silica gel, benzene) to give colorless needles (8.7 g., 71%), m.p. 139–140°C. (lit.³⁴ m.p. 137.5–138.5°C.).

ANAL. Calcd. for C₁₇H₁₄O₂Br₂: C, 49.78%; H, 3.44%. Found: C, 49.64%; H, 3.74%.

The infrared spectrum (Nujol) is characterized by bands at 1715 (carbonyl) and 1220 cm.⁻¹ (CH₂Br).

4,4'-Bis(bromoacetyl)diphenyl Ether. To a vigorously stirred mixture of 34 g. (0.20 mole) diphenyl ether, 93 g. (0.70 mole) aluminum chloride, and 200 ml. dry carbon disulfide was added over a 1-hr. period 121 g. (0.60 mole) of reagent grade bromoacetyl bromide. After total addition the mixture was stirred for 30 min., then refluxed for an additional 2 hr. and, finally, poured onto 3 l. of crushed ice containing 25 ml. of concentrated hydrochloric acid. The resulting semisolid mass was dissolved in chloroform and this solution added to the chloroform extracts of the aqueous layer. After drying, solvent was removed to leave crude product as a purple-gray mass. After seven recrystallizations from methanol (with Norit) followed by column chromatography (silica gel, ether), 11.1 g.

(13%) of colorless needles were obtained, m.p. 120–121°C. (lit.³⁵ m.p. 121°C.).

ANAL. Calcd. for $C_{16}H_{12}O_3Br_2$: C, 46.63%; H, 2.94%; Br, 38.78%. Found: C, 46.62%; H, 2.84%; Br, 38.33%.

The infrared spectrum (Nujol) has strong bands at 1700 and 1675 (carbonyl), 1255 (ether), and 1200 cm^{-1} (CH_2Br).

***p,p'*-Bis(bromoacetyl)-1,6-diphenylhexane.** 1,6-Diphenylhexane³⁶ was bromoacetylated in the manner described above for diphenyl ether. The crude product which precipitated on hydrolysis of the reaction mixture was dissolved in benzene. The benzene solution was treated with Norit, dried, concentrated, and then subjected to column chromatography (silica gel, benzene). Fractions yielding crystalline material were combined and recrystallized twice from carbon tetrachloride, affording pure monomer (10% yield) as off-white needles, m.p. 136–137°C.

ANAL. Calcd. for $C_{22}H_{24}O_2Br_2$: C, 55.01%; H, 5.04%; Br, 33.28%. Found: C, 54.91%; H, 5.23%; Br, 33.18%.

The NMR spectrum ($CDCl_3$) displays an A_2B_2 pair of doublets (J 8 cycle/sec.) at τ 1.96 and 2.61 (aromatic), a singlet at 5.51 (CH_2Br), a multiplet at 7.28 ($ArCH_2$), and a multiplet centered at 8.5 (tetramethylene). The infrared spectrum has strong bands at 1705 (carbonyl) and 1210 cm^{-1} (CH_2Br).

General Methods of Polymerization and Polymer Characterization

A solution containing equimolar amounts (ca. 3 mmole) of the bis-bromomethyl ketone and DTOA in dimethylformamide was heated to reflux (153°C.) in a 500-ml., three-necked flask fitted with a reflux condenser and mechanical stirrer. Precipitation of polymer generally commenced ca. 15 min. after initial reflux; reflux maintained for a total of 1.5 hr. At the end of this time the mixture was filtered while hot and the resulting solids continuously extracted (Soxhlet) for 15 hr. each with dimethylformamide, absolute ethanol, and ether, in that order. The residual polymer, after being dried at 100°C./0.2 mm. for 5 hr., was used for yield calculation and subsequent characterization.

Inherent viscosities were determined with the use of a Cannon-Fenske Series 150 viscometer at 25.0°C. and at concentrations of 0.25 g./100 ml. in concentrated sulfuric acid (filtered solutions); x-ray powder patterns were obtained with the use of $CuK\alpha$ radiation.

Polymer thermal stabilities were examined (nitrogen atmosphere) by a static method much like the one previously described.⁸ After pre-drying at 140–145°C./0.2 mm. for 30 min., samples were placed into an electrically heated chamber and held at 300, 350, 400, 500, and 600°C. consecutively for 1-hr. periods each. At the end of each hour of heating the sample was cooled under nitrogen and removed to determine weight loss.

Infrared spectra were obtained in KBr disks by use of conventional sample preparation techniques; data on all model and polymeric bithiazoles are from calibrated spectra (polystyrene). Potassium bromide disks

proved to be invaluable media for examining the insoluble polymers in the ultraviolet region; some care in disk preparation is required in order to obtain satisfactory spectra. Approximately 0.1 mg. of polymer and 300 mg. of infrared-grade KBr contained in a stainless steel capsule with two ball bearings are shaken for 30 sec. in a mechanical vibration-grinder. The use of a plastic capsule is generally unsatisfactory. A portion of the mixture, ca. 40 mg., is diluted with 260 mg. KBr and the resulting sample shaken for an additional 30 sec.; the necessary dilution factor is determined empirically. The sample is dried at 130°C. for 30 min. and then transferred while still hot to the disk mold; failure to remove adsorbed moisture at this point results in the formation of opaque rather than transparent disks. The mold assembly is evacuated at ca. 1 mm. for no less than 10 min.; 4,000 psi pressure is applied and held for 5 min., followed by 16,000 psi for an additional 5 min. The pressure is released and the disk removed in the conventional manner.

CONCLUSION

The use of dithiooxamide for the polycondensation of bifunctional bromomethyl ketones is particularly effective. Both high yields and molecular weights are obtained—undoubtedly a consequence of the enhanced reactivity¹¹ of the thionamide functions of dithiooxamide. Synthetic routes to halomethyl ketones are sufficiently diverse that polymer recurring units can be varied greatly and in a controlled manner. Monomers which allow the incorporation of heteroaromatic, organometallic, and perfluoroalkyl moieties are accessible. In addition, the use of aromatic bromomethyl ketones less symmetric than the ones reported here should lead to more tractable polymerizates with little loss of thermal stability. We are currently examining these variations.

References

1. Longone, D. T., and H. H. Un, *Am. Chem. Soc. Div. Polymer Chem. Preprints*, **4**, No. 2, 49 (1963).
2. Brinker, K. C., and I. M. Robinson, U. S. Pat. 2,895,948 (1959).
3. Brinker, K. C., D. D. Cameron, and I. M. Robinson, U. S. Pat. 2,904,537 (1959).
4. Serlin, I., and A. H. Markhart, *J. Polymer Sci.*, **60**, S59 (1962).
5. de Gaudemaris, G. P., and B. J. Sillion, *J. Polymer Sci.*, **B2**, 203 (1964).
6. Stille, J. K., and J. R. Williamson, *J. Polymer Sci.*, **B2**, 209 (1964).
7. Mulvaney, J. E., and C. S. Marvel, *J. Org. Chem.*, **26**, 95 (1961).
8. Vogel, H., and C. S. Marvel, *J. Polymer Sci.*, **50**, 511 (1961); *ibid.*, **A1**, 1531 (1963).
9. Mulvaney, J. E., J. J. Bloomfield, and C. S. Marvel, *J. Polymer Sci.*, **62**, 59 (1962).
10. Abshire, C. J., and C. S. Marvel, *Makromol. Chem.*, **44-46**, 388 (1961).
11. Hurd, R. N., and G. DeLaMater, *Chem. Rev.*, **61**, 45 (1961).
12. Lehr, H., and H. Erlenmeyer, *Helv. Chim. Acta*, **27**, 489 (1944).
13. Shukri, J., *J. Indian Chem. Soc.*, **39**, 651 (1962).
14. Karrer, P., P. Leiser, and W. Graf, *Helv. Chim. Acta*, **27**, 624 (1944).
15. Bischoff, G., O. Weber, and H. Erlenmeyer, *Helv. Chim. Acta*, **27**, 947 (1944).
16. Sheinker, Yu. N., V. V. Kushkin, and I. Ya. Postovskii, *Zh. Fiz. Khim.*, **31**, 214 (1957).

17. Weisiger, J. R., W. Hausmann, and L. C. Craig, *J. Am. Chem. Soc.*, **77**, 3123 (1955).
18. Klein, G., and B. Prijs, *Helv. Chim. Acta*, **37**, 2057 (1954).
19. Goerdeler, J., *Ber.*, **87**, 57 (1954).
20. Kuhn, R., and F. Drawert, *Ann.*, **590**, 55 (1954).
21. Karrer, P., and M. C. Sanz, *Helv. Chim. Acta*, **26**, 1778 (1943).
22. Karrer, P., and F. Forster, *Helv. Chim. Acta*, **28**, 315 (1945).
23. Mijovic, M. P. V., and J. Walker, *J. Chem. Soc.*, **1961**, 3381.
24. Bossignana, P., C. Cogrossi, and M. Gandino, *Spectrochim. Acta*, **19**, 1885 (1963).
25. Johns, I. B., E. A. McElhill, and J. O. Smith, *J. Chem. Eng. Data*, **7**, 277 (1962).
26. Dey, B. B., *J. Chem. Soc.*, **107**, 1606 (1915).
27. Evans, D. D., D. S. Morris, S. D. Smith, and D. Tivey, *J. Chem. Soc.*, **1954**, 1687.
28. Kipper, H., *Ber.*, **38**, 2490 (1905).
29. Tomita, M., H. Kumaoka, and M. Takase, *J. Pharm. Soc. Japan*, **74**, 850 (1954).
30. Longone, D. T., and F. P. Boettcher, *J. Am. Chem. Soc.*, **85**, 3436 (1963).
31. Kröhnke, F., and I. Vogt, *Ber.*, **86**, 1132 (1953).
32. Sloan, G. J., and W. R. Vaughan, *J. Org. Chem.*, **22**, 750 (1957).
33. Long, J. P., and F. W. Schueler, *J. Am. Pharm. Assoc.*, **43**, 79 (1946).
34. Lutz, R. E., et al., *J. Org. Chem.*, **12**, 617 (1947).
35. von Schickh, O., U. S. Pat. 1,717,424 (1929).
36. Van Alphen, J., *Rec. Trav. Chim.*, **59**, 580 (1940).

Résumé

La polycondensation du dithiooxamide avec des cétones aromatiques bifonctionnelles bromométhylées fournit une série de poly-4,4'-diaryl-2,2'-bithiazoles. Ces polymères présentent une stabilité thermique remarquable. Ils sont spécifiquement insolubles, infusibles, fortement cristallins et de poids moléculaires élevés. Des variations structurales contrôlées à l'intérieur de l'unité polymérique permet des modifications des propriétés macroscopiques du polymère. On discute de la détermination de la structure et des mesures de stabilité thermique.

Zusammenfassung

Die Polykondensation von Dithiooxamid mit bifunktionellen, aromatischen Brommethylketonen liefert eine Reihe von Poly-4,4'-diaryl-2,2'-bithiazolen. Diese Polymeren besitzen eine ungewöhnliche thermische Stabilität. Sie sind in charakteristischer Weise unlöslich, unschmelzbar, hochgradig kristallin und von hohem Molekulargewicht. Eine kontrollierte Strukturvariation des Polymerbausteins erlaubt eine Modifizierung der Polymereigenschaften. Strukturcharakterisierung und thermische Stabilitätsmessung werden diskutiert.

Received January 19, 1965

Prod. No. 4678A

Dye-Sensitized Polymerization of Vinyl Monomers in Aqueous Solution

A. I. MD. SHERIFF and M. SANTAPPA, *Department of
Physical Chemistry, University of Madras, Madras, India*

Synopsis

The kinetics of the polymerization of the vinyl monomers methyl methacrylate, methyl acrylate, and acrylonitrile sensitized by dye-reducing agent systems have been studied systematically. The systems were irradiated with light of 350-450 $m\mu$ wavelength. The induction period before the onset of polymerization was kept to a minimum by suitable experimental conditions. All the experiments were conducted in the presence of oxygen. The redox system sodium fluorescein (Uranine)-ascorbic acid was used for polymerization. The systems were buffered with phosphate buffer. The effects of temperature, viscosity, etc., on the reaction system were studied. The course of the reactions was followed by the measurements of rate of monomer disappearance (gravimetrically), rate of dye disappearance (spectrophotometrically) and the chain length of the polymer formed (viscometrically). Light intensity, wavelength, monomer concentration, dye concentration, reducing agent concentration, temperature, etc., were variable. The tentative kinetic scheme proposed is examined in the light of the experimental results. The values for the specific rate constants for the various steps have been evaluated.

INTRODUCTION

Dyes as photosensitizers for the polymerization of vinyl monomers have been the subject of extensive investigations for the past few years.¹⁻²⁹ Dyes, with and without reducing agents, under the influence of visible light initiate vinyl polymerization both in aqueous and nonaqueous media. Conflicting views with regard to the mechanism of initiation by the dyes abound in literature. Research workers in this field have expressed contrary opinions, with regard to the necessity or otherwise of oxygen, reducing agent, buffer, etc. Oster,⁹ who worked extensively in this field, has stressed the importance of both oxygen and a mild reducing agent. Takemura⁴ as well as Oster's school⁵ maintain that the initiating radicals are formed by the direct interaction of the dye and monomer. Various suggestions have been made with regard to the nature of initiation reaction. The interaction of transient tin ion (Sn^{3+}) (produced by the interaction of dye and Sn^{2+}) with the vinyl monomer to produce initiating species has been suggested by Koizumi and Watanabe.⁸ Delzenne, et al.¹⁰ have proposed the formation of initiating radicals from hydrogen peroxide, formed during the reoxidation of leuco derivative or semiquinone form of the dye

by molecular oxygen, the leuco or semiquinone form of the dye having been formed by interaction of excited dye with the reducing agent. These authors¹² are of the opinion that a transient activated complex (DT . . . HOH) and the monomer react together to form the initiating radicals under the influence of light. Shepp et al.⁷ have maintained that the initiating radicals are formed by the interaction of (ST-OH) (where ST denotes the semiquinone form of thionine) with the vinyl monomer in the primary photochemical reaction. Various views with regard to the initiation mechanism may be summarized as conforming to one of the three types: (1) energy transference between the excited dye and monomer;¹ (2) production of radicals as a result of interaction of the excited dye with the monomer;²⁻⁵ (3) production of radicals by the self-decomposition of the dye⁶ or by interaction of the dye with a third substance such as oxygen, OH, or reducing agent.⁷⁻¹⁰ With this blurred picture of dye initiation as a background, a systematic investigation has been carried out by us with the dye-reducing agent-vinyl monomer system in aqueous solution. Sodium fluorescein and ascorbic acid have been used as the dye and reducing agent, respectively, for polymerization of vinyl monomers, i.e., methyl methacrylate, methyl acrylate, and acrylonitrile. Light in the 350-450 m μ wavelength region has been employed for irradiation of the system. As a result of this investigation we have tried to throw some light on the nature of the initiation and termination reactions in the polymerization and on the importance of reducing agent, oxygen, etc., in the system.

EXPERIMENTAL

Optical Arrangement

The light sources used were (1) 250-w. high-pressure mercury vapor lamp supplied by B. T. H. Co. (Mazda box type fitted with a glass window); (2) 250-w. high-pressure mercury vapor lamp (bulb type provided by Pradip Lamp Works, Patna, India); (3) 125-w. bulb-type ultraviolet Mazda lamp. The lamps were connected to the mains through the necessary chokes. The first two lamps were used as sources of light of $\lambda=405$ and 435 m μ and the last type for $\lambda=365$ m μ . The light from the lamp was collimated by means of a quartz condenser lens and the resulting parallel beam allowed to pass through a series of filter solution combinations for isolating the various monochromatic radiations:³⁰ for 365 m μ : copper sulfate (CuSO₄·5H₂O, 125 g./1 liter water) in a quartz cell of 1 cm. light path, combined with chance glass OXI 2-3 mm.; for 405 m μ : copper nitrate [Cu(NO₃)₂·6H₂O, 200 g. of the salt dissolved in 100 ml. of water] in a 2 cm. cell combined with a solution of iodine in carbon tetrachloride (0.75 g. in 100 ml. of carbon tetrachloride) in a 1 cm. cell; for 435 m μ : copper nitrate [Cu(NO₃)₂·6H₂O, 200 g. of the salt dissolved in 100 ml. of water] in a 2 cm. cell combined with sodium nitrite (NaNO₂, 75 g. dissolved in 100 ml. of water) in a 1 cm. cell.

The parallel beam of light consisting of monochromatic radiation is allowed to fall on the quartz window of a metal thermostat, inside which the reaction cell is mounted. The reaction cell (length 4.6 cm. in the direction of the beam and 5 cm. in diameter, capacity about 75 ml.) fused at both ends with flat Pyrex plates, is fitted with two outlet tubes, of standard B-14 cones on the top.

Reagents

All the chemicals used in the preparation of solutions were B. D. H., A. R., E. Merck, G. R., or M & B reagent grade. Water doubly distilled (over alkaline permanganate) in an all-glass quickfit set-up and then passed through Biodeminrolit (Permutit, London) resin was used throughout for the preparation of solutions. The sensitizing dye, Uranine, was obtained from M & B Chemicals. The monomers methyl methacrylate and methyl acrylate were kindly supplied by Rohm & Haas Co., U. S. A., and acrylonitrile was supplied by American Cyanamid Co., New York. The monomers were washed free of the inhibitor with a 5% solution of sodium hydroxide and then with water and finally distilled under reduced pressure in an atmosphere of nitrogen. The monomers were distilled frequently before use and stored at 5°C. L-Ascorbic acid (G. R., E. Merck) was used as a reducing agent.

Estimation

A typical experiment is described below in brief and the procedures for various measurements are given. The reaction mixture, vinyl monomer-dye-reducing agent in aqueous solution, at pH 6 was introduced into the reaction cell and deaerated by passing through oxygen-free nitrogen.³¹ Loss of monomer in the deaeration process was kept to a minimum and corrected for. The reaction cell was then mounted inside a thermostat, maintained at $35 \pm 0.1^\circ\text{C}$. by use of toluene regulator and a hot wire vacuum switch relay (Gallenkamp), in the path of the monochromated light beam and the reaction allowed to proceed for 30–75 min., depending on the type of monomer. The precipitated polymer was then filtered off, dried, and weighed. Most of the experiments were conducted under nondeaerated conditions, for the polymerization is found to commence almost immediately under these conditions. For comparison some of the experiments have been repeated under deaerated conditions.

The rate of monomer disappearance was followed by gravimetric determinations on the precipitated polymer dried to constant weight. Poly(methyl acrylate) was precipitated from the reaction mixture by coagulation with the addition of an electrolyte such as ammonium nitrate. Poly(methyl methacrylate) and polyacrylonitrile were precipitated as fine flocculent precipitates.

The rate of dye disappearance was followed by measuring the optical density of the reaction mixture before irradiation and that of the filtrate obtained after removal of the polymer. The dye sensitizer was found to

obey Beer's law, and the absorption maximum for Uranine was $\lambda_{\max.} = 484 \text{ m}\mu$. All absorptiometric measurements were made in a Hilger-Watts Uvispek spectrophotometer, H-700 type, with matched Corex and silica cells. For measurement of chain length, the polymers were purified by reprecipitation with methanol from their solutions in benzene [poly(methyl methacrylate) and poly(methyl acrylate)] and dimethylformamide (polyacrylonitrile). The purified samples were then dried, and the viscosities of 0.1% solutions of poly(methyl methacrylate) and poly(methyl acrylate) in benzene and at a 0.1% solution of polyacrylonitrile in dimethylformamide measured in a PCL Ubbelohde-type viscometer, thermostated to $\pm 0.01^\circ\text{C}$. in a viscometric bath designed for precision viscometry (Krebs Electrical & Manufacturing Co., New York). Chain lengths n were then computed from the measured viscosities by using Mark-Houwink type relationships between limiting viscosity number and molecular weights of polymers:

$$n = 2.81 \times 10^3 [\eta]^{1.32}$$

at 25°C . for poly(methyl methacrylate);³⁴

$$\eta = 1.282 \times 10^{-4} M^{0.7143}$$

at 35°C . for poly(methyl acrylate);³⁵ and

$$\eta = 2.43 \times 10^{-4} M^{0.75}$$

at 25°C . for polyacrylonitrile.³⁶

The light intensity of the mercury vapor lamp was determined by chemical actinometry. Both uranyl oxalate³⁰ and potassium ferrioxalate^{32,33} were employed as chemical actinometers. The former method was found to be suitable for measuring high light intensities and is based on the photochemical decomposition of uranyl oxalate, the extent of decomposition being determined by permanganate titration. The latter method, which makes use of potassium ferrioxalate, was found to be suitable for measuring low intensities. The amount of ferrous ion produced was determined colorimetrically by forming a colored complex with *o*-phenanthroline and taking absorption measurements at $510 \text{ m}\mu$ in a Hilger-Watts ultraviolet spectrophotometer.

KINETIC RESULTS

The buffered system containing the vinyl monomer, dye, reducing agent, and oxygen, was found to be effective for polymerization. The effects of concentrations of monomer, dye, and ascorbic acid and the light intensity on the rates of monomer disappearance, dye disappearance, and also chain length were studied in detail.

Effect of Monomer Concentration

The rates of monomer disappearance were found to be proportional to the square of the monomer concentration (Fig. 1) with all the monomers at

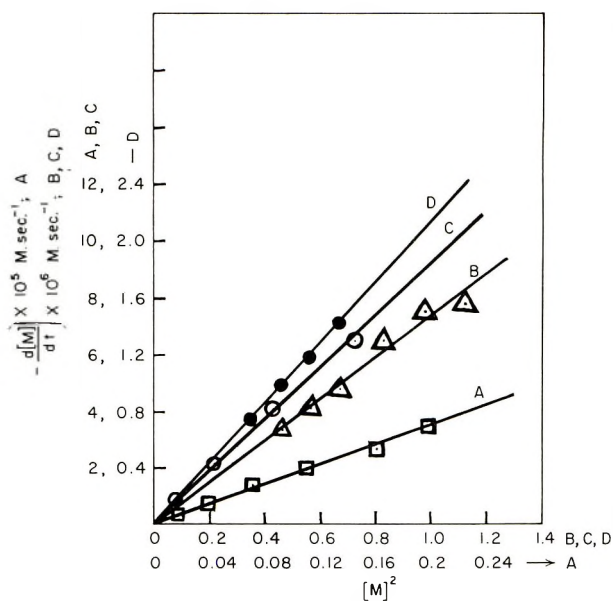


Fig. 1. Plots of rate of monomer disappearance vs. square of the monomer concentrations for the Uranine-ascorbic acid system at 35°C., $\lambda = 365$ and 435 μ : (A) methyl acrylate; (B), (D) acrylonitrile; (C) methyl methacrylate.

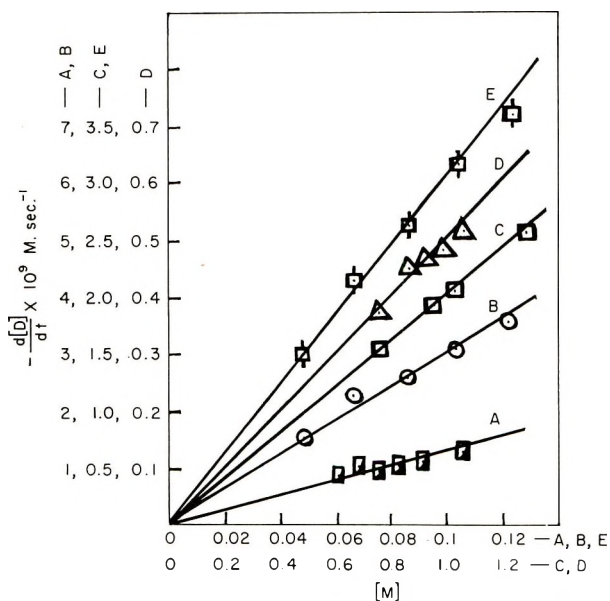


Fig. 2. Plots of rate of dye disappearance vs. first power of the monomer concentrations for the Uranine-ascorbic acid system at 35°C., $\lambda = 365$, 405, and 435 μ : (A), (D) acrylonitrile; (B), (C), (E) methyl methacrylate.

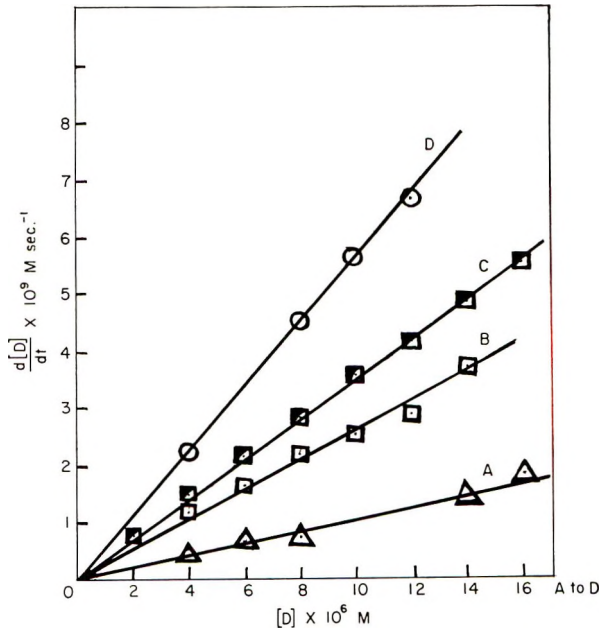


Fig. 3. Plots of rate of dye disappearance vs. dye concentration for the Uranine-ascorbic acid system at 35°C., $\lambda = 365$ and 435 $m\mu$: (A), (D) acrylonitrile; (B), (C) methyl methacrylate.

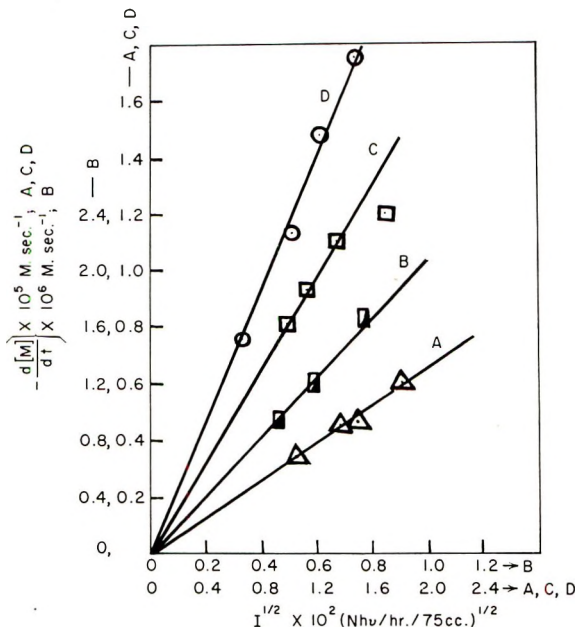


Fig. 4. Plots of rate of monomer disappearance vs. square root of the incident light intensity for the Uranine-ascorbic acid system at 35°C., $\lambda = 405$ and 435 $m\mu$: (A), (B) acrylonitrile, (C) methyl methacrylate, (D) methyl acrylate.

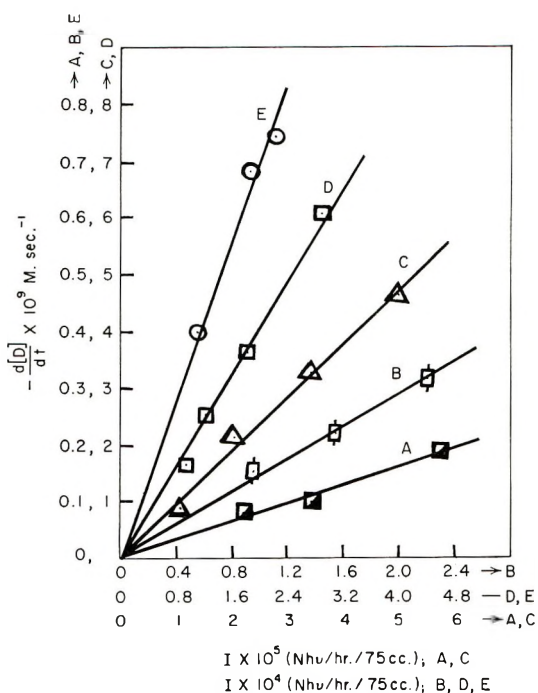


Fig. 5 Plots of rate of dye disappearance vs. incident light intensity for the Uranine-ascorbic acid system at 35°C., $\lambda = 365, 405, \text{ and } 435 \text{ m}\mu$: (A), (B), (E) acrylonitrile; (C), (D) methyl methacrylate.

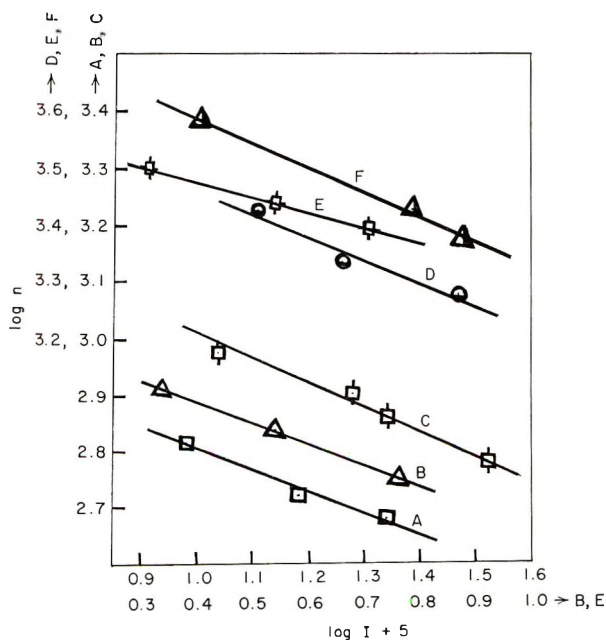


Fig. 6. Plots of $\log n$ vs. $\log I$ for the Uranine-ascorbic acid system at 35°C., $\lambda = 365, 405, \text{ and } 435 \text{ m}\mu$: (A), (B), (C) acrylonitrile; (D), (E), (F) methyl methacrylate. Slope = 0.5.

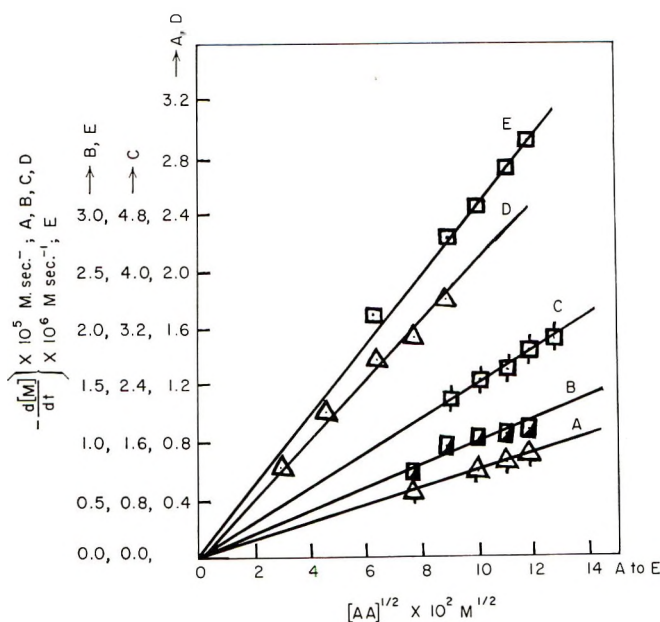


Fig. 7. Plots of rate of monomer disappearance vs. square root of the ascorbic acid concentrations for the Uranine-ascorbic acid system at 35°C., $\lambda = 365, 405,$ and $435 \text{ m}\mu$: (A), (E) acrylonitrile; (B), (D) methyl methacrylate; (C) methyl acrylate.

various wavelengths employed. Also the rates of dye disappearance were found to be proportional to the first power of the monomer concentration (Fig. 2), and the chain lengths were independent of the monomer concentration.

Effect of Dye Concentration

At high concentrations of the dye ($>10^{-3}M$) the rate of dye disappearance could not be followed. The rate of monomer disappearance was found to be independent of the dye concentration in the range 10^{-6} – $10^{-5}M$. At very low concentrations of the dye ($10^{-7}M$) there is negligible dependence of $-d[M]/dt$ on the dye concentration. The rate of dye disappearance varied directly with the first power of the dye concentration (Fig. 3) with the three monomers. The chain lengths of polymers were found to be independent of the dye concentration.

Effect of Light Intensity

The light intensity was varied by using variable diaphragms. The intensity of the lamp output remained quite constant. The rates of monomer disappearance and dye disappearance were found to vary directly with the square root and first power of light intensities, respectively, with the monomers studied (Figs. 4 and 5). Chain lengths were found to vary inversely with the square root of incident light intensity (Fig. 6).

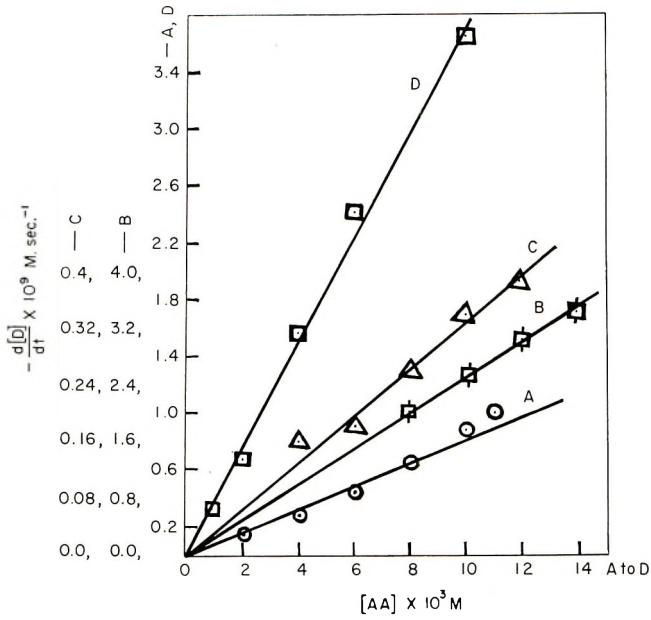


Fig. 8. Plots of rate of dye disappearance vs. ascorbic acid concentrations for the Uranine-ascorbic acid system at 35°C., $\lambda = 365$ and 435μ : (A), (C) acrylonitrile; (B), (D) methyl methacrylate.

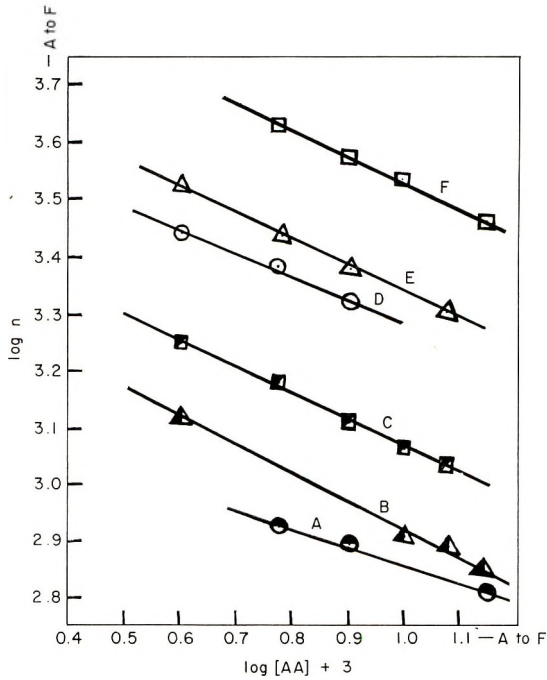


Fig. 9. Plots of $\log n$ vs. $\log [AA]$ for the Uranine-ascorbic acid system at 35°C., $\lambda = 365, 405,$ and 435μ . (A), (B), (C) acrylonitrile; (D), (E), (F) methyl methacrylate. Slope = 0.5.

Effect of Reducing Agent Concentration

Ascorbic acid was found to be a mild reducing agent and most effective for the system under study. The rates of monomer disappearance were proportional to the square root of the ascorbic acid concentration (Fig. 7), and the rate of dye disappearance was directly proportional to the first power of ascorbic acid concentration with the monomers studied (Fig. 8). The chain length varied inversely with the square root of ascorbic acid concentration (Fig. 9).

Quantum Yield for Dye Disappearance

From the data on the rate of dye disappearance and light absorption fraction, the quantum yields γ_{net} for dye disappearance were calculated. These values were found to be independent of the concentrations of dye and ascorbic acid, but dependent on the monomer concentration and incident light intensity.

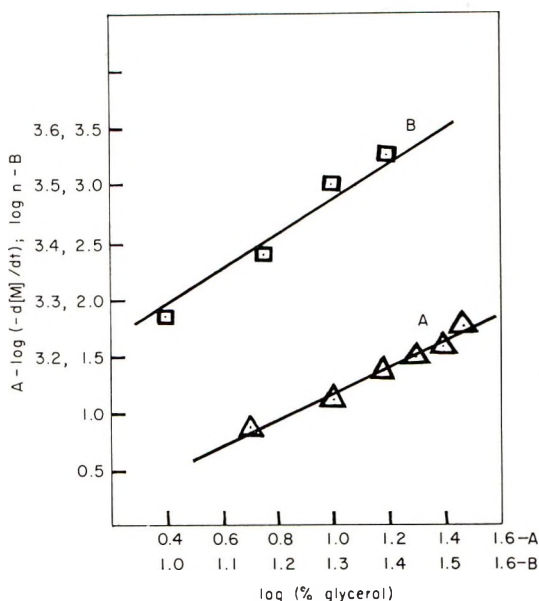


Fig. 10. Plots of log rate of monomer disappearance and log chain lengths vs. log percentage of glycerol for methyl methacrylate at 35°C., $\lambda = 435 \text{ m}\mu$.

The effects of temperature and viscosity on the reaction have been studied to a limited extent. Both the rates of monomer disappearance and dye disappearance were independent of temperature (30–50°C.). The rate of monomer disappearance and the chain length were dependent on the first power of the viscosity of the medium. The rate of dye disappearance was independent of the viscosity of the medium (Fig. 10). The viscosity of the medium was varied by using different glycerol–water mixtures.

KINETIC SCHEME AND DISCUSSION

The reaction scheme shown in eqs. (1)–(7) embodies the reactions that are likely to occur.

Excitation of the “initiator” cluster:



where initiator is a transient photosensitive cluster consisting of dye, monomer, and ascorbic acid.

Emission of fluorescence:



Radical formation:



Deactivation:



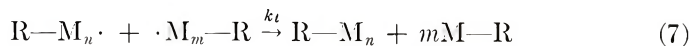
Initiation:



Propagation:



Termination:



The light absorption fraction involved in the reaction scheme is actually that due to the photosensitive cluster, $k_{e(\text{cluster})}$. It can be shown that

$$k_{e(\text{cluster})} = k_{e(\text{total})} K[\text{AA}][\text{M}]/(1 + K[\text{AA}][\text{M}]) \quad (8)$$

where [AA] and [M] denote concentrations of ascorbic acid and vinyl monomer, respectively, if equilibrium is assumed:



Also the extinction coefficients with respect to cluster and free dye are the same. Since under our experimental conditions $K[\text{AA}][\text{M}] \ll 1$, eq. (8) simplifies to:

$$k_{e(\text{cluster})} = k_{e(\text{total})} K[\text{AA}][\text{M}] \quad (10)$$

The radical formation step, eq. (3), appears to be the most probable. According to usual stationary-state kinetics,

$$d[\text{Initiator}^*]/dt = 0$$

$$d[\text{R}\cdot]/dt = 0$$

$$d[\text{R—M}\cdot]/dt = 0$$

The kinetic expressions for the rates of monomer disappearance $d[M]/dt$, dye disappearance $d[D]/dt$, and chain length of the polymers n which may be derived are given in eqs. (11)–(14).

$$-d[M]/dt = (k_p/k_t^{1/2})[M]^2\{k_i k_{\epsilon(\text{total})}K/(k_i[M] + k_d)\}^{1/2}[AA]^{1/2}I^{1/2} \quad (11)$$

where I is incident light intensity.

When $k_i[M]$ is neglected when compared to k_d we have:

$$-d[M]/dt = (k_p/k_t^{1/2})[M]^2(k_i k_{\epsilon(\text{total})}K/k_d)^{1/2}[AA]^{1/2}I^{1/2} \quad (12)$$

$$-d[D]/dt = k_{\epsilon(\text{total})}K[AA][M]I \quad (13)$$

$$n = (k_p/k_t^{1/2})(k_d/k_i k_{\epsilon(\text{total})}K)^{1/2}(1/[AA]^{1/2}I^{1/2}) \quad (14)$$

In the polymerization of vinyl monomers photosensitized by the dye-reducing agent system described in this paper, the most probable primary photochemical reaction appears to be the excitation of the photosensitive cluster composed of dye, monomer, and ascorbic acid. The excited cluster reacts with the monomer in a dark reaction to form the free radical $R\cdot$. Most of the kinetic results presented here may be conveniently explained, on the basis of formation of such a cluster. Delzenne et al.,¹⁰ in their study on the photopolymerization of acrylamide by different dye-reducing agent systems, have reported that the excitation of the dye to the triplet state is the primary photochemical step. The triplet state reacts with the reducing agent to give as intermediates semiquinone and leuco forms of the dye. Reoxidation of these two latter reduced forms with oxygen present in the system leads to the formation of the original dye and hydrogen peroxide. The initiation of polymerization has been attributed to the radicals formed by the reaction between hydrogen peroxide and reducing agent. In a subsequent publication by Delzenne et al.,¹¹ the photosensitizing agent (initiator) was assumed to consist of the dye sensitizer, reducing agent, and oxygen present in the system. In our study, direct interaction between the dye and monomer to form the initiating radicals has been discounted, for no polymerization could be detected if dye and monomer alone, without reducing agent, are present in the system. We are of the opinion that for our system oxygen is not an absolutely necessary ingredient in the photosensitizing cluster. Initiation with short induction periods is always possible in the presence of oxygen. That oxygen plays a significant part in the secondary reactions is obvious because of the observed enhanced rates in its presence. A. Watanabe⁸ has observed the same type of phenomenon in her study on the photopolymerization of acrylonitrile initiated by the stannous chloride–acriflavine system. The formation and reaction of the photosensitizing cluster appears to be pH-dependent. For $\text{pH} < 6$ the rates are steady, while for $\text{pH} > 6$ the rates decrease, and at $\text{pH} 8$ there is negligible polymerization. The rate of monomer disappearance has been found to be proportional to the square of the monomer concentration. This dependence is in accord with the observations of earlier workers.^{4,5,8,11} The second-power dependence of monomer concentration on rates has

been explained^{4,5,11} on the basis of participation of monomer in the formation of an initiator having a very low efficiency for initiation. Experimentally observed high molecular weights of the polymers in our systems also lend support to these views. The rate of monomer disappearance has been found to be directly proportional to the square root of ascorbic acid concentration. It has been observed that the rate reaches a maximum and remains constant when $[\text{ascorbic acid}] > 1.4 \times 10^{-2}M$. Delzenne et al.¹¹ have reported that a rate maximum is obtained for $[\text{ascorbic acid}] > 1.35 \times 10^{-3}M$ and further increase in the concentration of ascorbic acid decreases the rate. Similar observations have been made by Takayama¹⁷ in his study of the polymerization of vinyl acetate in methanol sensitized by the system acriflavine-ascorbic acid. According to Delzenne et al.,¹¹ this behavior is due to the powerful reducing capacity of ascorbic acid at high concentrations and consequently most of the dye molecules are directly reduced to the leuco form of the dye which may not be completely reoxidized. Watanabe and Koizumi⁸ have reported in their study on the polymerization of acrylonitrile sensitized by the system stannous chloride-acriflavine, that the rate of polymerization remains constant when the reducing agent concentration exceeds $1.2 \times 10^{-2}M$. The square-root dependence of the rate of polymerization on the incident light intensity has been reported by various workers,^{5,7,8} which clearly shows that the termination is of the mutual type. The rate of dye disappearance has been found to be directly proportional to the first powers of the concentrations of monomer, dye, reducing agent, and incident light intensity. Toppet et al.¹² reported similar views with regard to the dependence of photoreduction of dye on the monomer concentration and light intensity in their study on the polymerization of acrylamide sensitized by eosin. Shepp et al.,⁷ in their study on the thionine-sensitized polymerization of acrylamide, also expressed similar conclusions. The chain lengths of the polymers vary inversely with the square roots of both ascorbic acid concentration and incident light intensity. Oster et al.,⁵ in their study on the polymerization of acrylamide sensitized by riboflavine, reported that the degree of polymerization is inversely proportional to $I^{1/2}$. The inclusion of the step with respect to primary radical deactivation is justified by the assumption that the radicals are occluded in the giant polymer aggregates or being changed to a noninitiating free radical. This is supported by the increase in the rate with increase in the viscosity of the medium which lowers the rate of termination, contributing to the increase in the rate of polymerization.

The values of the equilibrium constant K have been evaluated from the plots of rate of dye disappearance versus $[M]$, $[AA]$, or I (Figs. 2, 5, 8). The values of the ratio $k_p/k_t^{1/2}$ have been evaluated from the plots of rate of monomer disappearance versus $[M]^2$, $[AA]^{1/2}$, or $I^{1/2}$ (Figs. 1, 4, 7) as well as by substituting the values for $k_{e(\text{total})}K$ obtained from the plots (Figs. 2, 5, 8). The numerical values for the ratios of the rate constants and the equilibrium constants are presented in Table I along with the

TABLE I
 Values of K and $k_p/k_t^{1/2}$

Wavelength, $m\mu$	$K \times 10^4$		$k_p/k_t^{1/2}, (l./mole)^{-1/2}\text{-sec.}^{-1/2}$		
	MMA	AN	MMA	MA	AN
			Aqueous solution (precipitating media)		
365	240.6	4.574	1.403	—	0.0479
405	389.0	4.829	1.473	—	0.0372
435	327.2	6.545	1.560	1.19	0.0756
			0.2700 ^a	—	0.0420 ^a
			0.2895 ^b	0.2700 ^b	0.1003 ^b
			0.3009 ^c	0.3743 ^c	0.0636 ^c
			0.5591 ^d	—	—
			12.30 ^e	—	—
			Bulk (homogeneous media)		
			0.0586 ^f	0.5275 ^f	0.0389 ^g

^a Data of Evans et al.³⁷

^b Data of Subramaniam and Santappa.³⁸

^c Data of Mahadevan and Santappa.³⁹

^d Data of Atkinson and Cotton.⁴⁰

^e Data of Baxendale et al.⁴¹

^f Data of Matheson et al.⁴²

^g Data of Bamford and Jenkins.⁴³

values of $k_p/k_t^{1/2}$ evaluated by other workers in similar or allied fields for comparison. The values for the precipitation media are considerably higher than the values for homogeneous media in the cases of methyl methacrylate and methyl acrylate but are of the same order for acrylonitrile. However, the values are in fairly good agreement with the values reported under precipitating conditions.

Grateful acknowledgment is made to the Council of Scientific and Industrial Research, New Delhi, for the award of a Junior Research Fellowship to one of us (A.I.M.S.) during the course of this work.

References

1. Ueberreiter, K., and G. Sorge, *Z. Elektrochem.*, **57**, 795 (1953).
2. Koizumi, M., A. Watanabe, and Z. Kuroda, *Nature*, **175**, 770 (1955).
3. Koizumi, M., and A. Watanabe, *Bull. Chem. Soc. Japan*, **28**, 136 (1955); *ibid.*, **28**, 141 (1955); A. Watanabe, *ibid.*, **32**, 557 (1959).
4. Takemura, F., *Bull. Chem. Soc. Japan*, **35**, 1074 (1962); *ibid.*, **35**, 1078 (1962).
5. Oster, G. K., G. Oster, and G. Prati, *J. Am. Chem. Soc.*, **79**, 595 (1957).
6. Miyama, H., *Nippon Kagaku Zasshi*, **76**, 1013 (1955); *ibid.*, **77**, 691 (1956).
7. Shepp, A., S. Cheberek, and R. MacNeil, *J. Phys. Chem.*, **66**, 2563 (1962).
8. Watanabe, A., and M. Koizumi, *Bull. Chem. Soc. Japan*, **34**, 1086 (1961); A. Watanabe, *ibid.*, **35**, 1562 (1962).
9. Oster, G., *Photo. Eng.*, **4**, 173 (1953); *Nature*, **173**, 300 (1954).
10. Delzenne, G., S. Toppet, and G. Smets, *J. Polymer Sci.*, **48**, 347 (1960).
11. Delzenne, G., W. DeWinter, S. Toppet, and G. Smets, *J. Polymer Sci.*, **A2**, 1069 (1964).
12. Toppet, S., G. Delzenne, and G. Smets, *J. Polymer Sci.*, **A2**, 1539 (1964).

13. Kuroda, Z., and M. Koizumi, *J. Inst. Polytech. Res., Osaka City Univ.*, **C5**, 135 (1956); M. Koizumi, Z. Kuroda, and A. Watanabe, *ibid.*, **C2**, 1 (1951).
14. Watanabe, A., and M. Koizumi, *J. Inst. Polytech. Res. Osaka City Univ.*, **C5**, 114 (1956); *ibid.*, **C5**, 124 (1956).
15. Uri, N., *J. Am. Chem. Soc.*, **74**, 5808 (1952).
16. Oba, H., and I. Fujita, *Kobunshi Kagaku*, **15**, 455 (1958).
17. Takayama, G., *Kobunshi Kagaku*, **17**, 644 (1960).
18. Oster, G. K., G. Oster, and J. R. Nusbaum, paper presented to Division of Polymer Chemistry, American Chemical Society; *Preprints*, No. 2, 290 (1960).
19. Delzenne, G., S. Toppet, and G. Smets, *Bull. Soc. Chim. Belges*, **71**, 857 (1962).
20. Jellinek, Z. K., *Plaste Kautschuk*, **2**, 131 (1955).
21. Oster, G., and Y. Mizutani, *J. Polymer Sci.*, **22**, 73 (1956).
22. Oster, G., and M. Taniyama, *Bull. Chem. Soc. Japan*, **30**, 856 (1957).
23. Korsunovskii, G. A., *Zhur. Fiz. Khim.*, **32**, 1926 (1958).
24. Yoshida, Z., K. Maeda, and R. Oda, *Kogyo Kagaku Zasshi*, **50**, 1161 (1957).
25. Nishijima, Y., *Kyoto Daigaku Nippon Kagakuseni Ken Kyusho Koenshu*, **16**, 141 (1959).
26. Giacintov, N., V. Stannett, and E. W. Abrahamson, *Makromol. Chem.*, **36**, 52 (1959); *J. Appl. Polymer Sci.*, **3**, 54 (1960).
27. Lagercrantz, C., and M. Yhland, *Acta Chem. Scand.*, **16**, 508 (1962).
28. Kransnovskii, A., and H. Umbrikina, *Dokl. Akad. Nauk SSSR*, **104**, 882 (1955).
29. Md. Sheriff, A. I., and M. Santappa, *Current Sci. (India)*, **33**, 302 (1964).
30. Bowen, E. J., *Chemical Aspects of Light*, Oxford Univ. Press, London, 1946, p. 279.
31. Fieser, L. F., *J. Am. Chem. Soc.*, **46**, 2639 (1924).
32. Parker, C. A., *Proc. Roy. Soc. (London)*, **A220**, 104 (1953).
33. Parker, C. A., and C. G. Hatchard, *Proc. Roy. Soc. (London)*, **A235**, 518 (1956).
34. Baxendale, J. H., S. Bywater, and M. G. Evans, *J. Polymer Sci.*, **1**, 237 (1946).
35. Sen, J., S. R. Bannerjee, and S. R. Palit, *J. Sci. Ind. Res.*, **11B**, 90 (1952).
36. Cleland, R. L., and W. H. Stockmeyer, *J. Polymer Sci.*, **17**, 473 (1955).
37. Evans, M. G., M. Santappa, and N. Uri, *J. Polymer Sci.*, **7**, 243 (1951).
38. Subramaniam, R. V., and M. Santappa, *Makromol. Chem.*, **22**, 147 (1956).
39. Mahadevan, V., and M. Santappa, *J. Polymer Sci.*, **50**, 361 (1961).
40. Atkinson, B., and G. R. Cotton, *Trans. Faraday Soc.*, **54**, 877 (1958).
41. Baxendale, J. H., M. G. Evans, and K. Kilham, *Trans. Faraday Soc.*, **42**, 668 (1946).
42. Matheson, M. S., E. B. Bevilacqua, E. E. Auer, and E. J. Hart, *J. Am. Chem. Soc.*, **71**, 497 (1949); *ibid.*, **73**, 1700 (1951).
43. Bamford, C. H., and A. D. Jenkins, *Proc. Roy. Soc. (London)*, **A216**, 515 (1953).

Résumé

On a étudié systématiquement les cinétiques de polymérisation du méthacrylate de méthyle, de l'acrylate de méthyle et de l'acrylonitrile sensibilisés au moyen de systèmes colorant-agent réducteur. Les systèmes ont été irradiés par de la lumière de longueur d'onde comprise entre 350 et 450 μ . La période d'induction avant le commencement de la polymérisation a été maintenue à un minimum au moyen de conditions expérimentales appropriées. Toutes les expériences ont été effectuées en présence d'oxygène. Le système rédox, sel de sodium de la fluorescéine(uranine)-acide ascorbique, a été employé pour la polymérisation. Les systèmes ont été tamponnés au moyen d'un tampon phosphaté. On a étudié l'influence de la température, de la viscosité etc., sur le système réactionnel. Le degré d'avancement des réactions a été suivi par des mesures de la vitesse de disparition du colorant (spectrophotométriquement) et de la longueur de chaîne du polymère formé (viscosimétriquement). Les variables employées sont l'intensité lumineuse, la longueur d'onde, la concentration en monomère, la concentration en colorant, la concentration en agent réducteur, la température, etc. Le schéma

cinétique proposé est examiné à la lumière des résultats expérimentaux. On a évalué les valeurs des constantes spécifiques de vitesse pour les différentes étapes.

Zusammenfassung

Die Kinetik der durch Farbstoff-Reduktionssysteme sensibilisierten Polymerisation der Vinylmonomeren Methylmethacrylat, Methylacrylat und Acrylnitril wurde systematisch untersucht. Die Systeme wurden mit Licht von Wellenlängen im Bereich 350–450 $m\mu$ bestrahlt. Durch geeignete Versuchsbedingungen wurde die Induktionsperiode vor Eintritt der Polymerisation auf einem Minimalwert gehalten. Alle Versuche wurden in Gegenwart von Sauerstoff ausgeführt. Das Redoxsystem Natriumfluoreszein(uranin)–Ascorbinsäure wurde für die Polymerisation verwendet. Die Systeme wurden mit Phosphatpuffer gepuffert. Der Einfluss von Temperatur, Viskosität, etc., auf das Reaktionssystem wurde untersucht. Der Verlauf der Reaktion wurde durch Messung der Geschwindigkeit des Monomerumsatzes (gravimetrisch), der Geschwindigkeit des Farbstoffumsatzes (spektrophotometrisch) und der Kettenlänge des gebildeten Polymeren (viskosimetrisch) verfolgt. Lichtintensität, Wellenlänge, Monomerkonzentration, Farbstoffkonzentration, Reduktionsmittelkonzentration, Temperatur, etc., wurden variiert. Ein versuchsweise aufgestelltes kinetisches Schema wird im Lichte der experimentellen Ergebnisse überprüft. Die Werte der spezifischen Geschwindigkeitskonstanten für die verschiedenen Schritte wurden ermittelt.

Received December 28, 1964

Prod. No. 4677A

Average Lifetime of Growing Chain in Propylene Polymerization

SANAE TANAKA and HIROYUKI MORIKAWA, *Mizonokuchi Research
Laboratory, Mitsubishi Petrochemical Company, Ltd., Kawasaki, Japan*

Synopsis

The value of the active lifetime of the growing chain of propylene polymer obtained with $\text{TiCl}_3\text{-Al}(\text{C}_2\text{H}_5)_2\text{Cl}$ as catalyst was determined to be 33-40 min. by the method of calculating changes of number-average molecular weight from measurements of molecular weight distribution. In addition, the influence of reaction conditions (reaction temperature, monomer concentration, catalyst concentration, reaction time, terminating agent) upon the active lifetime was examined. The data obtained support the theory of the occurrence of chain transfer. An expression was obtained for the lifetime distribution of the polymer.

INTRODUCTION

In their studies of the polymerization of α -olefins by use of Ziegler-Natta catalysts, Natta,¹ Bier,^{2,3} and Kontos⁴ indicated that the average lifetime of the growing polymer chain was rather long.

In the case of the polymerization of propylene, it was reported that the average lifetime was 4-7 min.⁵ when $\text{TiCl}_3\text{-Al}(\text{C}_2\text{H}_5)_3$ catalyst was used, and was of the same order (1-30 min.)⁶ when $\text{TiCl}_3\text{-Al}(i\text{-C}_4\text{H}_9)_3$ catalyst was used. On the other hand, with $\text{TiCl}_3\text{-Al}(\text{C}_2\text{H}_5)_2\text{Cl}$ as catalyst, the data are conflicting: some authors^{2,3,7,8} report a very long lifetime of (more than 10 hr.), while Caunt⁹ has found a short lifetime (about 12 min.). All of the previous calculations were made from intrinsic viscosity (or number-average molecular weight calculated from the latter) data versus polymerization time. However, it has been found that the number-average molecular weight of polypropylene is greatly influenced by the width of the molecular weight distribution ($\overline{M}_w/\overline{M}_n$)¹⁰ and also that the molecular weight distribution depends on time.¹¹ The values for the lifetime of the growing chain were derived from the above-mentioned method which ignores these effects.

In the present study, the active polymer lifetime was obtained for polymerization of propylene with $\text{TiCl}_3\text{-Al}(\text{C}_2\text{H}_5)_2\text{Cl}$ catalyst, by calculating changes of number-average molecular weight from the measurements of molecular weight distribution of polypropylene by a turbidimetric method.¹¹

EXPERIMENTAL

Materials

Propylene (Sinclair Co.; C. P. Grade) had a purity of 99.5%.

n-Heptane (Enjay Co.) was purified by distillation after refluxing on sodium metal.

Diethylaluminum chloride (Ethyl Corp.) was purified by distillation.

Titanium trichloride (Stauffer Chemical Co., A. A. Grade), having a surface area of 20 m.²/g. as measured by the B.E.T. method, was used.

Polymer Preparation

Polymerization was carried out in a 3-liter stainless steel autoclave, which was purged with nitrogen and then charged with 1.5 liters of *n*-heptane and catalysts [2g. TiCl₃ and 2.5 g. Al(C₂H₅)₂Cl] in that order. Then, propylene was charged under a constant pressure (2 kg./cm.²) at constant temperature (70°C.). The polymerization was quenched with a mixture of 300 ml. of *n*-butanol and 30 ml. of 1*N* hydrochloric acid; the catalysts were then decomposed by refluxing at 80°C. for 4 hr.

The polymer slurry was filtered by centrifugation at 80°C., washed with water, then dried at 60°C. in a vacuum oven.

Determination of Molecular Weight

The molecular weights of the polymers were calculated from intrinsic viscosity and turbidimetric titration measurement.

Intrinsic viscosities were measured in decalin containing 0.1% phenyl β -naphthylamine at 135°C. under nitrogen atmosphere.

Although the viscosity-molecular weight equation of Chiang¹² was employed:

$$[\eta] = 1.00 \times 10^{-4} [\bar{M}_w]^{0.80}$$

it was recognized that this correlation could not be applied quantitatively to samples having widely different molecular weight distributions; therefore, \bar{M}_w values were calculated from the molecular weight distribution.¹¹

Determination of Molecular Weight Distribution

Molecular weight distributions were measured by the turbidimetric titration method¹³ (Desreux type) under the following conditions: solvent: mixture of tetralin and butylcellosolve (6:4); precipitant: butylcellosolve; temperature: 110°C.; initial concentration: 3 mg. polymer/100 ml. solvent; feed rate of precipitant: 2 ml./min.

It was found that the type of molecular weight distribution could be expressed by the modified log normal distribution.^{11,13,14} The value of \bar{M}_w calculated by using this type of distribution from the molecular weight distribution agreed with the values calculated by the intrinsic viscosity method.

Calculation of \bar{M}_n and \bar{M}_w from Molecular Weight Distribution

When molecular weight distribution of polypropylene is expressed by a modified log normal distribution, its weight-average (\bar{M}_w) and number-average molecular weights (\bar{M}_n) are expressed by eqs. (1) and (2), respectively.¹¹

$$\bar{M}_n = M_0 e^{-\sigma^2/2} (2/f) \{1 + \operatorname{erf} [\rho + (\sigma/\sqrt{2})]\}^{-1} \quad (1)$$

$$\bar{M}_w = M_0 e^{-\sigma^2/2} (f/2) \{1 + \operatorname{erf} [\rho - (\sigma/\sqrt{2})]\} \quad (2)$$

where M_0 is molecular weight when the integral weight fraction of distribution function is equal to 0.5, and f and ρ are parameters of distribution defined by eqs. (3) and (4), respectively,

$$f = 2 (1 + \operatorname{erf} \rho)^{-1} \quad (3)$$

$$\rho = \frac{\ln M_m/M_0}{\sqrt{2} \sigma} \quad (4)$$

where M_m , is the maximum molecular weight reached and σ is standard deviation, calculated from the slope of probability plot.

Calculation of the Average Lifetime of the Growing Chain, $\bar{\tau}$

The average lifetime of the chain $\bar{\tau}$ can be determined by eq. (5), assuming Natta's mechanism:⁵

$$\bar{\tau} = [d(1/\bar{x}_n)/d(1/t)] \bar{x}_n \quad (5)$$

where t is polymerization time and \bar{x}_n is the number-average degree of polymerization.

If the number of active sites [C*] is known for the steady state, $\bar{\tau}$ can be determined from eq. (6).

$$\bar{\tau} = [C^*](\bar{x}_n/r_p) \quad (6)$$

where r_p is the rate of polymerization.

The conventional method for estimating the order of the lifetime in the steady state is obtained by use of eq. (7) from the curve of x_n versus time.

$$x_{\bar{\tau}} = x_n/2 \quad (7)$$

RESULTS AND DISCUSSION

Average Lifetime of the Growing Chain

The variation of the number-average degree of polymerization \bar{x}_n with reaction time t under certain conditions is illustrated in Figure 1.

The average lifetime of the growing chain $\bar{\tau}$ derived from eq. (5) is about 33–40 min. To check this, we tried to compare the number of active sites.

The reaction rate r_p and the number-average degree of polymerization x_n (at 70°C., under 2 kg./cm.² propylene pressure) are $r_p = 1.63 \times 10^{-2}$ mole C₃H₆/min.-g. TiCl₃; $\bar{x}_n = 7.25 \times 10^3$.

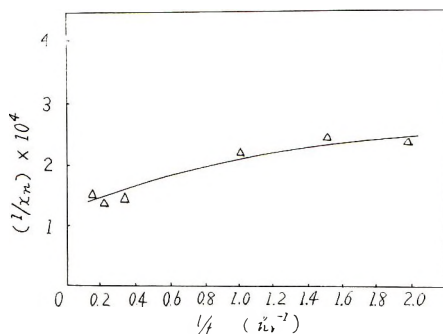


Fig. 1. Relationship between \bar{x}_n and reaction time t at 70°C ., 2 kg./cm.² propylene pressure, 2 g. TiCl_3 , 1.5 liters n -heptane, Al/Ti = 2.5.

The number of active sites $[\text{C}^*]$, as determined from eq. (6), is then

$$[\text{C}^*] = 7.45 \times 10^{-5} - 9.0 \times 10^{-5} \text{ mole site/g. TiCl}_3$$

or

$$[\text{C}^*] = 1.16 \times 10^{-2} - 1.4 \times 10^{-2} \text{ mole site/mole TiCl}_3$$

This value suggests that the most of the surface of the solid TiCl_3 can be accounted by the number of active sites, since the surface area of the TiCl_3 used (A. A. type) is of the order of 20 M.²/g., and the adsorbed $\text{AlEt}_2\text{-Cl}$ molecules occupy an area of about 40 A.²/molecule.

The number of active sites is influenced by many variables, such as the extent of poisoning of the used TiCl_3 , the amount of alkylaluminum reversibly adsorbed on the TiCl_3 surface, the particle size of the TiCl_3 , conditions of catalyst preparation, and reaction conditions.

Therefore, it seems very difficult to determine the exact value. Since there is agreement between $\bar{\tau}$ derived from eq. (6) for a value of $[\text{C}^*] = 1.0 \times 10^{-2}$ mole site/mole TiCl_3 (A. A.) and that derived from eq. (5) by the graphical method, it seems reasonable to calculate the approximate value of $\bar{\tau}$, in the stationary state from eq. (6), assuming minor variations in $[\text{C}^*]$ depending on reaction conditions.

Absolute Rate

It is of interest to calculate the absolute propagation rate constant k_p in the $\text{AlEt}_2\text{Cl-TiCl}_3$ catalyst system. The number of active sites $[\text{C}^*]$ is 1.0×10^{-2} mole site/mole TiCl_3 , and the observed polymerization rate r_p is 2.52 mole C_3H_6 /min.-mole TiCl_3 at 70°C . and under at a propylene pressure 2 kg./cm. (the concentration of propylene $[\text{C}_p]$ in n -heptane is 0.75 mole/l.).

Therefore, the absolute rate constant k_p can be described by eq. (8):

$$k_p = r_p/[\text{C}^*][\text{C}_p] = 5.6 \text{ l./mole-sec.} \quad (8)$$

By comparison with this value in free radical polymerization, the polymerization of the coordinated complex catalyst can be regarded as com-

TABLE I
Absolute Rate Constant in Ziegler-Natta Catalyst Systems

Monomer	Catalyst system	Temp., °C.	k_p , l./mole-sec.	Reference
Propylene	AlEt ₂ Cl-TiCl ₃ (A.A.)	70	5.6	
Propylene	AlEt ₃ -TiCl ₃	70	2.5	5
Propylene	AlEt ₂ Cl-TiCl ₃ (A.A.)	50	1.2	7
Propylene	AlEt ₂ Cl-TiCl ₃	50	0.426	8
		70	1.15	
		90	3.50	
Ethylene	Al(<i>i</i> -C ₄ H ₉) ₃ -TiCl ₄	54.5	127	6
Ethylene	Al(CH ₃) ₂ Cl-(C ₂ H ₅) ₂ TiCl ₂	30	13.6	17

paratively mild. The absolute rates in other systems are listed in Table I.

The differences in k_p value in Table I are due partly to the method calculation of the number of the active sites.

Changes of Average Lifetime with Reaction Conditions

Data illustrating the effects of the reaction conditions (temperature, monomer concentration, catalyst concentration, polymerization time) in the AlEt₂Cl-TiCl₃/*n*-heptane system are presented in Table II. The dependence of the average lifetime on polymerization temperature, mono-

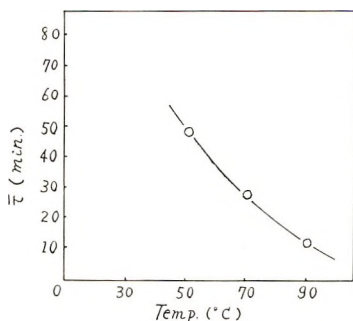


Fig. 2. Relationship between $\bar{\tau}$ and polymerization temperature at $t = 3$ hr., propylene pressure 2 kg./cm.², 2 g. TiCl₃, 1.5 liters *n*-heptane, Al/Ti = 2.5.

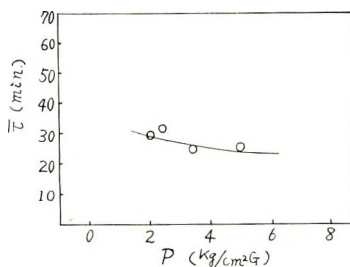


Fig. 3. Relationship between $\bar{\tau}$ and monomer pressure at 70°C., $t = 3$ hr., 2 g. TiCl₃, 1.5 liters *n*-heptane, Al/Ti = 2.5.

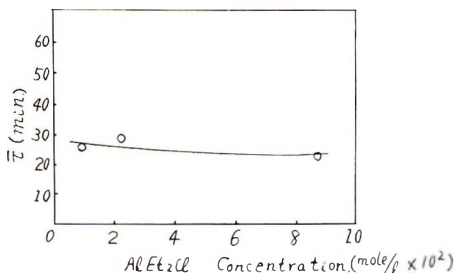


Fig. 4. Relationship between $\bar{\tau}$ and catalyst concentration at 2 kg./cm.² propylene pressure, 70°C., $t = 3$ hr., 2 g. TiCl₃, 1.5 liters *n*-heptane.

TABLE II
Changes of $\bar{\tau}$ with Reaction Conditions^a

Run no.	Propylene pressure, kg./cm. ²	Temp., °C.	Al/Ti	$r_p \times 10^2$ mole C ₃ H ₆ /min.	$[\eta]$, dl./g.	$\bar{M}_n \times 10^{-3}$	$\bar{\tau}$, min.
12	2	30	2.5	0.77	10.0	13.5	226
17	2	50	2.5	2.12	7.62	7.95	48.6
1	2	70	2.5	3.26	5.70	7.25	28.8
7	2	70	10.0	3.27	4.60	5.65	22.5
25	2	70	1.0	3.37	5.76	6.66	25.6
66	2.4	70	2.5	3.61	6.0	9.10	32.7
67	3.4	70	2.5	6.64	7.9	12.4	24.4
68	5	70	2.5	8.15	9.2	16.0	25.3
13	2	90	2.5	3.14	2.76	2.88	11.9

^a Conditions: 1.5 liters *n*-heptane, $t = 3$ hr., 2.0 g. TiCl₃.

mer concentration, and catalyst concentration are shown in Table II and Figures 2-4.

With decreasing reaction temperature, the average life time $\bar{\tau}$ increases; such a tendency is peculiar to "living" polymer (Fig. 2). The average lifetime does not change regularly with monomer concentration but it seems to be slightly higher at lower monomer concentrations (Fig. 3).

The change of the average lifetime with polymerization time is shown in Table III and Figure 5. It is noticed that $\bar{\tau}$ changes with polymerization time initially but after this period it becomes a constant.

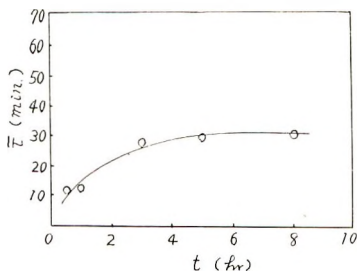


Fig. 5. Relationship between $\bar{\tau}$ and reaction time t at 70°C., 2 kg./cm.² propylene pressure 2 g. TiCl₃, 1.5 liters *n*-heptane, Al/Ti = 2.5.

TABLE III
Changes of $\bar{\tau}$ with Reaction Conditions^a

Run no.	Time t , hr.	$r_p \times 10^2$, mole C ₃ H ₆ /min.	$[\eta]$, dl./g.	$\bar{x}_n \times 10^{-3}$	$\bar{\tau}$, min.
16	0.5	4.0	3.38	4.05	13.0
19	1.0	4.5	3.44	4.50	13.0
1	3.0	3.26	5.70	7.25	28.8
20	5.0	3.36	5.70	7.56	29.2
21	8.0	2.97	5.74	6.95	30.4

^a Conditions: 70°C., 2 kg./cm.² propylene pressure, 1.5 liters *n*-heptane, 2.0 g. TiCl₃, Al/Ti = 2.5.

It is difficult to interpret the increase of $\bar{\tau}$ except at the beginning of the polymerization for this reaction model.

TABLE IV
Changes of $\bar{\tau}$ with Concentration of Termination Agent (H₂)^a

Run no.	H, % (in gas phase)	$r_p \times 10^2$, mole C ₃ H ₆ /min.	$[\eta]$, dl./g.	$\bar{x}_n \times 10^{-3}$	$\bar{\tau}$, min.
1	0	3.26	5.7	7.25	28.8
4	2.8	3.81	2.75	4.50	15.3
5	7	3.65	1.38	2.17	7.74

^a Conditions: 70°C., 2 kg./cm.² propylene pressure, 1.5 liters *n*-heptane, 2.0 g. TiCl₃, Al/Ti = 2.5, $t = 3$ hr.

Changes of Average Lifetime Depending on Terminating Agent (Hydrogen)

The effect of the addition of a terminating agent such as hydrogen is shown in Table IV and Figure 6. The average lifetime $\bar{\tau}$ decreases rapidly with hydrogen concentration (Fig. 6).

Relationship between Lifetime and Molecular Weight

The relationship between the average lifetime $\bar{\tau}$ and the number-average molecular weight M_n , under 2 kg./cm.² of monomer pressure is illustrated in Figure 7.

In a Ziegler-Natta catalyst system, polypropylene has a linear, unbranched structure, and during polymerization the combination or decomposition of polymer may not occur. Therefore, a simple one-to-one relationship between the lifetime of the growing chain and the degree of polymerization is reasonable. When the rate constants do not depend on chain length, this relation should be linear.

However, the plot in Figure 7 tends to deviate from a straight line in the region of high molecular weight ($\bar{M}_n > 30 \times 10^4$), which would indicate that the rate constants depend to some degree on chain length. Similar observations on polyethylene were previously reported by Feldman and Perry.⁶

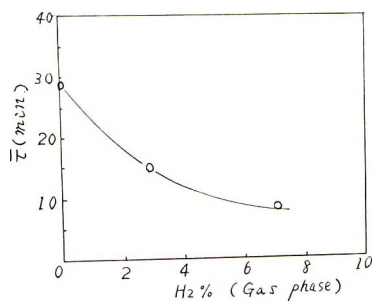


Fig. 6. Relationship between $\bar{\tau}$ and termination agent (H_2) at $70^\circ C.$, $t = 3$ hr., 2 kg./cm.², propylene pressure 2 g. $TiCl_3$, 1.5 liters n -heptane, $Al/Ti = 2.5$.

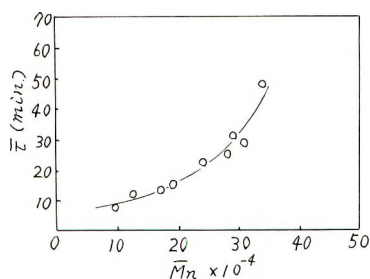


Fig. 7. Lifetime of growing chains as a function of molecular weight at 2 kg./cm.² propylene pressure, 2 g. $TiCl_3$, $Al/Ti = 2.5$, 1.5 liters n -heptane.

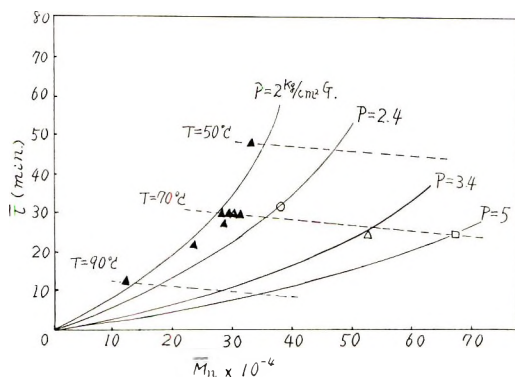


Fig. 8. Changes of M_n - $\bar{\tau}$ relation with reaction conditions.

Gordon and Roe¹⁵ also derived the log normal distribution of molecular weight, assuming that rate constants depend on chain length, and they obtained the value of \bar{M}_w/\bar{M}_n on the basis of their theory.

However, it seems very difficult to decide the true mechanism from the \bar{M}_w/\bar{M}_n dependence. The change in the \bar{M}_n - $\bar{\tau}$ relation with reaction conditions is shown in Figures 8 and 9.

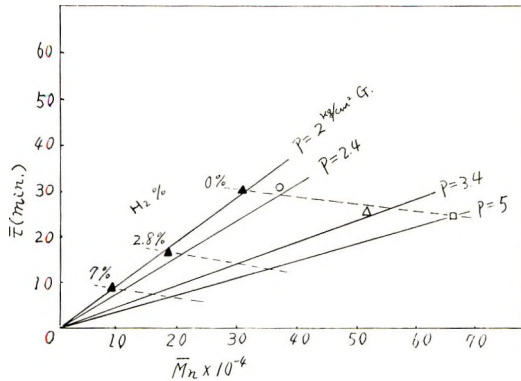


Fig. 9. Changes of \bar{M}_n - $\bar{\tau}$ relation at 70°C. with level of terminating agent (H_2).

Lifetime Distribution

When the \bar{M}_n - $\bar{\tau}$ relation is established, the lifetime distribution of the growing chain can be derived from the molecular weight distribution. Now, assuming that the rate constant k_p of each active site is approximately uniform, the log normal feature of molecular weight distribution is translated to a non-Gaussian nature (negative skewness) in the lifetime distribution, as shown in Figure 10.

Mussa¹⁶ showed that the log normal feature is derived from the Gaussian nature of the lifetime distribution, assuming the distribution of the rate constant of each catalyst site.

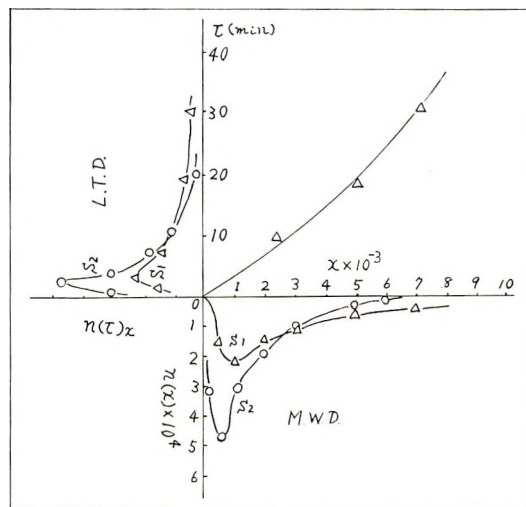


Fig. 10. Plot of molecular weight distribution (MWD) and lifetime distribution (LTD) with polymerization at propylene pressure of 2 kg./cm.²: (O) $\bar{M}_w = 100 \times 10^4$, $\sigma = 1.15$; (Δ) $\bar{M}_w = 50 \times 10^4$, $\sigma = 1.15$. Here, x is the degree of polymerization ($M/42$) and $n(x)$, the number fraction of x , is defined by $n(x) = [w(x)/x] \bar{x}_n$, where $w(x) = (1/\sigma\sqrt{2\pi})(1/x) \exp \{-(1/2\sigma^2) \ln(x/x_0)\}$, $\bar{x}_n = x_0 \exp \{-\sigma^2/2\}$, $\bar{x}_w = x_0 \exp \{\sigma^2/2\}$.

Since the region of high molecular weight tail is also shown for a sample obtained with a short polymerization time, homogeneity for all active sites does not appear likely.

It is concluded that the average lifetime of polymerization in $AlEt_2Cl-TiCl_3$ catalyst system is shorter than indicated by the results of Bier² and Chien⁸ and that polypropylene in such a case has a lifetime distribution dependent on the transfer reaction.

References

1. Natta, G., *J. Polymer Sci.*, **34**, 531 (1959).
2. Bier, G., G. Lehman, and H. J. Levgering, *Plastic Inst. Trans. J.*, **28**, 98 (1960).
3. Bier, G., et al., *Makromol. Chem.*, **44/46**, 347 (1961).
4. Kontos, E. G., E. K. Easterbrook, and R. D. Gilbert, *J. Polymer Sci.*, **61**, 69 (1962).
5. Natta, G., et al., *J. Polymer Sci.*, **34**, 21 (1959).
6. Feldman, C. F., and E. Perry, *J. Polymer Sci.*, **46**, 217 (1960).
7. Bier, G., W. Hoffmann, G. Lehman and G. Seydel, *Makromol. Chem.*, **58**, 1 (1962).
8. Chien, J. C. W., *J. Polymer Sci.*, **A1**, 425 (1963).
9. Caunt, A. D., *J. Polymer Sci.*, **C4**, 49 (1963).
10. Koningsveld, R. and C. A. F. Tvijan, *J. Polymer Sci.*, **39**, 445 (1959); *Makromol. Chem.*, **38**, 39 (1960).
11. Tanaka, S., H. Morikawa, and A. Nakamura, paper presented at the 12th Annual Meeting of the Society of Polymer Science of Japan, May 25, 1963.
12. Chiang, R., *J. Polymer Sci.*, **28**, 235 (1957).
13. Tanaka, S., A. Nakamura, and H. Morikawa, paper presented at the 11th Annual Meeting of the Society of Polymer Science of Japan, May 26, 1962.
14. Davis, T. E., R. T. Tobias, and E. B. Peterli, *J. Polymer Sci.*, **56**, 485 (1962).
15. Gordon, M., and R. J. Roe, *Polymer*, **2**, 41 (1961).
16. Mussa, C., *J. Appl. Polymer Sci.*, **1**, 300 (1959).
17. Chien, J. C. W., *J. Am. Chem. Soc.*, **81**, 86 (1959).

Résumé

On a obtenu la valeur de la durée de vie active de la chaîne en croissance du polypropylène en utilisant $TiCl_3-Al(C_2H_5)_2Cl$ comme catalyseur, par la méthode de calcul des changements de poids moléculaire moyen en nombre à partir de mesures de la distribution du poids moléculaire. Cette durée de vie est de 33 à 40 minutes. En outre, on a examiné l'influence des conditions de réaction (température de réaction, concentration en monomère, concentration en catalyseur, durée de réaction, agent de terminaison), sur la durée de vie active. A partir des résultats obtenus, la théorie de l'existence d'un transfert de chaîne est confirmée et la distribution de la durée de vie du polymère à été également exprimée.

Zusammenfassung

Für die aktive Lebensdauer einer wachsenden Propylenpolymerkette mit einem $TiCl_3-Al(C_2H_5)_2Cl$ -Katalysator wurde nach der Methode der Berechnung der Änderung des Zahlenmittelmolekulargewichts aus der Messung der Molekulargewichtsverteilung ein Wert von 33–40 min erhalten. Weiters wurde der Einfluss der Reaktionsbedingungen (Reaktionstemperatur, Monomerkonzentration, Katalysatorkonzentration, Reaktionsdauer, Abbruchmittel) auf die aktive Lebensdauer untersucht. Die erhaltenen Daten bilden eine Stütze für die Theorie des Auftretens von Kettenübertragung und gestatten eine Angabe der Lebensdauerverteilung des Polymeren.

Received December 3, 1964

Prod. No. 4690A

Catalyst and Solvent Effects in the Terpolymerization of Ethylene, Propylene, and Dicyclopentadiene

ROBERT E. CUNNINGHAM, *Research Division, Goodyear Tire and Rubber Company, Akron, Ohio*

Synopsis

Ethylene, propylene, and dicyclopentadiene were terpolymerized to form unsaturated, sulfur-curable elastomers, by use of catalysts of VCl_4 or $VOCl_3$ (with $Al_2Et_3Cl_3$ cocatalyst) and polymerization solvents of heptane, benzene, or tetrachloroethylene. Of the various possible catalyst-solvent combinations, best overall balance of results was given by $VOCl_3$ catalyst in benzene solvent. All other combinations, except one, also gave good results, however, with some having special points of merit. The exception was $VOCl_3$ in heptane solvent, which produced erratic yields of highly gelled polymer. A limited study was made of the effect of the dicyclopentadiene concentration on polymerization. Increasing the diene concentration decreased polymer yield but increased its unsaturation; it had no gross effect on the inherent viscosities of the polymers. Terpolymers containing more than about 0.30 mole $C=C/kg.$ can be cured tightly with sulfur-based vulcanizing recipe.

INTRODUCTION

In the last few years, considerable research has been carried out on the copolymerization of ethylene and propylene with the use of Ziegler-Natta catalysts to an amorphous elastomer. More recently, most research effort has been directed toward the terpolymerization of ethylene, propylene, and a nonconjugated diene to produce an unsaturated, sulfur-curable elastomer. Published data indicate that a wide variety of dienes may be used for this purpose, but perhaps the main one that has been used is dicyclopentadiene. Several groups have reported various results with this terpolymerization system,¹⁻⁵ but experimental data on the effects of different possible catalyst-solvent combinations were scanty. Detailed studies were undertaken in our laboratories to attempt to determine, if possible, the best combination of catalyst and solvent for the preparation of elastomeric ethylene-propylene-dicyclopentadiene terpolymers by use of catalysts and solvents that were known to be satisfactory for the copolymerization of ethylene and propylene.

EXPERIMENTAL

Materials

n-Heptane was obtained from Phillips Petroleum Company. It was washed successively with concentrated H_2SO_4 , potassium carbonate solution, and distilled water, then distilled and stored over Drierite. Benzene

was ACS reagent grade; it was passed through a silica gel column before use. Tetrachloroethylene was superior grade from Matheson, Coleman and Bell; it was also passed through silica gel before use.

Aluminum ethyl sesquichloride was from Ethyl Corporation, and was used as received. It was listed by the manufacturer as containing 21.5% Al (21.8% theor.) and 42.8% Cl (43.0% theor.). Vanadium oxytrichloride and vanadium tetrachloride were obtained from Anderson Chemical Division of Stauffer Chemical Company and were used as received.

Ethylene and propylene were C.P. grades from The Matheson Company. They were passed through two scrubbing towers of Fieser's solution⁶ to remove oxygen traces, then through calcium chloride, Drierite, and a 10% Al(*i*-Bu)₃ solution in kerosene before passage into the reactor.

Dicyclopentadiene was high-purity grade from Union Carbide Olefins Company. It was vacuum-distilled in a nitrogen atmosphere before use, b.p. 58°C./13 mm. It was a white solid at room temperature and was stored under nitrogen.

Catalyst Solutions

For all runs, the Al₂Et₃Cl₃ was handled as a 1.0*M* (in Al) solution in heptane (0.50*M* for the formula weight of Al₂Et₃Cl₃). The VCl₄ was made up as a 0.1*M* solution in heptane, and VOCl₃ as a 0.32*M* solution in heptane. All solutions were kept under nitrogen in 4-oz. bottles that were capped with self-sealing rubber gaskets and were transferred with hypodermic syringes. It is known that VCl₄ decomposes slowly to VCl₃ and Cl₂, especially under the influence of heat or light. By keeping the VCl₄ stock solution fairly dilute and storing it in a refrigerator, it was found that it could be kept for several weeks before any visible precipitate of VCl₃ could be seen. The VCl₄ stock solutions were generally used, however, within a few days after they were prepared.

Polymerizations

Reactions were carried out in a 1-liter resin kettle, fitted with a Teflon paddle stirrer, reflux condenser, thermometer, gas-inlet tube, and rubber serum cap. Glassware was thoroughly cleaned and dried. The apparatus was assembled and placed in an ice-water bath. In all runs, 500 ml. of solvent was used.

Ethylene and propylene were metered in at 1200 and 800 cc./min., respectively, by use of calibrated flowmeters. Mass spectrographic analysis was made of a feed gas sample for each run, and it was found to average very close to 58 mole-% ethylene. The gases were passed through a T-tube to form a common stream, then through the purification train and into the resin kettle through the inlet tube, which went well below the surface of the solvent. The feed stream was bubbled through the entire system and out the reflux condenser for at least 15 min., both to purge the system of air and to saturate the solvent with the monomers.

The appropriate amount of dicyclopentadiene was added. It was warmed slightly to melt it (literature m.p. = 33°C.) and transferred by injecting it into the resin kettle through the serum cap with a hypodermic syringe. All reactions were initiated at 5°C. The catalysts were all formed *in situ*, the $\text{Al}_2\text{Et}_3\text{Cl}_3$ being injected first. Both catalyst components were added all at the start of the reaction, with no subsequent incremental additions. Catalyst colors ranged from purple through rose shades, all of which faded rapidly in a few minutes to light rose or perhaps even colorless solutions. In all runs, the vanadium concentration was 0.001*M* and the Al/V molar ratio was 10.

Initial polymerization activity in all cases was very high. Rapid reaction took place for a few minutes and the exotherm raised the temperature of the reaction mixture 20–30°C. in less than 5 min., even with the ice-water cooling bath around the resin kettle. Reaction then began slowing down as evidenced by increasing flow of gases through a flowmeter attached to the exit of the reflux condenser. Reaction was continued for 30 min., agitation as vigorous as possible being maintained. At the end of this time, the reaction mixture was a viscous cement. It was coagulated in isopropanol containing a small amount of a phenolic antioxidant. After soaking 24 hr., the polymer was cut up and soaked another 24 hr. in a fresh portion of isopropanol. It was then dried in a vacuum oven at moderate temperatures (< 50°C.).

Polymer Evaluation

Inherent viscosity was measured in toluene at 30°C. with 0.25 g. of polymer in 50 ml. of toluene. The inherent viscosity of only that portion of polymer soluble in toluene at 30°C. is measured, of course; the insoluble portion is reported in Table I. This insoluble polymer can apparently arise in two different ways: from short blocks of crystalline polymer, or true, crosslinked gel. No quantitative measurements of crystallinity were attempted on these insoluble portions. A qualitative test was made however, by checking the solubility of the polymers in hot toluene (80°C.); short blocks of crystalline polymer are apparently soluble under such a condition, but crosslinked gel is not. Nearly all the polymers in Table I, which have fairly low amounts of insoluble content at 30°C., are found to be completely soluble in hot toluene. The exceptions are noted in the Results and Discussion section.

Crosslinked gel may be formed by polymerization of both double bonds of the dicyclopentadiene. Gladding et al.² showed that the 9, 10 double bond of the dicyclopentadiene is the one most reactive toward polymerization, but that the 1,2 double bond is also slightly reactive. They did not list the catalyst-solvent combination used for this study, but it seems reasonable that the reactivity of both double bonds would vary with different catalysts and solvents. Thus polymerization conditions might arise in which the reactivity of the 1,2 double bond becomes appreciable, relative to the reactivity of the 9,10 double bond. Both would then take part to

TABLE I
Ethylene-Propylene-Dicyclopentadiene Terpolymerization with Various Catalysts and Solvents^a

Run no.	Solvent	Dicyclopentadiene, g./500 ml.	Terpolymer yield, g.	Inherent viscosity	Insoluble polymer, %	Unsaturation, mole C=C/kg.	Volume swelling, % 15 min. cure	Volume swelling, % 60 min. cure
VOCl ₃ Catalyst								
418	Benzene	0	37.5	1.49	7.2	—	—	—
419	Benzene	0.5	34.5	1.40	4.9	0.09	1710	992
420	Benzene	1.0	32.5	1.51	1.9	0.19	1200	608
421	Benzene	1.5	30.5	1.55	1.6	0.29	545	404
422	Benzene	3.0	29	1.45	1.0	0.58	321	298
423	Benzene	4.5	26	1.58	10.2	1.00	245	232
439	Tetrachloroethylene	0	32	1.82	4.8	—	—	—
438	Tetrachloroethylene	0.5	29	2.05	1.4	0.12	1280	768
435	Tetrachloroethylene	1.0	28.5	1.92	2.1	0.24	780	527
436	Tetrachloroethylene	1.5	25.5	1.95	4.1	0.40	437	342
437	Tetrachloroethylene	3.0	21	1.62	26.1	0.97	227	226
VCl ₄ Catalyst								
427	Benzene	0	37.5	1.65	2.0	—	—	—
428	Benzene	0.5	30	1.82	1.7	0.12	2070	906
429	Benzene	1.0	27.5	2.04	1.9	0.26	738	383
430	Benzene	1.5	26.5	2.24	0.8	0.34	582	316
431	Benzene	3.0	24	2.06	4.1	0.74	247	225
432	Benzene	4.5	24	1.84	5.3	1.14	211	204
441	Heptane	0	27	2.31	1.9	—	—	—
442	Heptane	0.5	24.5	2.68	4.1	0.14	838	523
443	Heptane	1.0	21.5	2.62	24.9	0.32	419	313
444	Heptane	1.5	20	1.60	52.2	0.52	290	253
445	Heptane	3.0	17	1.49	36.0	1.22	198	183
446	Tetrachloroethylene	0	41	1.86	3.5	—	—	—
447	Tetrachloroethylene	0.5	38	2.18	2.9	0.17	1526	839
448	Tetrachloroethylene	1.0	30.5	2.28	2.0	0.28	569	387
449	Tetrachloroethylene	1.5	25.5	2.21	16.6	0.51	361	286
450	Tetrachloroethylene	3.0	22.5	1.62	29.9	0.98	223	215

^a Experimental section gives details of the polymerization conditions and the method of measuring the various tabulated quantities.

some extent in polymerization, resulting in crosslinking. Concentration of the dicyclopentadiene in the polymerization system should also play a small role in the degree to which the 1,2 double bond polymerizes. Unsaturation was measured by the iodine monochloride method.

Cured Polymer Properties

All terpolymers were compounded with the following recipe: 100 parts rubber, 5 parts zinc oxide, 1.5 parts tetramethylthiuram monosulfide, and 1.25 parts sulfur. Samples were press-cured at 320°F. for 15 or 60 min. They were then swollen at least 48 hr. in toluene at room temperature, weighed, and dried to constant weight by the usual techniques to determine volume swell. Values are reported in terms of volumes of toluene per volume of dry rubber, the dry weight being determined after swelling (i.e., with all toluene-soluble matter removed from the network).

RESULTS AND DISCUSSION

The two catalysts used in these studies were VOCl_3 and VCl_4 , with $\text{Al}_2\text{Et}_3\text{-Cl}_3$ as cocatalyst. Three solvents were used: heptane, benzene, and tetrachloroethylene. With each catalyst-solvent combination, the dicyclopentadiene level in the polymerization mixture was varied over a small range. The complete experimental results are given in Table I. Some important points can be noted about each of the catalyst-solvent combinations that were investigated.

VOCl_3 with Benzene Solvent. This system gave slightly better terpolymer yields than any other. (Mechanical factors may sometimes be rate-controlling in these reactions, however, and thus may influence polymer yields.) Inherent viscosities of the polymers averaged about 1.5, and insoluble portions of the polymers were low. Polymers with the higher unsaturations cured tightly with the sulfur recipe. All these results are satisfactory for the preparation of unsaturated ethylene-propylene rubber. It was felt that this particular system gave the best overall balance of results of those that are reported in this paper.

VCl_4 with Benzene Solvent. This is also a very satisfactory system, giving good yields of terpolymer. Their inherent viscosities were slightly higher than those made with VOCl_3 in benzene, averaging about 2.0. Insoluble portions of the terpolymers were quite low, and they had slightly higher unsaturation than those made with VOCl_3 . Direct comparison of terpolymer unsaturation between various catalyst-solvent systems cannot be made in these series of experiments, except where terpolymer yields are the same. Since all dicyclopentadiene is charged at the start of the run, but monomers are fed in continually, terpolymer unsaturation changes continuously during a run. Were reactions carried far enough, all dicyclopentadiene would be exhausted, and only copolymer would be formed; our reactions are always terminated before this point is reached. Additional experiments are underway in our laboratories to determine which system is

most efficient for introducing unsaturation into the terpolymer. These terpolymers all cured tightly, especially at the higher levels of unsaturation.

VOCl₃ with Tetrachloroethylene Solvent. This system also gave good yields of terpolymer with satisfactory inherent viscosities, averaging about 1.9. Insoluble polymer content was low, except at the highest dicyclopentadiene level, and polymers cured tightly. Tetrachloroethylene, because of its high density and boiling point, is difficult to remove from the polymers.

VCl₄ with Tetrachloroethylene Solvent. This system gave slightly better yields than did VOCl₃ in this solvent, with concomitantly higher inherent viscosities for the corresponding terpolymers. The fractions of insoluble polymer were low, except at the highest dicyclopentadiene levels, and the polymers cured very tightly.

VCl₄ with Heptane Solvent. This system gave the lowest yields of any of the systems reported here. The inherent viscosities of the terpolymers were high when the dicyclopentadiene concentration was low, but fell off sharply as the dicyclopentadiene concentration increased. Undoubtedly part of this phenomenon was caused by the high content of insoluble polymer in the latter samples, the highest of any reported here. The samples could be compounded, however, and gave very tight cures.

VOCl₃ with Heptane Solvent. No data are reported here on this system, since all of our experiments have given very erratic results, usually producing polymers with high proportions of insoluble material.

Much of the insoluble portions of polymers mentioned in the above sections is soluble in hot toluene (80°C.), and probably consists of short blocks of crystalline polymer. With the VOCl₃-heptane combination, however, much of the insoluble polymer appears to be true, crosslinked gel; apparently both of the double bonds of the dicyclopentadiene will polymerize to some extent in this system.

The effect of dicyclopentadiene concentration on polymerization can also be noted from the data. As the initial diene concentration increases, terpolymer yield in all systems decreases, and unsaturation increases as expected. There is no gross effect of dicyclopentadiene on the inherent viscosities of the terpolymers, but there does appear to be a slight increase of a few tenths of a unit in the viscosities as the diene concentration increases (those samples which have high insoluble content being neglected). The highest levels of insoluble content are associated with the highest dicyclopentadiene concentrations. Evidently a concentration level is reached at which the second double bond of the diene begins to polymerize, causing crosslinking, or the terpolymer composition is altered by the diene to the point where insoluble, crystalline polyolefin blocks may begin to appear in the chains. Both effects may come into play in some cases. Our efforts at determining the propylene content of the terpolymers have given erratic results to date and hence are not included here. There is some evidence, however, that as dicyclopentadiene content of the terpolymer increases, propylene content decreases. Under these conditions, small blocks of crys-

talline polyethylene units might form, producing portions of insoluble polymer.

In spite of both the variations in terpolymer yields and the margin of error in the unsaturation analysis, there is fairly good correlation, within each catalyst-solvent series, between the amount of dicyclopentadiene charged and the resultant terpolymer unsaturation, i.e., doubling the charge of dicyclopentadiene doubles the terpolymer unsaturation, etc. Had all reactions been carried to the same polymer yield, however, this relation probably would not have held true.

It can be seen that, in general, polymers with unsaturations of about 0.30 mole of $C=C/kg.$ of terpolymer will have volume swells of less than 400% at the 60-min. cure. This is indicative of fairly tight cure. The polymers with higher unsaturations may have volume swells of < 300% at the 15-min. cure. It would appear from the data that polymers with more than about 0.50 mole $C=C/kg.$ are fairly completely cured in 15 min. at 320°F., with this particular vulcanizing recipe. There are some discrepancies between the amount of unsaturation in the terpolymers and their respective volume swells, particularly at the low levels of unsaturation. This may be due in part to the experimental error in the unsaturation analysis, but it may also reflect to some extent differences in the distribution of the diene units (and the subsequent crosslinks) throughout the polymer chains.

The author wishes to thank the Goodyear Tire and Rubber Company for permission to publish these results. Acknowledgements are also due Mrs. V. A. Bittle for determination of the inherent viscosities and percentages of insoluble polymer, E. E. Fauser for the vulcanizing recipe, Frank Chan for the unsaturation analyses, and J. K. Phillips for mass spectrographic analyses of the ethylene-propylene mixtures.

This is contribution number 320 from the Goodyear Research Laboratories.

References

1. Natta, G., G. Crespi, A. Valvassori, and G. Sartori, *Rubber Chem. Technol.*, **36**, 1583 (1963).
2. Gladding, E. K., B. S. Fisher, and J. W. Collette, *Ind. Eng. Chem. Prod. Res. Devel.*, **1**, 65 (1962).
3. Tarney, R. E., U. S. Pat. 3,000,866 (1961).
4. Adamek, S., and A. D. Dingle, Can. Pat. 639,401 (1962).
5. Amberg, L. O., and B. F. Brown, paper presented before the Southern Rubber Group, New Orleans, November 9, 1962.
6. Fieser, L. F., *Experiments in Organic Chemistry*, Part II, Heath, New York, 1941, p. 395.

Résumé

L'éthylène, le propylène et le dicyclopentadiène ont été terpolymérisés pour former des élastomères insaturés, vulcanisables au soufre, en utilisant VCl_3 ou $VOCl_3$ comme catalyseurs (avec $Al_2Et_3Cl_3$ comme co-catalyseur) et avec l'heptane, le benzène ou le tétrachloroéthylène comme solvants de polymérisation. Des diverses combinaisons possibles catalyseur-solvant, les meilleurs résultats ont été obtenus avec $VOCl_3$ comme catalyseur dans le benzène comme solvant. Toutes les autres combinaisons, sauf une, donnent également de bons résultats bien que certains possèdent des points particulièrement intéressants. L'exception est $VOCl_3$ dans l'heptane, ce qui produit des rendements variables en poly-

mères fortement gélifiés. On a effectué une étude partielle de l'influence de la concentration en dicyclopentadiène sur la polymérisation. Une augmentation de la concentration en diène diminue le rendement en polymère mais augmente son insaturation; elle n'a pas d'influence macroscopique sur les viscosités inhérentes des polymères. Les terpolymères contenant plus de 0.30 moles de C=C par kilo peuvent être fortement vulcanisés au moyen d'un agent vulcanisant à base de soufre.

Zusammenfassung

Die Terpolymerisation von Äthylen, Propylen und Dicyclopentadien unter Bildung ungesättigter, Schwefel-vulkanisierbarer Elastomere wurde mit VCl_4 oder $VOCl_3$ (und mit $Al_2Et_3Cl_3$ als Cokatalysator) als Katalysatoren und Heptan, Benzol oder Tetrachloräthylen als Lösungsmittel durchgeführt. Von den verschiedenen möglichen Katalysator-Lösungsmittelkombinationen liefert $VOCl_3$ als Katalysator in Benzol als Lösungsmittel im Mittel das beste Ergebnis. Alle üblichen Kombinationen mit Ausnahme einer eintigen lieferten ebenfalls gute Resultate, wobei jedoch einige noch spezielle Vorzüge aufwiesen. Die Ausnahme bildete $VOCl_3$ in Heptan als Lösungsmittel, wobei stark streuende Ausbeuten an Polymeren mit hohem Gelgehalt erhalten wurden. In gewissen Ausmass wurde der Einfluss der Dicyclopentadienkonzentration auf die Polymerisation untersucht. Eine Erhöhung der Dienkonzentration setzte die Polymerausbeute herab, erhöhte aber den Doppelbindungsgehalt; es bestand aber kein starker Einfluss auf die Viskositätszahl der Polymeren. Terpolymere mit mehr als etwa 0,30 Molen C=C pro Kilogramm können nach Vulkanisationsrezepten auf Schwefelgrundlage stark vulkanisiert werden.

Received February 16, 1965

Prod. No. 4697A

Adsorption of Poly-4-vinylpyridine onto Glass Surfaces

PAUL PEYSER, *National Bureau of Standards, Washington, D. C.*, and
ROBERT ULLMAN, *Scientific Laboratory, Ford Motor Co., Dearborn,
Michigan*

Synopsis

Some data on the adsorption of poly-4-vinylpyridine on a glass surface are presented. The results on the un-ionized polymer are characteristic of the adsorption of organic polymers; the adsorption isotherm has a flat top and the amount adsorbed depends on the solvent used. The adsorption of ionized poly-4-vinylpyridine decreases with increasing ionization and increases with increasing ionic strength. The effect of increased ionic strength is presumably associated with the greater tendency of an ionized polymer to coil in the presence of excess salt. These results tend to confirm the general hypothesis that the coiling of a polymer molecule at a liquid-solid interface reflects the tendency of the polymer to coil in solution.

Introduction

The adsorption of polymers from solution has been investigated by a number of workers.¹⁻³ The special properties of a polymer molecule, i.e., internal flexibility and multiple adsorption sites on a single molecule, have a considerable effect on the character of the adsorption isotherm and on the structure of adsorbed layer. In many cases, the isotherm is that of a monolayer, and yet the weight of polymer adsorbed per unit area is in excess of that which can be fitted in a single layer on the surface. The amount of polymer adsorbed at full surface coverage is a function of solvent power and solvent polarity. It has also been possible to show by a variety of methods, i.e., capillary flow,⁴ infrared investigation at a surface,^{5,6} ellipsometry,⁷ and differential capacity at a mercury electrode,⁸ that polymer chains are more or less folded in the adsorbed layer at an interface, this folding presumably reflecting the natural tendency of the polymer molecule to take the form of a random coil in solution.

One of the ways in which the arrangements of a polymer molecule may be controlled is, if the polymer molecule may be made into an electrolyte, to put a charge on the molecule. Because of the long range of action of electrostatic forces, charges on a molecule tend to repel each other; and consequently, the molecular coil is extended. The degree to which the molecule is extended may be reduced by adding foreign salts to the system, thus shielding the electrostatic repulsions between charged groups. Accord-

ingly, an investigation of the adsorption of polymeric electrolytes has certain interesting aspects which are not present in uncharged polymeric systems.

There have been a few investigations of the adsorption of polyelectrolytes on solid adsorbents.⁹⁻¹² These works have, in some cases, been carried out with objectives which are different from those indicated here; nevertheless, our choice of materials and experiments has been dependent, in part, on the results of earlier studies. The polymer used here, poly-4-vinylpyridine, henceforth referred to as PVP, was prepared by free-radical initiation. The solvents used in the adsorption experiments are chloroform, methanol, and water (the electrolyte influence could only be investigated in water or in methanol-water mixtures), and the adsorbent used was Vycor, a 96% silica glass (Corning Glass Co., Corning, New York).

EXPERIMENTAL

Preparation of Materials

The monomer, 4-vinylpyridine, was distilled under vacuum, mixed with toluene in a ratio of 10 ml. of toluene to 1 ml. of monomer, and an initiator, azobisisobutyronitrile, was added. The monomer/initiator mole ratio was approximately 180. The polymerization was carried out at 60°C. in an evacuated and sealed vessel. The final polymer was generally light yellow in color, the deeper the yellow the greater the oxidation. Most of the colored products could be removed by a crude fractionation procedure based on solution in tertiary butanol and precipitation with benzene. A middle fraction of the polymer was retained for subsequent experiments. The intrinsic viscosities of PVP-1 and PVP-2 in absolute ethanol at 25°C. were 1.19 and 1.50 in units of 100 ml./g. The viscosity-average molecular weights¹³ were 2.55×10^5 and 3.60×10^5 , respectively.

The Vycor glass powder contained small quantities of hydrochloric acid which could be removed by washing with distilled water until a silver nitrate test for chloride was found to be negative. The presence of this excess acid had a significant effect in those experiments where the degree of ionization was varied. In those cases, the hydrochloric acid was removed from the Vycor adsorbent. The surface area of the powder determined by the B.E.T. method with the use of nitrogen was 2.68 m.²/g.*

Adsorption Procedure

A polymer solution of known concentration was added to a weighed amount of adsorbent and shaken mechanically at a controlled temperature. The agitation was as gentle as possible (to prevent chain scission), but consistent with the requirement that the adsorbent and solution be thoroughly mixed.

* The authors wish to express their thanks to Dr. Y. F. Yu of the Scientific Laboratory at the Ford Motor Company for carrying out this determination.

Analysis

The concentration of polymer after an adsorption experiment was measured by determining the ultraviolet absorption of the supernatant liquid. The extinction coefficient of the un-ionized polymer at its maximum (2560 Å) was $\epsilon = 1655$ l./mole-cm., and of the fully ionized polymer at its maximum (2540 Å) was $\epsilon = 3945$ l./mole-cm. The unit mole is based on monomer molecular weight. These extinction coefficients are the same in all solvent systems used.

Because of the large difference in extinction coefficient of the un-ionized and ionized form of the polymer, it was possible to obtain reasonably accurate determinations of the per cent of ionized pyridyl groups on the polymer from the ultraviolet spectrum. It was assumed that the per cent ionization could be obtained by linear interpolation between the values obtained for the un-ionized and 100% ionized polymer. The extinction coefficient of the fully ionized polymer was determined from solutions of the perchloric acid salt in a sufficient excess of perchloric acid.

Preliminary Experiments

The amount of polymer adsorbed as a function of time was measured on a few samples to determine an appropriate time scale of the experiment. The amount of polymer adsorbed was found not to change with time after the adsorbent and polymer solution had been shaken together for more than $1/2$ hr.

Experiments were carried out to insure that the adsorption isotherms were independent of the relative amounts of adsorbent and polymer solution used in the experiment. Only those experiments which satisfied this test are reported. The presence of impurities on the surface or in the polymer solution would be seen in these experiments. As a matter of fact, unless a crude fractionation of the polymer was carried out before the polymer was used in an adsorption experiment, this criterion was not satisfied. The impurities which were removed by fractionation are not known; presumably they are highly oxidized fractions of the polymer or low molecular weight species.

RESULTS

The adsorption isotherms of PVP in the un-ionized form in chloroform, methanol, and 50% methanol-50% water solvents is shown in Figure 1. Note that more polymer is adsorbed from chloroform than from methanol or methanol-water mixtures. The adsorption of ionized poly-4-vinylpyridinium chloride (PVP Cl) from methanol-water and water in the presence of varying quantities of sodium chloride and hydrochloric acid is shown in Figures 2 and 3. In Figure 4 the adsorption of polymer from salt solutions in methanol and water is presented as a function of the fraction of polymer ionized. The ionic strength was controlled by adding appropriate quantities of sodium chloride, magnesium chloride, and hydrochloric acid. The

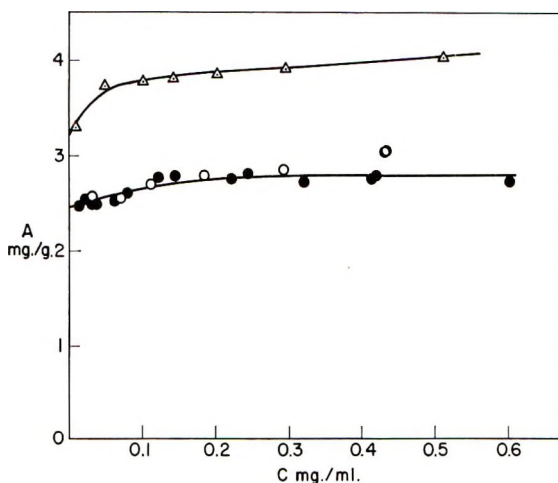


Fig. 1. Adsorption isotherms of PVP-1 on Vycor at 30°C. from (Δ) chloroform; (\bullet) methanol; a (\circ) 50% methanol-water mixture. The ordinate A is the weight of polymer adsorbed per weight of adsorbent; the abscissa C is the concentration of polymer in solution after adsorption.

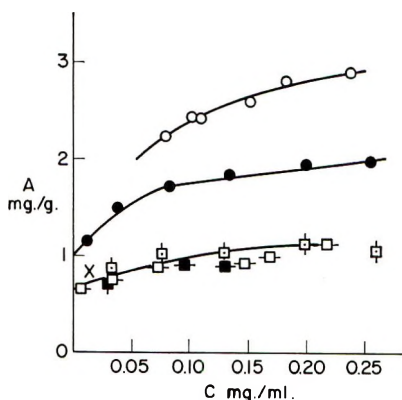


Fig. 2. Adsorption isotherms of ionized PVP-1 on Vycor at 30°C. from methanol-water mixture in solution with varying concentrations of HCl and NaCl: (\circ) 0.9N HCl; (\bullet) 0.5N HCl (\times) 0.2N HCl; (\blacksquare) 0.15N HCl; (\square) 0.1N HCl; (\blacksquare) 0.02N HCl; (\square) 0.1N HCl + 0.1N NaCl.

fraction ionized was determined by ultraviolet spectroscopy as discussed above. In all cases in which the amount of polymer adsorbed as a function of ionization was treated, the concentration of polymer remaining in solution after adsorption was between 75 and 100 mg./100 ml., which insures that the surface is essentially saturated with polymer.

It has been shown elsewhere that polymer adsorption is not always reversible in the time scale of an usual experiment, and several experiments were performed to find out whether PVP adsorption is reversible upon ionization and neutralization. This could be done easily, since the un-

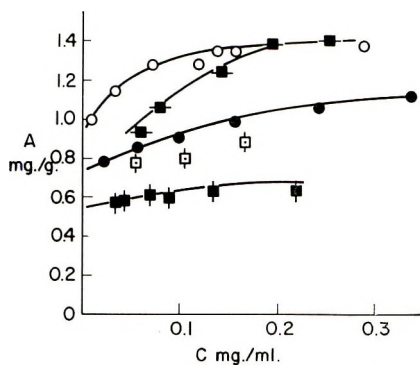


Fig. 3. Adsorption isotherms of ionized PVP-1 on Vycor at 30°C. from water in solution with varying concentrations of HCl and NaCl: (○) 0.9*N* HCl; (●) 0.5*N* HCl; (■) 0.1*N* HCl; (◻) 0.1*N* HCl + 0.1*N* NaCl; (◼) 0.1*N* HCl + 1*N* NaCl.

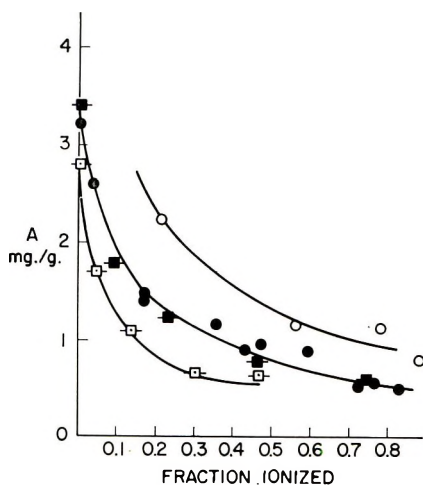


Fig. 4. Adsorption of ionized PVP-2 on Vycor at 0°C. from a methanol-water mixture (this ionization is produced by HCl + added salt): (○) 0.2*N* Cl⁻, NaCl; (●) .04*N* Cl⁻, NaCl; (■) 0.4*N* Cl⁻, MgCl₂; (◻) 0.007*N* Cl⁻, NaCl. The ordinate A_{∞} is the weight of polymer adsorbed per weight of adsorbent on the fully covered surface; the abscissa is the fraction of ionized pyridyl groups on the polymer.

ionized polymer is adsorbed in much greater quantities per unit area than the ionized material. The results are set down in Table I. Desorption upon ionization is mostly but not entirely reversible; adsorption upon neutralization is entirely reversible as far as can be told from this experiment.

DISCUSSION

The amount of polymer adsorbed from solution onto a solid depends on a number of factors which have been explored with a considerable variety of

TABLE I
 Adsorption Reversibility^a

No.	Initial ingredients	Ingredients added at 4 hr. adsorption time	Polymer concentration after 42 hr. adsorption, mg./ml.	Amount polymer adsorbed after 42 hr., mg./g.
1	Polymer solution, 15 ml.; solvent, 10 ml.; adsorbent, 1.740 g.	—	0.816	2.94
2	Polymer solution, 15 ml. 1 <i>N</i> NaCl, 1 ml.; solvent, 9 ml.; adsorbent, 1.511 g.	—	0.821	3.31
3	Polymer solution, 15 ml.; 0.5 <i>N</i> HCl, 2 ml.; solvent, 8 ml.; adsorbent, 10.177 g.	—	0.810	0.52
4	Polymer solution, 15 ml.; solvent, 8 ml.; adsorbent, 9.595 g.	0.5 <i>N</i> HCl, 2 ml.	0.643	0.98 (partially reversible)
5	Polymer solution, 15 ml.; 0.5 <i>N</i> HCl, 2 ml.; solvent, 6 ml.; adsorbent, 1.540 g.	0.5 <i>N</i> NaOH, 2 ml.	0.802	3.55 (reversible)

^a All experiments were carried out with the use of Vycor as an adsorbent, and a solution of PVP-2 in 50% methanol-50% water solvent. The initial concentration of the polymer solution was 1.721 mg./ml.; the temperature at which adsorption took place was 30°C.

materials. One of these factors is the solvent from which adsorption takes place. It has generally been established that polymer adsorption is greatest from the poorest solvent unless the solvent strongly competes with the polymer segment for surface sites. If strong competition occurs, the energy of solvent adsorption as compared with the energy of adsorption of the polymer segment at the surface is the significant quantity, and for polar surfaces (such as are used here), a more highly polar or polarizable solvent tends to reduce the amount of polymer adsorbed. As applied to the present experiments this factor would lead to the result that the maximum amount of PVP adsorbed on a surface, A_{∞} , satisfies the following inequalities:

$$A_{\infty}(\text{CHCl}_3) \geq A_{\infty}(\text{CH}_3\text{OH}) \geq A_{\infty}(\text{CH}_3\text{OH} + \text{H}_2\text{O})$$

On the other hand, since the polymer coil is expanded in a good solvent, and to the extent that the coiled character of the polymer molecule is maintained after adsorption, one usually finds that adsorption is greatest from the poorest solvent. This leads to the inequalities:

$$A_{\infty}(\text{CHCl}_3) \geq A_{\infty}(\text{CH}_3\text{OH} + \text{H}_2\text{O}) \geq A_{\infty}(\text{CH}_3\text{OH})$$

The experimental results show that adsorption is greatest from chloroform, which would be expected regardless of which of the above factors is dominating, and that adsorption from methanol-water mixtures and pure water is essentially the same.

The adsorption of the ionized polymer on a solid surface is controlled by the various factors already considered for the un-ionized material plus the attraction or repulsion brought about by the charge on the polymer molecule, and the charge on the surface. The charge on the polymer molecule tends to bring about an uncoiling of the polymer chain, and this would tend to reduce the amount of polymer which can fit on an adsorbent surface. The presence of excess salt tends to counteract this coil expansion.

Silica and glass surfaces are normally negatively charged in aqueous suspension, and it is known that the adsorption of polymeric acids is reduced and sometimes completely inhibited by ionization of the polymer.⁹⁻¹² PVP in acid solution tends to be positively charged, and, indeed, it is found that PVP is adsorbed on glass and Vycor in the charged state. However, it has been shown that quaternized PVP derivatives tend to adsorb excess bromide ion from potassium bromide solutions,¹⁴ so much so that at sufficiently high ($\sim 1N$) concentrations of potassium bromide, the quaternized PVP salts become negatively charged. It is likely that similar effects take place with the hydrochloride of PVP in the presence of excess chloride; some changes in the ultraviolet spectrum indicate that this is so, but the magnitude of the effect is not known.

The charge and ζ potential on silica particles in the presence of sodium chloride, hydrochloric acid, and magnesium chloride has been determined by a sedimentation method.¹⁵ Briefly, the results are that silica is generally negatively charged in these systems, the magnitude of the charge and the ζ potential is greater in NaCl than in HCl, and is still less in $MgCl_2$, the bivalent magnesium ion being much more strongly adsorbed than Na^+ or H_3O^+ ions. As the concentration of salt is increased, the total charge on the surface increases if NaCl or HCl is added, the charge on silica in $MgCl_2$ solutions increases in magnitude with concentration up to a normality of 10^{-4} and then decreases with a further increase of $MgCl_2$. No measurements have been reported for $MgCl_2$ concentrations greater than 5×10^{-4} , and it is possible that the glass particles become positively charged at higher concentrations.

The presence of foreign electrolytes in a solution from which polymer is adsorbed may influence the adsorption phenomenon in a number of different ways. First of all, the expansion of the polymer coil arising from electrostatic repulsion of charged groups on the polymer coil is diminished by the addition of salt. The expanded chain in solution would presumably tend to maintain a similar arrangement while adsorbed and would occupy more space on the surface. If this were the only effect the capacity of the adsorbent would be high for the uncharged polymer where there is no coil expansion, least for the case of low salt concentration where the chain is charged and the coil is highly extended, and higher again in high salt concentrations

where the expansion of the coil is suppressed. It may be seen from Figure 4 that the capacity of the surface for polymer is decreased if the ionic strength is lowered, as would be expected from these considerations. The adsorption of ionized polymer in the presence of large quantities of salt is about the same as that of uncharged polymer. It is not clear whether this is purely a chain coiling phenomenon, or whether these are accidentally compensating forces from electrostatic charges on the polymer or at the interface.

If the charge on the surface were an important factor in controlling the adsorption capacity in these experiments, the adsorption of PVP from NaCl solution would be greater than from MgCl₂ solutions because the adsorbent (silica) carries a higher negative charge in NaCl than in MgCl₂ as may be seen from the ζ potential measurements of Dulin and Elton.¹⁵ However, the adsorption of the polymer does not depend on whether MgCl₂ or NaCl is used, as may be seen in Figure 4. Accordingly, this factor is not important here.

The excess salt concentration probably reduces the positive charge on the polymer molecule because of counterion binding. There is no evidence that this plays a significant role in PVP adsorption.

The principal effect of foreign salts on the adsorption of PVP seems to arise from the inflation (low salt concentration) or deflation (high salt concentration) of the polymer coil in solution and at the interface, thus bringing about a saturation of the surface of the adsorbent by lower quantities of polymer when the coil occupies more space. The increase or decrease of electrostatic charges on the polymer and surface play, if anything, a minor role.

Table I contains results on adsorption experiments designed to test whether the amount of polymer adsorbed under a given set of conditions is dependent on the experimental path. If equilibrium were attained, the amount adsorbed in systems 2 and 5 would be equal, and the amount adsorbed in systems 3 and 4 would be equal. The results in systems 2 and 5 agree, but in 3 and 4 they do not. By reference to system 1, it is evident that the addition of HCl in system 4 should bring about a sixfold desorption. In fact, only a threefold desorption took place. This partial desorption is similar to the one-sided irreversibility with temperature noted elsewhere.^{16,17} This sluggishness or lack of reversibility in polymer adsorption shows clearly the pitfalls inherent in the interpretation of polymer adsorption experiments in terms of equilibrium theories.

The authors thank the S. C. Johnson Foundation for a grant supporting this research.

This work was submitted by P. Peyser in partial fulfillment of the requirements for the degree of Doctor of Philosophy.

References

1. Jenckel, E., and B. Rumbach, *Z. Elektrochem.*, **55**, 612 (1951).
2. Kraus, G., and J. Dugone, *Ind. Eng. Chem.*, **47**, 1809 (1955).
3. Koral, J., R. Ullman, and F. R. Eirich, *J. Phys. Chem.*, **62**, 541 (1958).
4. Öhrn, O. E., *Arkiv. Kemi*, **12**, 397 (1958).
5. Fontana, B. J., and J. R. Thomas, *J. Phys. Chem.*, **63**, 1376 (1959).

6. Thies, C., P. Peyser, and R. Ullman, *Proceedings of the 4th International Congress on Surface Active Substances, Brussels, 1964*, in press.
7. Stromberg, R. R., E. Passaglia, and D. J. Tutas, *J. Res. Natl. Bur. Std.*, **67A**, 431 (1963).
8. Miller, I. R., *Trans. Faraday Soc.*, **57**, 301 (1961).
9. Michaels, A. S., and O. Morelos, *Ind. Eng. Chem.*, **47**, 1801 (1955).
10. Schmidt, W., and F. R. Eirich, *J. Phys. Chem.*, **66**, 1907 (1962).
11. Lopatin, G., Ph.D. Dissertation, Polytechnic Institute of Brooklyn, 1961.
12. Lauria, R., Ph.D. Dissertation, Polytechnic Institute of Brooklyn, 1962.
13. Berkowitz, J. B., M. Yamin, and R. M. Fuoss, *J. Polymer Sci.*, **28**, 69 (1958).
14. Strauss, U. P., N. L. Gershfeld, and H. Spiera, *J. Am. Chem. Soc.*, **76**, 5909 (1954).
15. Dulin, C. I., and G. A. H. Elton, *J. Chem. Soc.*, **1953**, 1168.
16. Ellerstein, S., and R. Ullman, *J. Polymer Sci.*, **55**, 123 (1961).
17. Stromberg, R. R., A. R. Quasius, S. D. Toner, and M. S. Parker, *J. Res. Natl. Bur. Std.*, **62**, 71 (1959).

Résumé

On présente certains résultats sur l'adsorption de poly-4-vinyl-pyridine sur une surface de verre. Les résultats obtenus avec le polymère non ionisé sont caractéristiques de l'adsorption de polymères organiques; l'isotherme d'adsorption possède un plateau et la quantité adsorbée dépend du solvant employé. L'adsorption de la poly-4-vinyl-pyridine ionisée diminue avec une augmentation de l'ionisation et augmente avec une augmentation de la force ionique. L'influence d'une augmentation de la force ionique est probablement associée à une tendance plus grande d'un polymère ionisé à s'enrouler en présence d'un excès de sel. Ces résultats tendent à confirmer l'hypothèse générale suivant laquelle l'enroulement d'une molécule de polymère à l'interface liquide-solide reflète la tendance du polymère à s'enrouler en solution.

Zusammenfassung

Einige Daten über die Adsorption von Poly-4-vinylpyridin an einer Glasoberfläche werden vorgelegt. Die Ergebnisse an nicht-ionisierten Polymeren sind für die Adsorption organischer Polymerer charakteristisch. Die Adsorptions-isotherme besitzt ein flaches Maximum, und die adsorbierte Menge hängt vom verwendeten Lösungsmittel ab. Die Adsorption von ionisiertem Poly-4-vinyl-pyridin nimmt mit steigender Ionisation ab und mit steigender Ionenstärke zu. Der Einfluss der Erhöhung der Ionenstärke hängt wahrscheinlich mit der grösseren Verknäuelungstendenz eines ionisierten Polymeren in Gegenwart von überschüssigem Salz zusammen. Die Ergebnisse bilden eine Bestätigung der allgemeinen Hypothese, dass die Verknäuelung eines Polymermoleküls an einer Flüssig-Fest-Grenzfläche die Verknäuelungstendenz des Polymeren in Lösung widerspiegelt.

Received March 5, 1965

Prod. No. 4698A

Silver Perchlorate-Initiated Polymerization of Vinyl Monomers

J. P. HERMANS and G. SMETS, *Laboratoire de Chimie Macromoléculaire,
Université de Louvain, Belgium*

Synopsis

The polymerization of vinyl compounds can be initiated by soluble silver salts. In this paper, the kinetics of the silver perchlorate-initiated polymerization of styrene and methyl methacrylate in organic solution has been examined. The rates were measured dilatometrically at 70°C.; the solutions were prepared by a high vacuum technique. With respect to the monomer, either styrene or methyl methacrylate, the order of reaction is equal to two. In the case of styrene, the rate of polymerization is proportional to the silver perchlorate concentration when this concentration is $\leq 10^2$ mole/l. Above this value, the rate becomes proportional to the square of the silver perchlorate concentration. For methyl methacrylate, the order with respect to the silver salt concentration varies from 0.5 to 1, depending on the concentration range. These kinetic results are interpreted on the basis of the assumption that a silver perchlorate-monomer complex, instead of a silver perchlorate molecule, participates in the polymerization. Moreover, the examination of styrene and benzene solutions of silver perchlorate indicates a formation of silver salt-aromatic hydrocarbon complexes of the 1:1 and 2:1 types. Consequently, good agreement is found between the kinetics of those two different initiator systems. A coordination polymerization mechanism is proposed, in which hydrogen transfer alternates with each propagation step. The mechanism is corroborated by an isotope effect equal to two, when didenterostyrene is compared to styrene. The internal structure of the poly(methylmethacrylate) obtained with AgClO_4 , corresponds to that of a conventional polymer. The presence of traces of water inhibits the polymerization.

Metal salt-initiated polymerizations of vinyl derivatives¹⁻⁴ have been examined by several authors during the last two decades. It is generally thought that the reaction proceeds through a cationic mechanism. In the particular case of the silver perchlorate initiation, it is assumed that traces of perchloric acid are responsible for the cationic, sometimes explosive, polymerization.⁵⁻⁷ Similarly, Solomon and Dimonie⁸ proposed recently a cationic mechanism for the polymerization of *N*-vinylcarbazole in the presence of magnesium perchlorate.

The role of metal salts is not restricted to the initiation step, however; they can also affect the rate of polymerization by formation of a complex with the monomer molecules and/or with the growing chains. This effect was shown by Bamford⁹ and Imoto and co-workers¹⁰⁻¹² in the case of the radical polymerization of acrylonitrile initiated with azobisisobutyronitrile, where the rate increases appreciably in the presence of lithium chloride.

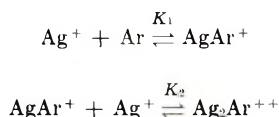
Similarly, olefin-silver nitrate complexes are able to polymerize under low pressure and in a strongly polar medium in the presence of a radical initiator.^{13,14} Besides these kinetic effects, metal salts can also modify the internal structure, i.e., the tacticity of the polymer, as in the cases of silver salts in the polymerization of butadiene with azobisisobutyronitrile and zinc or magnesium halides in the polymerization of methyl methacrylate in the presence of a Grignard reagent.¹⁵⁻¹⁷

It is the purpose of the present paper to examine the influence of pure silver perchlorate on the polymerization kinetics of styrene and of methyl methacrylate in the absence of any traces of perchloric acid, and to show the participation of silver perchlorate-double bond complex formation in the reaction mechanism.

NATURE OF THE SILVER PERCHLORATE COMPLEX INITIATOR

The complexes formed by interaction between unsaturated groups and a silver ion are of the electron donor-acceptor type, in which the olefin functions as an electron donor by sharing their π -electrons with the silver ion.¹⁷⁻¹⁹ Silver perchlorate-aromatic hydrocarbon complexes have been isolated in the solid state, e.g., in the cases of benzene,²⁰ styrene,^{21,22} polystyrene, and others.²³⁻²⁶ Their existence was also demonstrated on the basis of a decrease of the infrared absorption frequency of the C=C double bond^{27,28} as well as by an increased absorption intensity in the ultraviolet region.²⁹

From the solubility of the aromatic hydrocarbon in aqueous silver nitrate, equilibrium constants for the formation of water-soluble complexes of the AgAr^+ and $\text{Ag}_2\text{Ar}^{++}$ types have been evaluated; their values depend on the basicity of the aromatic ring. Both equilibria can be written



The first equilibrium constant K_1 , determined by this method for styrene, is equal to 18 and is much higher than K_2 ($= 0.8$); it corresponds to a reaction enthalpy of about 6 kcal./mole.³⁰⁻³² Since K_1 for toluene is equal to 3, it is very likely that in the case of styrene solutions in benzene the silver ion will be fixed preferentially on the styrene molecules.

The apparent molecular weight of silver perchlorate in benzene solution has been evaluated by cryoscopic measurements (Table I). It varies within the limits corresponding to a $\text{AgClO}_4\text{-C}_6\text{H}_6$ complex and a $(\text{AgClO}_4)_2\text{-C}_6\text{H}_6$ complex.

Although imprecise, these cryoscopic measurements indicate nevertheless values of K_2 much higher than those obtained from the water solubility measurements, where water and the aromatic hydrocarbon compete for the silver ion for complex formation.

TABLE I
Cryoscopic Molecular Weight Determination of Silver Perchlorate in Benzene

c , g./100 ml.	Δt , °C.	Molecular weight
4.5	0.08	289
5.9	0.094	364
4.99	0.095	304
7.2	0.115	362
6.74	0.122	320
8.56	0.134	370
8.4	0.135	362
10.2	0.155	380
10.8	0.167	371
13	0.201	374
13.9	0.214	380
15	0.225	385

These results were confirmed by vapor pressure measurements carried out at 37°C. with a Mechrolab vapor pressure osmometer; the data are shown in Figure 1.

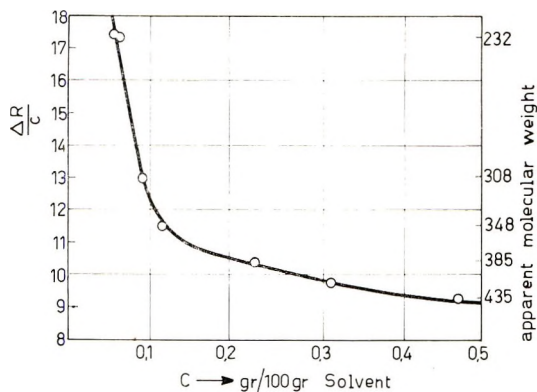


Fig. 1. Vapor pressure molecular weight determination of silver perchlorate in benzene solution at 37°C. ΔR = variation of electric resistivity (Mechrolab apparatus).

From these data it must be concluded that the amount of monomeric and dimeric complexes depends on the silver perchlorate concentration. Evidently the composition of the complex existing in a polymerization mixture affects the overall kinetics of the reaction.

KINETICS OF POLYMERIZATION: EXPERIMENTAL RESULTS

Styrene

The influence of the initiator concentration on the rate of polymerization of styrene has been examined in two concentration ranges, one in which the 1:1 complex of styrene is present alone ($[\text{AgClO}_4] = 0.02$ mole/l.)

TABLE II
Influence of the Silver Perchlorate Concentration on the Polymerization of Styrene at 70°C.

[Styrene] = 8.713 mole/l.			[Styrene] = 5.45 mole/l. ^a	
[Initiator] × 10 ² , mole/l.	$R_p \times 10^5$, mole/l.-sec.			
	Dry AgClO ₄	Benzene- AgClO ₄ complex	[Initiator] × 10, mole/l.	$R_p \times 10^5$, mole/l.-sec.
1.4		1.46	0.895	0.92
1.68	0.72		1.12	2.0
2.42		1.97	1.34	2.75
3.05		2.58	1.78	4.4
3.61	1.20		2.23	6.95
4.34	1.62			
4.80		3.48		
6.99	2.70			

^a Solvent: toluene.

and the one in which both 1:1 and 2:1 complexes are present ($[\text{AgClO}_4] = 0.1$ mole/l.).

In the low concentration range, the rate is proportional to the first power of the silver perchlorate concentration independently if dry silver perchlorate or its benzene complex is used as initiator.

In the higher concentration range the rate becomes proportional to the square of the silver perchlorate concentration. The results are summarized in Table II and represented in Figure 2.

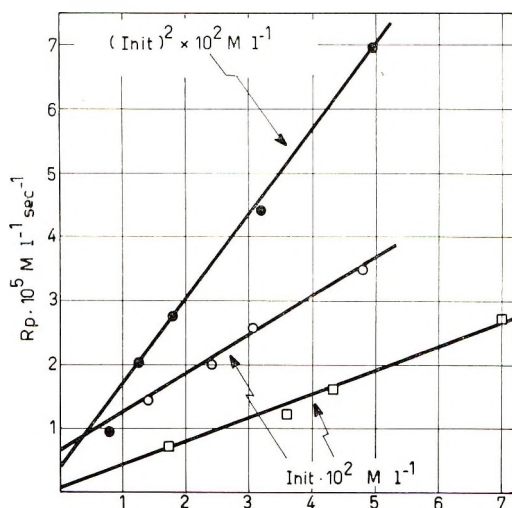


Fig. 2. Influence of the silver perchlorate concentration on the polymerization of styrene at 70°C.: (O) with AgClO₄-benzene complex, $[M] = 8.713$ mole/l.; (□) with dry AgClO₄, $[M] = 8.713$ mole/l.; (●) with dry AgClO₄, $[M] = 5.45$ mole/l.

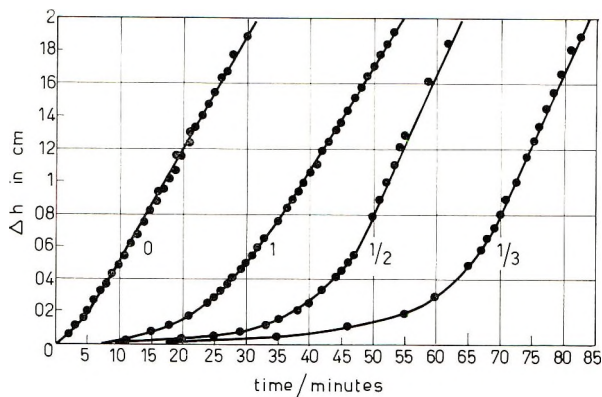


Fig. 3. Influence of concentration in the styrene polymerization at $[AgClO_4-C_6H_6] = 2 \times 10^{-2}$ mole/l., $70^\circ C.$, and silver perchlorate/water ratios of 0, $1/1$, $1/2$, and $1/3$.

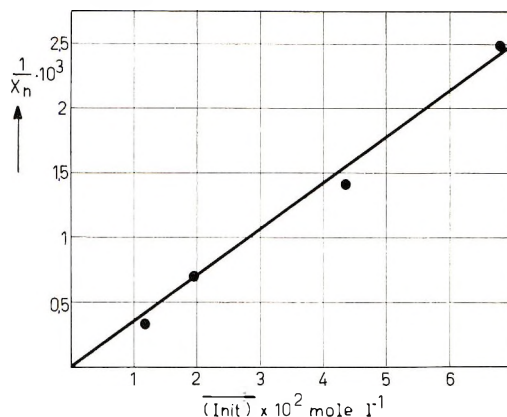


Fig. 4. Influence of the initiator concentration on the degree of polymerization \bar{X}_n of styrene at $70^\circ C.$, $[M] = 8.713$ mole/l.

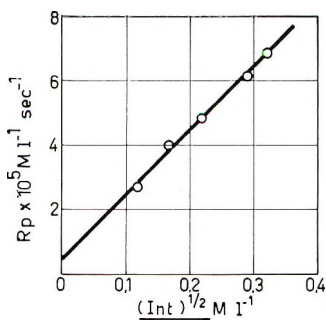


Fig. 5. Influence of the $AgClO_4$ concentration in the polymerization of methyl methacrylate at $70^\circ C.$, $[M] = 8.85$ mole/l.

It must also be pointed out that, depending on the nature of the AgClO_4 -aromatic hydrocarbon complex used for the initiation, the overall energy of activation is different, attaining values of 17 and 21 kcal./mole with the styrene and benzene complexes, respectively (Table III). When silver perchlorate is used as a complex with dioxane or with alcohol the rate of polymerization decreases appreciably. In the presence of water, inhibition occurs, and its duration is proportional to the water content. After the inhibition period the rate increases progressively and reaches practically the same value as in the polymerization in the complete absence of water (Fig. 3). These results indicate that water behaves not as a cocatalyst, but as an inhibitor, as long as it is not consumed in a side reaction. It can be shown that silver perchlorate is an efficient catalyst for the hydration of styrene; indeed during the inhibition period methylphenylcarbinol, $\text{C}_6\text{H}_5\text{CHOHCH}_3$, is formed and was detected with gas chromatographic analysis.

TABLE III
Energy of Activation of the Polymerization of Styrene at $[\text{Styrene}] = 8.713$ mole/l.

Initiating complex	Temperature, °C.	$R_p \times 10^5$, mole/l.-sec.	E^a , kcal./mole
AgClO_4 -styrene, 0.4×10^{-2} mole/l.	77	0.52	17
	85	1.00	
	92	1.50	
	99	2.50	
AgClO_4 -benzene, 0.12×10^{-2} mole/l.	70	0.10	21
	79	0.19	
	88	0.39	
	98	1.0	

With respect to the monomer concentration, the rate in toluene solution is proportional to the second power of styrene, a plot of the rate versus $[\text{M}]^2$ being linear and passing through the origin. The results are given in Table IV.

TABLE IV
Influence of the Monomer Concentration on Rate of Polymerization of Styrene at 70°C .,
 $[\text{AgClO}_4] = 0.178$ mole/l.

$[\text{Styrene}]$, mole/l.	$R_p \times 10^5$, mole/l.-sec.
1.57	0.40
2.36	0.90
3.14	1.40
3.49	1.65
4.36	2.62
5.24	3.50
5.45	4.40

TABLE V
Influence of the Styrene Concentration on the Degree of Polymerization of Styrene at
70°C., $[\text{AgClO}_4] = 0.175$ mole/l.

[Styrene], mole/l.	$[\eta]$	M_η	M_n
1.04	0.2	46,100	
1.39	0.3	78,200	72,000
1.74	0.325	88,300	82,000
2.61	0.4	117,000	110,000

The dependence of the molecular weight on the monomer and initiator concentrations has also been examined; the results with respect to the styrene concentration are given in Table V, while those for the silver perchlorate concentration are shown in Figure 4.

As a first approximation there is a roughly linear relationship between the degree of polymerization X_n and the monomer concentration as well as between the reciprocal degree of polymerization and the initiator concentration.

Methyl Methacrylate

The polymerization of methyl methacrylate was investigated in order to determine whether or not any significant change in the polymerization mechanism would occur when the polarity of the vinyl double bond was reversed.

At low initiator concentration in methyl methacrylate in bulk, the rate is proportional to the square root of the silver perchlorate concentration (Fig. 5). At higher concentration, e.g., in toluene solution when both 1:1 and 2:1 complexes are present ($[\text{AgClO}_4] = 0.08$ mole/l.), the polymerization becomes first-order with respect to the silver perchlorate concentration (Table VI).

The influence of the monomer concentration on the polymerization of methyl methacrylate follows practically the same course as in the case of

TABLE VI
Influence of the Silver Perchlorate Concentration on the Polymerization of Methyl
Methacrylate at 70°C.

[Monomer] = 8.85 mole/l.		[Monomer] = 4.75 mole/l. ^a	
[Initiator] $\times 10^2$, mole/l.	$R_p \times 10^5$, mole/l.-sec.	[Initiator] $\times 10$, mole/l.	$R_p \times 10^5$, mole/l.-sec.
1.48	2.7	0.515	0.78
2.92	4	0.849	1.3
4.77	4.8	1.03	1.5
8.48	6.1	1.54	2.42
10.5	6.8	2.06	3.1

^a Solvent: Toluene.

TABLE VII

Influence of the Monomer Concentration on Rate of Polymerization of Methyl Methacrylate at 70°C., $[\text{AgClO}_4] = 8.49 \times 10^{-2}$ mole/l.

[Monomer], mole/l.	$R_p \times 10^5$, mole/l.-sec.
3.267	0.6
4.75	1.3
5.936	2.0
6.848	2.1
7.606	3.8

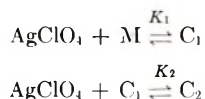
styrene, i.e., a second-order reaction with respect to the monomer (Table VII).

KINETIC INTERPRETATION

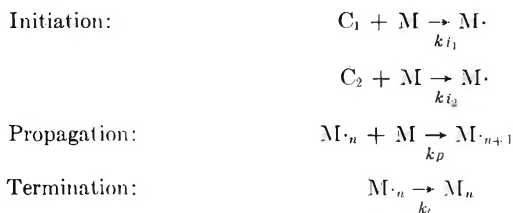
The experimental results indicate that the mechanism of polymerization depends on whether the AgAr^+ (1:1) complex or the $\text{Ag}_2\text{Ar}^{++}$ (2:1) complex is present in the solution; moreover the rate dependence with respect to the initiator concentration differs for the two monomers. The polymerization of styrene will therefore be considered first.

Styrene

The total silver perchlorate complex concentration $[\text{C}]$ is equal to the sum of both species $[\text{C}_1]$ and $[\text{C}_2]$, corresponding to the equilibria K_1 and K_2 ,



where M represents the monomer and C_1 and C_2 the AgAr^+ and $\text{Ag}_2\text{Ar}^{++}$ complexes, respectively. The individual reactions can be written as follows:



For steady-state conditions, i.e.,

$$[\text{M}\cdot] = [\text{M}]\{k_{i_1}[\text{C}_1] + k_{i_2}[\text{C}_2]\}/k_t$$

the rate is expressed by

$$R_p = (k_p/k_t)[\text{M}]^2(k_{i_1}[\text{C}_1] + k_{i_2}[\text{C}_2])$$

At low silver perchlorate concentration the complex C_1 is present alone and initiates the polymerization. Considering that K_1 is high ($k_1 \gg k_{-1}$) it follows that

$$k_1[\text{AgClO}_4][\text{M}] = k_{-1}[C_1] + k_{i_1}[C_1][\text{M}] \cong k_{i_1}[C_1][\text{M}]$$

and

$$[C_1] = (k_1/k_{i_1})[\text{AgClO}_4]$$

$$R_p = (k_p/k_t)k_1[\text{AgClO}_4][\text{M}]^2$$

the rate being directly proportional to the silver perchlorate concentration.

At higher silver perchlorate concentration, the complex $\text{Ag}_2\text{Ar}^{++}$ will also be present, and its catalytic activity is considered to be the highest. Since

$$[C_2] = K_2[\text{AgClO}_4][C_1] = K_2[\text{AgClO}_4]^2(k_1/k_{i_1})$$

the rate expression becomes

$$R_p = (k_p/k_t)k_1[\text{AgClO}_4][\text{M}]^2 \{1 + K_2(k_{i_2}/k_{i_1})[\text{AgClO}_4]\}$$

When $K_2(k_{i_2}/k_{i_1}) \gg 1$, the rate will be proportional to the square of the silver perchlorate concentration.

Independently of the initiator concentration it is always proportional to the square of the styrene concentration.

The proportionality between the degree of polymerization and the monomer concentration can be interpreted by assuming a predominance of monomolecular chain termination with respect to chain transfer, i.e., $\bar{X}_n = (k_p/k_t)[\text{M}]$.

Methyl Methacrylate

In the polymerization of methyl methacrylate in bulk the initiation step requires two monomer molecules for one silver perchlorate (see Discussion), while a bimolecular termination is considered to take place.

On the basis of the scheme

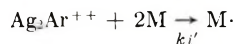


and assuming steady-state conditions the following rate expression is obtained:

$$R_p = k_p(k_i/k_t)^{1/2}[\text{AgClO}_4]^{1/2}[\text{M}]^2$$

Here the rate is proportional to the square root of the silver perchlorate concentration as a consequence of the bimolecular termination.

When methyl methacrylate is polymerized in toluene solution at relatively high silver perchlorate concentration, the initiating species will be $\text{Ag}_2\text{Ar}^{++}$, as in the case of styrene. The initiation step then becomes



Consequently,

$$R_p = k_p(k_i'/k_t)^{1/2}[\text{AgClO}_4][\text{M}]^2 \times \text{constant}$$

where the constant depends on the equilibrium constants K_1 and K_2 of the silver perchlorate-toluene complex formation.

The main differences between the polymerization kinetics of styrene and methyl methacrylate lie in the participation of one or two monomer molecules in the initiation reaction and in the monomolecular or bimolecular nature of the termination step.

DISCUSSION OF THE REACTION MECHANISM

It was first suggested that the positively charged silver ion-aromatic hydrocarbon complex would induce a cationic polymerization by addition on the double bond of the styrene monomer, $\text{Ag}-\text{CH}_2-\text{CHC}_6\text{H}_5^+$. This hypothesis must however be rejected for three main reasons: (1) the absence of any light absorption characteristic of a cationic growing polystyrene chain, which normally absorbs at 4400 Å;³³ (2) the composition of a copolymer of styrene with methyl methacrylate prepared in the presence of silver perchlorate complex as initiator which had about the same composition as the monomer mixture (1:1); (3) the inhibition effect of traces of water on the rate of polymerization.

The formation of an organo-silver compound followed by homolytic scission of the Ag-carbon link and radical polymerization of the monomer was also very unlikely, taking into account the high unstability of organo-silver compounds, even below room temperature,³⁴ and the absence of an appreciable silver precipitate during reaction. Therefore, the polymerization is considered to proceed through a coordination mechanism in which the initiation consists in the formation of a complex between the silver ion and the unsaturated group of the monomer, i.e., the vinyl group or the aromatic nucleus for styrene, the carboxymethyl group for methyl methacrylate.

The monomer-complexed silver ion enhances the addition of a second monomer molecule through the formation of a transient complex, in which hydrogen transfer is favored by the presence of the Ag^+ . After the addition, the Ag^+ ion is located at the unsaturated end of the growing chain, and thus further monomer addition with simultaneous isomerization (hydrogen shift) can be repeated. The monomolecular chain termination reaction results from the deactivation of the Ag^+ -unsaturated endgroup complex. The reaction scheme is represented in Figure 6.

The proposed reaction mechanism assumes a hydrogen transfer reaction alternating with each propagation step and can be compared with the isomerization-polymerization as described recently.³⁵⁻³⁸ In order to test the validity of this hypothesis, 1,1'-dideutero styrene, $\text{CD}_2=\text{CH}-\text{C}_6\text{H}_5$, has been used. Preliminary experiments showed that the rates of the radical polymerization of styrene and the dideuterated styrene in the presence of azobisisobutyronitrile are equal, showing no detectable isotopic effect in the radical propagation. On the contrary, when both styrenes are submitted to silver perchlorate-initiated polymerization, an appreciable isotopic effect ($= 2$) has been measured, the rate of the deuterated styrene

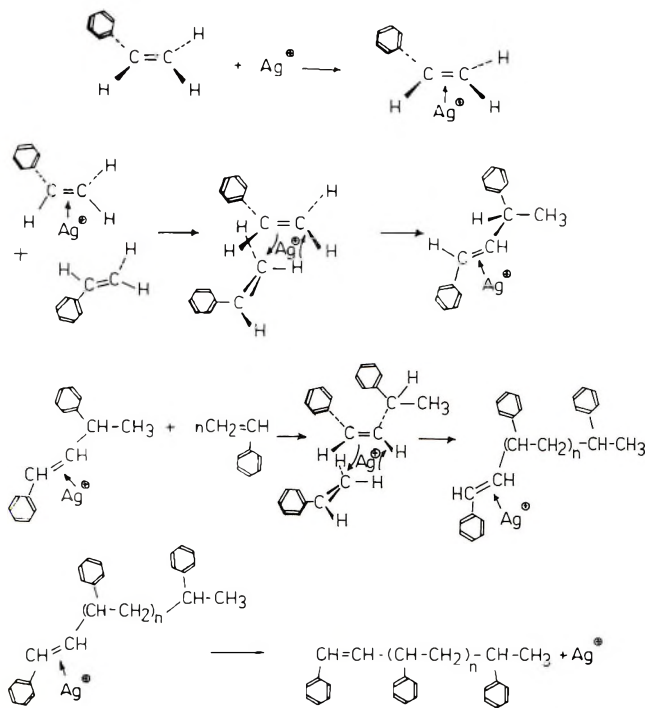


Fig. 6. Polymerization mechanism of styrene in the presence of silver perchlorate.

being half that of conventional styrene. This effect shows that, even it is not very important, the hydrogen (or deuterium) transfer must intervene in the rate-determining process; undoubtedly it supports the mechanism, as shown in Figure 6.

A similar reaction mechanism has been proposed for the methyl methacrylate polymerization with silver perchlorate as initiator. In this case it is assumed that the hydrogen transfer proceeds through the allylic α -hydrogen atoms of the monomer. As can be seen from the reaction scheme (Fig. 7), the poly(methyl methacrylate) resulting from this isomerization polymerization has the same overall structure as the usual polymer; moreover, the nuclear magnetic resonance spectra show that its internal

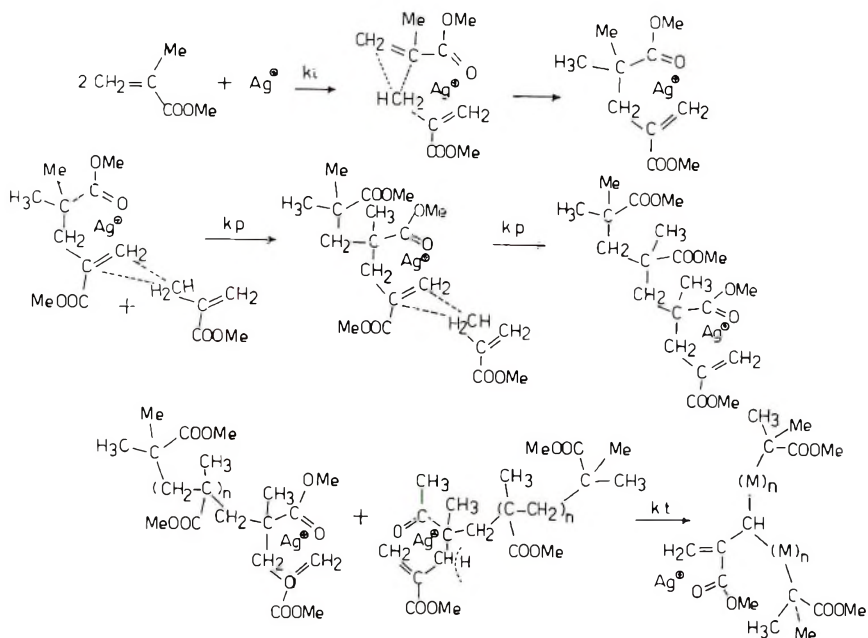


Fig. 7. Polymerization mechanism of methyl methacrylate in the presence of silver perchlorate.

structure is also identical with that of conventional (radical-polymerized) poly(methyl methacrylate).

Experiments with deuterium-tagged methyl methacrylate have not been carried out. The bimolecular termination reaction agrees quite well with the extremely high molecular weights of the polymers (3×10^6 – 4×10^6). The existence of a coordination complex between a silver ion and two molecules of methyl methacrylate was assumed on the basis of the kinetic results. The existence of such 2:1 complexes has, however, been described in the literature for oxygenated compounds³¹ and some nitriles with inorganic halides.³⁹

In conclusion, silver perchlorate and silver perchlorate–aromatic hydrocarbon complexes initiate the polymerization of styrene and methyl methacrylate through a coordination mechanism in which an intramolecular hydrogen transfer alternates with each propagation step.

EXPERIMENTAL

Silver perchlorate was purified, traces of perchloric acid being removed by formation of its complex with benzene. This pure silver perchlorate was stored over P₂O₅ and heated under high vacuum at 120°C. to constant weight.

The silver perchlorate–dioxane complex was prepared by the method described by Comyns and Lucas.⁴⁰ The silver perchlorate–benzene com-

plex was prepared by dissolving AgClO_4 in anhydrous benzene to saturation. On cooling, a 1:1 complex precipitates which can be isolated.⁴¹ The silver perchlorate-styrene complex (1:1) was obtained by dropwise addition of AgClO_4 solution in styrene to cyclohexane. After several hours the precipitate was isolated and washed with cyclohexane.⁴² Styrene and methyl methacrylate were carefully dried over calcium hydride and freshly distilled under vacuum before use.

The solvents were refluxed over metallic sodium for 24 hr. and distilled under nitrogen atmosphere. Before use they were dried again over calcium hydride and distilled in high vacuum. Traces of water in monomers and solvents were determined by the Karl Fischer method by the dead-stop technique.⁴³

In the polymerization, high vacuum filling technique was used in order to avoid inhibition due to humidity or pressure of oxygen. All taps in the apparatus were made of Teflon and used without grease.

Anhydrous silver perchlorate was always kept in break-seal tubes. Solvents, monomers, and initiator solutions were stored under high vacuum in cylindric vessels connected with a graduated tube which permitted given volumes of monomer or solutions to be taken off and introduced in the reaction vessel. Dilatometers and polymerization tubes were filled in high vacuum by turning over the sealed apparatus. For the polymerization initiated by silver perchlorate hydrate, a known volume of water vapor was condensed into the mixing vessel from a large bulb of a known volume, the walls of which were made hydrophobic with silicones in order to eliminate loss of water by adsorption.

The rate of polymerization was followed dilatometrically at 70°C. Plots of the per cent polymerization against time were strictly linear.

Osmotic molecular weights were determined in a Fuoss and Mead osmometer in benzene solution at 25°C. In the equation, $[\eta] = KM^a$, values of K and a were taken to be 1.7×10^{-4} and 0.74, respectively.

The apparent molecular weight of AgClO_4 in benzene was determined by cryoscopic and ebullioscopic methods. Thermoelectric microdetermination of the molecular weight was also carried out at 37°C. in benzene in a Mechrolab vapor pressure osmometer, model 301A. A preliminary calibration was made to relate the difference in vapor pressure, i.e., of electrical resistance, with the molarity of the solution.

The authors are indebted to the Fonds National de la Recherche Scientifique (FNRS) for a fellowship to one of them (J. P. H.) and for supporting this research. They acknowledge also the financial support of Gevaert-Agfa N.V., Antwerp, Belgium.

References

1. Salomon, G., *Proceedings of the International Colloquium on Macromolecules, Amsterdam, 1949*, Centen's, Amsterdam 1950, p. 77.
2. Richards, A. W., and D. D. Eley, *Discussions Faraday Soc.*, **2**, 378 (1947).
3. Eley, D. D., and A. W. Richards, *Trans. Faraday Soc.*, **45**, 425 (1949).
4. Hodgson, R. B., *J. Polymer Sci.*, **47**, 259 (1960).

5. Lilley, H. S., and G. L. Foster, *Nature*, **160**, 131 (1947).
6. Burton, H., and P. F. G. Prail, *J. Chem. Soc.*, **1953**, 837.
7. Losev, B. I., and Yu. I. Zakharova, *Dokl. Akad. Nauk SSSR*, **116**, 609 (1957).
8. Solomon, D. F., and M. Dimonie, paper presented at I.U.P.A.C. International Symposium on Macromolecular Chemistry, Paris, July 1963; *J. Polymer Sci.*, **C4**, 969 (1963).
9. Bamford, C. H., A. D. Jenkins, and R. Johnston, *Proc. Roy. Soc. (London)*, **A241**, 364 (1957).
10. Imoto, M., T. Otsu, and S. Shimizu, *Makromol. Chem.*, **65**, 174 (1963).
11. Imoto, M., T. Otsu, and T. Ito, *Bull. Chem. Soc. Japan*, **36**, 310 (1963).
12. Imoto, M., T. Otsu, and Y. Harada, *Makromol. Chem.*, **65**, 180 (1963).
13. Henglein, A., and W. Schnabel, *Angew. Chem. Intern. Ed.*, **1**, 54 (1962).
14. Bier, G., and G. Messwarb, *Angew. Chem. Intern. Ed.*, **1**, 274 (1962).
15. Goode, W. E., F. H. Owens, R. P. Fellman, W. H. Snyder, and J. E. Moore, *J. Polymer Sci.*, **46**, 317 (1960).
16. Kargin, V. A., V. A. Kabanov, and V. P. Zubov, *Vysokomol. Soedin.*, **2**, 765 (1960).
17. Yamashita, I., J. Furukawa, T. Saegusa, and A. Kawasaki, *Kogyo Kagaku Zasshi*, **65**, 239 (1962).
18. Pepper, C. D., *Quart. Rev.*, **8**, 88 (1954).
19. Dewar, M. J. S., *Bull. Soc. Chim. France*, **18**, C79 (1951).
20. Hill, A., *J. Am. Chem. Soc.*, **44**, 1163 (1922); A. Hill and F. W. Miller, *ibid.*, **47**, 2702 (1925).
21. Peyronel, G., I. M. Vezzosi, and S. Buffalagni, *Gazz. Chim. Ital.*, **93**, 1462 (1963); *ibid.*, **89**, 1863 (1959); *Ann. Chim. (Rome)*, **50**, 343, 348 (1960);
22. Peyronel, G., G. Belmondi, and I. M. Vezzosi, *Atti Soc. Nat. Modena*, **35**, 87 (1957).
23. Andrews, L. G., and R. M. Keefer, *J. Am. Chem. Soc.*, **71**, 3644 (1949).
24. Smith, H. J., and R. E. Rundle, *J. Am. Chem. Soc.*, **80**, 5075 (1958).
25. Mulliken, R. S., *J. Am. Chem. Soc.*, **74**, 811 (1952).
26. Slough, W., *Trans. Faraday Soc.*, **58**, 1360 (1962).
27. Taufen, H. J., J. M. Murray, and F. F. Cleveland, *J. Am. Chem. Soc.*, **63**, 3500 (1941).
28. Daasch, I. W., *Spectrochim. Acta*, **15**, 726 (1959).
29. Keefer, R. M., and L. J. Andrews, *J. Am. Chem. Soc.*, **74**, 640 (1952).
30. Ogimachi, M., L. J. Andrews, and R. M. Keefer, *J. Am. Chem. Soc.*, **78**, 2210 (1956).
31. Winstein, S., and A. G. Lucas, *J. Am. Chem. Soc.*, **60**, 836 (1938).
32. Keefer, R. M., and L. J. Andrews, *J. Am. Chem. Soc.*, **72**, 5034 (1950).
33. Jordon, P. O., and F. E. Trebor, *J. Chem. Soc.*, **1961**, 734.
34. Bawn, C. E. H., W. H. Jones, and A. M. North, *J. Polymer Sci.*, **58**, 335 (1962).
35. Krentsel, B. A., L. G. Siderova, and A. V. Topchiev, paper presented at I.U.P.A.C. International Symposium on Macromolecular Chemistry, Paris, July 1963; *J. Polymer Sci.*, **C4**, 3 (1963).
36. Edwards, W. R., and N. F. Chamberlain, *J. Polymer Sci.*, **A1**, 2299 (1963).
37. Kennedy, J. P., and R. M. Thomas, *Makromol. Chem.*, **53**, 28 (1962).
38. Kennedy, J. P., L. S. Minckler, Jr., G. G. Wanless, and R. M. Thomas, *J. Polymer Sci.*, **C4**, 289 (1963).
39. Coerver, H. J., and C. Curran, *J. Am. Chem. Soc.*, **80**, 3522 (1958).
40. Comyns, A. E., and H. J. Lucas, *J. Am. Chem. Soc.*, **76**, 1019 (1954).
41. Rundel, R. E., and J. H. Goring, *J. Am. Chem. Soc.*, **72**, 5337 (1950).
42. Peyronel, G., G. Belmondi, and V. Gaglioti, *Gazz. Chim. Ital.*, **93**, 1163 (1963).
43. Levy, G. B., J. J. Murtangh, and M. Rosenblatt, *Ind. Eng. Chem.*, **17**, 194 (1945).

Résumé

La polymérisation de dérivés vinyliques peut être initiée au moyen de sels d'argent solubles. Dans ce travail, on étudie la cinétique de polymérisation en solution du styrène et du méthacrylate de méthyle, initiée au perchlorate d'argent. Les vitesses ont été suivies dilatométriquement à 70°C; les solutions étaient préparées sous vide poussé. L'ordre de la réaction, par rapport à la concentration en monomère, est égal à deux, aussi bien pour le styrène que pour le méthacrylate de méthyle. Dans le cas du styrène, la vitesse de polymérisation est proportionnelle à la concentration en AgClO_4 lorsque celle-ci est inférieure ou égale à 10^{-2} mole/l. Au-dessus de cette valeur, la vitesse est proportionnelle au carré de la concentration en perchlorate. Dans le cas du méthacrylate de méthyle, l'ordre de la réaction varie de 0,5 à 1, suivant le domaine des concentrations en AgClO_4 . Ces résultats sont interprétés sur la base de l'existence de complexes AgClO_4 -monomère qui participent à la réaction au lieu de AgClO_4 libre. Par ailleurs, l'examen de solutions de AgClO_4 dans le styrène et de benzène indique la formation de complexes AgClO_4 -hydrocarbure aromatique de composition 1:1 et 2:1. Il en résulte un bon accord entre la cinétique de polymérisation et l'existence de deux types d'initiateurs. On propose un mécanisme de polymérisation par coordination dans lequel une réaction de transfert d'hydrogène alterne avec chaque étape de propagation. Ce mécanisme est corroboré par l'existence d'un effet isotopique égal à deux, lorsqu'on compare le comportement du dideutérostyrène à celui du styrène usuel. La structure interne du polyméthacrylate de méthyle, obtenu en présence de perchlorate d'argent, correspond à celle d'un polymère conventionnel. La présence de traces d'eau inhibe ces polymérisations.

Zusammenfassung

Die Polymerisation von Vinylverbindungen kann durch lösliche Silbersalze angeregt werden. In der vorliegenden Arbeit wurde die Kinetik der durch Silberperchlorat angeregten Polymerisation von Styrol und Methylmethacrylat in organischen Lösungsmitteln untersucht. Die Geschwindigkeit wurde dilatometrisch bei 70°C gemessen; die Lösungen wurden unter Hochvakuum hergestellt. In Bezug auf das Monomere ist die Reaktionsordnung sowohl für Styrol als auch für Methylmethacrylat gleich zwei. Im Falle von Styrol ist die Polymerisationsgeschwindigkeit bei Silberperchloratkonzentrationen $\leq 10^{-2}$ Mol/l dieser Konzentration proportional. Oberhalb dieses Werts wird die Geschwindigkeit dem Quadrat der Silberperchloratkonzentration proportional. Bei Methylmethacrylat variiert die Ordnung in Bezug auf die Silbersalzkonzentration in Abhängigkeit vom Konzentrationsbereich von 0,5 bis 1. Die kinetischen Ergebnisse werden durch die Annahme der Teilnahme eines Silberperchlorat-Monomerkomplexes anstatt einer Silberperchloratmolekel an der Polymerisation interpretiert. Überdies lässt die Untersuchung von Lösungen von Silberperchlorat in Styrol und Benzol die Bildung von Silbersalz und aromatischen Kohlenwasserstoffkomplexen vom 1:1- und 2:1-Typ erkennen. Es besteht also eine gute Übereinstimmung zwischen der Kinetik der beiden verschiedenen Initiatorsysteme. Es wird ein Koordinationspolymerisationsmechanismus angenommen, bei welchem Wasserstoffübertragung mit jedem Wachstumsschritt abwechselt. Dieser Mechanismus wird durch einen Isotopeneffekt gleich zwei beim Vergleich von Bideuterostyrol zu gewöhnlichem Styrol gestützt. Die innere Struktur des mit AgClO_4 erhaltenen Polymethylmethacrylats entspricht derjenigen eines konventionellen Polymeren. Die Gegenwart von Wasserspuren verhindert die Polymerisation.

Received February 3, 1965

Prod. No. 4703A

Aliphatic Poly-1,3,4-Oxadiazoles

TERUNOBU UNISHI and MASAKI HASEGAWA, *The Textile Research Institute, Yokohama, Japan*

Synopsis

Three high molecular weight aliphatic polyoxadiazoles have been prepared by a new route from equimolar amounts of a diphenyl ester of dicarboxylic acid and an anhydrous hydrazine (or a dihydrazide). The resulting polymers have been characterized by microanalysis, intrinsic viscosity, x-ray diffraction patterns, infrared absorption spectra, and by differential thermal analysis. Such polymers are soluble in several solvents and show very low melting temperature and high crystallinity.

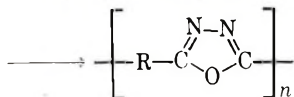
INTRODUCTION

A few extensive studies on polyoxadiazoles have recently been carried out. Frazer reported the results of a preparative study of several aromatic, a few aliphatic and some aliphatic-aromatic polyoxadiazoles which were converted from the corresponding high molecular weight polyhydrazides.¹

The synthesis of poly[1,8-octamethylene-2,5-(1,3,4-oxadiazole)] from diphenyl sebacate and anhydrous hydrazine was reported in our previous paper.²

In this reaction it is interesting that the self-condensation of the hydrazide group does not interfere with the polyoxadiazole formation under the melt conditions used and that high molecular weight polyoxadiazoles are produced from low molecular weight polyhydrazides by melt polymerization.

Successive attempts to obtain several kinds of aliphatic and aromatic polyoxadiazoles from diphenyl esters of carboxylic acids with an anhydrous hydrazine or carboxylic acid dihydrazides were also investigated. Iso-phthalic, terephthalic, adipic, 1,7-heptanedicarboxylic, 1,8-octanedicarboxylic, 1,9-nonanedicarboxylic, and 1,10-decanedicarboxylic acids were used as the phenyl ester component. Three aliphatic polyoxadiazoles were obtained successfully i.e., those from 1,8-octanedicarboxylic, 1,9-nonanedicarboxylic, and 1,10-decanedicarboxylic acids:



where R is (CH₂)₈, (CH₂)₉, and (CH₂)₁₀.

These three aliphatic polymers are soluble in several common polymer solvents, e.g., dimethylformamide and *m*-cresol, and unusually soluble in benzene, cyclic ethers, etc.

Films could be cast from solvent, and fibers were made by melt spinning.

All of these linear polyoxadiazoles showed low melting points and high crystallinities. Differential thermal analysis was used to characterize some thermal properties of the polymer.

RESULTS AND DISCUSSION

Preparation and Properties of Polyhydrazides

Comparatively low molecular weight polyhydrazide was produced by heating a diphenyl ester with an anhydrous hydrazine or a dihydrazide in dimethylformamide at 110–150°C. for 2–5 hr. The precipitated white substance was isolated by removal of solvent and eliminated phenol under the reduced pressure. These compounds were shown to be polyhydrazides by their infrared spectra.

Data on some polyhydrazides obtained by this procedure are shown in Table I. The amount of phenol eliminated from the diphenyl esters of the aliphatic acids was 80–90% of the theoretical amount; this suggests that the polyhydrazides contain 3–5 repeating units.

TABLE I
Polyhydrazides

Diphenyl ester component	Reaction conditions		Extent of time, hr.	Melting point, °C. reaction % ^a
	Temp., °C.			
Terephthalic acid	140–150	2	65	>350 (dec)
Isophthalic acid	140–150	2	70	>350 (dec.)
Adipic acid	110–120	2	86	300–305
1,7-Heptane-dicarboxylic acid	110–120	2	90	285–298
1,8-Octane-dicarboxylic acid	110–120	2	90	280–285
1,9-Nonane-dicarboxylic acid	110–120	4	80	257–263
1,10-Decane-dicarboxylic acid	110–120	5	85	265–270

^a This value was evaluated from the amount of phenol eliminated.

The use of two other solvents, *m*-cresol and nitrobenzene, in this procedure in place of dimethylformamide was tried, but the results were, not better than those obtained in the following melt polymerization.

Preparation of Polyoxadiazoles

A melt process was used for further polymerization of polyhydrazide. That both cyclodehydration and chain growth occur was proved by

detection of phenol and water in the distillate during the process. Only about $\frac{1}{2}$ hr. of melt polymerization was required for the melting temperature of the product to become as low as that of the corresponding polyoxadiazole.

Polyhydrazide from isophthalic or terephthalic acid degraded before it melted, and that from adipic acid was crosslinked with progression of melt polymerization.

Melt polymerization of the polyhydrazide from 1,7-heptanedicarboxylic acid proceeded successfully, and the melting temperature dropped to that of poly[1,7-heptamethylene-2,5-(1,3,4-oxadiazole)], but contents of the apparatus began to show an appearance characteristic of slightly cross-linked polymer after a few hours. This polymer produced very strong film and showed an apparent melting temperature near 300°C . but was soluble only in concentrated sulfuric acid, so it was concluded that the product was a mixture consisting of mainly polyoxadiazole and a small part of cross-linked substance.

The above observations indicate a bath temperature around 300°C . seems to be the upper limit for the reaction of phenyl ester of carboxylic acid with hydrazide to proceed exclusively, with other undesirable side reactions depressed. Also, aliphatic polyhydrazides appear to resist thermal degradation.

Solid-state polymerization was attempted for high-melting ($>300^{\circ}\text{C}$.) polyhydrazides but has not been successful. Since hardly any cyclodehydration occurs below a temperature of 200°C ., the final step required a temperature of $230\text{--}240^{\circ}\text{C}$. for several hours. The polymer increases its melt viscosity gradually during the procedure, and a tan opaque substance with high molecular weight was obtained from polyhydrazides of 1,8-octanedicarboxylic, 1,9-nonanedicarboxylic, and 1,10-decanedicarboxylic acids.

Elementary analysis of the final products supported the polyoxadiazoles structures (Table II).

TABLE II
Polyoxadiazoles

Poly-oxadiazole ^a	Calculated			Found			Intrinsic viscosity (30°C., <i>m</i> -cresol)	Specific gravity, g./cm. ³	Melting point, °C. ^b
	C, %	H, %	N, %	C, %	H, %	N, %			
I	66.61	8.95	15.55	65.60	9.16	15.38	0.45	1.21	90–110
II	67.17	9.34	14.42	67.38	8.73	14.24	0.40	1.28	66–82
III	69.17	9.68	13.45	68.99	9.69	13.27	0.41	1.22	64–100

^a Polyoxadiazoles I, II, and III correspond to poly[octamethylene-2,5-(1,3,4-oxadiazole)], poly[nonamethylene-2,5-(1,3,4-oxadiazole)] and poly[decamethylene-2,5-(1,3,4-oxadiazole)], respectively.

^b Melting temperature was determined by differential thermal analysis.

Infrared Spectra of Polyoxadiazoles

Infrared spectra of the model compound and of the polyoxadiazoles are shown in Figure 1. When 1,2-dibutylhydrazine was heated, 2,5-dipropyl-(1,3,4-oxadiazole) (IV) was produced. New absorption peaks

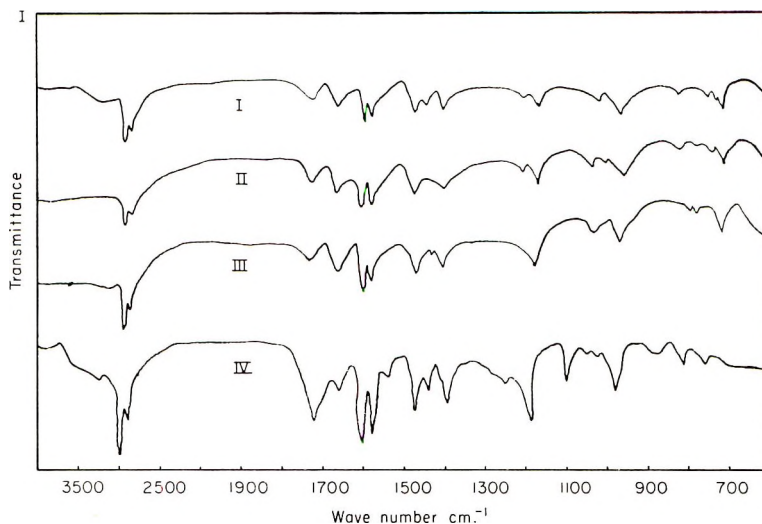


Fig. 1. Infrared spectra of (I) poly[1,8-octamethylene-2,5-(1,3,4-oxadiazole)]; (II) poly[1,9-nonamethylene-2,5-(1,3,4-oxadiazole)]; (III) poly[1,10-decamethylene-2,5-(1,3,4-oxadiazole)]; (IV) 2,5-dipropyl-(1,3,4-oxadiazole).

appeared in the 1720–1730, 1600–1605, 1570–1575, 1170, and 970 cm^{-1} regions. These peaks are due to the oxadiazole ring in aliphatic compounds. The infrared spectra of the three linear polyoxadiazoles (I, II, and III) are in agreement with that of the model compound (IV) (Fig. 1).

Physical Properties of Polyoxadiazoles

Aliphatic polyoxadiazoles show unexpectedly low melting temperatures and are soluble in several solvents including benzene, tetralin, and cyclic ethers. Films could be cast conveniently from the solutions in chloroform. These properties are summarized in Tables II and III.

Differential Thermal Analysis of Polyoxadiazoles

Both films and fibers from these polymers lose their plasticities gradually on standing at room temperature for several days. These brittle substances regain their plasticities if they are melted and kept at the molten state for 30 min. These polymers have been investigated by differential thermal analysis, and the DTA curves are shown in Figure 2.

An inflection point is observed before the melting temperature which seems to be some crystalline transition point of the polymer (arrow in

TABLE III
Solubilities of Polyoxadiazoles^a

Solvent	Polymer I	Polymer II	Polymer III
<i>m</i> -Cresol	++	++	++
Ethylenechlorohydrine	++	++	++
1,2-Dichloroethane	++	++	++
Chloroform	++	++	++
Dichloromethane	++	++	++
Tetrachloromethane	±	-	-
Benzyl alcohol	++	++	++
Formic acid	++	++	++
Benzene	+	+	+
Tetrahydrofuran	+	+	+
Dioxane	+	+	+
Cyclohexanone	+	+	+
Tetralin	+	+	+
Dimethylformamide	+	+	+
Methanol	±	±	±
Dimethyl sulfoxide	-	-	-

^a ++ = soluble at room temperature; + = soluble at below 50°C.; ± = swollen at 50°C.; - = insoluble.

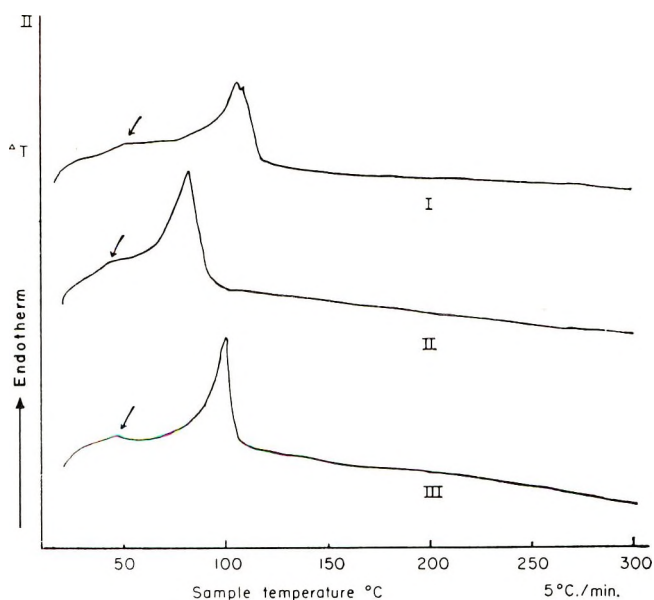


Fig. 2. Differential thermal analysis in He of (I) poly[1,8-octamethylene-2,5-(1,3,4-oxadiazole)]; (II) poly[1,9-nonamethylene-2,5-(1,3,4-oxadiazole)]; (III) poly[1,10-decamethylene-2,5-(1,3,4-oxadiazole)].

Fig. 2). Polymers I, II, and III have such transition points at 46–52, 39–45, and 40–43°C., respectively.

The polymer melting temperature was determined from the heat absorption peak in Figure 2. The melting temperature of poly[1,8-octamethylene-2,5-(1,3,4-oxadiazole)] was reported by Frazer¹ to be at 300°C., but no heat absorption peak was observed near 300°C. in the diagram. The analysis was also attempted in air, but it did not indicate any oxydative degradation up to a temperature of 300°C.

Fiber Properties of Polyoxadiazoles

Fiber formed from polyoxadiazole by melt spinning with a flow tester machine, was wound on a reel and could be stretched at 65–80°C. in silicon oil.

By x-ray studies these three polymers have been shown to be highly crystalline, and their stretched fibers show good orientation.² The relation between their birefringences and the stretching ratios is shown in Table IV.

TABLE IV

Polyoxadiazole	Spinning temp., °C.	Stretching ratio % ^a	Birefringence
I	115	0	4.30×10^{-3}
		66	6.25×10^{-3}
II	95	0	$<10^{-3}$
		133	2.69×10^{-3}
III	100	0	—
		100	$<10^{-3}$

^a Fibers wound on a reel are already stretched because of the small difference between spinning and room temperatures, so the term stretching ratio is really not valid.

TABLE V

Dicarboxylic acid	Melting point of diphenyl ester, °C.	
	Observed (this work)	Literature value
Terephthalic	196 – 197	191 ^a
Isophthalic	134.5 – 135.5	134–135 ^b
Adipic	105 – 106	105.5–106 ^c
1,7-Heptanedicarboxylic	51 – 52	49–50 ^d
1,8-Octanedicarboxylic	69 – 70	65–66 ^d
1,9-Nonanedicarboxylic	62 – 63	New compound
1,10-Decanedicarboxylic	76 – 76.5	New compound

^a Data of Schreder.³

^b Data of Hasegawa and Suzuki.¹

^c Data of Hill.⁵

^d Data of Marongoni.⁶

EXPERIMENTAL

Preparation of Phenyl Esters

The phenyl esters were prepared by a standard method from the phenol and the carbonyl chloride. These were recrystallized from absolute ethanol (Table V).

Preparation of Polyoxadiazoles

Anhydrous hydrazine (0.01 mole) was dissolved in 7 ml. of dimethylformamide. This solution was added to the dicarboxylic acid diphenyl ester (0.01 mole).

Dihydrazide could be substituted in place of anhydrous hydrazine in this procedure. Since dihydrazide does not dissolve in dimethylformamide, the solvent was added to a mixture of dihydrazide and diphenyl ester. The resulting solution or mixture was held at room temperature for 1 hr. and then was heated at 110–120°C. for 2 hr. A white oligomer (polyhydrazide) separated.

Dimethylformamide and phenol were removed under reduced pressure. Then the polyhydrazide was heated above its melting temperature and held at this temperature for $\frac{1}{2}$ hr. under reduced pressure in an N_2 atmosphere; it was then held at 230–240°C. under reduced pressure in an N_2 atmosphere for 15–20 hr.

Differential Thermal Analysis

The differential thermal analysis apparatus consisted of cylindrical nickel sample holders. Twin cavities were drilled symmetrically from the axis of the cylinder.

Alumel–chromel thermocouples were placed exactly in the center of each palladium sample cell. A two-recorder system was used (recorders with range of -25 and $25 \mu v.$ deflection). The sample holders were heated in a cylindrical block in an electric furnace. Usually a 0.03–0.04 g. sample was tamped into place between two layers of aluminum oxide (0.7 g.). The reference cell contained 0.07 g. of aluminum oxide.

The author wishes to express his thanks to Dr. H. Kanetsuna for help in obtaining and interpreting DTA curves and to Mr. T. Kurita for the x-ray study.

References

1. Frazer, A. H., W. Sweeny, and F. T. Wallenberger, *J. Polymer Sci.*, **A2**, 1157 (1964).
2. Hasegawa, M., and T. Unishi, *J. Polymer Sci.*, **B2**, 237 (1964).
3. Schreder, *Ber.*, **7**, 707 (1874).
4. Hasegawa, M., and F. Suzuki, *Kogyo Kagaku Zasshi*, **66**, 218 (1963).
5. Hill, J. W., *J. Am. Chem. Soc.*, **52**, 4110 (1930).
6. Marongoni, C., *Atti. Ist. Veneto. Sci.*, Pt. II, *Sci. Mat. Nat.*, **97**, 209 (1937).

Résumé

On a préparé trois polyoxadiazoles aliphatiques de poids moléculaires élevés au moyen d'une nouvelle méthode, à partir de quantités équimoléculaires d'un ester diphenylique de l'acide dicarboxylique et d'une hydrazine anhydre (ou d'un dihydrazide). Les polymères obtenus ont été caractérisés par microanalyse, par viscosité intrinsèque, par les diagrammes de diffraction aux rayons-X, par les spectres d'absorption infrarouge et par analyse thermique différentielle. De tels polymères sont solubles dans plusieurs solvants, présentent des températures de fusion très basses et une cristallinité élevée.

Zusammenfassung

Drei hochmolekulare aliphatische Polyoxadiazole wurden auf einem neuen Weg aus äquimolaren Mengen eines Diphenylesters einer Dicarboxylsäure und eines wasserfreien Hydrazins (oder eines Dihydrazides) dargestellt. Die erhaltenen Polymeren wurden durch Mikroanalyse, Viskositätszahl, Röntgenbeugungsdiagramm, Infrarotabsorptionsspektren und durch Differentialthermoanalyse charakterisiert. Die Polymeren sind in einigen Lösungsmitteln löslich, zeigen eine sehr niedrige Schmelztemperatur und hohe Kristallinität.

Received July 20, 1964

Revised February 2, 1965

Prod. No. 4685A

Copolymerization of *p*-Triphenyltinystyrene and *p*-Triphenylleadstyrene with Styrene or Vinyltoluene*

STANLEY R. SANDLER, J. DANNIN, and K. C. TSOU,
*Central Research Laboratory, The Borden Chemical Company,
Philadelphia, Pennsylvania*

Synopsis

The reactivity ratios for the copolymerization of *p*-triphenyltinystyrene (M_1) and styrene (M_2) have been determined by the Fineman and Ross method to be $r_1 = 2.55$ and $r_2 = 0.93$. The values for vinyltoluene copolymerization are $r_1 = 3$, and $r_2 = 0.60$. The latter values indicate that *p*-triphenyltinystyrene-copolymers with styrene or vinyltoluene contain blocks of the former monomer unit. The rate of homopolymerization of *p*-triphenyltinystyrene and *p*-triphenylleadstyrene in toluene was shown to be the same at 50°C.

INTRODUCTION

In the previous report,¹ scintillation plastics had been prepared by the copolymerization of *p*-triphenylleadstyrene or *p*-triphenyltinystyrene with vinyltoluene. Since the scintillation efficiency of the plastics could be affected by the distribution of such organometallic monomers in the polymer chain, it was considered to be of interest to investigate the reactivity ratio of these organometallic monomers with vinyl toluene and styrene. The latter solvent was used in most of the reactivity ratio determinations because it avoids the difficulty in using two isomeric monomers as is present in commercial vinyltoluene. No initiators were used, and the monomers were thermally polymerized.

In addition, a brief kinetic study of these two organometallic monomers was carried out in a toluene solution in order to learn some of the characteristics of the homopolymerization.

EXPERIMENTAL

p-Triphenyltinystyrene² (m.p. 104–105°C.) and *p*-triphenylleadstyrene³ (m.p. 112–113°C.) were prepared by an improved procedure¹ to yield a pure product. Earlier Koton⁴ reported that *p*-triphenylleadstyrene had a melting point of 87–89°C. and *p*-triphenyltinystyrene had a melting point of 101–103°C.

* This work was supported by the U. S. Atomic Energy Commission under Contract No. AT(30-1)-1931.

The reactivity ratio determination was performed according to procedure 3 described by Mayo and Lewis⁵ at a temperature of $108 \pm 1^\circ\text{C}$. The analysis of the copolymers for tin or lead facilitated the reactivity ratio determination.*

The homopolymerization of the organometallic monomers was followed by a dilatometric method. The description of the solutions is reported in the Results section of this paper.

Tetraphenyllead and tetraphenyltin were obtained from Peninsular Chem-Research, Inc. and recrystallized several times from benzene to give melting points of 226 and 225°C ., respectively.

RESULTS

Reactivity Ratio of *p*-Triphenyltinstyrene and Styrene

The copolymer was prepared in the usual manner to low conversion and the molar ratio of the polymer calculated from the tin analysis. The Fineman and Ross⁶ method was used for the calculation of r_1 and r_2 . The data are summarized in Table I, and a plot of $(f-1)/F$ versus f/F^2 is shown in Figure 1. From the intercept and slope, r_1 (*p*-triphenyltinstyrene) = 2.55, r_2 (styrene) = 0.93 are obtained.

TABLE I
Composition of *p*-Triphenyltinstyrene and Styrene in Copolymerization Ratio Study

Sn in polymer, %	Conversion, %	$F = M_1/M_2$		f/F^2	$(f-1)/F$
		(initial monomer composition) ^a	$f = m_1/m_2$ (polymer composition) ^a		
11.10	14.33	0.1332	0.1690	9.54	-6.24
11.56	15.51	0.1573	0.1807	7.31	-5.20
15.39	16.99	0.2875	0.3280	3.96	-2.34
16.39	18.21	0.3050	0.3830	4.23	-2.02
14.80	17.09	0.2300	0.2990	5.66	-3.05
8.37	12.40	0.1060	0.1080	9.65	-8.41
21.38	14.70	0.6080	1.0260	2.77	0.043

^a Molar ratios.

Reactivity Ratio of *p*-Triphenyltinstyrene and Vinyltoluene

The vinyltoluene used is a 60% *meta*-40% *para* mixture. No correction was made, as it is assumed that the reactivity of either isomer to the organometallic monomer is the same. The data are shown in Table II, and a plot based on these data is shown in Figure 2. The calculated values are $r_1 = 3.0$ and $r_2 = 0.63$.

* Microanalyses were performed by Dr. Stephen M. Nagy, Microchemical Laboratory, Belmont, Mass.

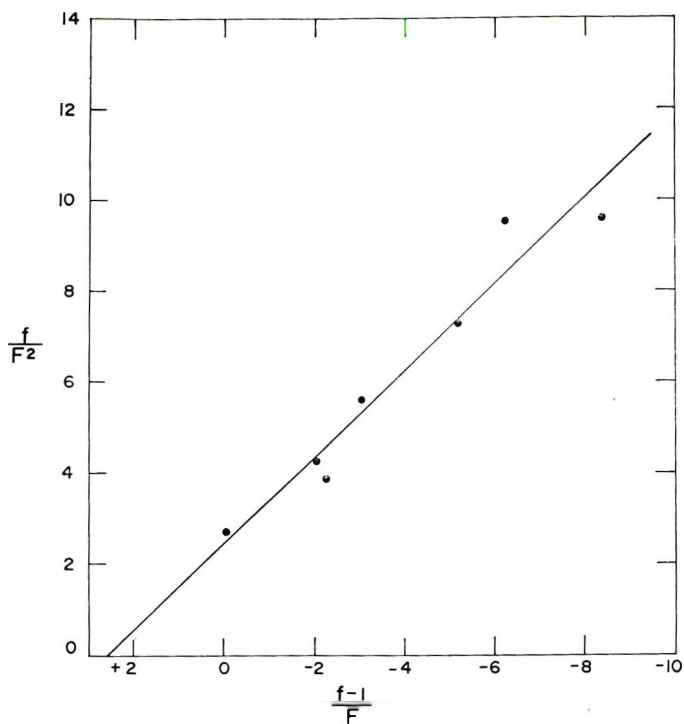


Fig. 1. Fineman and Ross plot of f/F^2 vs. $(f - 1)/F$ for the copolymerization of *p*-triphenyltinystyrene and styrene.

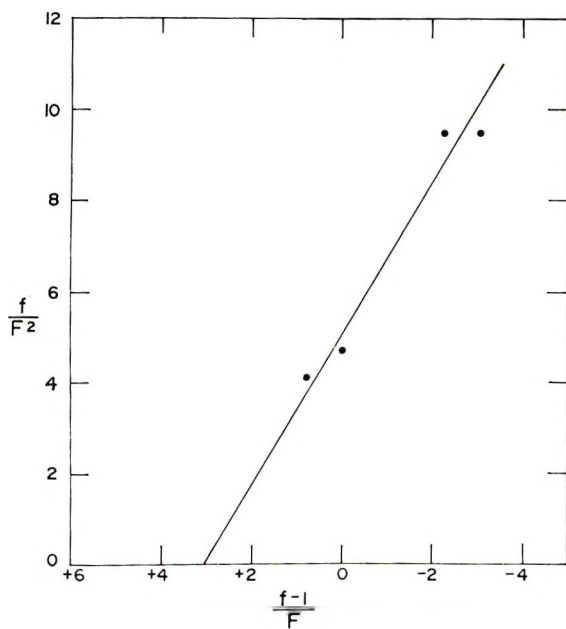


Fig. 2. Fineman and Ross plot of f/F^2 vs. $(f - 1)/F$ for the copolymerization of *p*-triphenyltinystyrene and vinyl toluene.

TABLE II
Composition of *p*-Triphenyltinstyrene and Vinyltoluene in Copolymerization Ratio Study.

Sn in polymer, %	Conversion, %	$F = M_1/M_2$	$f = m_1/m_2$	f/F^2	$(f - 1)/F$
22.27	9.20	0.6020	1.489	4.11	0.813
20.79	12.40	0.4640	1.007	4.67	0.0151
15.45	12.40	0.1989	0.377	9.51	-3.13
16.95	29.78	0.2245	0.478	9.51	-2.32

TABLE III
Summary of Monomer Reactivity Ratios for Copolymerization at 108°C.

Monomer 1	Monomer 2	r_1	r_2
<i>p</i> -Triphenyltinstyrene	Styrene	2.55	0.93
<i>p</i> -Triphenyltinstyrene	Vinyltoluene	3.0	0.63

Rates of Thermal Copolymerization of Styrene in the Presence of Organometallics

The rate of homopolymerization of pure styrene in presence of tetraphenyllead or tetraphenyltin was determined at $100 \pm 1^\circ\text{C}$.; the data are presented in Table IV. It is seen that the organometallics accelerate the polymerization almost to the same extent for tin or lead.

To ascertain the influence of the vinyl group on the organometallics, the effect on the rate of small amounts of *p*-triphenylleadstyrene and *p*-tri-

TABLE IV
Conversion versus Time for Tetraphenyllead and Tetraphenyltin in Thermal Polymerization with Styrene at $100 \pm 1.0^\circ\text{C}$.

Wt. tetraphenylmetallic, g.	Wt. styrene, g.	Time, min.	Conversion, %
$(\text{C}_6\text{H}_5)_4\text{Pb}$			
0.30 (0.0608 molal)	9.6	63.0	1.96
0.30	9.6	116.5	3.87
0.30	9.6	193.8	5.44
0.30	9.6	238.0	7.22
0.30	9.6	300.0	10.8
0.30	9.6	374.0	11.2
$(\text{C}_6\text{H}_5)_4\text{Sn}$			
0.30 (0.0735 molal)	9.6	63.0	2.73
0.30	9.6	116.5	4.17
0.30	9.6	238.0	8.02
0.30	9.6	300.0	9.59
0.30	9.5	374.0	12.6

TABLE V
Rate of Copolymerization of $(C_6H_5)_2M-C_6H_4CH=CH_2$ with Styrene^a

Composition and experiment no.	Time, min.	Wt. polymer, g.	Conversion, %
$(C_6H_5)_2SnC_6H_4CH=CH_2$, 0.0610 molal			
1	64.7	0.1983	2.01
2	115.5	0.3883	3.94
3	210.0	0.7489	7.59
4	295.5	1.2178	12.35
5	351.5	1.5109	15.32
$(C_6H_5)_2PbC_6H_4CH=CH_2$, 0.0610 molal			
1	63.0	0.1322	1.33
2	208.6	0.7876	7.94
3	294.0	1.2088	12.19
4	352.5	1.4026	14.15

^a The temperature of the oil bath was $105 \pm 1^\circ C$.

phenyltinstyrene in styrene copolymerization is shown in Table V for comparison. Evidently, the styrene organometallics are even better accelerators of the rate than the tetraarylmatallics. For comparison, we determined also the rate of homopolymerization of styrene under identical conditions. There is an initial induction period of polymerization in styrene as well as in the other two-component systems. The per cent conversion for styrene (after the induction period) versus time is 2.15%/hr., and this checks with the literature value.⁴ The combined results are also shown in Figure 3.

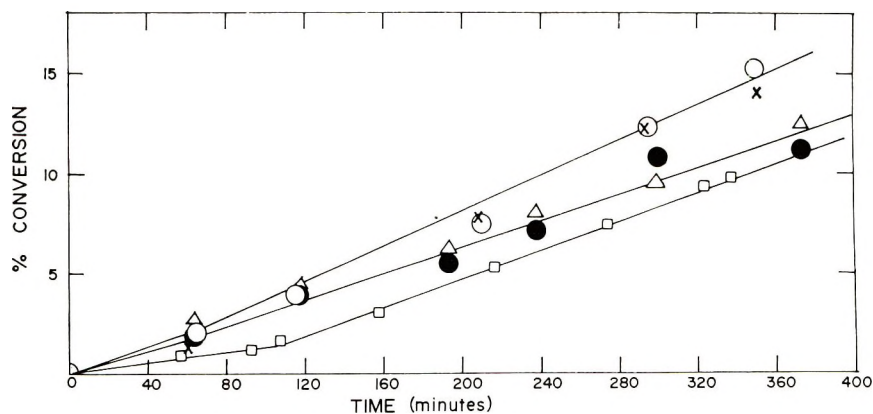


Fig. 3. Per cent conversion vs. time for copolymerization of styrene and *p*-triphenyltinstyrene or *p*-triphenylleadstyrene at 0.0610 molal concentration (in addition tetraphenyllead (0.0608 molal) and tetraphenyltin (0.0735 molal) was added to styrene to determine the effect on the rate.): (O) *p*-triphenyltinstyrene; (X) *p*-triphenylleadstyrene; (Δ) tetraphenyltin; (●) tetraphenyllead; (□) curve for pure styrene also shown for comparison.

Homopolymerization of *p*-Triphenylleadstyrene and *p*-Triphenyltinstyrene

The rate of polymerization of pure *p*-triphenylleadstyrene and *p*-triphenyltinstyrene were determined at 49.95°C. in toluene by use of 0.3000*M* solutions with 0.5 wt.-% (based on the solution) azobisisobutyronitrile (AIBN) as initiator. The data are shown in Table VI.

TABLE VI
Homopolymerization of *p*-Triphenyltinstyrene and *p*-Triphenylleadstyrene in Toluene

<i>p</i> -Triphenyltinstyrene			<i>p</i> -Triphenylleadstyrene		
Time, min.	Height <i>h</i> , cm.	Δh , cm.	Time, min.	Height, <i>h</i> , cm.	Δh , cm.
0	31.00	—	0	33.5	—
80.8	30.96	0.04	80.0	33.4	0.10
112.5	30.90	0.10	136.5	33.30	0.20
169.1	30.80	0.20	176.0	33.25	0.25
275.0	30.70	0.30	224.0	33.20	0.30
340.0	30.65	0.35	279.5	33.16	0.34
381.0	30.60	0.40	322.0	33.10	0.40
434.0	30.58	0.42	420.0	33.05	0.45
454.0	30.56	0.44	453.0	33.00	0.50
462.0 ^a					

^a End of polymerization; precipitation in methanol.

The density of the solution of *p*-triphenyltinstyrene was 0.89 g./ml. and the volume was 5.50 ml. (0.745 g. monomer). The weight of the polymer formed was 0.4793 or 64.4%/7.7 hr. or 8.37%/hr.

The density of the *p*-triphenylleadstyrene solution was 0.927 g./ml. and the volume used was 5.88 ml. (0.955 g. monomer). The weight of the polymer was 0.5776 g. or 60.5%/7.7 hr. or 7.85%/hr. Thus the rate of polymerization of the tinstyrene sample seems to be greater by 0.52%/hr. However, the slopes show more accurately that the rates are the same since the slopes of the lines are almost identical (Fig. 4).

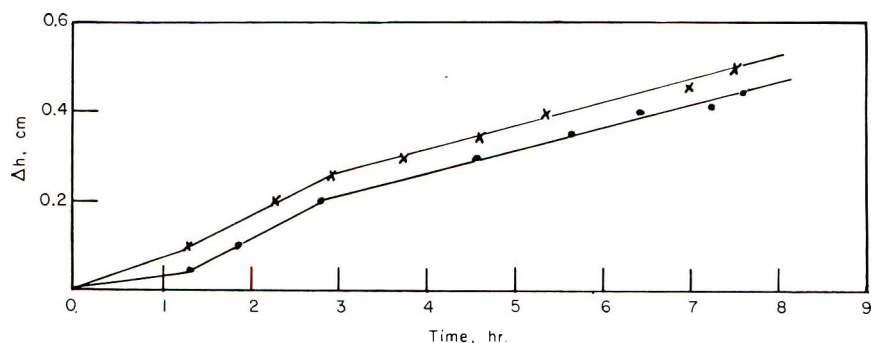
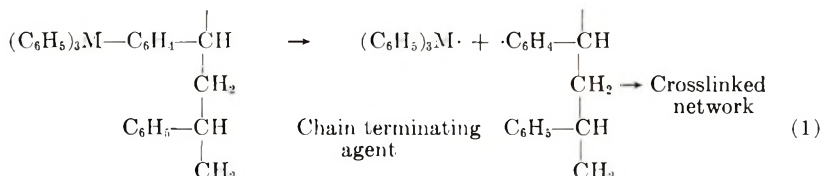
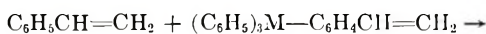


Fig. 4. Change in height of the dilatometer Δh vs. time for *p*-triphenyltinstyrene and *p*-triphenylleadstyrene at 0.3000*M* concentration in toluene at 49.95°C.: (●) *p*-triphenyltinstyrene; (×) *p*-triphenylleadstyrene.

DISCUSSION

For *p*-triphenyltinstyrene (M_1)-styrene (M_2) copolymerization $r_1 = 2.6$, $r_2 = 0.93$. Similarly, in vinyltoluene, $r_1 = 3.0$, $r_2 = 0.60$. Therefore, the rate of addition of a *p*-triphenyltinstyrene monomer to its own radical is greater than the addition of a styrene or vinyl toluene monomer unit. These results suggest that small blocks of the tin monomer units are found in the polymer network.

The copolymers obtained at low mole fractions of organometallics at 10–30% conversion are, for the most part, soluble in benzene. Higher mole fractions of tin or lead monomer give crosslinked polymers even for low conversions. Since decomposition of the monomers is not evidenced by free tin or lead, an increase in the radical concentration and subsequent crosslinking must take place. The process shown in eqs. (1) may take place, as is evidenced by a sudden increase in viscosity, rate, and exotherm.⁸ (Noltes, Buddery, and van der Kerk suggested homolytic cleavage of the trimethylleadstyrene at 70–90°C. to give a branched and crosslinked polymer.⁸)

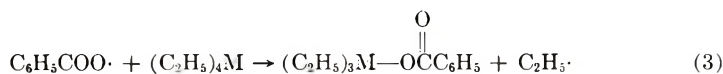


The crosslinked polymers and copolymers are not soluble in any organic solvent but swell to a great extent in benzene. The latter suggests a loose network. It is interesting to note from Figure 3 that tetraphenyllead and tetraphenyltin also accelerate the rate of polymerization of styrene.⁹ In addition, both organometallic monomers accelerate the rate of polymerization to about the same extent and both give rates that are greater than those for the tetraarylmetallics. The fact that the tetraarylmetallics also cause an acceleration suggests that the latter cleave homolytically to give free radicals as suggested for the organometallic monomers:



where $M = Pb$ or Sn .

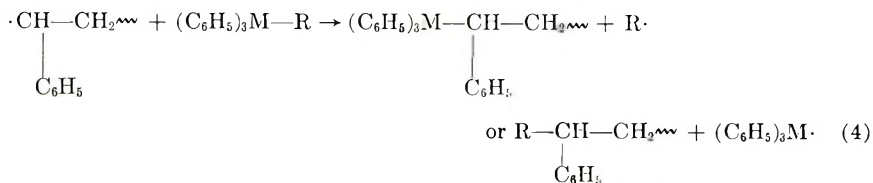
In addition, a radical-induced decomposition of the organometallics is possible, as has been recently suggested by studies with radicals from benzoyl peroxide:¹⁰



where $M = Sn, Pb$, or Si .

It is possible that styrene or vinyltoluene radicals produced during the course of the thermal copolymerizations can act in the same way as the

benzoyl peroxy radical to give a radical-induced decomposition of the tin and lead aryl organometallics used in this investigation, as shown in eq. (4):



where M = Sn or Pb and R = C₆H₅ or C₆H₄CH=CH₂.

Previously it was our belief that because *p*-triphenylleadstyrene and tetraphenyllead are thermally more unstable than the corresponding tin compounds, that the lead compounds are more readily polymerized. However, if the polymerizations are conducted at 49.95°C. or lower so that decomposition is avoided and the vinyl group is the only site of reaction, then the metallic portion exerts only a substituent effect on the reactivity of the vinyl group. This is supported by the fact that the polymer formed was soluble in toluene. The results in this work seem to indicate that the tin and lead styrene monomers homopolymerize and copolymerize at about the same rate. However, Koton, Kiseleva, and Florinskii⁴ found that *p*-triphenyltinstyrene homopolymerizes faster than the analogous lead monomer. The difference between their data and ours could be due to the purity of the monomers¹ used or the limitations of the methods used. The melting points of our samples are higher. The ultraviolet spectra confirms their purity. The homopolymerization studies were carried out almost exactly as that reported by Koton, except that a lower temperature, 49.95°C., was used. In their work the higher temperature of 80°C. was used, and this may result in C—Pb scission as shown in the earlier part of our discussion.

Since all of our scintillation plastics are prepared at approximate 100% conversion, a crosslinked network is the predominant structure in the organometallic-styrene copolymers. Thus, as reported recently by us elsewhere,¹ energy transfer and quenching have to be examined in a cross-linked network.

We are grateful to Dr. B. D. Halpern for his interest and suggestions in the course of this work, and to Mr. R. Mihailovich for his assistance in dilatometric study.

References

1. Sandler, S. R., and K. C. Tsou, *J. Phys. Chem.*, **68**, 300 (1964).
2. Loebnick, J. L., and H. E. Ramsden, *J. Org. Chem.*, **23**, 935 (1958).
3. Pars, H. G., W. A. G. Graham, E. R. Atkinson, and C. R. Morgan, *Chem. Ind. (London)*, **1960**, 693.
4. Koton, M. N., T. M. Kiseleva, and F. S. Florinskii, *Vysokomol. Soedin.*, **2**, 1639 (1960).
5. Mayo, F. R., and F. M. Lewis, *J. Am. Chem. Soc.*, **66**, 1594 (1944).
6. Fineman, M., and S. D. Ross, *J. Polymer Sci.*, **5**, 259 (1950).

7. Boundy, R. H., and R. F. Boyer, *Styrene Its Polymers, Copolymers and Derivatives*, Reinhold, New York, 1952, p. 216.
8. Noltes, J. G., H. A. Buddeny, and G. J. M. van der Kerk, *Rec. Trav. Chim.*, **79**, 1076 (1960).
9. Koton, M. M., *Dokl. Akad. Nauk SSSR*, **88**, 991 (1953).
10. Vyzankin, N. S., and O. A. Tschepetkova, *Dokl. Akad. Nauk SSSR*, **137**, 618 (1961).

Résumé

On a déterminé, par la méthode de Fineman et Ross, les rapports de réactivité pour la copolymérisation du *p*-triphényl-étain styrène (M_1) et du styrène (M_2), et on trouve $r_1 = 2.55$ et $r_2 = 0.93$. Les valeurs pour la copolymérisation avec le vinyl-toluène sont $r_1 = 3.1$ et $r_2 = 0.60$. Ces dernières valeurs indiquent que les copolymères du *p*-triphényl-étain-styrène ou du vinyl-toluène contiennent des blocs de la première unité monomérique. On montre que la vitesse d'homopolymérisation du *p*-triphénylétain-styrène et du *p*-triphénylplombstyrène dans le toluène est la même à 50°C.

Zusammenfassung

Die Reaktivitätsverhältnisse für die Copolymerisation von *p*-Triphenylzinnstyrol (M_1) und Styrol (M_2) wurden nach der Methode von Fineman und Ross zu $r_1 = 2,55$ und $r_2 = 0,93$ bestimmt. Die Werte für die Vinyltoluolcopolymerisation sind $r_1 = 3,1$ und $r_2 = 0,60$. Letztere Werte zeigen, dass *p*-Triphenylzinnstyrol-Styrol- oder-Vinytoluol-copolymere Blöcke ersterer Monomereinheit enthalten. Die Geschwindigkeit der Homopolymerisation von *p*-Triphenylzinnstyrol und *p*-Triphenylbleistyrol in Toluol erwies sich bei 50°C als gleich.

Received August 21, 1963

Revised January 19, 1965

Prod. No. 4656A

Polymers Containing the 3,3,3',3'-Tetramethyl-1,1'-Spirobiindane Residue

K. C. STUEBEN, *Union Carbide Corporation, Plastics Division, Research and Development Department, Bound Brook, New Jersey*

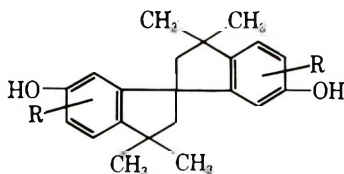
Synopsis

A variety of condensation polymers were prepared from the 6,6'-dihydroxy-3,3,3',3'-tetramethyl-1,1'-spirobiindanes including polyesters, polyurethanes, and a polyhydroxy-ether. The polycarbonate displayed good oxidative resistance at 200°C. but was found to lack toughness despite the presence of a low temperature transition at -100°C. A tendency toward brittleness was also evident in the other polymers and copolymers prepared. The contribution of the spiroindane structure to polymer properties is discussed. All of the polymers studied were amorphous and displayed high glass transition temperatures.

INTRODUCTION

Over the past several years the search for polymers having improved thermal and oxidative stability has led to the development of heterocyclic and aromatic systems which are stable up to 500°C. While such structures are required at the upper extremes of temperature, other more conventional polymer types, such as polyesters,^{1,2} will suffice at intermediate temperatures (200-300°C.) if they are devoid of oxidatively sensitive groups and have adequate heat distortion temperatures. As a class, the alkylaryl bisphenols, e.g., bisphenol A [2,2-bis(4-hydroxyphenyl) propane], have received little attention in this area because many contain oxidatively sensitive tertiary hydrogen atoms or because they afford polymers with insufficient heat distortion temperatures.

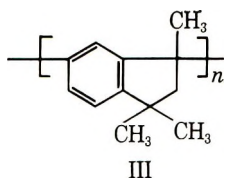
A class of bisphenols which might be expected to be useful for the preparation of high temperature polymers are the 6,6'-dihydroxy 3,3,3',3'-tetramethyl-1,1'-spirobiindanes (hereafter shortened to spiroindanes) (I, II).



I, R = H
II, R = CH₃

This class of compounds has been known for over thirty years but remained incorrectly characterized until recently.³ Thus, the product originally formulated⁴ as a dimethyldiphenylcyclobutane resulting from the acid-catalyzed decomposition of 2,2-bis(4-hydroxyphenyl) propane was shown to be the spiroindane (I).

Polymers derived from the spiroindanes should possess high glass transition temperatures because both aromatic rings are held rigidly together through the spiro-carbon atom. In addition, these monomers are devoid of oxidatively sensitive tertiary hydrogen atoms in the nucleus so that good oxidation resistance should result. In fact, the spiroindanes are closely related to a polyindane (III) which is reported to have excellent



thermal and oxidative stability.^{5,6} The latter class of polymers, however, is brittle even at high molecular weights, probably due to the fact that the chain is composed solely of rigid rings interconnected by single bonds. The spiroindanes, however, offer the possibility of building in flexibility by standard polycondensation reactions with the phenolic hydroxyl groups.

EXPERIMENTAL

Bisphenols

Preparation of 6,6'-Dihydroxy-3,3,5,3',5',5'-hexamethyl-1,1'-spirobiindane (II). The procedure outlined by Baker and Besley⁷ was followed. The yield of crude spiroindane (II) diacetate, m.p. 248–251°C. was 13%. After crystallization from acetic acid, the product had m.p. 260–266°C. and analyzed satisfactorily. Saponification of the diacetate with sodium hydroxide afforded the crude dihydroxyspiroindane (II), m.p. 218–228°C. After one recrystallization from water-acetic acid followed by three from xylene, it melted at 242–248°C. (reported⁷ m.p. 245–246°C.), with no change on further recrystallization. Sublimation did not improve the melting point. The spread in melting point is believed to be due to the presence of positional isomers. It is noteworthy that a sample of the spiroindane recovered from the saponification of a high molecular weight copoly-carbonate displayed this same broad melting point. This result rules out any suspicion that this melt behavior resulted from the presence of terminator.

ANAL. Calcd. for $C_{23}H_{28}O_2$: C, 82.10%; H, 8.39%; mol. wt. 336.51. Found: C, 81.99%; H, 8.11%; mol. wt. 331 ($\pm 1\%$) (in acetone).

6,6-Dihydroxy-3,3,3',3'-tetramethyl-1,1'-spirobiindane (I). This monomer was conveniently prepared by the *p*-toluenesulfonic acid-catalyzed disproportionation of 2,2-bis(4-hydroxyphenyl) propane. The conditions used were those described by Petropoulos and Sullivan,⁸ although in our hands the product obtained was the dihydroxyspiroindane (I) and not the 1-(4-hydroxyphenyl)-1,3,3-trimethylindanol-6 as claimed. To obtain evidence as to the structure of the product of the reaction above, it was reduced* to the hydrocarbon (b.p. 200–230°C./15 mm.) by a published method.⁹ Recrystallization from alcohol afforded a 27% yield of crystals, m.p. 130–131°C.¹⁰ whose infrared spectrum was identical with that reported for the parent spiroindane hydrocarbon (m.p. 132°C.).

The crude crystalline product from the *p*-toluenesulfonic acid decomposition (m.p. 212.5–215°C., ca. 50–55% yield) was washed four times with chloroform, air-dried, and then converted to the disodium salt with excess sodium hydroxide and recrystallized from 50:50 EtOH–H₂O under a nitrogen atmosphere. After four more recrystallizations from this solvent, the free bisphenol was liberated by treatment with hydrochloric acid. Two to three recrystallizations from methanol–water gave the pure dihydroxyspiroindane (I), m.p. 215.5–217°C. (lit.¹¹ m.p. 213–214°C.) after drying *in vacuo* at 100°C. Elemental analysis and NMR were consistent with the desired structure.

Bischloroformates

A. A mixture of 16.82 g. (0.05 mole) of the spiroindane (II), 9.89 g. (0.1 mole) of phosgene, 125 ml. of chlorobenzene, and 1.74 g. (0.005 mole) of stearyltrimethyl ammonium chloride† was heated sufficiently to cause the phosgene to reflux. Over 4 hr. the temperature of the contents of the flask rose to 133°C. (reflux), after which reflux was continued for 1 hr. longer. On cooling the resultant mixture a precipitate containing both catalyst and product formed. (Some product remained in the supernatant liquid but was not worked up.) The quaternary ammonium catalyst was washed out with water and the residual bischloroformate dried. This material was then taken up in methylene chloride and chromatographed on silica gel. Several fractions totaling 50% yield of the bischloroformate were thus obtained with melting points between 243 and 247°C. A fraction with m.p. 244–247°C. had the following analysis.

ANAL. Calcd. for C₂₃H₂₆O₄Cl₂: C, 65.08%; H, 5.68%; Cl, 15.37%; Found: C, 65.21%; H, 5.68%; Cl, 15.34%.

B. The 6,6'-dihydroxyspirobiindane (I) was dissolved in a dioxane–toluene mixture containing an excess of phosgene. Addition of dimethylaniline completed the reaction. Recrystallization from heptane gave 81% crystalline bischloroformate, m.p. 122–124°C.

* Performed by Dr. A. G. Farnham of these laboratories.

† This general procedure for chloroformate preparation was developed by Dr. R. J. Cotter of these laboratories.

ANAL. Calcd. for $C_{23}H_{22}O_4Cl_2$: C, 63.75%; H, 5.12%; Cl, 16.36%. Found: 63.82%; H, 5.25%; Cl, 16.21%.

The large difference in the melting point of this dichloroformate and that from the *o*-cresol derivative above is noteworthy.

Polyesters

Polycarbonates. Conventional melt polymerization of stoichiometric amounts of the spiroindane and diphenyl carbonate with a trace of lithium hydroxide as catalyst were not fruitful. The most satisfactory preparation of the homopolycarbonate employed interfacial techniques.¹² In a micro blender was placed a mixture of 1.31 g. (0.00425 mole) of spiroindane (I) and 0.41 g. (0.0125 mole) of sodium hydroxide in 15 ml. of water. During vigorous stirring a solution of 1.845 g. (0.0043 mole) of the dichloroformate (from I) in 19 ml. of methylene chloride was added all at once, followed by the addition of one drop of triethylamine catalyst. The mixture was stirred 1 min. and then one drop of triethylamine was added. After an additional 2 min. of stirring, the methylene chloride layer was removed, washed with water, coagulated in isopropanol, redissolved, and then re-coagulated. The product (IV) isolated in 68% yield had a reduced viscosity (25°C., chloroform) of 0.75. A similar procedure was used for the preparation of copolycarbonates (V, VI, VII) with 2,2-bis(4-hydroxyphenyl) propane as well as for the polyurethanes (VIII, IX).

Polyisophthalate. Interfacial polymerization of the dihydroxyspiroindane(I) and isophthaloyl chloride catalyzed by triethylamine in a CH_2Cl_2 - H_2O system afforded a 92% yield of the isophthalate (X) with a reduced viscosity (25°C., chloroform) of 0.39.

Polyadipate. The polyadipate (XI) was prepared by reacting the dihydroxyspiroindane (0.00578 mole) with 1 equiv. of adipoyl chloride in 7 ml. of nitrobenzene at 150°C. for 5 days. Removal of the solvent afforded polymer with a reduced viscosity (25°C., chloroform) of 0.29.

Polyethers

A variation of the general method¹³ for the preparation of polyhydroxyethers was employed. Equivalent amounts of the dihydroxy-spiroindane (I) and epichlorohydrin were treated with a 10% excess of 25% aqueous sodium hydroxide added dropwise and with stirring. The reaction product partially gelled at the end of the reaction period. The gel was extracted with dioxane and then with chloroform. Coagulation of these extracts in water and isopropanol, respectively, gave a cumulative yield of 17% of polymer (XII) having a reduced viscosity of 0.75–0.87.

Characterization of Polymers

Elemental analyses of the various polymers prepared are summarized in Table I.

TABLE I
 Elemental Analyses of Spiroindane Polymers

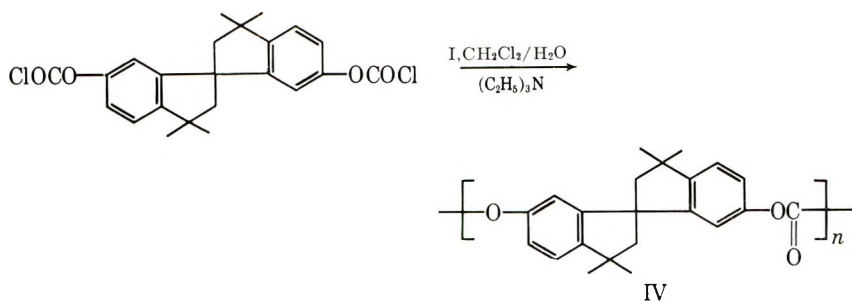
No.	Polymer ^a	Calculated			Found		
		C, %	H, %	O(N), %	C, %	H, %	O(N), %
IV	Polycarbonate	79.1	6.63	14.27	79.32	6.43	13.92
V	Copolycarbonate 50% spiroindane and 50% bisphenol A	77.52	6.16	16.32	77.61	6.15	16.49
VI	Copolycarbonate 35% spiroindane and 65% bisphenol A	77.03	6.01	16.96	76.93	6.21	16.98
VII	Copolycarbonate 25% spiroindane and 75% bisphenol A	76.63	5.88	—	76.59	5.77	—
VIII	Polyurethane from piperazine	72.62	6.77	6.28(N)	71.20	6.68	5.84
IX	Polyurethane from hexamethylenediamine and spiroindane (II)	73.38	7.22	5.90(N)	72.58	7.50	5.79
X	Polyisophthalate	79.43	5.98	14.59	79.50	6.09	14.22
XI	Polyadipate	77.48	7.25	—	77.23	6.94	—
XII	Polyhydroxyether	79.09	7.74	13.17	78.18	7.88	13.78

^a Derived from spiroindane (I) unless otherwise noted.

Measurements of transition temperature T_g were determined by measuring resiliency as a function of temperature by using the method described by Brown.¹⁴ Determination of elongation, tensile strength, and tensile modulus were carried out in accordance with ASTM procedure D638-58T while tensile impact measurements utilized ASTM procedure D1822-61T. A recording torsion pendulum¹⁵ was used to determine the low temperature transitions.

DISCUSSION

Of the many polymers which might be prepared, the polycarbonate was chosen as being most likely to exhibit both thermal stability and flexibility. Initial attempts to prepare this polymer by standard melt techniques were thwarted by the high melting (ca. 245°C.) insoluble nature of the monomer (II). Somewhat more success was achieved using interfacial polymerization but here the almost complete insolubility of the spiroindane (II) disodium (or other) salt made the attainment of high molecular weights difficult. Similar difficulties were encountered with the lower melting spiroindane (I, R=H) based on phenol. Examination of monomer (I) by NMR disclosed the presence of impurities even after several recrystallizations. In order to increase the ease of separating the monomer and the impurity, the disodium salt was prepared and recrystallized. This approach gave immediate improvement in the ease with which high polymer could be obtained and it was ultimately possible to reach reduced viscosities of 0.75 dl./g. by interfacial polymerization.



The polycarbonate (IV) was amorphous and displayed a glass transition temperature of 240°C ., some 90°C . higher than the bisphenol A analog. Even at the high levels of reduced viscosity obtained (fractionation afforded the polycarbonate with a reduced viscosity of 0.99), the polymer was too brittle for thorough evaluation and it was hoped that the properties of some copolymers might be more enlightening. An examination of the copolycarbonates of bisphenol A and the spiroindane reveals an apparent decrease in the toughness (per cent elongation, tensile impact) of the polymer as the spiroindane content increases (Table II). Based on the data

TABLE II
Properties of Spiroindane Copolycarbonates

	Polymer content, mole-% bis A/% spiro (I)				
	100/0	75/25	65/35	50/50	0/100
Reduced viscosity (25°C .; CHCl_3)	—	1.20	1.10	1.54	0.99
T_g , $^{\circ}\text{C}$.	150	175	180	195	240
Tensile modulus, psi	280,000	242,000	250,000	370,000	—
Tensile strength, psi	8000	5820	8800	8300	—
Elongation, %	150	7-20	8-9	4-5	—
Tensile impact, ft.-lb./in. ³	200-400	39	65	<10	low

of Table II, it would appear that the homopolycarbonate is inherently brittle. The energy absorbing ability of a polymer is a function of the flexural mobility of the repeat unit and, in polycarbonates, presumably dependent upon the carbonate group to a large extent. Thus, the polycarbonate of bisphenol A is a tough, high-impact plastic while that of the corresponding polymer from 4,4'-dihydroxy-3,3',5,5'-tetrachlorodiphenyl-2,2-propane in which the rotation of carbonate groups is hindered much less so.¹⁶ In general, polymers possessing secondary low temperature "transitions" are tougher than those lacking such a transition.^{17,18} In agreement with this, Reding and co-workers have demonstrated the absence of such a transition in the brittle tetrachloro polymer.¹⁹ Bisphenol A polycarbonate, on the other hand, does have a low temperature transition at -100°C .

Although the correlation of toughness and low temperature transitions is still in the preliminary stages,^{15,18,20,21} it was of interest to determine whether the brittle spiroindane polycarbonate (IV) exhibited any such peak. An examination of the low temperature mechanical loss spectrum of the spiroindane polycarbonate did show a peak at -100°C ., essentially identical in position and intensity to that found in bisphenol A polycarbonate. These results could be taken to mean that the experimental polymer would be tough at higher levels of molecular weight, although this is by no means certain. The flexibility of the carbonate group and apparently the ability to transmit stress is diminished considerably in the spiroindane polycarbonate because the whole monomer nucleus must move as a unit. Bisphenol A, with its flexible isopropylidene bridge, permits easier distribution of stress by the carbonate link itself.

It was possible to improve the properties of the spiroindane polycarbonate by uniaxial orientation (stretched 450% at 230°C .) as shown in Table III.

TABLE III
Properties of Partially Oriented Spiroindane Polycarbonate

Property	
Tensile modulus, psi	200,000-300,000
Tensile strength, psi	10,000
Elongation at break, %	12-32
Elongation at yield, %	5-7

The thermal and oxidative stability of the polycarbonate (IV) was examined by exposing films to air at 200°C . No apparent change in the reduced viscosity or infrared spectrum of the film was noted after heating in air for 2 days at 170°C ., followed by 4 days at 200°C . A slight drop in reduced viscosity was noted after one week at 200°C ., however, (0.99-0.84). Since no special precaution was taken to purify the polymer before heat treatment, its stability appears to be excellent.

In order to determine whether the brittleness observed in the polycarbonate (IV) was characteristic of all polymers of this class, a number of others were prepared, including the isophthalate (X), adipate (XI), hydroxyether (XII), and urethane (VIII,IX) (Table IV). Without exception, all of the polymers prepared were brittle, amorphous* materials with high glass transition temperatures. The amorphous nature of these polymers is not unexpected in view of the rigid bulky nature and lack of symmetry (D and L forms are possible) displayed by the spiroindane nucleus. A comparison of the softening points of the spiroindane (I) derived polymers with those of the corresponding bisphenol A (Table IV) analogs reveals the former to be higher by $40-145^{\circ}\text{C}$. In general, little difference

* Polyurethane (IX) gave an ambiguous x-ray pattern. Unlike most polymers, it showed many rings at high radius.

TABLE IV
Glass Transition Temperatures of Spiroindane Polymers and Analogous Bisphenol A Polymers

No.	Structure ^a	T_g , °C.	T_g of Bis A analog, °C.
IV		240	150 ^b
V		195	150
VII ^f		295	205 ^c
IX		240	—
X		260	125 ^d
XI		140	45 ^e
XII		140	100 ^f

^a The spiroindane nucleus has been abbreviated as "spiro." Unless otherwise indicated, the polymers were derived from (I).

^b Data of Schnell.¹⁶

^c Data of Cotter.²²

^d Data of Conix.²³

^e Data of Levine and Temin.²⁴

^f Data of Reinking et al.²⁵

was noted between the polymers derived from the two spiroindanes (I and II) studied.

The author is indebted to Dr. C. N. Merriam of these laboratories for the determination of the physical properties of these polymers and to W. Niegisch for the x-ray units.

References

1. Sheehan, D., A. P. Bentz, and J. C. Petropoulos, *J. Appl. Polymer Sci.*, **6**, 47 (1962).
2. Ehlers, G. F. L., ASD Report No. ASD TR 61-622, Feb. 1962.
3. Curtis, R. F., *Chem. Ind. (London)*, **1960**, 928.
4. von Braun, J., *Liebigs Ann.*, **472**, 65 (1929).
5. Brunner, H., A. Palluel, and D. J., Walbridge, *J. Polymer Sci.*, **28**, 629 (1958).
6. Mitin, Y. V., and N. A. Glukhov, *Dokl. Akad. Nauk SSSR*, **115**, 97-99 (1957).
7. Baker, W., and D. M. Besley, *J. Chem. Soc.*, **1939**, 1421.
8. Petropoulos, J. C., and F. A. V. Sullivan, U. S. Pat. 2,979,535 (April 11, 1961).

9. Kenner, G. W., and N. R. Williams, *J. Chem. Soc.*, **1955**, 522.
10. Adams, L. M., R. J. Lee, and F. T. Wadsworth, *J. Org. Chem.*, **24**, 1186 (1959); see ref. 11 for correct proof of structure.
11. Curtis, R. F., *J. Chem. Soc.*, **1962**, 415.
12. Wittbecker, E. L., and P. W. Morgan, *J. Polymer Sci.*, **40**, 289 (1959).
13. Wynstra, J., N. H. Reinking, and A. E. Barnabeo, French Pat. 1,309,491 (Oct. 8, 1962).
14. Brown, A., *Textile Res. J.*, **25**, 891 (1955).
15. Nielsen, L. E., *Rev. Sci. Instr.*, **22**, 690 (1951).
16. Schnell, H., *Ind. Eng. Chem.*, **51**, No. 2, 157 (1959).
17. Nielsen, L. E., *Mechanical Properties of Polymers*, Reinhold, New York, 1962, p. 125.
18. Boyer, R. F., *Rubber Chem. Technol.*, **36**, 1395 (1963).
19. Reading, F. P., J. A. Faucher, and R. D. Whitman, *J. Polymer Sci.*, **54**, S56 (1961).
20. Zutty, N. L., and F. P. Reding, and J. A. Faucher, *J. Polymer Sci.*, **62**, S172 (1962).
21. Faucher, J. A., and G. Ingraham, private communication.
22. Cotter, R. J., private communication.
23. Conix, A., *Ind. Eng. Chem.*, **51**, No. 2, 147 (1959).
24. Levine, M., and S. C. Temin, *J. Polymer Sci.*, **28**, 179 (1958).
25. Reinking, N. H., A. E. Barnabeo, and W. F. Hale, *J. Appl. Polymer Sci.*, **7**, 2135 (1963).

Résumé

On a préparé une variété de polymères de condensation à partir des 6,6'-dihydroxy-3,3,3',3'-tétraméthyl-1,1'-spirobiindanes comprenant des polyesters, des polyuréthanes et un polyhydroxyéther. Le polycarbonate présente une bonne résistance à l'oxydation à 200°C mais manque de dureté malgré la présence d'une basse température de transition à -100°C. Une tendance à la fragilité est également mise en évidence dans d'autres polymères et copolymères préparés. On discute de la contribution de la structure spiroindane aux propriétés du polymère. Tous les polymères étudiés sont amorphes et présentent des températures de transition vitreuse élevées.

Zusammenfassung

Eine Reihe von Kondensationspolymeren, darunter Polyester, Polyurethane und ein Polyhydroxyäther wurde aus den 6,6-Dihydroxy-3,3,3',3'-tetramethyl-1,1'-spirobiindanen dargestellt. Das Polycarbonat zeigte gute Oxydationsbeständigkeit bei 200°C, besass aber trotz des Vorhandenseins einer Tieftemperaturumwandlung bei -100°C keine Zähigkeit. Eine Tendenz zur Sprödigkeit trat auch bei den anderen dargestellten Polymeren und Copolymeren auf. Der Beitrag der Spiroindanstruktur zu den Polymereigenschaften wird diskutiert. Alle untersuchten Polymeren waren amorph und wiesen hohe Glasumwandlungstemperaturen auf.

Received December 16, 1964

Revised March 8, 1965

Prod. No. 4687A

Effects of Rate of Shear on the Viscosity of Polymer Solutions

SHOEI FUJISHIGE, *The Textile Research Institute of Japanese Government, Sawatari, Kanagawa, Yokohama, Japan*

Synopsis

Viscosities of dilute solutions of poly(methyl methacrylate) in toluene and in chloroform were measured with a modified capillary viscometer. By tilting the viscometer one can control the solvent flow time to any desired condition, and by use of this technique it was possible to determine the extent to which such variables affect the resulting rate of shear if one measures the viscosities with two or more viscometers of the same type having different flow times of solvent. The reduced viscosities measured with the modified capillary viscometer at several tilting angles were plotted in the usual way against the polymer concentrations, and values of the intrinsic viscosity for a given solution at each tilting angle were thus obtained for both of the solutions studied. For a rather high molecular weight polymer fraction, the maximum variation in the molecular weight estimated from the intrinsic viscosity by the Mark-Houwink relation was of the order of 20% between the values obtained with the viscometer fixed at a vertical and at another extreme angle. All the experimental data are also reproduced as a function of the rate of shear, and reliable values for the intrinsic viscosity at zero rate of shear and hence for the molecular weight are obtained. Other possible differences noted in the determination of such molecular characteristics as the Huggins' constant which could be attributed to this kind of experimental condition were discussed.

INTRODUCTION

It is well known that viscometry of dilute polymer solutions is one of the more useful and convenient methods of characterization of high polymers. Recent theoretical treatments on the intrinsic viscosity enable us to estimate the molecular dimensions and other characteristics of the polymer molecules in solutions. However, there are still rather complicated experimental problems to be solved to permit us to obtain a reliable measurement of the intrinsic viscosity at zero rate of shear.

The effects of rate of shear have long attracted the interest of many researchers.¹⁻⁴ In fact, it seems to be one of the most significant but little explored experimental problems in determination of the intrinsic viscosity of dilute polymer solutions.

In the present work we will discuss the effects of rate of shear on viscosities of polymer solutions in determination of the intrinsic viscosity in relation to the characterization of a given polymer in solution, e.g., the determination of the molecular weight.

By making use of a modified Ubbelohde type capillary viscometer⁵ a series of round-robin measurements was carried out with the use of two or more viscometers of the same type but with variable efflux times for solvent flow. How such variables affect the experimental results was determined. All the experimental data obtained are also reproduced as a function of the rate of shear, and a reliable value of the intrinsic viscosity at zero rate of shear was estimated by extrapolation.

It was also confirmed that Huggins' constant has a marked dependence on the rate of shear or/and on the flow condition which has been defined so far as a constant value for a given polymer-solvent system at a given temperature.⁶

EXPERIMENTAL

Materials

Purified methyl methacrylate monomer was polymerized at 60°C. with the use of benzoyl peroxide as the catalyst. The polymer thus obtained was fractionated by fractional solution method from thin films deposited on Celite (diatomaceous earth), and the high molecular weight portion was used for this investigation.

Toluene and chloroform were both reagent grade and purified by standard procedures before use.

Viscosity

Solution viscosities for the polymer fraction in each of the two solvents, toluene and chloroform, were determined at $25 \pm 0.01^\circ\text{C}$. Flow times of the solvents and the solutions were measured in modified Ubbelohde type capillary viscometer maintained at several different tilting angles. Kinetic energy corrections for the viscometer at each angle were made with water, carbon tetrachloride, and toluene at various temperatures. Experimental techniques employed in this work were identical to those in a previous paper.⁵

The following relationships were applied for calculation of the relative viscosity, η_{rel} at each tilting angle

$$\eta_{\text{rel}} = \frac{\eta}{\eta_0} = \frac{\rho t}{\rho_0 t_0} \left[1 + \frac{B}{A} \left(\frac{1}{t_0^2} - \frac{1}{t^2} \right) \right] \quad (1)$$

and of the average rate of shear, \bar{q}

$$\bar{q} = 8\bar{V}/3\pi r^3 t \quad (2)$$

where η and η_0 are the viscosity of the solution and of the solvent, ρ and ρ_0 are the density, t and t_0 are the efflux time in seconds for the solution and the solvent, respectively. A and B are constants characteristic of a given viscometer at a given tilting angle. \bar{V} is the volume of the efflux bulb, and r is the capillary radius of the viscometer employed.

Results

The concentration dependence of solution viscosities η_{sp}/c versus c for the poly(methyl methacrylate) fraction in each of the two solvents at 25°C. is shown in Figures 1 and 2. A linear relationship between the reduced viscosities and the polymer concentrations was noted in both the solutions; however, the intrinsic viscosity thus obtained according to the definition of eq. (3) differs markedly for the two solvents.

$$\eta_{sp}/c = [\eta] + k'[\eta]^2c + \dots \quad (3)$$

Here $[\eta]$ is the intrinsic viscosity, η_{sp}/c is the reduced viscosity for solutions of polymer concentration c , and k' is a constant for a given polymer-solvent system at a given temperature which has been so defined by Huggins.⁶

Even the flow times were measured on the same polymer solutions in the same capillary viscometer; the variations in experimental results obtained were due only to the variation of flow conditions of the solutions, i.e., the tilting angle of the viscometer in this work.

Table I shows the experimental results, values of the apparent intrinsic viscosity, and Huggins' constant obtained from the relationship shown in Figures 1 and 2, the average rate of shear for the solvent flow at each tilting angle as an indication of the flow conditions, and also the resulting molecular weights calculated by eqs. (4) and (5),⁷ respectively.

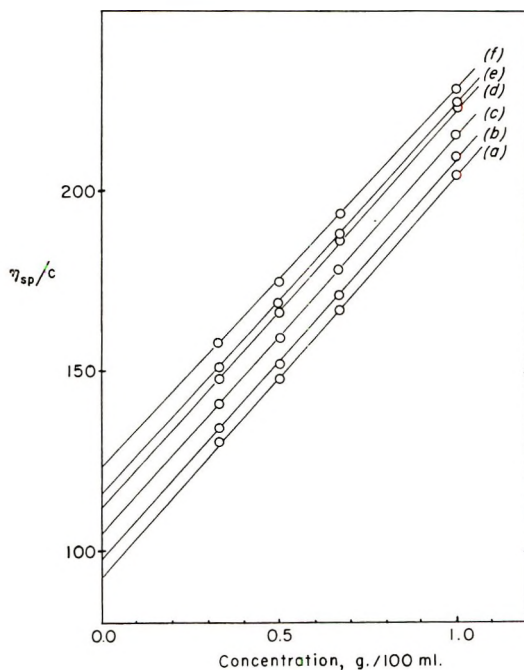


Fig. 1. Concentration dependence of the viscosities of poly(methyl methacrylate)-toluene solutions obtained at various tilting angles: (a)-(f) as in Table I.

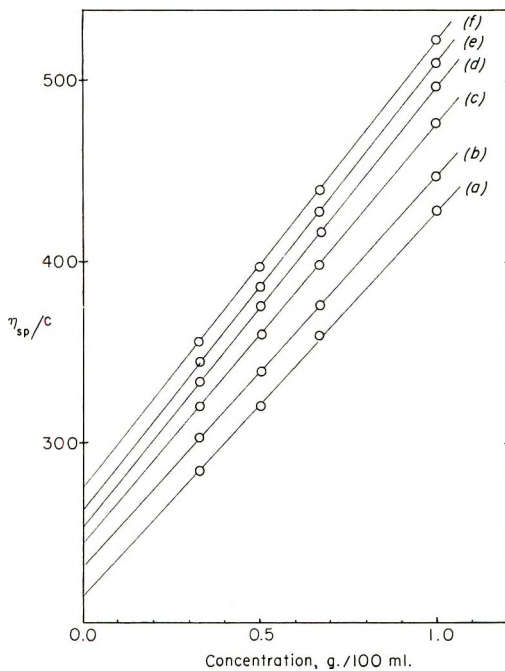


Fig. 2. Concentration dependence of the viscosities of poly(methyl methacrylate)-chloroform solutions obtained at various tilting angles: (a)-(f) as in Table I.

TABLE I

Apparent Values of the Intrinsic Viscosity, Molecular Weight, and Huggins' Constant for Poly(methyl Methacrylate) in Toluene and in Chloroform Solutions Obtained at Various Tilting Angles

No. ^a	In toluene				In chloroform			
	\bar{q} , sec. ⁻¹	k'	$[\eta]$	M	\bar{q} , sec. ⁻¹	k'	$[\eta]$	M
<i>a</i>	912	1.311	92	440,000	1,450	0.472	213	600,000
<i>b</i>	824	1.190	97		1,404	0.401	232	
<i>c</i>	635	1.016	104		1,049	0.393	245	
<i>d</i>	465	0.908	110		785	0.373	257	
<i>e</i>	395	0.830	114		677	0.356	266	
<i>f</i>	322	0.698	122	640,000	559	0.331	276	830,000

^a Refers to curves in Figs. 1 and 2.

In toluene:

$$[\eta] = 7.1 \times 10^{-3} M^{0.73} \quad (4)$$

In chloroform:

$$[\eta] = 3.4 \times 10^{-3} M^{0.83} \quad (5)$$

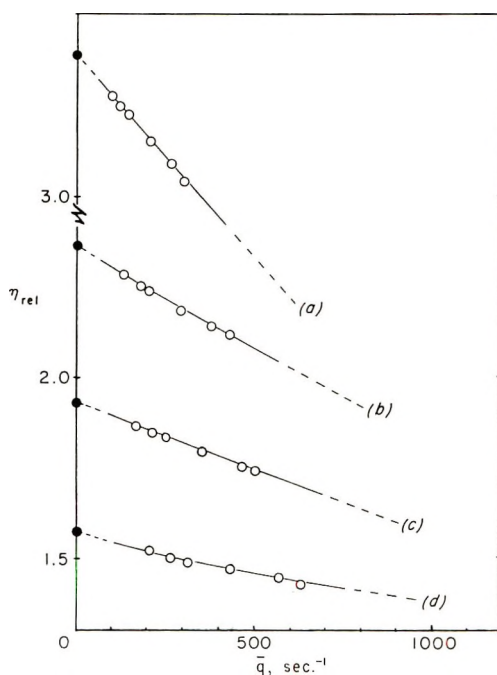


Fig. 3. Shear rate dependence of the viscosities of poly(methyl methacrylate)-toluene solutions: (a) $c_1 = 1.0$ g./100 ml.; (b) $c_2 = 0.67$ g./100 ml.; (c) $c_3 = 0.50$ g./100 ml.; (d) $c_4 = 0.33$ g./100 ml.

The shear rate dependence of the relative viscosities of each of the solutions is represented in Figures 3 and 4. The values of the relative viscosity for the solutions of various concentrations at zero and/or any desired rate of shear are all estimated by extrapolating the measured values as a function of the rate of shear.

The concentration dependence of the solution viscosities thus estimated from the relationship in Figures 3 and 4 for the poly(methyl methacrylate)

TABLE II
Values of the Intrinsic Viscosity, Molecular Weight, and Huggins' Constant for Poly-(methyl Methacrylate) in Toluene and in Chloroform Solutions Estimated for Various Average Rates of Shear

\bar{q} , sec. ⁻¹	In toluene			In chloroform		
	k'	$[\eta]$	M	k'	$[\eta]$	M
0	0.505	140	780,000	0.230	330	1,000,000
200	0.515	130	700,000	0.193	308	980,000
400	0.544	119	620,000	0.129	292	880,000
600	0.519	111	560,000	0.119	280	840,000
0 ^a	—	143	800,000	—	350	1,100,000

^a The values of the intrinsic viscosity were determined in Figs. 7 and 8.

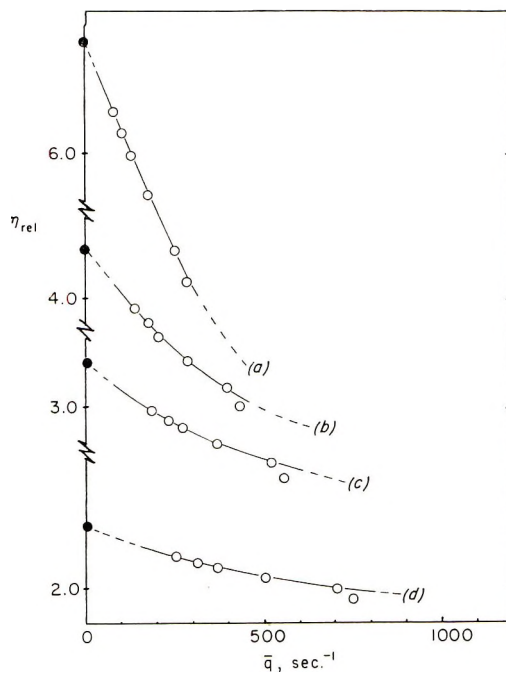


Fig. 4. Shear rate dependence of the viscosities of poly(methyl methacrylate)-chloroform solutions: (a) $c_1 = 1.0$ g./100 ml.; (b) $c_2 = 0.67$ g./ml.; (c) $c_3 = 0.50$ g./100 ml.; (d) $c_4 = 0.33$ g./100 ml.

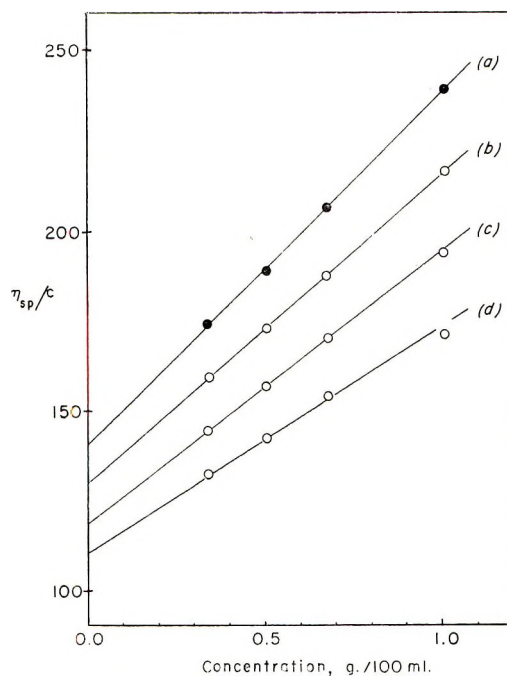


Fig. 5. Concentration dependence of the viscosities of poly(methyl methacrylate)-toluene solutions for fixed rates of shear: (a) $q = 0$; (b) $q = 200$ sec. $^{-1}$; (c) $q = 400$ sec. $^{-1}$; (d) $q = 600$ sec. $^{-1}$.

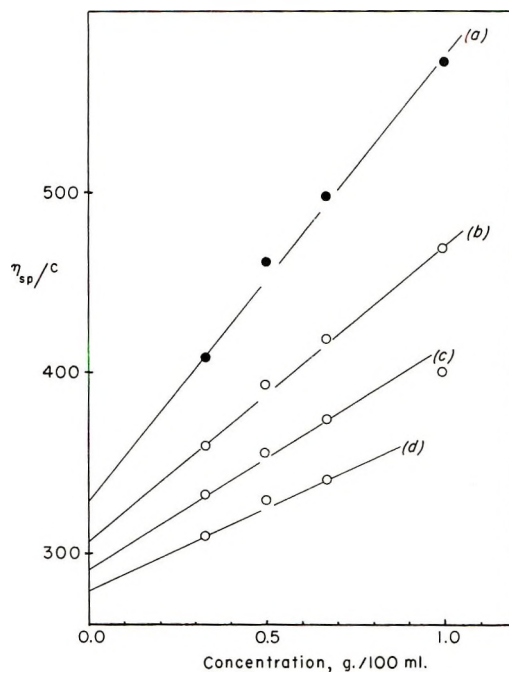


Fig. 6. Concentration dependence of the viscosities of poly(methyl methacrylate)-chloroform solutions for fixed rates of shear: (a) $q = 0$; (b) $q = 200 \text{ sec.}^{-1}$; (c) $q = 400 \text{ sec.}^{-1}$; (d) $q = 600 \text{ sec.}^{-1}$.

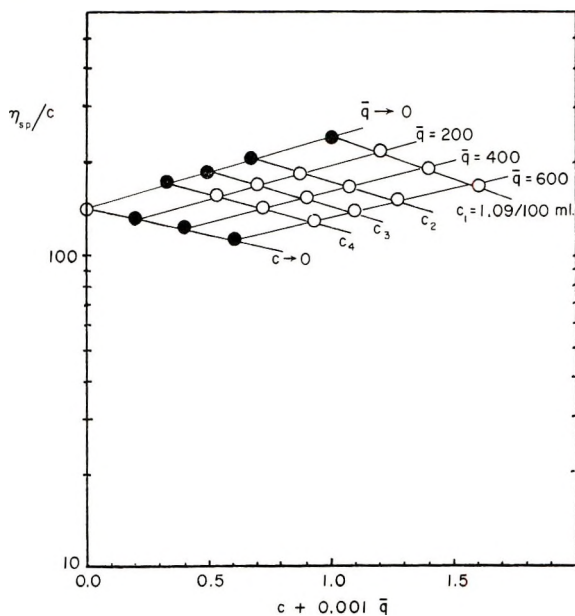


Fig. 7. Method of extrapolation according to Schurz⁸ for determining the intrinsic viscosity at zero rate of shear of poly(methyl methacrylate)-toluene solutions. $[\eta] = 143$.

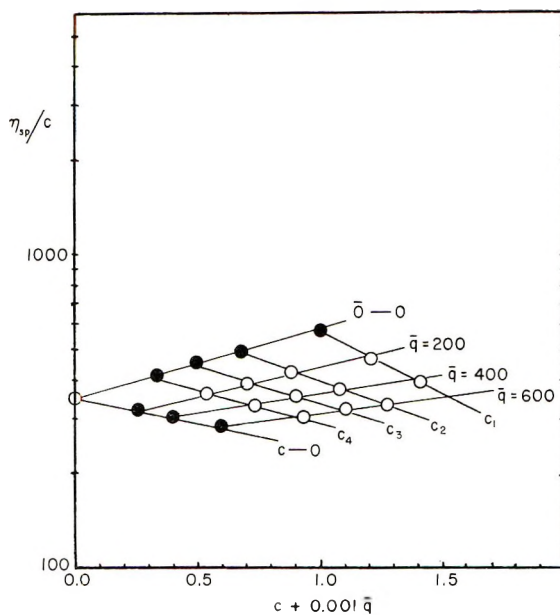


Fig. 8. Method of extrapolation according to Schurz⁸ for determining the intrinsic viscosity at zero rate of shear of poly(methyl methacrylate)-chloroform solutions. $[\eta] = 350$.

fraction in each of the solvents at various fixed rates of shear is shown in Figures 5 and 6, respectively.

The relationship represented in Figures 3 and 4 leads also to another method of extrapolation for estimating the intrinsic viscosity at zero rate of shear; Figures 7 and 8 are obtained according to Schurz.⁸

The values of the intrinsic viscosity and Huggins' constant, the molecular weight for the polymer fraction in toluene and in chloroform solutions thus estimated for each average rate of shear are shown in Table II.

DISCUSSION

The possible significant effects of the rate of shear and/or of the flow conditions for measurement of the efflux times on determination of the intrinsic viscosity of polymer solutions were obviously shown through this investigation.

The results enable us to conclude that in many of the round-robin measurements for the determination of the intrinsic viscosity of a given polymer solution the results should always be accompanied by a significant value for the experimental variables, not the error, because of the effects of the flow conditions in the experimental study.

In an extreme case, as shown in Table I, the maximum difference in the variables such the molecular weight estimated from the intrinsic viscosity was the order of 20% between the values obtained with the viscometer at a vertically fixed angle (a) and at the extreme angle (f).

A marked variation in Huggins' constant k' was also noted, and it decreases with increasing rate of shear but varies inversely with the flow condition, as shown in Tables I and II.

The theoretical complications of the constant, k' are not quantitatively known; as was considered for the second virial coefficient in the case of osmometry of dilute polymer solutions, it seems to give a significant amount of useful information for the characterization of polymer molecules in solution.

References

1. Staudinger, H., and M. Sorkin, *Ber.*, **70**, 1993 (1937).
2. Conrad, C. M., *J. Phys. Colloid Chem.*, **55**, 1474 (1951).
3. de Wind, G., and J. J. Hermans, *Rec. Trav. Chim.*, **70**, 521 (1951).
4. Claesson, S., and U. Lohmander, *Makromol. Chim.*, **46**, 461 (1961).
5. Fujishige, S., J. Kuwana, and M. Shibayama, *J. Polymer Sci.*, **B1**, 355 (1963).
6. Huggins, M. L., *J. Am. Chem. Soc.*, **64**, 2712 (1942).
7. Chinai, S. N., J. D. Matlack, A. L. Resnick, and R. J. Samuels, *J. Polymer Sci.*, **17**, 391 (1955).
8. Schurz, J., *Rheol. Acta*, **3**, 43 (1963).

Résumé

On a mesuré les viscosités de solutions diluées de polyméthacrylate de méthyle dans le toluène et le chloroforme avec un viscosimètre capillaire modifié. En inclinant le viscosimètre, on peut contrôler le temps d'écoulement du solvant pour toutes les conditions voulues. En faisant usage de cette technique, il a été possible de confirmer comment plusieurs variables pouvaient être attribuées aux effets de la vitesse de cisaillement résultante sur les mesures expérimentales si on mesure les viscosités avec deux ou plusieurs viscosimètres du même type mais possédant des temps d'écoulement de solvants différents. Les viscosités réduites, mesurées avec le viscosimètre capillaire modifié à des angles différents, sont mises en graphique suivant la méthode habituelle en fonction des concentrations en polymère, et les valeurs variables de la viscosité intrinsèque pour une solution donnée à chaque angle sont ainsi obtenues pour les deux solutions étudiées. Pour une fraction de polymère de poids moléculaire relativement élevé, la différence maximum dans le poids moléculaire, estimé à partir de la viscosité intrinsèque par la relation Mark-Houwink, était de 20% entre les valeurs obtenues avec le viscosimètre fixé verticalement et celui fixé sur l'autre angle extrême dans le domaine étudié dans ce travail. Tous les résultats expérimentaux sont aussi reproduits en fonction de la vitesse de cisaillement et on obtient des valeurs sûres pour la viscosité intrinsèque à une vitesse de cisaillement nulle et de là pour le poids moléculaire. On a discuté d'autres différences possibles notées dans la détermination des caractéristiques moléculaires telles que la constante de Huggins, qui pourraient être aussi attribuées à des conditions expérimentales analogues.

Zusammenfassung

Die Viskosität verdünnter Lösungen von Polymethakrylsäuremethylester in Toluol und Chloroform wurde in einem modifizierten Kapillarviskosimeter bestimmt. Durch Verschiebung des Viskometers aus senkrechter Lage ist es möglich den Einfluss des Gefälles auf die Viskosität zu bestimmen. Die reduzierten Viskositäten wurden bei verschiedenen Winkeln der Kapillare gemessen und gegen die Konzentration der Lösungen aufgetragen. Dadurch erhält man die Viskositätszahl als Funktion des Winkels. Für Fraktionen von höheren Molekulargewicht findet man einen Unterschied von 20% zwischen dem Molekulargewicht aus des Viskositätszahl mit senkrechter Kapillare, und

dem aus der Viskositätszahl mit der Kapillare welche mit dem grössten Winkel von der Senkrechten abweicht. Die Viskositätszahlen wurden auch auf ein Gefälle von Null estapoliert was erlaubt korrekte Molekulargewichte zu bestimmen. Der Einfluss des Gefälles auf andere Eigenschaften, wie die Huggins'che k' Konstante, wird auch diskutiert.

Received May 26, 1964

Revised October 7, 1964

Prod. No. 4518A

Polymer-Filler Interaction. Thermodynamic Calculations and a Proposed Model

T. K. KWEI,* *Central Research Laboratories, Interchemical Corporation, Clifton, New Jersey*

Synopsis

From a study of the sorption of water vapor by epoxy polymers filled with titanium dioxide, the differences in enthalpy and entropy of the filled and the unfilled polymers are calculated. The enthalpy and the entropy of the filled polymer are smaller than those of the unfilled polymer by about 2 cal./g. and 6×10^{-3} e.u., respectively. These differences may be explained by the existence of a higher degree of local ordering of the polymer segments. A model is proposed to describe the interaction between the polymer and the filler as a function of the distance from the interface. It appears that polymer segments at a distance less than 1500 Å. from the surface of the filler particle are within the sphere of influence of the filler. The effects of filler incorporation on the thermal expansion coefficient, heat capacity, and partial molar heat of solution of the polymer are discussed in terms of the model.

INTRODUCTION

It is generally known that the incorporation of a filler in a polymer may result in changes in the physical and mechanical properties of the material. These changes in the properties of a material presumably may be interpreted as an indication of some structural changes in the polymer accompanying filler incorporation. However, the structural changes which may exist have not been expressed in quantitative terms, and the mechanism of filler-polymer interaction is still open to speculation.

In our laboratories, attempts have been made to study polymer-filler interaction by the measurement of glass transition temperatures¹ and by the study of vapor sorption.² It may be inferred from the observed changes in the glass transition temperatures of vinyl chloride-acetate copolymer when it is filled with titanium dioxide that the presence of filler particles modifies the mobility of polymer segments.¹ A comparison of the results of organic vapor sorption by filled and unfilled poly(vinyl acetate) and epoxy polymer has led to the postulation that filled polymers have sorptive properties like those of glassy polymers.² In this report, additional studies of water vapor sorption by filled epoxy polymers is presented. The differences in free energy, enthalpy, and entropy of the filled and the unfilled polymer are calculated and a simple model for describing filler-polymer interaction outlined.

* Present address: Bell Telephone Laboratories, Murray Hill, New Jersey.

In this paper the term filled polymer is used to refer strictly to the polymer component of the system of polymer plus filler. The symbol f which appears later in the text refers to the free polymer and has a different meaning than in the previous paper.²

EXPERIMENTAL

Epon 828 (Shell Chemical Company, essentially 4,4'-bisglycidylphenyl-2,2'-propane) and 1,6-hexanediamine (Matheson Coleman and Bell Company) were mixed in stoichiometric proportion to prepare the cross-linked epoxy film. The detailed procedure was described in previous reports.³ In the preparation of the filled epoxy film titanium dioxide (Rutile 610, du Pont, average size 0.2μ) was dispersed in Epon 828 by the use of a three-roller mill. Stoichiometric quantities of the diamine were dissolved in a small amount of butanone-2 and added slowly with vigorous stirring to the dispersion of TiO_2 in Epon. The method of film preparation was described earlier.³ The amount of titanium dioxide in the film was determined by ash analysis to be 14.31% by weight (or 4.41% by volume). The film was the same as the one used in a previous study.³

The glass transition temperatures of the filled and the unfilled polymer were determined by a dilatometric method. Both samples show transition at $54^\circ C$.

The water vapor sorption of the polymer film was measured by means of a quartz helix microbalance. The final pressure and the amount of vapor sorption by the sample were recorded when the weight gain was less than 0.003 mg. (for a polymer sample of about 80 mg.) overnight. Usually, equilibrium sorption was attained in about 1 hr.

RESULTS

The sorption water vapor by the unfilled epoxy polymer appears to obey Henry's law in that the isotherms may be represented by straight lines (Fig. 1). The temperature coefficient of water sorption is negative. The sorption isotherms of water by the filled epoxy polymer at 60, 70, and $80^\circ C$. are also shown in Figure 1. At low vapor pressures, the amount of water vapor sorbed by the filled polymer is less than that sorbed by the two polymers diminishes with increasing vapor pressure; the isotherms for the two materials appear to become identical above P/P_0 of 0.56, 0.51, and 0.44 at 60, 70, and $80^\circ C$., respectively. All the sorption measurements are reversible.

DISCUSSION

Assumptions

The sorption of low molecular substances by polymers is often sensitive to any change in segment mobility or spatial arrangement of chains.⁴ The observed difference in the water vapor sorption by the filled and the

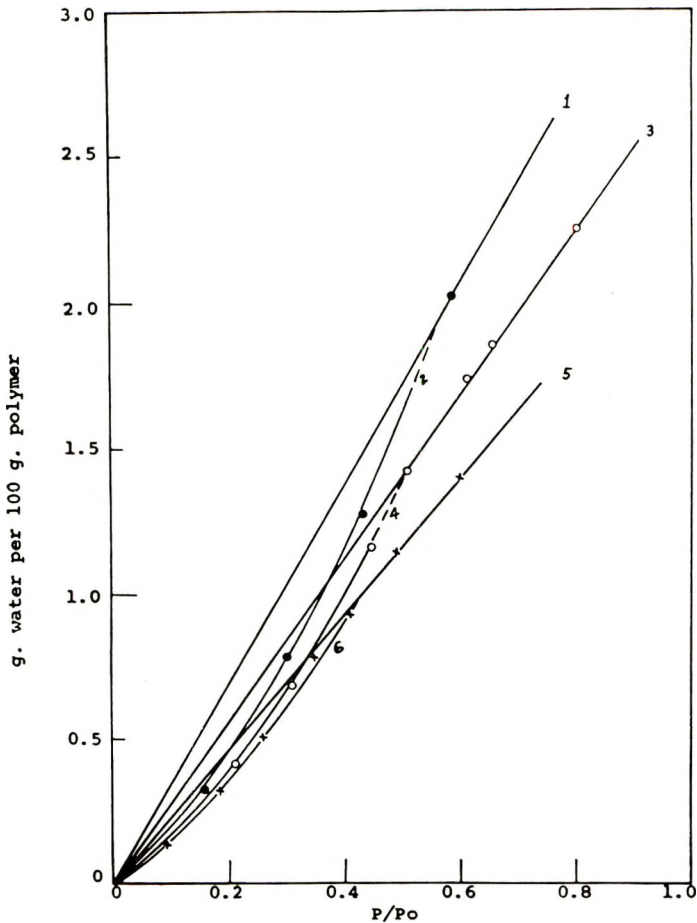
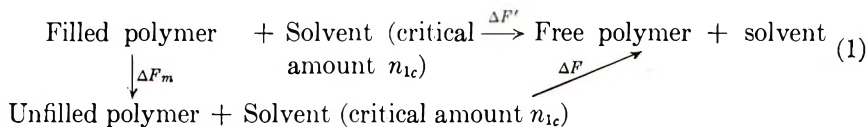


Fig. 1. Sorption of water vapor by epoxy polymers: (1) 60°C., unfilled; (2) 60°C., filled; (3) 70°C., unfilled; (4) 70°C., filled; (5) 80°C., unfilled; (6) 80°C., filled.

unfilled materials at low vapor pressures may be viewed perhaps as a reflection of the difference in the chain configuration or mobility of the two polymers. With increasing vapor pressure, the difference in vapor sorption lessens. The two isotherms coincide after a critical vapor pressure is reached. Apparently the filled polymer appears to possess the same sorptive properties as the unfilled one when a critical amount of certain diluent is introduced into the system. The significance of this critical concentration of diluent in a filled polymer may be similar to that of the critical volume concentration, pointed out by Long,⁵ in a polymer-diluent system at which the diffusion of the organic diluent becomes Fickian. We would like to propose that all the physical properties of the filled polymer become identical with those of the unfilled polymer when the diluent concentration is at or above a certain critical amount. It was also noted that the amount of sorption by the filled polymer in no case exceeded the sorption by the

unfilled polymer. It appears that, in our system, filler particles do not tend to sorb water independently. It is likely that in this system a monolayer (perhaps several) of adsorbed polymer molecules remains in contact with the filler surface even when the critical amount of solvent is present, and prevents the filler surface from adsorbing water in an independent manner. (In the water sorption of filled vinyl chloride-acetate copolymer,¹ it has been observed that the amount of water sorbed by the polymer-filler system is essentially equal to the sum of the individual sorptions of the polymer and the filler.) We assume, without strong justification, that the displacement of polymer segments from the filler surface by water molecules may not have occurred to a significant extent in this system. As a first approximation we neglect the water-filler interaction temporarily from our thermodynamic calculations. It is hoped that the thermodynamic quantities thus calculated, while possibly inexact in absolute values, may still provide an estimate of the order of magnitude of the polymer-filler interaction.

Under the aforementioned premise, it is possible to construct the thermodynamic cycle shown in eq. (1)



It may be shown from this above cycle that the free energy ΔF_m or the enthalpy ΔH_m of the transformation of the filled polymer to the unfilled state can be obtained as the difference between $\Delta F'_c$ and ΔF_c , $\Delta H'_c$ and ΔH_c . The quantities $\Delta F'$, ΔF , $\Delta H'$, and ΔH denote the free energy and enthalpy of the vapor sorption process, the primed symbols referring to the filled polymer and the subscript c referring to the sorption of the critical amount of solvent n_{1c} by the polymer. In the following paragraphs, the calculations of these quantities from vapor sorption isotherms will be described.

Calculations

Equations (2)-(7) are used in the calculation of thermodynamic quantities:

$$\Delta \bar{H}_1 = RT^2 (\partial \ln a_1 / \partial T)_{n_1} \quad (2)$$

$$\Delta \bar{H}_{2c} = - \int_{n_1=0}^{n_{1c}} (n_1/n_2) d \Delta \bar{H}_1$$

(graphical integration) (3)

$$\Delta H = n_1 \Delta \bar{H}_1 + n_2 \Delta \bar{H}_2 \quad (4)$$

$$\Delta \bar{F}_1 = RT \ln a_1 \quad (5)$$

$$\Delta \bar{F}_{2c} = - \int_{n_1=0}^{n_{1c}} (n_1/n_1) d \Delta \bar{F}_1$$

(graphical integration) (6)

$$\Delta F = n_1 \Delta \bar{F}_1 + n_2 \Delta \bar{F}_2 \quad (7)$$

Here n_1 and n_2 are the number of moles of the solvent and the polymer segment, respectively. The graphical integration leading to the evaluation of ΔF is carried out by a procedure based on that proposed by Conway⁶ to circumvent the uncertainty of extrapolation to infinity. Where the sorption process obeys Henry's law, the following equations are obtained:

$$\Delta \bar{H}_1 = \text{constant} \quad (8)$$

$$\Delta \bar{H}_2 = 0$$

$$\Delta \bar{F}_2 = -RT (n_1/n_2) \quad \text{For } n_1 \ll n_2 \quad (9)$$

The molecular weight M of the polymer segment need not be known if the ΔF and ΔH values are calculated in calories per gram of polymer. The results of our calculation are summarized in Table I.

TABLE I
Thermodynamic Quantities

	80°C.	70°C.
Unfilled polymer ^a		
ΔH_c , cal./g. polymer	-2.54	-3.49
ΔF_c , cal./g. polymer	-0.74	-0.91
Filled polymer ^b		
$\Delta \bar{H}'_{2c}$, cal./g. polymer	0.25	0.28
$\Delta H'_c$, cal./g. polymer	-0.73	-1.02
$\Delta H_m = \Delta H'_c - \Delta H_c$, cal./g. polymer	1.81	2.47
$\Delta F'_c$, cal./g. polymer	-0.66	-0.76
$\Delta F_m = \Delta F'_c - \Delta F_c$, cal./g. polymer	0.08	0.15
$T \Delta S_m = \Delta H_m - \Delta F_m$, cal./g. polymer	1.72	2.32
ΔS_m , cal./deg./g. polymer	4.9×10^{-3}	6.7×10^{-3}

^a $\Delta \bar{H}_1 = -4.40$ kcal./mole at all concentrations of sorbed water; $\Delta \bar{H}_2 = 0$.

^b $\Delta \bar{H}'_1$ changes with the concentration of sorbed water, but is more positive than $\Delta \bar{H}_1$, at any water concentration when the concentration is less than the critical amount.

Conclusions

The principal conclusion which may be drawn from the calculations of Table I is that the unfilled polymer has higher free energy, enthalpy, and entropy content than the filled polymer. The inference is very strong that the transformation of a filled polymer to the unfilled state is accompanied by increases in both enthalpy and entropy.

It may be instructive to compare the differences in enthalpy (about 2 cal./g.) and in entropy (about 5×10^{-3} cal./deg./g.) of the two states with those involved in the melting of a crystalline polymer, for example, polyethylene,⁷ where $T_{\text{melting}} = 137.5^\circ\text{C}$., $\Delta H = 68.5$ cal./g, $\Delta S = 0.167$ cal./deg./g. Our calculated values of ΔH_m and ΔS_m are about 30 times smaller than the ΔH and ΔS values for polyethylene melting. In the case of acetone sorption by poly(vinyl acetate)² filled with TiO_2 (12.1% by volume), similar calculation gives the following values at 40°C .: $\Delta H_m \cong 1.7$ cal./g. $\Delta F_m \cong 0.5$ cal./g., and $T \Delta S_m \cong 1.2$ cal./g.-deg. It appears that there may exist in the filled state local ordering of the polymer segments rather than the well defined, periodic order observed in crystalline polymers.

The presence of order in amorphous polymers has been investigated only cursorily. Kargin⁸ concluded from electron diffraction, electron microscope, and x-ray studies of polymer films in the amorphous state that mutual ordering of chain molecules can arise even in the amorphous state. According to him, "The principal source of this order appearing in the system of many polymer chains is their mutual orientation. This mutual orientation of chains may be caused by intermolecular interaction (resulting at most in crystallization) by an orientation arising from considerable distortion and particularly from the flow of polymers due to mechanical strain applied to the polymers and . . . in the case of natural polymers . . . by an orientation resulting from the morphological conditions of polymer formation The mutual orientation and ordering of chains in polymers may lead to the formation of clusters in the manner which occurs in liquids."

Mikhailov and Fainberg⁹ determined the heats of solution of isotropic and oriented cellulose in quaternary ammonium bases and found that they differed by only 1–1.5 cal./g. It is of interest to note that the difference in the heats of solution of the isotropic and the oriented cellulose, which is a direct measure of the difference in the enthalpies of the two states, is of the same order of magnitude as our calculated ΔH_m values.

PROPOSED MODEL

We would like to propose now a simple model to describe the interaction between the polymer and the filler.

1. There exists between the filler and polymer chains an interaction which manifests itself in a decrease in the chemical potential of the polymer—a postulate based on thermodynamic calculations.

2. One boundary condition of this interaction is that it becomes negligible as the distance between the filler and the polymer becomes infinite. It is obvious, therefore, that the interaction must be a function of distance. We assume that the interaction decreases rapidly with distance so that a polymer segment at a distance greater than r^* from the center of the filler would experience negligible interaction and has all the properties of an unfilled polymer and may be called "free" polymer. Chain segments at distances smaller than r^* from the center of the filler would fall within the

sphere of influence of the filler particle and may be called "bound" polymer. The chemical potential of the chain segments in the bound layer is assumed to increase with distance from the center of the filler particle. (The justification of thermodynamic treatment of nonuniform systems has been discussed; for example, by Cahn and Hilliard.¹⁰) The choice of r^* is subject to the stipulation that $\mu_{b(r^*)} \cong \mu_f^\circ$, where μ_f° is the chemical potential of the free polymer in the pure state and $\mu_{b(r)}$ is the chemical potential of the bound polymer at distance r .

3. Solvent molecules have a greater tendency to mix with the free polymer than the bound polymer because the free energy of mixing with the former is more negative (based on thermodynamic calculations). It is assumed that the bound polymer absorbs negligible amount of water vapor. The justification of this assumption was discussed elsewhere.²

4. The mixing of the free polymer with solvent molecules of activity a_1 results in a decrease in the chemical potential of the free polymer from μ_f° to $\mu_{f(a_1)}$. The chemical potential of the bound polymer at distance r^* , $\mu_{b(r^*)}$, is now larger than $\mu_{f(a_1)}$. Consequently, some of the bound polymer will dissolve and become "free" until a new boundary at r is established satisfying the relation $\mu_{b(r)} = \mu_{f(a_1)}$. In effect, the bound layer would shrink, in the presence of solvent, from r^* to r . Upon further increase in solvent activity, the bound layer will decrease progressively in thickness until at a critical value of solvent activity, all bound polymer dissolves.

The following relationships may be derived on the basis of the above model, where μ_f is the chemical potential of free polymer:

$$\mu_b(r) = \mu_f \quad (10)$$

For Henry's law sorption at small n_1 ,

$$\mu_f = \mu_f^\circ - RT \ln n_1/n_2 \quad (11)$$

$$\Delta\mu = \mu_f^\circ - \mu_{(b)} = RT \ln n_1/n_2 \quad (12)$$

The distance from the center of the filler particle to the periphery of the bound polymer is r . The boundary conditions of eq. (12) are:

$$\mu_{b(r)} = \mu_{b(r^*)} = \mu_f^\circ \quad \Delta\mu = 0 \quad \text{At } n_1 = 0 \quad (13)$$

$$r = r_0 \quad \text{At } n_1 \geq n_{1c} \quad (14)$$

where r_0 is the radius of the filler particle; here all segments are free.

Since it is assumed that only the free polymer sorbs water vapor, the fraction f of the free polymer in the total polymer at a given P/P_0 is given by:

$$f = \frac{\text{Amount of vapor sorption by the filled polymer}}{\text{Amount of vapor sorption by the unfilled polymer}} \quad (15)$$

The fraction of bound polymer is $(1-f)$; it is related to r by eq. (16):

$$(r/r_0)^3 - 1 = (1-f) \left(\frac{\text{Volume of the polymer in filled specimen}}{\text{Volume of the filler in a filled specimen}} \right) \quad (16)$$

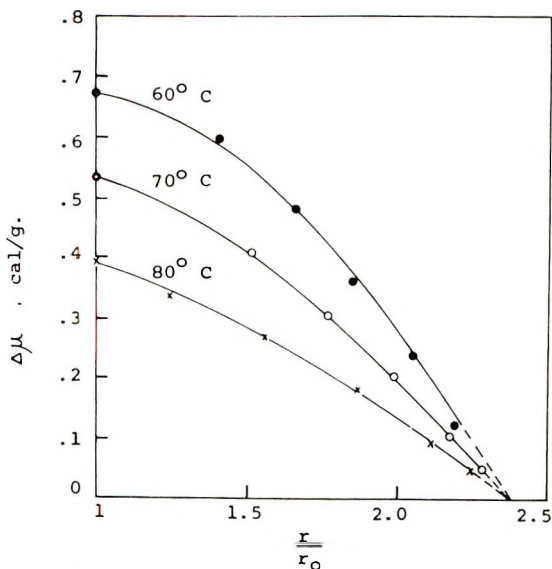


Fig. 2. Plot of $\Delta\mu$ as a function of distance.

From eqs. (12) and (16), one can obtain $\Delta\mu$ and r/r_0 from experimentally measurable quantities. Plots of $\Delta\mu$ versus r/r_0 are shown in Figure 2. Extrapolation of the three curves yields a common intercept with the abscissa. (More realistically, the curves probably should approach the axis of abscissa asymptotically.) Application of the aforementioned boundary conditions to the plots in Figure 2 yields: at $\Delta\mu = 0$, $r = r^*$, and $(r^*/r_0) = 2.36$. Also, at $n = n_{1c}$, $r/r_0 = 1$, $\Delta\mu = \Delta\mu_{(r_0)}$. The $\Delta\mu_{(r_0)}$ values are 0.672 cal./g. at 60°C., 0.533 cal./g. at 70°C., and 0.394 cal./g. at 80°C.

The thickness of the bound layer in the dry state, which is $(r^* - r_0)$, is about 1430 Å. The fraction of bound polymer, $(1 - f)$, calculated by eq. (16), is 56.2%. These results are in good agreement with the corresponding values obtained from a consideration of the chloroform vapor sorption² of the same epoxy polymer filled with TiO_2 at various concentrations; namely, $(1 - f) = 58.6\%$, $(r^*/r_0) = 2.39$, and $(r^* - r_0) = 1460$ Å.

From the values of $\Delta\mu_{(r_0)}$ at the three temperatures, it is obtained:

$$\Delta S_{(r_0)} = -\partial \Delta\mu_{(r_0)} / \partial T = 1.39 \times 10^{-2} \text{ cal./g.-deg.} \quad (17)$$

and

$$\Delta H_{(r_0)} = \Delta\mu_{(r_0)} + T \Delta S_{(r_0)} = 5.30 \text{ cal./g.} \quad (18)$$

Hence,

$$\Delta\mu_{(r_0)} = 5.30 - 1.39 \times 10^{-2} T \text{ cal./g.} \quad (19)$$

The magnitude of $\Delta H_{(r_0)}$ is such that London forces appear to be operative. According to our model, the interaction will vanish when $\Delta\mu_{(r_0)} = 0$, at a temperature of 381°K.

It is difficult to find a simple analytical expression for the dependence of $\Delta\mu$ on r satisfying all the boundary conditions. Equation (20) represents the data in Figure 2 satisfactorily in the range $r < r < r^*$.

$$\Delta\mu_{(r)} = \Delta\mu_{(r_0)} \{1 - \beta [(r^3/r_0^3) - 1]\} \quad (20)$$

For $r > r^*$, eq. (20) gives a negative value of $\Delta\mu$ and is thus inapplicable. It also appears that one single value of β , namely, 8.6×10^{-2} , suffices to describe the decay of $\Delta\mu$ with distance at the three temperatures of our experiment. To check the internal consistency of our calculation, an average value of $\Delta\mu$ per gram of bound polymer, $\langle\Delta\mu\rangle$, may be calculated as shown in eq. (21).

$$\begin{aligned} \langle\Delta\mu\rangle &= \int_r^{r^*} \Delta\mu dV / \int_{r_0}^{r^*} dV \\ &= \int_{r_0}^{r^*} \Delta\mu r^2 dr / 1/3 (r^{*3} - r_0^3) \end{aligned} \quad (21)$$

where V is the volume of the bound polymer.

The $\langle\Delta\mu\rangle$ values are 0.35, 0.26, and 0.18 cal./g. bound polymer at 60, 70, and 80°C., respectively. They are in agreement with the ΔF_m values obtained previously, namely, 0.15 cal./g. at 70°C. and 0.08 cal./g. at 80°C., if one takes into consideration that about 56% of the total polymer is bound and that ΔF_m is expressed in calories per gram of total polymer. If one equates the temperature-dependent term of $\Delta\mu$ to ΔS , one obtains $\langle\Delta S\rangle$ as 6.7×10^{-3} cal./g.-deg., and from the temperature-independent term of $\Delta\mu$, one obtains $\langle\Delta H\rangle$ as 2.54 cal./g. These values are in fair agreement with the ΔH_m and ΔS_m values listed in Table I, suggesting that the omission of the water-filler interaction in the thermodynamic cycle has not introduced serious errors, and that the validity of our conclusion is not substantially affected by this omission.

We now proceed to discuss the significance of $\Delta\bar{H}'_1$, for the sorption of a vapor by a filled polymer in terms of our model. The enthalpy of a mixture of a solvent and a filler polymer is:

$$\begin{aligned} H' &= n_1\bar{H}_1 + n_f\bar{H}_f + n_b\bar{H}_b \\ &= n_1\bar{H}_1 + n_2 [f\bar{H}_f + (1-f)\bar{H}_b] \end{aligned} \quad (22)$$

where the subscripts 1, f , and b , denote solvent, free polymer, and bound polymer, respectively, and n_2 is the total number of moles of polymer segments. Differentiation of eq. (22) gives eq. (23):

$$\partial H' / \partial n_1 = \bar{H}_1 + n_2 (\bar{H}_f - \bar{H}_b) \partial f / \partial n_1 \quad (23)$$

The quantity $\Delta\bar{H}'_1$ is, by definition, $[(\partial H' / \partial n_1) - H_1^\circ]$:

$$\Delta\bar{H}'_1 = (\bar{H}'_1 - H_1^\circ) + n_2 (\partial f / \partial n_1) (\bar{H}_f - \bar{H}_b) \quad (24)$$

The first term on the right-hand side of eq. (24), $(\bar{H}'_1 - H_1^\circ)$, is just $\Delta\bar{H}_1$, the heat of sorption of the solvent by the unfilled polymer. The quantities

TABLE II
Partial Molar Heat of Sorption of Water by Filled Epoxy Polymer^a

Sorbed water, g./100 g. polymer	$m\bar{H}'_1$, kcal./mole
0.2	-2.53
0.4	-2.06
0.6	-1.83
0.8	-1.80
1.0	-1.69

^a $\Delta\bar{H}_1 = -4.40$ kcal./mole.

$(H_f - H_b)$ and $\partial f/\partial n$, are both positive. Therefore, it is expected that $\Delta\bar{H}'_1$ is more positive than $\Delta\bar{H}_1$. Experimental data are shown in Table II. A cursory examination of Table II reveals that $\Delta\bar{H}'_1$ increases with solvent concentration, which may be viewed as a reflection of the lower \bar{H}_b and hence higher $(\bar{H}_f - \bar{H}_b)$ values for polymer segments nearer to the surface. It may also be mentioned that in the sorption of acetone by TiO₂-filled poly(vinyl acetate), $\Delta\bar{H}'_1$ is about 4.3 kcal./mole,² which is more positive than the $\Delta\bar{H}_1$ value for the unfilled PVAc, reported to be about -0.6 kcal./mole.¹¹

Similar consideration may be applied to the interpretation of the thermal expansion coefficient and heat capacity of a filled polymer. For example, the change of specific volume with temperature is:

$$d\bar{V}/dT = f(d\bar{V}_f/dT) + (1 - f)(d\bar{V}_b/dT) \quad (25)$$

The experimentally observed $d\bar{V}/dT$ of a filled polymer would be smaller than $d\bar{V}_f/dT$ of the unfilled polymer if $d\bar{V}_b/dT$ is less than $d\bar{V}_f/dT$. This was observed in the case of a filled poly(vinyl acetate) sample where $d\bar{V}/dT$ at 40°C. is about 4.7×10^{-4} cm.³/g.-deg., in comparison with the $d\bar{V}_f/dT$ value for the unfilled polymer of about 5.9×10^{-4} cm.³/g.-deg.¹² The same treatment may be applied to heat capacity C_p .

It appears from the above calculations that the influence exerted by the filler particles probably is not limited to the immediate vicinity of the particle surface. The subject of the depth of the surface zone of a liquid in contact with a solid has been reviewed many years ago by Henniker.¹³ Refractive index, x-ray diffraction, and electron diffraction data suggest that the effective depth of the surface zone having different structure from the bulk liquid may reach hundreds to thousands of Angstroms. Recent viscosity studies of dilute polymer solutions led to the interpretation that the adsorbed polymer layer on glass capillary has an "apparent" thickness of the order of 1000 Å.¹⁴⁻¹⁷ The thickness of adsorbed polystyrene on chrome plate was measured, by ellipsometry, to be about several hundred Angstroms.¹⁸ The distance of effective interaction between a filler particle and the surrounding polymer in the solid state, estimated by us to be about 1500 Å. in our system, therefore does not seem to be unreasonable. It is generally acknowledged that the configuration of adsorbed polymer

molecules is not necessarily the same as the configuration of the same polymer chains in solution or in bulk. It appears possible that the packing of the polymer molecules on top the adsorbed layer may be different from the packing of chains in the unfilled state. According to our calculation, a higher state of order exists in the packing of polymer chains near the filler surface. It is not entirely unexpected that the order of polymer packing may decrease progressively with increasing distance from the filler surface. A detailed molecular mechanism of chain packing or order in amorphous polymers, however, is still lacking.

References

1. Kumins, C. A., and J. Roteman, *J. Polymer Sci.*, **A1**, 527 (1963); *ibid.*, **A1**, 541 (1963).
2. Kwei, T. K., and C. A. Kumins, *J. Appl. Polymer Sci.*, **8**, 1483 (1964).
3. Kwei, T. K., *J. Polymer Sci.*, **A1**, 2977 (1963).
4. Kargin, V. A., *J. Polymer Sci.*, **23**, 47 (1957).
5. Kokes, R. J., F. A. Long, and J. L. Hoard, *J. Chem. Phys.*, **20**, 1711 (1952).
6. Lakhanpal, M. L., and B. E. Conway, *Can. J. Chem.*, **38**, 199 (1960).
7. Mandelkern, L., *Crystallization of Polymers*, McGraw-Hill, New York, 1964, p. 119.
8. Kargin, V. A., *J. Polymer Sci.*, **30**, 247 (1958).
9. Mikhailov, N., and E. Fainberg, *Dokl. Akad. Nauk SSSR*, **109**, 1160 (1956).
10. Cahn, J. W., and J. E. Hilliard, *J. Chem. Phys.*, **28**, 258 (1958).
11. Kokes, R. J., A. R. DiPietro, and F. A. Long, *J. Am. Chem. Soc.*, **75**, 6319 (1953).
12. Kwei, T. K., *J. Polymer Sci.*, in press (1965).
13. Henniker, J. C., *Rev. Mod. Phys.*, **21**, 322 (1949).
14. Ohrn, O. E., *J. Polymer Sci.*, **17**, 137 (1955).
15. Takeda, M., and R. Endo, *J. Phys. Chem.*, **60**, 1202 (1956).
16. Hugue, M. M., M. Fishman, and D. A. I. Goring, *J. Phys. Chem.*, **63**, 766 (1959).
17. Tuijnman, C. A. F., and J. J. Hermans, *J. Polymer Sci.*, **25**, 385 (1957).
18. Stromberg, R. R., E. Passaglia, and D. J. Tutas, paper presented at 144th National meeting, American Chemical Society, Los Angeles, April 1963.

Résumé

A partir d'une étude de la sorption de vapeur d'eau par les polymères Epoxy chargés de bioxyde de titane, on a calculé les différences d'enthalpie et d'entropie des polymères chargés et non-chargés. L'enthalpie et l'entropie du polymère chargé sont plus petites que celles du polymère non chargé d'environ 2 cal/g et 6×10^{-3} u.e. respectivement. Ces différences peuvent être expliquées par l'existence d'un degré plus élevé d'ordre local des segments de polymère. On propose un modèle pour décrire l'interaction entre le polymère et la charge en fonction de la distance à partir de l'interface. Il semble que les segments de polymère situés à une distance inférieure à 1.500 Å. de la surface de la particule de remplissage sont à l'intérieur de la sphère d'influence de la charge. Sur la base du modèle, on discute de l'influence de l'incorporation de charge sur le coefficient de dilatation thermique, sur la capacité calorifique et sur la chaleur molaire partielle de la solution de polymère.

Zusammenfassung

Aus den Ergebnissen einer Untersuchung der Sorption von Wasserdampf durch titandioxydgefüllte Epoxy-polymere wurden die Enthalpie- und Entropieunterschiede zwischen gefüllten und ungefüllten Polymeren berechnet. Die Enthalpie und die Entropie des gefüllten Polymeren sind um etwa 2 kal/g bzw. $6 \cdot 10^{-3}$ cal. grad⁻¹ kleiner als diejenigen des ungefüllten Polymeren. Diese Unterschiede können durch das Bestehen

eines höheren lokalen Ordnungsgrads der Polymersegmente erklärt werden. Ein Modell zur Beschreibung der Wechselwirkung zwischen Polymerem und Füllstoff als Funktion des Abstandes von der Grenzfläche wird angegeben. Es scheint, dass Polymersegmente bei einem geringeren Abstand von der Oberfläche der Füllstoffteilchen als 1500 Å sich innerhalb der Einflussphäre des Füllstoffes befinden. Der Einfluss des Füllstoffeinbaus auf den thermischen Expansionskoeffizienten, die Wärmekapazität und die partielle molare Lösungswärme des Polymeren werden an Hand des Modells diskutiert.

Received December 22, 1964

Revised February 7, 1965

Prod. No. 4666A

Kinetics of the Initiation of Styrene Polymerization by *n*-Butyllithium

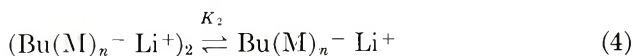
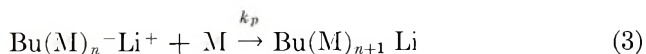
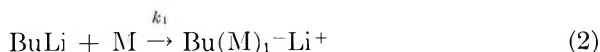
K. F. O'DRISCOLL,* E. N. RICCHEZZA,† and J. E. CLARK,‡
Department of Chemistry, Villanova University, Villanova, Pennsylvania

Synopsis

The reaction between styrene and *n*-butyllithium in benzene has been studied by spectrophotometry and calorimetry at 25°C. It was observed that the initiation of polymerization was first-order in styrene and one-third-order in butyllithium at styrene concentrations of 0.5 mole/l. and that addition of butyllithium to styrene solutions caused an evolution of 1.7 kcal./mole of butyllithium. It was also noted that the rate of initiation was approximately an order of magnitude larger than that previously reported in very dilute styrene solutions (0.03 mole/l.) and comparable butyllithium concentrations. It is concluded that styrene stabilizes trimeric butyllithium relative to its hexamer by a nonstoichiometric, exothermic solvation process.

Introduction

In the more than five years since the first publication^{1,2} on the subject appeared, the unusual kinetics of the *n*-butyllithium (BuLi)-initiated polymerization of styrene has excited considerable interest. It had appeared that the work of Worsfold and Bywater³ had essentially solved the kinetic problem. They proposed a mechanism for polymerization in benzene involving hexameric BuLi and dimeric polystyryllithium chain ends. Their kinetic results exhibited extremely precise agreement with the mechanism expressed in eqs. (1)–(4), where *n* has a value of 6.



* Present address: Department of Polymer Chemistry, Kyoto University, Kyoto, Japan (on leave of absence, 1964–65)

† Present address: Olin Mathison Corp., Fayetteville, N. C.

‡ Present address: W. R. Grace and Co., Silver Springs, Md.

Recent work by Morton et al.⁴ has sustained the concept of dimeric chain ends, and vapor pressure studies by Margerison and Newport⁵ confirm the existence of BuLi as a hexamer. When these works are considered together, the kinetic scheme above cannot be questioned. However, the work which established the above initiation mechanism was done at a maximum styrene concentration of 0.03 mole/l.³ We will show in this paper that at concentrations of 0.2–1.0 mole/l. of styrene, the kinetics of initiation indicates that BuLi exists as a trimer.

Experimental

Three distinct types of experiments (A, B, and C) were performed, all at 25°C.

In experiments A, mixtures of styrene ($[\text{Sty}] \cong 10^{-4}M$) and commercial *n*-butyllithium ($[\text{BuLi}] = 1.29M$) were prepared in cyclohexane under a helium atmosphere. The samples were contained in cylindrical, 1.0 cm. spectrophotometer cells which were sealed under vacuum. A vertical line scribed on the cell permitted reproducible alignment. The absorbance of the solution was followed at 440 $m\mu$ for a period of days, until a limiting absorbance was reached. Simultaneous absorbance measurements were also made at 334 $m\mu$ until those more intense readings went above 2.0.

In series B, catalytic amounts of benzene solutions of BuLi were added through a breakseal to 0.5*M* styrene in benzene. The entire process was carried out in a vacuum-jacketed reaction flask containing a thermistor. The thermistor formed one arm of a Wheatstone bridge, and the potential required to balance the bridge was recorded as a function of time. Temperature changes as small as 0.01°C. could be measured. Knowledge of the various heat capacities, the heat of polymerization, and the rate of heat loss from the flask enabled us to calculate conversion of monomer to polymer to within $\pm 0.1\%$. In all of these experiments, the important observation was made that the addition of BuLi caused an immediate temperature increase of approximately 0.08°C. Since the solution was magnetically stirred and at temperature equilibrium with its surroundings before the addition of the BuLi, the temperature rise must represent a heat of solution of BuLi. Maximum temperature rise due to subsequent polymerization was approximately 2.0°C.

In experiment series C, solutions of the same concentrations as those in experiments B were prepared in spectrophotometer cells and the absorbance monitored at 540 $m\mu$ until a limiting absorbance was reached. This occurred in about 1 hr. when polymerization was only 60–80% complete. Frequent measurements were also made of the absorbance at 440 $m\mu$ until it went above 2.0.

All solvents and monomers were carefully dried over calcium hydride and distilled under vacuum immediately before use. In experiments B and C, all transfers were performed under a vacuum of 10^{-6} mm. Hg.

Solutions of BuLi were kindly supplied by the Foote Mineral Co. in a

hydrocarbon solvent which was a mixture of pentane and heptane. BuLi concentrations were determined by the double titration method of Gilman.⁶

A Beckman DK-1 equipped with a thermostatted cell holder was used for all spectrophotometric measurements.

Results

Figure 1 shows a plot of the limiting absorbance at $440\text{ m}\mu$ of the solutions containing small amounts of styrene and a vast excess of BuLi ($1.29M$). Figure 2 shows a first-order plot of the absorbance as a function of time. The zero-zero intercept of Figure 1 and the linearity of Figures 1 and 2 justify the assumption that every styrene molecule added to a BuLi mole-

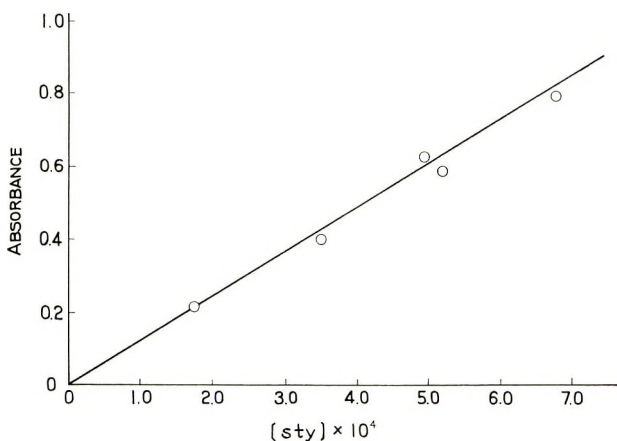


Fig. 1. Limiting absorbance at $440\text{ m}\mu$ as a function of the amount of styrene added to $1.29M$ BuLi.

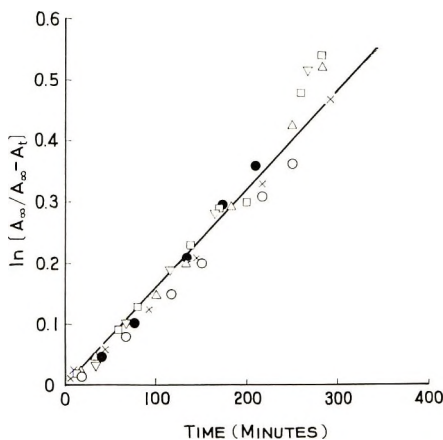


Fig. 2. Pseudo first-order behavior of absorbance at $440\text{ m}\mu$ when various amounts of styrene were added to $1.29M$ BuLi at 25°C .: (\times) $[\text{Sty}] = 7.15 \times 10^{-4}M$; (\circ) $[\text{Sty}] = 5.71 \times 10^{-4}$; (Δ) $[\text{Sty}] = 4.28 \times 10^{-4}M$; (\square) $[\text{Sty}] = 4.28 \times 10^{-4}M$; (\bullet) $[\text{Sty}] = 2.88 \times 10^{-4}M$; (∇) $[\text{Sty}]_i = 1.43 \times 10^{-4}M$.

cule and no polymerization took place. This permits us to calculate the extinction coefficient ϵ for the styryllithium chain end at 440 $m\mu$. From the simultaneous measurements which we made at 334 $m\mu$, we can calculate that extinction coefficient also. Values are given in Table I.

TABLE I
Molar Extinction Coefficients of the Species $R-CH_2-CH(C_6H_5)-Li$ in Hydrocarbon Solvent

λ , $m\mu$	ϵ , l./mole/cm.	Approximate concentration,		R	Reference
		[Sty]	[BuLi]		
334	13,000	0.09	0.0005	Polystyrene	3
334	13,600	0.0004	1.29	Butyl	This work, A
440	1,360	0.0004	1.29	Butyl	This work, A
440	1,450	0.5	0.04	Polystyrene	This work, C
540	39	0.5	0.04	Polystyrene	This work, C
550	>10	0.7	0.07	Polystyrene	7 ^a
530	~50	1.5	0.03	Polystyrene	2 ^b

^a Polymerization complete before BuLi consumed.

^b Not done under vacuum.

From the linearity of Figure 2 we can also deduce that initiation is first-order in styrene as was previously shown.^{3,7} From the slope of Figure 2 and the 440 $m\mu$ extinction coefficient, we can calculate the pseudo first-order rate constant for initiation. Assuming the reaction to be one-sixth-order with respect to BuLi, we obtain 1.53×10^{-3} (l./mole)^{1/6} min.⁻¹ at 25°C. Interpolation of the data of Worsfold and Bywater with an apparent activation energy of 18 kcal.³ gives a value of 0.82×10^{-3} (l./mole)^{1/6} min.⁻¹ at 25°C. Considering the more than three orders of magnitude

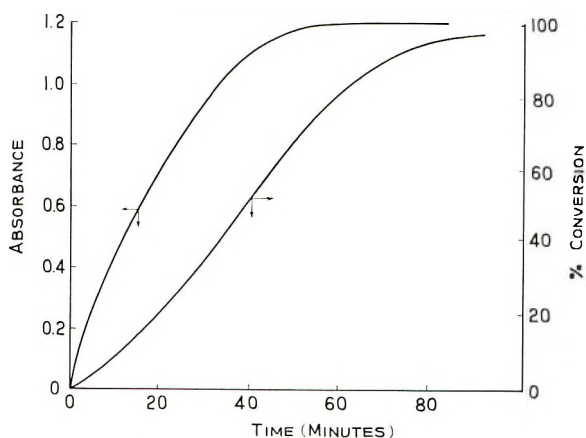


Fig. 3. Absorbance at 540 $m\mu$ and conversion as a function of time at 25°C. in benzene at [Sty] = 0.51*M*; [BuLi] = 0.030*M*.

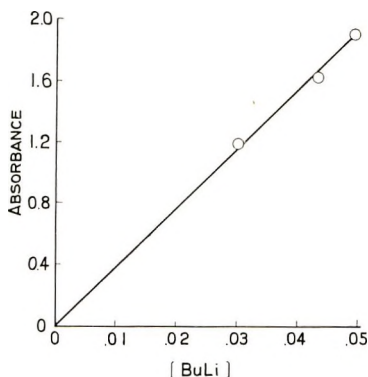


Fig. 4. Limiting absorbance at 540 $m\mu$ as a function of the amount of BuLi added to approximately 0.5*M* styrene.

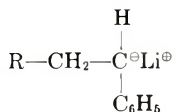
difference in BuLi concentrations, and the difference in solvents, the agreement is considered satisfactory.

Figure 3 shows a typical plot of the increase in absorbance and conversion in two separate experiments done under the same reaction conditions. In Figure 4 is shown a plot of the limiting absorbance at 540 $m\mu$ as a function of the initial BuLi concentration. From this plot and from simultaneous measurements made of absorbance at 440 $m\mu$, extinction coefficients were determined for the polystyryllithium chain ends. Values are contained in Table I.

In Table II are listed the temperature jumps which were noted at the start of all experiments B when BuLi in benzene was added to styrene in benzene. The average heat produced was 1.7 ± 0.3 kcal./mole of BuLi. Based on the BuLi existing as a hexamer in benzene, this is 10.2 ± 1.8 kcal./mole of hexameric BuLi.

Discussion of Results

The data of Figures 1-4 and Table I clearly show that the extinction coefficients we have determined are quantitative measures of the total concentration of the species



whether R is a butyl group or a polystyrene chain and regardless of the exact state of association. Furthermore, they show that these extinction coefficients are independent of monomer and BuLi concentrations. The use of the extinction coefficients and the rates of change of absorbance is therefore valid for determination of the rate of initiation, IR. We can write then, at time zero:

$$\text{IR} = -d[\text{B}_0]/dt = (1/\epsilon)(dA/dt) = k_1(K_1/n)^{1/n} [\text{B}_0][\text{Sty}]_0 \quad (5)$$

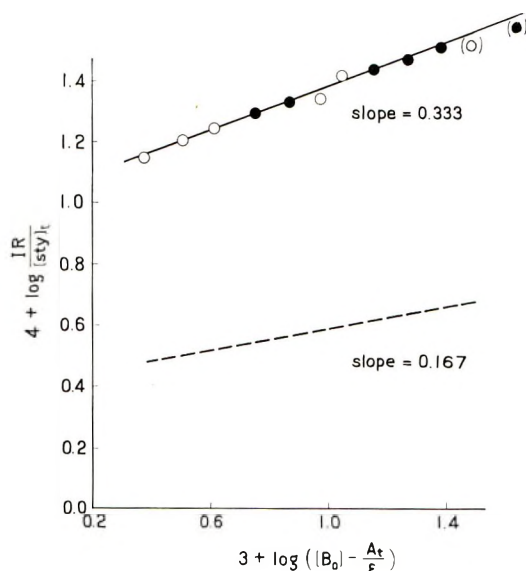


Fig. 5. Plot eq. (6) or 25°C.: (O) $[B_0] = 0.030M$, $[Sty]_0 = 0.509M$; (●) $[B_0] = 0.04M$, $[Sty]_0 = 0.491M$. Points in parentheses are from *initial* tangents; (--) of A vs. time plots. Expected value from Worsfold and Bywater.³

At some subsequent time, t :

$$IR/[Sty]_t = k_1(K_1/n)^{1/n} \{ [B_0] - A_t/\epsilon \}^{1/n} \quad (6)$$

Here $[B_0]$ is the analytically determined BuLi concentration, A_t is the absorbance at time t , and the other terms are defined in the Worsfold and Bywater mechanism of eqs. (1)–(4). A correct solution in closed form of the differential equations describing the kinetics of this mechanism has not been achieved, but we can use eq. (6) in a log-log plot where data such as Figure 3 are available, since the absorbance–time data were obtained at a fast recorder speed and dA/dt can be precisely calculated. A plot of eq. (6) from data such as those of Figure 3, is shown in Figure 5. Least-squares analysis of the data gives in units of moles, liters, and minutes:

$$1/n = 0.333$$

$$k_1(K_1/n)^{1/n} = 1.02 \times 10^{-2} \quad \text{at } 25^\circ\text{C.}$$

Not only does this indicate that a trimer rather than a hexamer is the dominant species, but the value of the observed rate is one order of magnitude greater than that predicted from the data of Worsfold and Bywater³ or by our own experiments A. For comparison in Figure 5 we show as a dotted line the value of $IR/[Sty]$ predicted from Worsfold and Bywater.

Because of this large discrepancy we have plotted data from the work of Cubbon and Margerison⁷ at 15°C. They measured initial rates of absorbance increase at 550 $m\mu$ using initial styrene concentrations of 0.72 mole/l. Since the spectrum of styryllithium is quite flat in this region, we have used

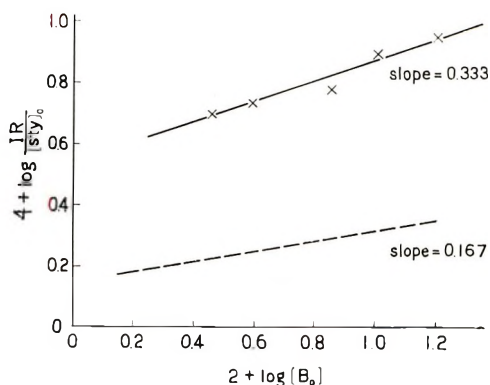


Fig. 6. Plot of (—) initial rate data from Cubbon and Margerison⁷ according to eq. (5) at $[Sty]_0 = 0.72M$; (---) expected value from Worsfold and Bywater.³

our extinction coefficient at $540\text{ m}\mu$ and show in Figure 6 the variation of initial IR with $[B_0]$. Again for comparison we include the prediction of Worsfold and Bywater³ at 15°C . and again we note a slope of $1/3$ for the higher styrene concentration and a difference in rate of more than one half of an order of magnitude.

Conclusions

We conclude that in the presence of approximately 0.5 mole/l. of styrene in benzene, BuLi exists as a trimer. From the data in Table II, we suggest that the heat of reaction for reaction (7) is $\Delta H_{6,3} = -10.2 \pm 1.8\text{ kcal}$.

$(BuLi)_6$ ($<0.03M$ styrene/benzene) \rightarrow



The possibility that cross-association between BuLi and the living chain end gives rise to the $1/3$ dependence in Figure 5 can be ruled out by noting the comparatively high initial rates of chain end formation obtained in both this work and in that of Cubbon and Margerison.⁷ Experimental difficulties associated with mixing of reactants and measuring changes in small absorbances cause these numbers to be somewhat more imprecise than the data at higher conversions. Therefore in Figure 5 we have not included the initial rate data in the least-squares analysis, but show only the points to indicate that cross-association cannot be the source of the rate enhancement over that of Worsfold and Bywater.³ Figure 6 also indicates the unimportance of cross-association, since there, too, higher rates were obtained for initial measurements.

The conclusion that monomer solvates hexamer to give trimer must be reconciled with the well established fact that initiation is first-order with respect to monomer.^{3,7} We suggest that styrene solvates the trimeric butyllithium in a nonstoichiometric fashion similar to the postulated solvation of monomeric polyisoprenyllithium by tetrahydrofuran.⁸

TABLE II
Initial Temperature Jump (ΔT) When BuLi Added to Benzene Solution of Styrene

[Sty], mole/l.	[BuLi], mole/l.	Heat capacity of system C , cal./deg.	Volume of system V , ml.	ΔT , °C.	Q , kcal./mole BuLi ^a
0.379	0.027	6.69	10.4	0.07	1.3
0.379	0.026	6.69	10.5	0.07	1.7
0.505	0.032	6.75	10.5	0.08	1.6
0.383	0.029	6.79	10.7	0.09	2.0
0.384	0.027	6.80	10.4	0.09	2.2
0.521	0.031	6.73	10.4	0.08	1.7
0.549	0.027	6.94	11.0	0.06	1.4

^a $Q = C \Delta T / V [\text{BuLi}]$.

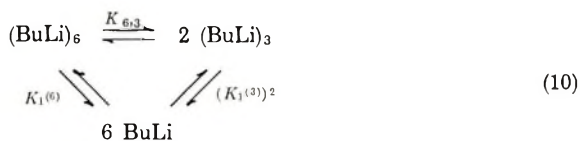
It would be interesting to know more about the thermodynamics of the association equilibria. From this work and that of Worsfold and Bywater,³ we can write at 25°C.:

$$k_1 (K_1^{(6)}/6)^{1/6} / k_1' (K_1^{(3)}/3)^{1/3} = 0.824 \times 10^{-3} / 10.2 \times 10^{-3} \quad (8)$$

where $K_1^{(n)}$ is the equilibrium constant for dissociation of the n -mer into monomeric BuLi and k_1 and k_1' are the respective rate constants for initiation by unsolvated and solvated monomeric BuLi. If these two rate constants were equal, we could calculate from eq. (8) that

$$(K_1^{(6)})^{1/6} / (K_1^{(3)})^{1/3} = 0.075 \quad (9)$$

However, the assumption that $k_1 = k_1'$ is equivalent to assuming that monomeric BuLi is unaffected by solvation. It would follow from a consideration of the isothermal cycle [eq. (10)] that $K_{6,3} = (0.075)^6$ and that $\Delta S_{6,3} = -65$ e.u. if $\Delta H_{6,3} = -10.2$ kcal./mole.



The small value of $K_{6,3}$ is inconsistent with the postulated predominance of trimeric BuLi, and the extremely large, negative entropy change is inconsistent with a dissociation process. It therefore seems that k_1 must be affected by solvation. Calculation shows that if the ratio k_1/k_1' is appreciably less than 0.1, $K_{6,3}$ will have a value that places more than 90% of the BuLi in the trimer. The ratio k_1/k_1' would have to be less than 0.004 for $\Delta S_{6,3}$ to be positive.

Sinn et al. have also postulated the existence of a trimer as well as a hexamer to account for the kinetics of isoprene initiation in hexane.⁹ They offer no conclusive evidence, but by assuming a single value of k_1 and curve

fitting to a polynomial equation they determined values for $K_1^{(3)}$ and $K_1^{(6)}$ such that we can calculate in isoprene/hexane at 20°C.

$$(K_1^{(6)})^{1/2}/(K_1^{(3)})^{1/3} = 0.29 \quad (11)$$

which contrasts with the value of eq. (9). Unfortunately, Sinn et al.⁹ do not report any temperature variation, so it is not possible to compare thermodynamic parameters directly.

Solvation has long been considered of importance in ionic polymerization, and the existence of a scale of solvating power for monomers has been suggested.¹⁰ The variation for different compounds in their solvating ability for the carbon-lithium bond is explicitly contained in the polymerization work of Tobolsky and Rogers¹¹ as well as in the spectroscopic investigations of Waack.¹² It appears that BuLi exists as a hexamer in benzene,^{3,5} a trimer in styrene, a dimer in methyl ether,¹³ and a monomer in tetrahydrofuran. The ability of vinyl or diene monomers to form π complexes with the carbon-lithium bond has also recently been invoked¹⁴ to explain anionic copolymerization behavior as well as the effect of durene on the homopolymerization kinetics of styrene. We believe that this paper offers some idea of the quantitative magnitude of the solvation enthalpies involved. They are surprisingly large even for relatively weak solvating agents such as styrene and isoprene. A surprisingly large value was also noted by Morton et al.⁴ for the solvation of polyisoprenyllithium by tetrahydrofuran.

Support of this work by the National Science Foundation, Grant G-9497, and by the Petroleum Research Fund, administered by the American Chemical Society, is gratefully acknowledged.

References

1. O'Driscoll, K. F., and A. V. Tobolsky, *J. Polymer Sci.*, **35**, 259 (1959).
2. Welch, F. J., *J. Am. Chem. Soc.*, **81**, 1345 (1959).
3. Worsfold, D. J., and S. Bywater, *Can. J. Chem.*, **38**, 1891 (1960).
4. Morton, M., L. J. Fetters, and E. E. Bostick, *J. Polymer Sci.*, **C1**, 311 (1963).
5. Margerison, D., and J. Newport, *Trans. Faraday Soc.*, **59**, 2058 (1962).
6. Gilman, H., and A. Haubein, *J. Am. Chem. Soc.*, **66**, 1515 (1944).
7. Cubbon, R., and D. Margerison, *Proc. Roy. Soc. (London)*, **A268**, 260 (1962).
8. Morton, M., and L. J. Fetters, *J. Polymer Sci.*, **A2**, 3311 (1964).
9. Sinn, H., C. Lundborg, and O. T. Onsager, *Makromol. Chem.*, **70**, 222 (1964).
10. Ludvig, E. B., A. R. Gantmakher, and S. S. Medvedev, *Vysokomol. Soedin.*, **1**, 1333 (1959).
11. Tobolsky, A. V., and C. E. Rogers, *J. Polymer Sci.*, **38**, 205 (1959).
12. Waack, R., and M. A. Doran, *J. Phys. Chem.*, **67**, 148 (1963).
13. Cheema, Z. K., G. W. Gibson, and J. F. Eastham, *J. Am. Chem. Soc.*, **85**, 3517 (1963).
14. O'Driscoll, K. F., and R. Patsiga, *J. Polymer Sci.*, **A3**, 1037 (1965).

Résumé

On a étudié la réaction entre le styrène et le *n*-butyllithium dans le benzène par spectrophotométrie et calorimétrie à 25°C. On a observé que l'initiation de la polymérisation était du premier ordre par rapport au styrène et de l'ordre un tiers par rapport au butyllithium pour des concentrations en styrène de 0,5 m/l., et que l'addition de butyllithium

aux solutions de styrène provoquait un dégagement de 1,7 kcal/mol. de butyllithium. On a également noté que la vitesse d'initiation était approximativement d'un ordre de grandeur plus grand que celle décrite antérieurement en solutions styréniques très diluées (0,03 m/l.) et avec des concentrations en butyllithium comparables. On peut conclure que le styrène stabilise le butyllithium trimère comparativement à son hexamère par un processus de solvatation exothermique non stoechiométrique.

Zusammenfassung

Die Reaktion zwischen Styrol und *n*-Butyllithium in Benzol wurde spektrophotometrisch und kalorimetrisch bei 25°C untersucht. Der Polymerisationsstart ist von erster Ordnung in bezug auf Styrol und von der Ordnung $\frac{1}{3}$ in bezug auf Butyllithium bei Styrolkonzentrationen von 0,5 m/l, und der Zusatz von Butyllithium zu Styrolösungen verursacht eine Entwicklung von 1,7 kcal/Mol Butyllithium. Weiters wurde festgestellt, dass die Startgeschwindigkeit ungefähr um eine Grössenordnung höher ist als sie früher für sehr verdünnte Styrollösungen (0,03 m/l) und vergleichbare Butyllithiumkonzentrationen berechnet wurde. Man kommt zu dem Schluss, dass Styrol das trimere Butyllithium im Verhältnis zu seinem hexameren durch einen nichtstöchiometrischen exothermen Solvatationsprozess stabilisiert.

Received January 19, 1965

Revised February 22, 1965

Prod. No. 4669A

Single Crystals of Amylose V Complexes

YUHIKO YAMASHITA, *Faculty of Engineering, Okayama University, Okayama, Japan*

Synopsis

In the present paper our previous results and Manley's results for single crystals of amylose V complexes are confirmed. A reasonable interpretation of electron diffraction patterns from lamellar crystals of the monohydrated complex and of the anhydrous complex is presented. It is concluded that the longer side of rectangular lamellae corresponds to the a axis of the unit cell of the wet complex, and that the crystal structure does not have hexagonal symmetry at the time when the lamellar crystals are formed in the supercooled solution. The mode of chain packing in the single crystals is described and discussed.

INTRODUCTION

Amylose is a linear polymer derived from naturally occurring starches. It is well known that amylose in the solid state exists in two basically different conformations: an extended form which yields either the A or B type of x-ray diffraction pattern and a helical form which yields the V pattern.¹⁻⁴ The V type conformation results from amylose complexes precipitated from aqueous solution with various alcohols. These precipitates have been studied by many investigators. Rundle et al.³ have determined the crystal structure of the n -butanol-amylose complex from x-ray powder diagrams. The unit cell is orthorhombic with the dimensions $a = 13.7$ A., $b = 23.8$ A., and $c = 8.05$ A. for the monohydrated complex (one water molecule per glucose residue) and $a = 13.0$ A., $b = 23.0$ A., and $c = 8.05$ A. for the anhydrous complex.⁵ The chain molecule assumes a helical conformation with six glucose residues per turn, and each unit cell contains two helices directed in opposite directions. On the other hand, rectangular platelets and six-segmented spherulites have been observed microscopically in crystal suspensions precipitated with n -butanol by Kerr et al.⁶ and Schoch.⁷ The difficulty of producing oriented fibers and films of amylose V complexes seems to have interrupted the elucidation of more detailed structure in the solid state.

However, various high polymers have been found in the form of single crystals in which the molecular chains are folded in segments of 100 A. since the polyethylene single crystal was discovered in 1957.⁸⁻¹⁰ These have given us an effective means for structural studies of crystalline polymers. We have reported previously^{11,12} that single crystals of amy-

lose V complexes can be crystallized as rectangular-shaped lamellae in which the helix axes are oriented perpendicular to the lamellar surface. In view of the lamellar thickness and average degree of polymerization, a given helical chain must necessarily be folded in the lamella repeatedly. It was interesting that the concept of chain folding could be applied to lamellar crystals of the *n*-butanol-amylose complex, which has the abnormally large helix diameter of 13.7 Å, just in the same way as the other various synthetic polymers. More recently, Manley¹³ has independently published a paper on chain folding in amylose crystals in which he presents conclusions substantially the same as our previous ones. In the present we will report in more detail morphological observations and structure studies on the lamellar crystals by electron microscopy and by electron and x-ray diffraction.

EXPERIMENTAL

Preparation of Amylose V Complexes

The amylose V complexes of *n*-butanol and *n*-propanol were prepared following Kerr's procedure.⁶ Amylose was extracted from potato starch with distilled water at 70°C. Precipitating agents were added to the resulting aqueous solutions at 95°C. Crystallization was performed at constant temperatures between 40 and 60°C. with gentle stirring. To obtain the degree of polymerization of our amylose, the intrinsic viscosity in 1*N* KOH at 22.5°C. was measured. This value was 11.5 l./g., and corresponds to an average degree of polymerization of 850 from the viscosity-molecular weight relation derived by Greenwood et al.¹⁴

Morphological Observations and Electron Diffraction Studies

Drops of the crystal suspension were placed on carbon-coated grids and the solvent was removed in a desiccator. The specimens were shadowed with Ge or Pt-Pd and were examined by direct transmission in a JEM 6A electron microscope. Selected area electron diffraction experiments were carried out in the same instrument. Calibration of the diffraction spots was made with the aid of a thin evaporated layer of aluminum on the same specimen.

X-Ray Diffraction Studies

Films obtained by filtering the crystal suspension, and powder samples obtained by centrifugation of the crystal suspension, were used for x-ray diffraction studies. High-angle x-ray diffraction photographs for oriented films of sedimented lamellar crystals were obtained in a flat film camera with the use of nickel-filtered CuK α radiation. High-angle x-ray powder patterns of the samples were obtained by a diffractometer by use of nickel-filtered CuK α radiation. Low-angle x-ray diffraction patterns of the oriented film were measured with a low-angle diffractometer (Rigaku Denki Co., Ltd.).

RESULTS

Morphology

The electron microscopic observations on crystals of the *n*-butanol and *n*-propanol complexes prepared by the procedure described above confirmed our previous results^{11,12} and also Manley's results.¹³ The micrograph in Figure 1 shows typical crystals obtained by adding *n*-butanol to 0.05% amylose solution. The crystals generally consist of aggregates composed of stacks of thin, rectangular-shaped lamellae. The thickness of each lamella is estimated to be about 100 Å. from shadow length measurements. Dislocation-centered spiral growth was not observed in these crystals.



Fig. 1. Electron micrograph of the *n*-butanol complex. These crystals show cracks along the direction of the longer side of the rectangular lamellae. Detailed aspects of the cracks also show the fibers pulled out perpendicular to the longer side.

This suggests that the crystals thicken by epitaxial growth oriented on the lower lamellae. Further, a single lamella can be crystallized from very dilute solution of concentration of about 0.005%. It is one of the most characteristic features that the crystals frequently show cracks only along the direction of the longer side of the rectangular lamellae (Fig. 1). These are associated with stress due to anisotropic shrinkage which occurs during the drying process of the wet complex to the monohydrated complex, as will be discussed later. Details of the cracks also show the presence of fibers pulled out perpendicular to the longer side. These fibers have the same appearance as those observed by Hirai et al.¹⁵ in torn polyethylene single crystals. An increase in concentration of the amylose solution favored the growth of the cross-shaped and rosette-shaped crystals which

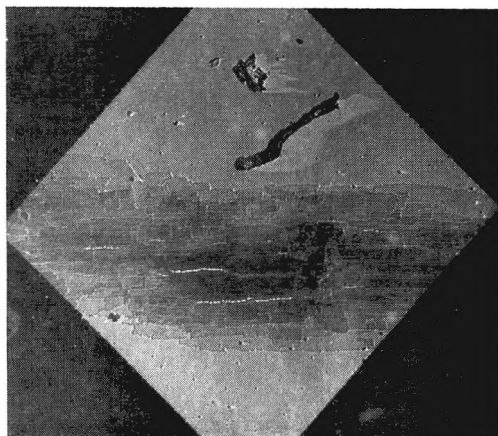
have been described by Manley as twinned crystals consisting of two or three platelets with a 60° angle of intersection.

Electron and X-Ray Diffraction Studies

A selected area electron diffraction pattern and a corresponding electron micrograph of the *n*-butanol complex dried in a desiccator for 8 hr. are shown in Figure 2, where their relative orientations have been corrected for rotation in the microscope. This pattern represents the $(hk0)$ reflections of the unit cell determined by Rundle et al.³ for the monohydrated complex. The reflection spots exist on three Debye-Scherrer rings with spacings of 11.9, 6.87, and 4.50 Å. The twelve spots of the outermost ring are indexed as $\{150\}$, $\{240\}$, $\{310\}$ for the orthorhombic unit cell. The next six spots and the innermost six spots are indexed as $\{200\}$, $\{130\}$ and



(a)



(b)

Fig. 2. *n*-Butanol complex: (a) selected area electron diffraction pattern and (b) a corresponding electron micrograph.

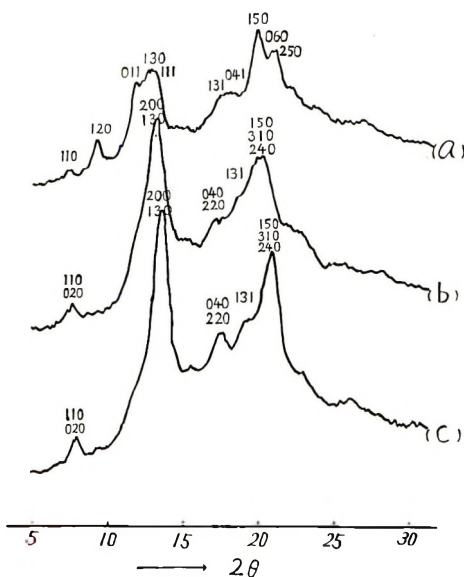


Fig. 3. X-ray diffraction curves of the powder samples of the *n*-butanol complex in various drying states: (a) wet samples dripping saturated *n*-butanol solution; (b) samples dried in a desiccator for 24 hr.; (c) samples dried *in vacuo* at 100°C. for 8 hr.

$\{110\}$, $\{020\}$, respectively. Because the pattern has a hexagonal symmetry in point of spacings and intensities, it seems to be more reasonable that three spacings should be indexed as $\{200\}$, $\{220\}$ and $\{420\}$ for a hexagonal unit cell with $a = 27.4$ Å. and $c = 8.05$ Å. This has been suggested as another possible unit cell by Rundle et al.³ This large unit cell contains four helices. Also, the $\{400\}$ and $\{600\}$ spots, corresponding to $\{220\}$, $\{040\}$ and $\{330\}$, $\{060\}$, respectively, for the orthorhombic unit cell, can be seen on the original plates. The helix diameter calculated from the above spacings was 13.8 Å.

We can not determine the plane corresponding to the longer side of the rectangular crystals from the correlation of the selected area electron diffraction pattern and electron micrograph. The difficulty arises from the fact that there is no difference in the $\{200\}$ and $\{130\}$ spacings of the orthorhombic unit cell, which have identical d values because of hexagonal nature. It seems reasonable, however, to assume that the a axis, and not the b axis as reported by Manley, corresponds to the longer side, as will be discussed later.

It was also found that the electron diffraction pattern from the specimen dried thoroughly at 100°C. *in vacuo* for 8 hr. shows a decrease in the spacings, and the helix diameter calculated from it is 13.2 Å. At present it is reasonable to assume that the two values obtained in different conditions of drying correspond to those of the monohydrated complex and the anhydrous complex determined by Rundle et al.⁵

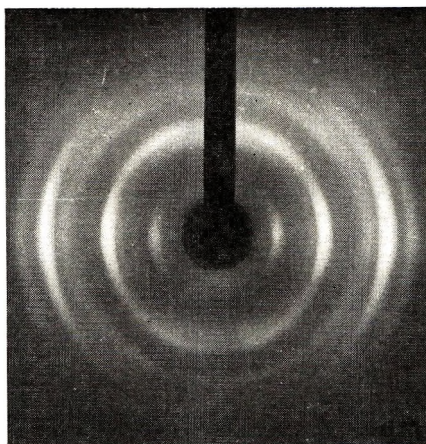


Fig. 4. X-ray diffraction photograph obtained from the film of the sedimented lamellar crystals. The x-ray beam was directed parallel to the film surface which was oriented along the equator.



Fig. 5. Low-angle x-ray diffraction curve obtained on the film with the beam parallel to the film surface.

X-ray powder patterns were obtained for samples dried under various conditions. X-ray diffraction curves for the wet samples dripping the saturated *n*-butanol solution are shown in Figure 3*a*. The diffraction curve does not indicate hexagonal symmetry. Figures 3*b* and 3*c* show curves obtained from the samples dried in a desiccator for 24 hr. and *in vacuo* at 100°C. for 8 hr., respectively. The helix diameters calculated from these x-ray patterns are 13.7 and 13.0 Å.

In order to obtain a film with basal planes of lamellar crystals parallel to the film surface, the crystal suspension was filtered carefully. When the x-ray beam was directed parallel to the film surface, the diffraction pattern showed preferential orientation, as shown in Figure 4. This result is consistent with Manley's and shows that the helices are oriented perpendicular to the lamellar surface. The low-angle x-ray diffraction curve in Figure 5 was obtained on the same specimen with the beam parallel to the film surface. The long spacing calculated by assuming the Bragg equation to be valid here is 98 Å. This value agrees with the thickness estimated from electron micrographs, but is inconsistent with that of 75 Å, which has led Manley to suggest an invariance of fold period with temperature of crystallization. However, it should be noticed that the concentration of amylose in our crystallization experiment was about 0.05%, much lower than Manley's.

DISCUSSION

Manley¹³ has postulated two interpretations for electron diffraction patterns such as those we have obtained from lamellar crystals identified with the anhydrous complex. The first interpretation, which was considered more probable, is based on the superposition of the diffraction patterns of three single orthorhombic lattices. Then it has been suggested that a rectangular lamella contains elements of repeated microtwinning. The second interpretation is based on the fact that the spacings and intensities of the $\{110\}$ and $\{020\}$; $\{200\}$ and $\{130\}$; and $\{150\}$, $\{240\}$, and $\{310\}$ points, respectively, are equal because of the pseudo-hexagonal nature of the anhydrous complex. We chose the second interpretation rather than the first, for the following reasons. There exists no evidence in morphological observations that single platelets grow by a mechanism involving repeated microtwinning. On the contrary, the fact that the cracks of single platelets always exist in the direction of the longer side lead us to conclude that the rectangular platelets are single crystals. Further, the reason why a lower symmetrical pattern having only the $\{110\}$, $\{200\}$, and $\{150\}$ spots is envisaged, in spite of the steadily evolved concept of the closed packed helices for anhydrous V complex, can not be understood. Finally, we will suggest that two similar patterns which were obtained from the specimens dried at different conditions can be explained unambiguously as the appearance of the $\{110\}$ and $\{020\}$; $\{200\}$ and $\{130\}$; and $\{150\}$, $\{240\}$, and $\{310\}$ points in the zero layer of the reciprocal lattice of the two orthorhombic unit cells which have been determined by Rundle et al.⁵ for the monohydrated and anhydrous complexes, respectively. Furthermore, the hexagonal features in the spacings and intensities indicate that the hexagonal unit cell may be more real than the orthorhombic in both cases.

We consider the question of the helix diameters of the amylose V complexes. It was mentioned earlier that the values of 13.8 and 13.2 Å, correspond to the monohydrated complex and the anhydrous complex helix

diameters, respectively. Such identification raises possibly objections: (1) these values differ a little from those of 13.7 and 13.0 Å. obtained by our x-ray powder patterns, and (2) the crystals bind the water tightly enough in the unheated specimens that they do not lose the water in the microscope vacuum. The former may probably be an effect¹⁶ of the beam on the spacings while the crystal is in the microscope. We do not have a clear answer to the latter but we notice that Germino et al. report¹⁷ a substantially anhydrous methyl ethyl ketone complex which has a helix diameter of 13.7 Å. Their result seems to suggest that the helix diameter of 13.7 Å. does not always depend on the presence or absence of water.

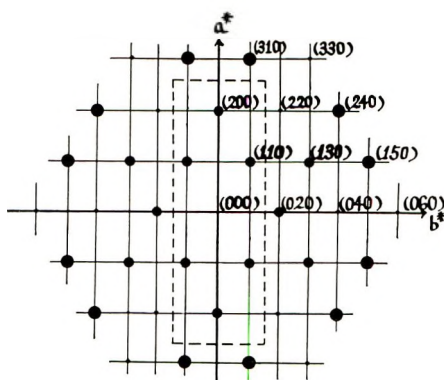


Fig. 6. Reflection spots of the electron diffraction and reciprocal lattice of (001) planes. Dots show observed reflections, the dotted lines show the outline of a single crystal.

We consider next the question of the shape of the crystals. The hexagonal symmetry of the unit cell in the basal plane obtained from the electron diffraction pattern would lead us to expect that the crystals may have a rhombic or hexagonal habit, but the real crystal has an apparent rectangular habit. This suggests that the crystal structure does not have hexagonal symmetry at the time when the lamellar crystals are formed in the supercooled solutions. This suggestion is supported by the fact that the x-ray curves of Figure 3a are inconsistent with a hexagonal structure but can be accounted for satisfactorily by an orthorhombic unit cell obtained by modifying slightly the unit cell found for the monohydrated complex: keeping a constant, increasing b by about 1.8 Å., and decreasing c by 0.25 Å. The unit cell dimensions thus obtained are $a = 13.7$ Å., $b = 25.6$ Å., and $c = 7.8$ Å.; these values are the same as those obtained by Rundle et al. for the wet *n*-butanol complex. Electron diffraction studies did not show the unit cell for the wet complex, because this state of the crystals was unstable under vacuum. However, we can conclude that the unit cell, with b lattice constant larger than that of the monohydrated complex, exists in the original crystals before drying.

If the crystal structure of the wet complex is changed to that of the monohydrated complex during drying, the value of a is unchanged, but that of b is decreased by a very large value of 1.8 Å. This should lead to an anisotropic shrinkage of the crystals and cause cracks on the lamella parallel to the longer side, as shown in Figure 1. In this way the direction of cracks on the lamella can be explained when the a axis is assigned as shown schematically in Figure 6.

It is now necessary to consider the mode of chain packing in the lamellar crystal. According to the work of Rundle et al., two helices contained in the unit cell of the wet complex are directed in opposite directions. On the basis of these facts, the mode of chain packing can be discussed. Consider the projection of a crystal on the (001) plane shown in Figure 7 in which the

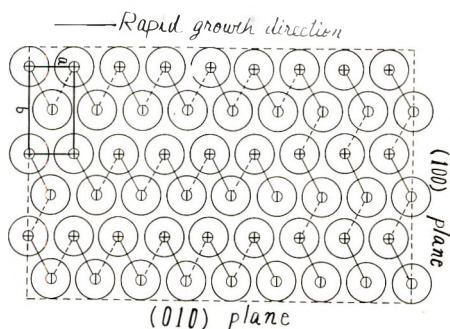


Fig. 7. Folding structure of chain molecules in lamellar crystals. The helices represented by circles are normal to the plane of the figure and the outline of a single crystal is represented by dotted lines. The directions of the chain (upward and downward) are designated by the symbols $+$ and $-$, respectively.

external form of the crystal is represented by dotted lines. The chain direction of upward and downward are designated by the symbols $+$ and $-$, respectively. As the folding must be formed between antiparallel chains, the chains should be connected by a fold between the corner and the center in the unit cell and the fold plane should be parallel to the (110) plane. Thus we have the folding structure as shown in Figure 7 which differs from Manley's.¹³

We can explain the twinning of the crystals based on our folding structure. Although the apparent growing faces are (100) and (010) planes, the growth rate in the (100) plane is faster than that in the (010) plane. On the other hand, the (130) plane is very similar to the (100) plane in respect of the intermolecular distance. Thus the molecule can deposit on the (130) plane as easily as on the (100) in the growing crystals and a twin can be formed.

The author would like to thank Prof. Nishio Hirai of the faculty of Science, Okayama University, for his many interesting and constructive suggestions and guidances throughout the investigation. The author also wishes to thank Mr. T. Yasui and Mr. S. Fujita for significant contributions to this work.

References

1. Rundle, R. E., I. Daasch, and D. French, *J. Am. Chem. Soc.*, **86**, 130 (1944).
2. Rundle, R. E., and D. French, *J. Am. Chem. Soc.*, **65**, 1707 (1943).
3. Rundle, R. E., and F. C. Edwards, *J. Am. Chem. Soc.*, **65**, 2200 (1943).
4. Bear, R., *J. Am. Chem. Soc.*, **66**, 2122 (1944).
5. Rundle, R. E., *J. Am. Chem. Soc.*, **69**, 1769 (1947).
6. Kerr, R. W., and G. M. Severson, *J. Am. Chem. Soc.*, **65**, 193 (1943).
7. Schoch, T. J., *J. Am. Chem. Soc.*, **64**, 2957 (1942).
8. Till, P. H., *J. Polymer Sci.*, **24**, 301 (1957).
9. Keller, A., *Phil. Mag.*, [8] **2**, 1171 (1957).
10. Fischer, E. W., *Z. Naturforsch.*, **12a**, 753 (1957).
11. Hirai, N., T. Yasui, S. Fujita, and Y. Yamashita, *Kobunshi Kagaku*, **20**, 413 (1963).
12. Yamashita, Y., *Kobunshi Kagaku*, **21**, 103 (1964).
13. Manley, R. St.-J., *J. Polymer Sci.*, **A2**, 4503 (1964).
14. Cowie, J. M. G., and C. T. Greenwood, *J. Chem. Soc.*, **1957**, 2862.
15. Hirai, N., H. Kiso, and T. Yasui, *J. Polymer Sci.*, **61**, S1 (1962).
16. Kobayashi, K., and T. Nagasawa, paper presented at annual meeting, Society for Polymer Science (Japan), Tokyo, June 1964.
17. Germino, F. J., R. J. Moshy, and R. M. Valletta, *J. Polymer Sci.*, **A2**, 2705 (1964).

Résumé

Dans cet article nos résultats précédents et ceux de Manley concernant les monocristaux de complexes d'amylose V sont confirmés. On propose une interprétation raisonnable des diagrammes de diffraction électronique à partir de cristaux lamellaires des complexes monohydratés et des complexes anhydres. En plus, on peut conclure que la longueur des lamelles rectangulaires correspond à l'axe a de la cellule unitaire du complexe hydraté, et que la structure du cristal n'a pas de symétrie hexagonale au moment où les cristaux lamellaires sont formés dans la solution surgelée. On décrit et discute de l'arrangement spatial des chaînes dans les monocristaux.

Zusammenfassung

In der vorliegenden Mitteilung werden unsere Ergebnisse sowie diejenigen von Manley für Einkristalle der Amylose-V-Komplexe bestätigt. Eine Interpretation der Elektronenbeugungsdiagramme lamellarer Kristalle des Monohydratkomplexes und des wasserfreien Komplexes wird gegeben. Weiters kommt man zu dem Schluss, dass die längere Seite der rechteckigen Lamellen der a -Achse der Elementarzelle des feuchten Komplexes entspricht und dass die Kristallstruktur zur Zeit der Bildung der lamellaren Kristalle in der unterkühlten Lösung keine hexagonale Symmetrie besitzt. Die Art der Kettenpackung in den Einkristallen wird beschrieben und diskutiert.

Received September 21, 1964

Revised February 17, 1965

Prod. No. 4712A

Oxonium Ion-Initiated Polymerization of Tetrahydrofuran

DAVID VOFSI* and ARTHUR V. TOBOLSKY, *Department of Chemistry, Princeton University, Princeton, New Jersey*

Synopsis

The kinetics of polymerization of tetrahydrofuran was studied, with the use of triethyloxonium tetrafluoroborate as initiator and dichloroethane as solvent. Conversion versus time and degree of polymerization versus time were measured at 0°C. at various monomer and initiator concentrations. The data were systematized by means of a kinetic equation, and the absolute rate constants for initiation and propagation were determined.

INTRODUCTION

The polymerization of tetrahydrofuran (THF) was first described by Meerwein¹ in 1939, who used as initiators trialkyloxonium salts.

In subsequent studies² it was shown that THF polymerization can be initiated by practically any catalyst (or catalyst-cocatalyst system) which is a strong generalized acid. More recently some very active catalysts were reported for this reaction. Muettterties and coauthors³ described the formation of extremely high molecular weight polymers by the action of PF_5 , while Saegusa et al.⁴ obtained similar polymers by the action of a trialkylaluminum- H_2O complex in the presence of a cocatalyst. The catalytic activity of trialkylaluminum-water complexes in ring-opening polymerizations of cyclic ethers was noted earlier by Colclough et al.⁵

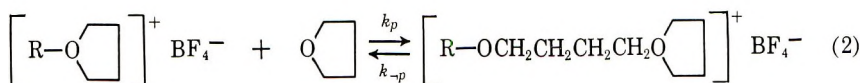
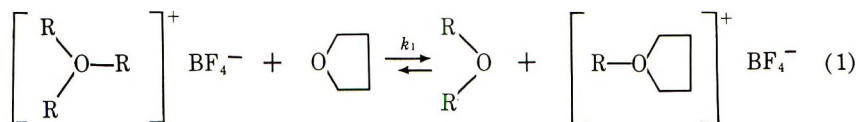
In all of these studies, it was mainly the synthetic aspect that was of interest to the various authors. Although it was recognized by Meerwein as a cationic type ring-opening equilibrium polymerization, kinetic studies of this reaction were not reported until recently.⁶⁻⁸ However, the catalyst systems chosen in these last studies probably involve rather complex initiation reactions, and the authors described mainly a kinetic pattern, rather than attempting a quantitative analysis of the various systems.

In the present work triethyloxonium tetrafluoroborate, $(\text{C}_2\text{H}_5)_3\text{O}^+\text{BF}_4^-$, was used as catalyst, and polymerization was carried out in a solution of dichloroethane. Furthermore, the catalyst was labeled with C^{14} , and this permitted the precise determination of molecular weights in the early stages of reaction.

* On leave from the Weizman Institute of Science, Rehovot, Israel.

The polymerization proceeds in the manner shown in eqs. (1) and (2).

Initiation:



The mechanism of chain growth, i.e., the structure of the active endgroup and the orientation of monomer during the act of addition, are not being discussed in the present work, so that eqs. (1) and (2) are to be regarded by way of a formal description only.

In these equations k_1 , k_p and k_{-p} are the specific rate constants of the initiation, the propagation, and depropagation reactions, respectively.

EXPERIMENTAL

Materials

Tetrahydrofuran. A Fisher Scientific Company product was refluxed over solid KOH for 48 hr., then distilled, the middle third being retained. This fraction was then refluxed over a potassium-sodium alloy until a green color developed upon addition of a trace of naphthalene. After removal of about one third by distillation, the middle fraction was made to condense in a number of ampules under a vacuum. The ampules were sealed off and stored until used. Four different batches thus prepared were used in the course of this work.

Dichloroethane. Dichloroethane (Matheson Coleman) was refluxed over calcium hydride for 48 hr. A procedure similar to the previous one was then followed, and a number of ampules were sealed and put to storage.

Preparation of Catalyst. Borontrifluoride etherate (Eastman Chemicals) was purified and made to react with epichlorohydrin (Aldrich) in an excess of ether, according to a procedure described by Meerwein et al.⁹ When the C¹⁴-labeled catalyst was prepared, about 150 mg. of C¹⁴-labeled diethyl ether (0.5 mC. activity, supplied by New England Nuclear) was added to the main portion of the ether. After filtration and washing with dry ether, the white crystals were dried in a vacuum at room temperature to remove traces of ether, and the crop was then transferred to a dry-box and distributed between several preweighed ampules. These were then taken to the vacuum line and sealed. The exact weight in each ampule was determined by difference.

The catalyst ampules were stored under liquid nitrogen until use. (Storage at room temperature results in darkening of the salt in a few weeks.)

The catalyst had an activity of 8.6×10^6 disintegrations/g./min.

Polymerization Procedure

The reaction was carried out in two compartment ampules (Fig. 1). The ampules were attached to the high vacuum line, and both compartments evacuated, flamed, and filled with pure dry nitrogen. With cocks closed, they were transferred to the dry-box and, after withdrawing the stopcock plug, they were filled in one compartment with a measured volume of THF. After closing the stopcocks, the ampules were removed from the dry-box, attached to the vacuum line, and after freezing the monomer, evacuated and sealed off at the constriction.

The same procedure was followed when filling the second compartment with catalyst solution. The catalyst solution was prepared in the dry-box by dissolving the contents of a catalyst ampule in dichloroethane. The proper amount was measured in by means of a syringe.

After temperature equilibrium had been attained in the thermostat, the ampule was vigorously shaken, the diaphragm broken, and the two components mixed instantaneously.

At specified intervals the ampules were withdrawn from the thermostat, quickly opened, and the reaction was stopped by injecting about 10 ml. of a 5% solution of diethylamine in dichloroethane. (This solution was

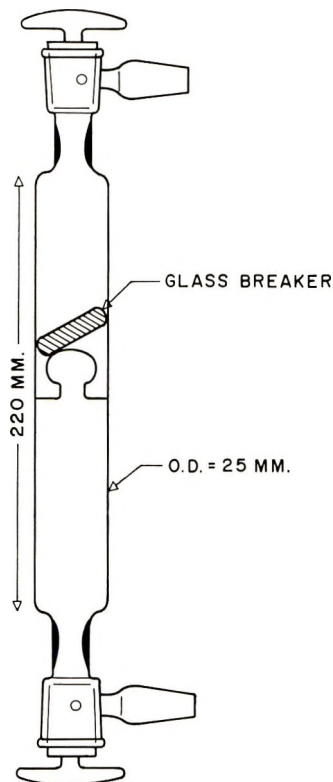


Fig. 1. Polymerization ampule.

always prepared a few minutes before use.) The opening, injecting, and mixing operations did take place within 1 min.

The polymer was isolated by liquid extraction. The contents of an ampule were poured into a separatory funnel, diluted with dichloroethane, and extracted with water to remove all water-soluble components. The extraction was repeated, and the final solution was transferred to a pre-weighed Claisen-type flask and evaporated at room temperature (water aspirator) until most solvent was removed. The flask with the residue was then transferred to a vacuum oven, and pumping (oil pump) was continued at 40°C. until constant weight was achieved. The yield was determined by weighing.

Equipment

Viscosities were measured in Ubbelohde viscometers. All measurements were made in benzene solution at 30°C.

Osmotic molecular weights were determined in a Mechrolab 301-A vapor pressure osmometer with benzene as solvent.

Endgroup analysis was carried out by means of a Chicago Nuclear liquid scintillation counter. The counting was done on samples of about 150 mg. polymer, and counting efficiencies determined by the channels ratio method. The average degree of polymerization was calculated according to:

$$DP = 1 + (190b - 188a)/72a$$

where $b = 1/3$ number of disintegrations per gram catalyst, and $a =$ number of disintegrations per gram polymer, per minute.

RESULTS AND DISCUSSION

Dependence of Rate of Polymerization on Catalyst Concentration

In Figure 2 are plotted the data of per cent monomer conversion versus time for five catalyst concentrations at 0°C.: run K, 6.1×10^{-2} mole/l. (1% of monomer concentration); run L, 3.05×10^{-2} mole/l. (0.5%); run M, 1.53×10^{-2} mole/l. (0.25%); run R, 0.61×10^{-2} mole/l. (0.1%); and run P, 0.31×10^{-2} mole/l. (0.05%). The monomer concentration throughout these experiments was 6.1 mole/l.

It is seen that in all cases an equilibrium conversion of 57–58% is reached.

In the experiments shown in Figure 2 there were used two different preparations of catalyst, and monomer as well as solvent were taken from four sets of ampules, each set involving a different batch of material.

Initial reaction rates versus initial catalyst concentrations are given in Table I and plotted in Figure 3.

While in the lower concentration range (up to about 2×10^{-2} mole/l.) linearity is observed with respect to catalyst concentration, a deviation of 10% from this relationship occurs already at a concentration of 3×10^{-2} mole/l. and is very marked at 6.1×10^{-2} mole/l.

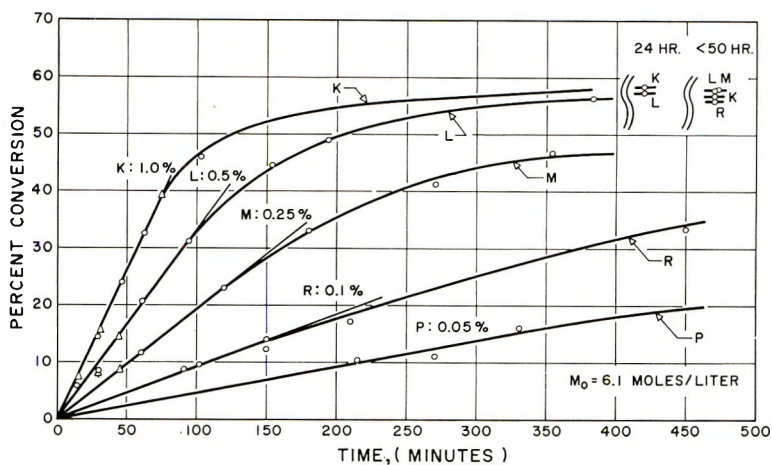


Fig. 2. Conversion vs. time plot. Letters and numbers designate run and percentage of catalyst to monomer. Triangles indicate duplicate runs.

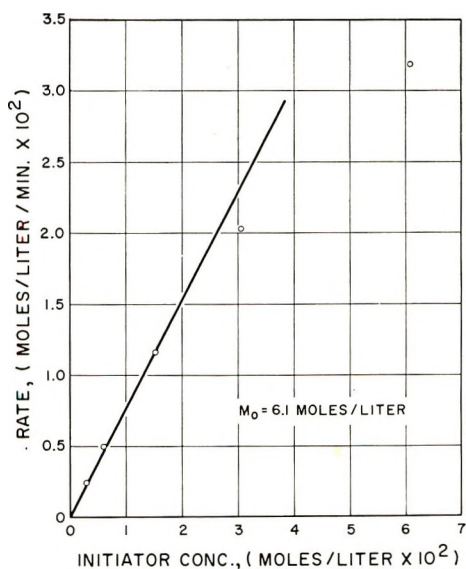


Fig. 3. Initial rate of polymerization vs. initial catalyst concentration.

TABLE I
Dependence of Initial Rate on Initial Catalyst Concentration $[I_0]$

Run	Rate, mole/l./min.	$[I_0]$, mole/l. $\times 10^2$
K	0.0319	6.10
L	0.0203	3.05
M	0.0116	1.53
R	0.0050	0.61
P	0.0025	0.31

The initiation step involves a nucleophilic displacement on the oxonium cation and would depend on the activity or concentration of this cation. This may be quite different from the overall catalyst concentration in the low dielectric medium under consideration. To elucidate the above deviation, conductivity measurements on catalyst solutions would be helpful.*

Rate Dependence on Initial Monomer Concentration

These data are given in Table II and shown in Figure 4. Catalyst concentration throughout these experiments was 0.61×10^{-2} mole/l., while initial monomer concentration varied from 3 to 9 mole/l. It follows from

TABLE II
Dependence of Initial Rate on Initial Monomer Concentration

Run	Rate, mole/l./min.	$[M_0]$, mole/l.
T1, T2	0.00930	9.15
S5, T5	0.00820	8.00
T6, T7	0.00680	7.00
R, S7	0.00500	6.10
T3	0.00350	5.00
S1, S2	0.00170	4.06
T4	0.00037	3.05

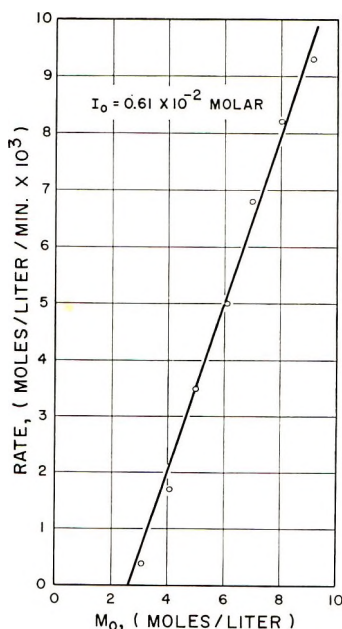


Fig. 4. Initial rate of polymerization vs. initial monomer concentration.

* The assumption that a simple Ostwald dilution law is operative failed to produce a constant of equilibrium when α was assumed to be given by the ratio actual rate/expected rate.

these data that a first-power dependence of the rate on monomer concentration is observed in the range of monomer concentrations covered.

The straight line extrapolates to a monomer concentration of 2.6 mole/l., which is the equilibrium concentration of monomer at 0°C. It is possible that the position of the first two points on this graph (for the lowest monomer concentrations) reflect a deviation from the straight line for reasons given below.

Rate of Initiator Consumption

The rate of initiator disappearance is given by

$$d[I]/dt = k_1 [I] ([M] - [M_{eq}]) \quad (3)$$

Equation (3) appears reasonable since we do not expect initiator to disappear when $[M] = [M_{eq}]$. Equation (3) is also justified by the experimental facts and will be shown in this section. From eq. (3) the following relations are obtained by integration.

$$2.3 \log [I_0]/[I] = k_1 \int_0^t ([M] - [M_{eq}]) dt \quad (4)$$

and

$$k_1 = \frac{2.3 \log ([I_0]/[I])}{\int_0^t ([M] - [M_{eq}]) dt} \quad (5)$$

In Table III are given data of activity measurements for a set of polymer samples from a single run ($[M_0] = 6.1$ mole/l. $[I_0] = 3.05 \times 10^{-2}$ mole/l., temperature = 0°C.). In column 5 is given the number of counts per gram polymer calculated with the assumption that all catalyst reacted, while in column 6 are listed the actual counts per gram per minute. Mon-

TABLE III
Rate of Catalyst Disappearance at $[M_0] = 6.1$ mole/l., $[I_0] = 3.05 \times 10^{-2}$ mole/l.

Run ^a	Wt. catalyst, g.	Wt. polymer, g.	Total Counts/g. polymer			Time, min.	Monomer conversion, %	Catalyst conversion, %
			/min. (calc.) $\times 10^{-5}$	/min. (calc.) $\times 10^{-5}$	Counts/g. polymer (found) $\times 10^{-5}$			
L1	0.174	1.12	5	4.46	3.41	30	8.5	76.5
P3	0.174	1.07	5	4.66	3.57	30	8.1	77
P4	0.116	1.27	3.3	2.60	2.37	45	14.4	91
L2	0.174	2.75	5	1.82	1.75	61	20.7	95
L3	0.174	4.08	5	1.22	1.18	94	31.0	97
L4	0.116	3.89	3.3	0.86	0.86	157	44.3	100
L5	0.116	4.30	3.3	0.78	0.80	194	49.0	100
L6	0.116	4.98	3.3	0.67	0.69	383	56.5	100

^a P and L are two different experiments run under an identical set of conditions.

omer and catalyst conversions are given in columns 8 and 9, respectively. It will be noted that when monomer was converted to the extent of about 15%, the conversion of catalyst was over 90%. In the absence of chain transfer reactions, this should lead to a sharp polymer distribution.

In Table IV are summarized the values of k_1 , calculated according to eq. (5) from three runs, with initial catalyst concentration of 6.1×10^{-2} , 3.05×10^{-2} , and 1.53×10^{-2} mole/l., and $[M_0]$ of 6.1 mole/l. The integrals were evaluated graphically.

TABLE IV
Calculation of k_1^a

Run	$[I_0]$, mole/l. $\times 10^2$	Time t , min.	$k_1 \times 10^2$
P3	3.05	30	1.56
L1	3.05	30	1.52
P4	3.05	45	1.64
L2	3.05	61	1.95
L3	3.05	94	1.52
P2	1.53	45	1.75
M1	1.53	60	1.51
K2	6.10	30	1.38
K3	6.10	47	1.32
K4	6.10	73	1.42

^a $k_1 = -2.3 \log [I]/[I_0] \int_0^t ([M] - [M_{eq}]) dt$, where $[M_{eq}] = 2.62$ mole/l., $[M_0] = 6.1$ mole/l.

DP-Viscosity Relationship

Degrees of polymerization were estimated by determination of C¹⁴-labeled endgroups assuming one third of original catalyst activity is incorporated in the polymer chain. To check this assumption, the DP of a number of polymer samples was determined by vapor pressure osmometry by use of the Mechrolab instrument. In the last two columns of Table V

TABLE V
Comparison of Osmotic \bar{M}_n with Endgroup Analysis

Run	Polymer concn., g./100 ml.	ΔR , (arbitrary units)	Endgroup concn., mole/ml. $\times 10^6$	\bar{M}_n	
				Osmotic	By end groups
M1	1.368	2.11	4.5	3040	3420
K2	1.719	5.27	11.2	1535	1280
K3	1.937	4.55	9.7	1997	1865
L1	1.878	5.60	12.0	1565	1405
L1	0.939	2.74	5.9	1590	1405
L2	2.517	4.54	9.7	2595	2795
L2	1.252	1.94	4.2	2990	2795

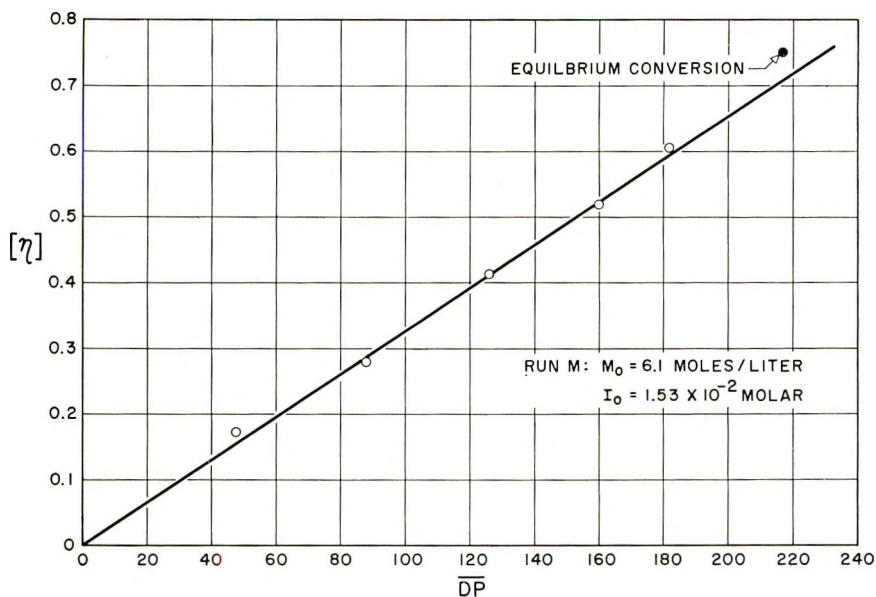


Fig. 5. Intrinsic viscosity vs. DP (from C^{14} analysis).

a comparison is given between the number-average molecular weights thus obtained.

The agreement is satisfactory, considering the rather low accuracy of the osmotic method. Inasmuch as intrinsic viscosity measures an average molecular weight which is close to a weight average, a change in the ratio of $[\eta]$ to DP would indicate a changing molecular weight distribution. When DP values calculated from endgroups were plotted against intrinsic viscosities at different degrees of conversion, a linear relationship between the two resulted in all cases up to conversions close to the equilibrium value. At these high conversions, however, the ratio of $[\eta]$ to DP showed an increase. This is perhaps to be expected. At low conversions

TABLE VI
Comparison of Intrinsic Viscosities and DP Values at Different Conversion Levels

Run	Conversion, %	Conversion % from eq. equilibrium conversion	DP ^a	$[\eta]$, dl./g ^b
M1	11.7	20.2	47.5	0.178
M2	23.0	39.5	87.5	0.280
M3	33.0	57.0	126	0.410
M4	41.3	71.0	160	0.520
M5	46.7	80.0	182	0.605
M6	58.0	100	217	0.750

^a From C^{14} activity measurements.

^b Determined at 30°C. in benzene solution.

the polymerization mechanism gives a Poisson distribution, with ratio of \bar{M}_w/\bar{M}_n close to unity. At equilibrium, however, the distribution of molecular weights must be random, with \bar{M}_w/\bar{M}_n close to 2.0.

In Table VI are given conversion, DP, and $[\eta]$ data from a single run ($[M_0] = 6.1$ mole/l., $[I_0] = 0.25$ mole-% of monomer, 0°C .), and a plot of (η) versus DP at different conversions is shown in Figure 5. Meerwein² suggested that transesterification is a possible mechanism at high conversions, and this would also tend to broaden the distribution.

Effect of Temperature

Figure 6 is an Arrhenius plot of the overall rate, measured at 0, 10, and 20°C . The activation energy is close to 10 kcal./base mole.

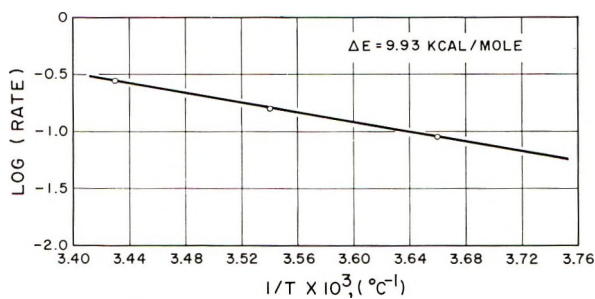


Fig. 6. Arrhenius plot of overall rate.

Equilibrium Conversion

The theory of equilibrium polymerization^{10,11} predicts an equilibrium concentration of monomer which is independent of initial monomer concentration, solvent concentration, or catalyst concentration. (This presumes that the thermodynamic activity of monomer is equal to its molar concentration.)

$$[M_{\text{eq}}] = 1/K_3 = k_p/k_{-p} \quad (6)$$

where K_3 is the equilibrium constant for the propagation reaction.

The conversion at equilibrium is given by

$$\text{Conversion} = ([M_0] - [M_{\text{eq}}])/[M_0] \quad (7)$$

We find that $[M_{\text{eq}}]$ is indeed a constant, namely 2.62 mole/l. at 0°C . provided that $[M_0]$ is larger than 5-6 mole/l. For lower values an apparent "equilibrium" conversion appears to be reached within our times of measurement. A comparison of experimental "equilibrium conversions" versus the calculated value from eq. (7) for $[M_{\text{eq}}] = 2.62$ mole/l. is shown in Table VII.

Above an initial monomer concentration of 5-6 mole/l., agreement between calculated and actual equilibrium conversions is within experimental error. At lower concentrations, however, a discrepancy shows up which is

TABLE VII
Comparison of Experimental and Calculated Equilibrium Conversions of Monomer

Run	[M ₀], mole/l.	Equilibrium conversion, %	
		Calculated	Found
S9	3.05	14	1.7
S8	4.06	35.5	22.7
N7	6.10	57.5	57.5
S10	8.00	67.5	70.4
--	12.20	78.0	75-77 ^a

^a These values were obtained by the present authors and by Dr. R. Bohme on polymerizing THF in bulk with a catalyst system made up of equimolar quantities of BF₃ etherate and various epoxides at 0°C.

very large at [M₀] = 3 mole/l. In all these experiments the catalyst concentration was 0.1 mole-% on monomer, and rates become exceedingly small when [M₀] is below about 5 mole/l. It is probable that under these conditions a slow termination reaction, caused by the collapse of the double ion end of the chain with elimination of BF₃ [eq. (8)] is gaining importance,



and a true equilibrium may not have been established within the time of these experiments (69 hr.). Although initial rates, when measured over a much shorter time interval, should be less influenced by this step, it may be that the low values of these rates, given in the last two rows of Table II (see also Fig. 4), are caused by some termination taking place. It is intended to check this assumption by fluorine endgroup analysis of these polymers. (It should be noted that BF₃ liberated in the termination step cannot catalyze polymerization of THF except at concentrations of about 10% of monomer.⁶)

CONCLUSION

The experimental data presented here seem to confirm the course of polymerization postulated by Meerwein in his early work on the polymerization of THF by oxonium salts.

For a "living" type polymerization,¹⁰ the rate of reaction is given by:

$$-dm/dt = k_1 [I] [M] + k_p ([I_0] - [I]) [M] \quad (9)$$

In the case of an equilibrium polymerization without termination, the validity of eq. (9) is maintained if [M] is replaced by ([M] - [M_{eq}]),

$$-dM/dt = k_1 [I] ([M] - [M_{eq}]) + k_p ([I_0] - [I]) ([M] - [M_{eq}]) \quad (10)$$

In view of the present data it seems safe to assume that within a monomer concentration range of 4-10 mole/l. and a catalyst concentration below 3.0×10^{-2} mole/l., the rate is closely approximated by:

$$-dM/dt = k_p [I_0] ([M] - [M_{eq}]) \quad (11)$$

or

$$2.3 \log \left\{ \frac{([M_0] - [M_{eq}])}{([M] - [M_{eq}])} \right\} / [I_0] = k_p t \quad (12)$$

A plot of eq. (12) is shown in Figure 7, from which a value of k_p of 0.290 l./mole-min. is deduced.

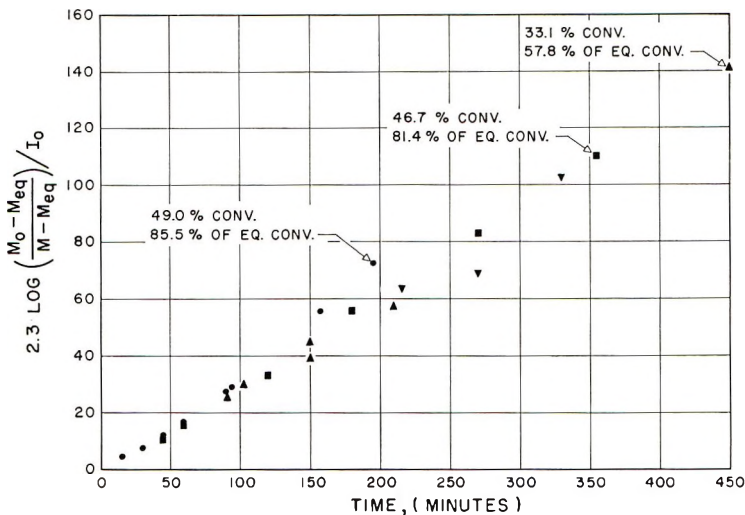


Fig. 7. Integrated form of conversion vs. time curves for runs L, M, R, and P (compare Fig. 2).

There is little doubt, however, that to cover a wider kinetic range, two constants, namely k_1 and k_p , are insufficient, and a termination term would have to be included to more fully describe the system.

Acknowledgments are due to Mr. Chubachi for assisting in the viscosity and osmotic measurements, to Miss Bamman for the help in measuring C^{14} activity, and to Dr. R. Bohme for aid with Table VI. The support of the AFOSR is greatly appreciated.

References

1. Meerwein, H., German Pat. 741,478 (1939).
2. Meerwein, H., D. Delfs, and H. Morschel, *Angew. Chem.*, **72**, 927 (1960).
3. Muettterties, E. L., T. A. Bither, M. W. Farlow, and D. D. Coffman, *J. Inorg. Nucl. Chem.*, **16**, 52 (1960).
4. Saegusa, T., H. Imai, and J. Furukawa, *Makromol. Chem.*, **65**, 60 (1963).
5. Colclough, R. O., G. Gee, and A. H. Jagger, *J. Polymer Sci.*, **48**, 273 (1960).
6. Burrows, R. C., and B. F. Crowe, *J. Appl. Polymer Sci.*, **6**, 465 (1962).
7. von Weissermel, K., and E. Nolken, *Makromol. Chem.*, **68**, 140 (1963).
8. Sims, D., *J. Chem. Soc.*, **1964**, 864.
9. Meerwein, H., E. Battenberg, H. Gold, E. Pfeil, and G. Willfang, *J. Prakt. Chem.*, **154**, 83 (1939).
10. Beste, L. F., and H. K. Hall, Jr., *J. Phys. Chem.*, **68**, 269 (1964).
11. Tobolsky, A. V., *J. Polymer Sci.*, **25**, 220 (1957).
12. Tobolsky, A. V., A. Rembaum, and A. Eisenberg, *J. Polymer Sci.*, **45**, 347 (1960).

Résumé

On a étudié les cinétiques de polymérisation du tétrahydrofurane en utilisant le triéthylxonium-tétrafluoroborate comme initiateur et le dichloroéthane comme solvant. On a mesuré à 0°C. la conversion en fonction du temps et le degré de polymérisation en fonction du temps, en employant différentes concentrations en monomère et en initiateur. Les résultats ont été systématisés au moyen d'une équation cinétique et on a déterminé les constantes absolues de vitesse pour l'initiation et la propagation.

Zusammenfassung

Die Kinetik der Tetrahydrofuranpolymerisation wurde mit Triäthylxoniumtetrafluorborat als Initiator und Dichloräthan als Lösungsmittel untersucht. Die Zeitabhängigkeit des Umsatzes und des Polymerisationsgrades wurde bei 0°C und verschiedenen Monomer- sowie Initiatorkonzentrationen gemessen. Die Ergebnisse wurden anhand einer kinetischen Gleichung in ein System gebracht und die absoluten Geschwindigkeitskonstanten für Start und Wachstum bestimmt.

Received December 3, 1964

Revised March 2, 1965

Prod. No. 4688A

Carborane Polymers. III. Vinyl Carboranes

JOSEPH GREEN, NATHAN MAYES, and MURRAY S. COHEN,
*Thiokol Chemical Corporation, Reaction Motors Division,
Denville, New Jersey*

Synopsis

Isopropenylcarborane could not be polymerized by conventional radical and ionic methods. A low molecular weight polymer of $\overline{DP} = 10$ was obtained by the use of aluminum chloride as catalyst at 150–170°C. Carboranymethyl acrylate was homopolymerized and copolymerized with fluoroacrylates by using benzoyl peroxide as catalyst. The T_g of the homopolymer was about 165°C. The difficulty in polymerizing the isopropenylcarborane and the high T_g value for carboranymethyl acrylate polymer have been partially attributed to the steric requirements of the carborane group.

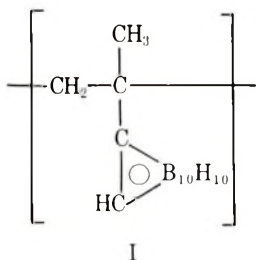
Introduction

In earlier papers¹⁻³ the size of the carborane nucleus based upon a model for its proposed structure was indicated as approximating a sphere with an effective van der Waals radius of 4 Å. The effect of such a large and bulky group on the ability of carborane vinyl compounds to polymerize and the resultant polymer properties were of interest. Two monomers were available for such a study, isopropenylcarborane and carboranymethyl acrylate. This paper discusses the polymerization studies with these two monomers.

Results

Attempts to polymerize isopropenylcarborane by conventional radical and ionic methods were unsuccessful. However, when the monomer was heated at 150–170°C. in the presence of 5% of aluminum chloride a benzene soluble solid was obtained. Precipitation from the benzene solution with heptane gave a 50% yield of a solid which did not melt below 300°C. The molecular weight of the product by vapor-phase osmometry in benzene was 1790 ($\overline{DP} = 10$). The infrared spectrum was consistent with the formation of polyisopropenylcarborane (I, as shown on following page).

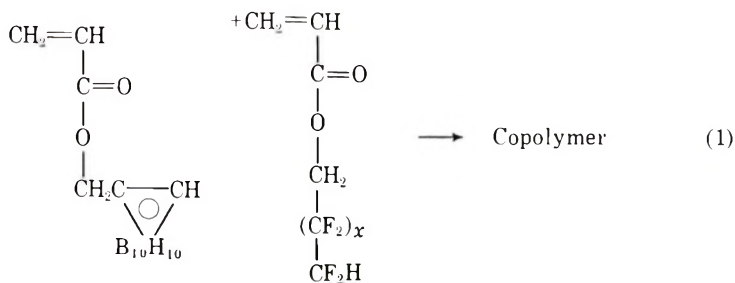
The use of catalytic quantities of di-*tert*-butyl peroxide at 150–160°C. did not yield any noticeable quantity of polyisopropenylcarborane. When large quantities of the peroxide (50% by weight) were used, a resinous solid was obtained. Molecular weight determinations indicated the product to be trimeric.



The copolymerization of isopropenylcarborane with methyl acrylate with azobisisobutyronitrile as catalyst was successful and acrylate-isopropenylcarborane copolymers, about 3:1, that contained up to 22% boron, were obtained. The concentration of boron in the polymer depended upon the concentration of isopropenylcarborane in the monomer feed. The polymers were glasslike materials that softened at 45–80°C. A polymer with a 10% boron content became rubbery at 45–50°C. and flowed above 80°C.

Carboranylmethyl acrylate was polymerized in bulk with the use of 2% benzoyl peroxide as the catalyst in evacuated sealed glass tubes heated at 60°C. with end-over-end agitation. The resulting hard, brittle solid dissolved only in boiling terphenyl. Precipitation of the polymer by the addition of heptane to the terphenyl solution yielded a powder which softened and became rubbery at about 165°C. and flowed at 270°C.

Carboranylmethyl acrylate was copolymerized with dodecafluoro heptyl acrylate and hexadecafluorononyl acrylate in bulk with benzoyl peroxide as catalyst [eq. (1)].



The physical properties of the polymers varied with composition, the brittleness and softening temperature increasing with carborane content. The fluoroacrylate homopolymers both were somewhat rubbery at room temperature. The introduction of an equimolar quantity of carboranyl methyl acrylate into the polymer resulted in stiffening of the polymer.

The C₉ fluoroalkyl acrylate and carboranylmethyl acrylate were copolymerized in acetone solution using azobisisobutyronitrile as catalyst. A high catalyst concentration, 2.1% based on monomer weights, was used to inhibit chain growth. The product was a tough, rubbery gum that could be dissolved in acetone, methyl ethyl ketone, or diethyl ketone. Infrared analysis showed no unsaturation and indicated 100% conversion. The

reaction was repeated and shown to be reproducible. Two reaction products of molecular weights 2170 and 3000, having densities of 1.503 and 1.497, respectively, were obtained.

Discussion

The high softening temperature of the carboranyl methyl acrylate polymer was predictable based upon experience with noncarboranyl acrylate polymers. As the chain length of the side chain is increased in a polyacrylate or polymethylacrylate the second-order transition temperature decreases. This is believed to be due to the influence of the side chain in increasing the free volume of the system, thereby increasing its mobility. Branching of the side chain, however, increases the volume required by a rotating segment, and may actually result in restriction of rotation about the carbon-carbon chain. For example, the polymer from *tert*-butyl methacrylate has a glass transition temperature of 104°C. as compared to 30°C. for *n*-butyl methacrylate.⁴ This effect is reported to be even more pronounced with cyclic groups such as cyclohexyl, and the polymers of cyclohexyl acrylate and methacrylate are considerably harder and have higher brittle points than the corresponding *n*-hexyl polymers.⁵ We have shown that a further increase in the bulk of the side chain by a methylcarboranyl group results in a polymer which softens at about 165°C.

The low molecular weights of the isopropenylcarborane polymer have been attributed to steric inhibition due to the bulk of the carborane group. Since this work was done it has been reported that 1-vinyl carborane, 1,2-methyl vinyl carborane, and 1,2-methyl isopropenylcarborane were polymerized in ether solution with the use of phenyllithium as the catalyst; isopropenylcarborane could not be homopolymerized but could be copolymerized.⁶ Molecular weights of 6,000–71,000 were reported.

This work was supported by the United States Air Force under Contract AF33(616)-5639.

References

1. Graftstein, D., and J. Dvorak, *J. Inorg. Chem.*, **2**, 1128 (1963).
2. Green, J., N. Mayes, and M. S. Cohen, *J. Polymer Sci.*, **A2**, 3113 (1964).
3. Green, J., N. Mayes, A. P. Kotloby, and M. S. Cohen, *J. Polymer Sci.*, **A2**, 3135 (1964).
4. Schildknecht, C. F., *Vinyl and Related Polymers*, Wiley, New York, 1952, p. 231.
5. Riddle, E. H., *Monomeric Acrylic Esters*, Reinhold, New York, 1954, p. 62.
6. Clark, S. L., and W. L. Taft, U. S. Pat. 3,093,687 (June 11, 1963).
7. Goldstein, H. L., and T. L. Heying, U. S. Pat. 3,109,031 (Oct. 29, 1963).

Résumé

L'isopropényl-carborane ne peut être polymérisé par les méthodes radicalaires et ioniques conventionnelles. On obtient un polymère de bas poids moléculaire de DP = 10 en utilisant le chlorure d'aluminium à 150–170° comme catalyseur. On homopolymérise et copolymérise le carboranyl-acrylate de méthyle avec les fluoroacrylates en em-

ployant le peroxyde de benzoyle comme catalyseur. Le T_g de l'homopolymère est d'environ 165°C. La difficulté de polymériser l'isopropényl carborane et la valeur élevée de T_g pour le polymère carboranyl acrylate de méthyle sont partiellement attribuées aux exigences stériques du groupe carborane.

Zusammenfassung

Isopropenylcarboran konnte nach den konventionellen radikalischen und ionischen Methoden nicht polymerisiert werden. Mit Aluminiumchlorid als Katalysator wurde bei 150–170° ein niedermolekulares Polymeres mit $\overline{DP} = 10$ erhalten. Carboranyl-methylacrylat wurde mit Fluoracrylaten unter Verwendung von Benzoylperoxyd als Katalysator homo- und kopolymerisiert. T_g des Homopolymeren lag etwa bei 165°C. Die Schwierigkeit, das Isopropenylcarboran zur Polymerisation zu bringen und der hohe T_g -Wert des Carboranymethylacrylatpolymeren wurden zum Teil den sterischen Bedingungen der Carborangruppe zugeschrieben.

Received March 9, 1965

Prod. No. 4704A

Critical Conditions for Formation of Infinite Networks in Branched-Chain Polymers

YOSHIO TANAKA and HIROSHI KAKIUCHI, *Department of Applied Chemistry, Faculty of Engineering, Yokohama National University, Yokohama, Japan*

Synopsis

The conditions necessary for infinite network formation due to the bifunctional interunit junction were reinvestigated, and the difference in theories between Flory and Case or Kahn was mentioned. The theory is extended to a more general case than those of Flory and of Case or Kahn. It also deals with the critical point in the condensation reaction between mixtures of two types of functional groups containing one or more functionalities. It is shown that at the critical point,

$$P_A P_B (1 - \rho_i)(1 - \sigma_i) \sum \rho_i (f_i - 1) \sum \sigma_i (g_i - 1) = 1$$

and/or

$$[1/(1 + r)] [r P_A \sum \sigma_i (g_i - 1) + P_B \sum \rho_i (f_i - 1)] = 1$$

where P_A and P_B are the respective probabilities that an A or B group has reacted, f_i and g_i are the functionalities of A_i and B_i monomers, r is the ratio of A groups to B groups at the initial state, and ρ_i , σ_i are the molar fractions of A_i and B_i , respectively.

Introduction

The theoretical treatment of the gel formation due to the bifunctional interunit junction has been established by Flory,¹ Stockmayer,² and many workers.³⁻⁹ Flory,^{1a} in discussing the condensation between two kinds of functional groups, limited his discussions to situations in which only one of the reactants ever had a functionality greater than 2. The extension to a condensation reaction between two types of functional groups in which each reacting group has a functionality greater than 2 has been treated by Stockmayer,^{2c} who calculated the molecular size distributions in branched-chain polymers by a method, different from Flory's, having the advantage of somewhat greater generality.

Recently, Kahn⁸ dealt with the critical conditions for the formation of infinite networks by the same calculating method as Case's⁷ and obtained the results coincident with Stockmayer's.^{2c} It is the purpose of this paper to reinvestigate the conditions necessary for infinite network formation due to the bifunctional interunit junction. In this paper the theory

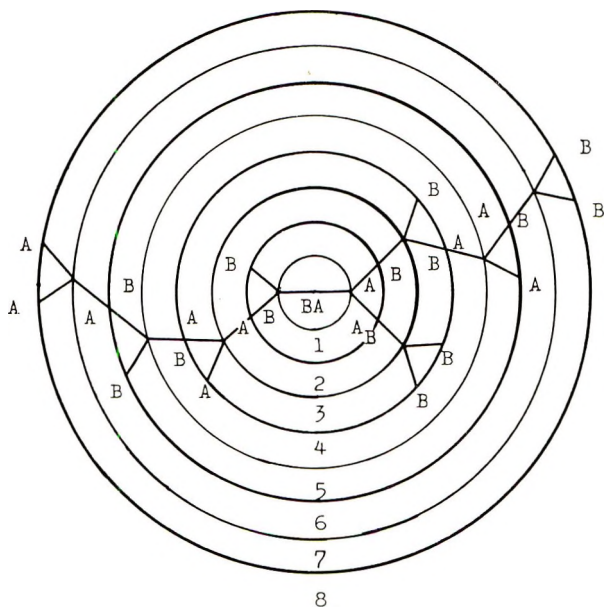


Fig. 1. Schematic representation of condensation between two trifunctional molecules

of the critical conditions for gelation is extended to a more general case than those¹⁻⁸ previously considered. It also deals with the condensation reaction between two types of functional groups in which each reacting group has a functionality greater than 1.

Symbols


The symbols used are as follows: A_i = A type monomer of functionality f_i ($i = 1, 2, \dots$); B_i = B-type monomer of functionality g_i ($i = 1, 2, \dots$); C_A = initial concentration of A groups; C_B = initial concentration of B groups; f_i = functionality of A-type monomer A_i ($i = 1, 2, \dots$); g_i = functionality of B-type monomer B_i ($i = 1, 2, \dots$); P = Case's propagation expectation (probability); P_A = probability or extent that an A group has reacted; P_B = probability or extent that a B group has reacted; p = fraction of A groups at circle 2 in Figure 1; q = fraction of B groups at circle 2 in Figure 1; r = ratio of A groups to B groups at the initial state; Y_i = number of branches or any reacting groups at circle i in Figure 1; Y_i' = number of any reacting groups except of monofunctional monomer at circle i in Figure 1; $Y_{i,A}$ = number of reacting A groups at circle i in Figure 1; $Y_{i,A}'$ = number of reacting A groups except of A_1 at circle i in Figure 1; $Y_{i,B}$ = number of reacting B groups at circle i in Figure 1; $Y_{i,B}'$ = number of reacting B groups except of B_1 at circle i in Figure 1; α = Flory's propagation expectation (probability); ρ_i = molar fraction of A-type monomer A_i with functionality f_i ($i = 1, \dots$); σ_i = molar fraction of B-type monomer B_i with functionality g_i ($i = 1, \dots$).

Critical Conditions of the Cases of Flory¹ and Case⁷ or Kahn⁸ for Gelation

It should be remarked at the outset that in the following presentation there are employed assumptions which also characterized the works of Flory,¹ Stockmayer,² and others³: (a) intramolecular reactions leading to cyclic structures are postulated not to occur; (b) at any stage during the reaction, all unreacted functional groups are considered to be equally reactive, regardless of the size of the molecule to which they are attached or of the fate of other functional groups on the same molecule.

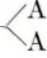
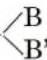
A possible course of reaction between a trifunctional A monomer and a trifunctional B monomer is given schematically in Figure 1. Suppose the chain within the first circle in Figure 1 has been selected at random from the polymer mixture. This chain gives rise to two branches, one at each end on circle 1. The four new chains extending from these branches lead to three branches on circle 3 and one terminal group. The resulting six chains on circle 4 lead to two branches on circle 5, etc. Then α is taken to be the probability, according to Flory,¹ that any given chain extending outward from one of the circles, $2i - 1$, ends in a branch on the circle $2i + 1$ ($i = 1, 2, \dots$) in Figure 1. In the simplest case of the system composed of identical monomeric units A, each carrying f (≥ 2) identical functional groups capable of reacting with each other, Flory^{1a} considered that the network may continue indefinitely, i.e., infinite networks are possible when $Y_{2i+1}/Y_{2i-1} \geq 1$, where Y_i are branches on the i th circles, and

$$Y_{2i+1} = \alpha[\sum \rho_i(f_i - 1)]Y_{2i-1}$$

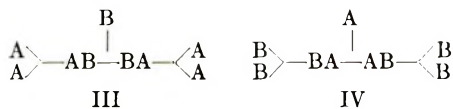
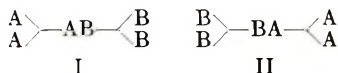
ρ_i is the molar fraction of monomer with functionality of f_i . On the other hand, Kahn⁸ concluded that for an infinite network to be possible, $Y_{2(i+2).B}/Y_{2i.B} \geq 1$ or $Y_{2(i+2).A}/Y_{2i.A} \geq 1$, where $Y_{i.A}$ and $Y_{i.B}$ are A and B groups at the i th circle. He also showed that, in the case of a system composed of A—A, A— and B—B, his result agreed with Flory's.

This coincidence can be explained clearly by Figure 1.

From Case's standpoint,⁷ if any given unit or structure in the chain has a mean expectation of 1 (or greater) of reappearing in the chain or branches of the chain which start at such a structure, then gelation will occur. Therefore, Kahn's calculation⁸ of the critical condition for gelation point has on the same theoretical basis as that of Case.⁷

The mean expectation of reappearance of the chain or branch, which Case⁷ called the propagation expectation, is not equivalent fundamentally to Flory's probability, α . A simple example of this criterion would be in the case of reaction between two types of functional groups in which each reacting group has a functionality greater than 3, such as A— and B—, where A and B can react only with each other.

The probability of Flory's α that any group belonging to a branch unit and selected at random is connected via a chain to another branch unit is obtained as follows. This state of affairs may come about in $2!_n C_1 \ m C_1$ ($n = m = 1$, in this case) = 2 possible ways for I and II:



Each case is equally valid for the purpose of evaluating α and has the individual probability of $P_A(g - 1)$ and $P_B(f - 1)$. The probability α is equal to the sum of the two individual probabilities of each of these two cases occurring in any selection taken at random, i.e., in this case,

$$P_A(g - 1) + P_B(f - 1) = 2(P_A + P_B)$$

Here f and g are 3.

However, from the point of view of Case⁷ and Kahn,⁸ the propagation expectation P that any given unit or structure in the chain selected at random reappears in the chain or branches of the chain which start at such a structure is obtained as follows. This state of affairs may not come about in the ways I and II, but as shown in III or IV, because of the definition^{7,8} of the partial propagation expectation. The propagation expectation P is obtained as

$$P = P_A P_B (f - 1)(g - 1)$$

for either III or IV. Both theories of Flory¹ and Case⁷ may coincide with each other when i is so large as discussed later, and for the reaction between two types of functional groups in which one reacting group has a functionality greater than 2 and the other has only a functionality of 2, as shown by Case⁷ and Kahn.⁸

Critical Condition for Gelation

Now the fundamental theory on which Kahn's⁸ treatment is based is extended as follows. For an infinite network to be possible, the relationship as shown by eq. (1) should be obtained.

$$Y_{2(i+j)} / Y_{2i} \geq 1 \quad i, j = 1, 2, \dots, \quad (1)$$

Flory's treatment would be the case of $i = 1/2, 3/2, \dots$, and $j = 1$, and Case's or Kahn's calculation would be the case of $i = 1, 2, \dots$, and $j = 2$, as shown in Figure 1.

Consider the reaction of an f -functional A monomer $\begin{array}{c} \diagdown \text{A} \diagup \\ \text{A} \end{array}$ with a g -functional B monomer $\begin{array}{c} \diagdown \text{B} \diagup \\ \text{B} \end{array}$. Here f and g are greater than 2. Let

the number of groups on circle 2 be Y_2 . In general, proportions p and q are A groups and B groups, respectively, at circle 2 ($p + q = 1$). Let P_A and P_B be probabilities, respectively, that an A and B group has reacted. There are $Y_{2.A}$ A groups and $Y_{2.B}$ B groups at circle 2, and there is a probability P_A or P_B that any particular A or B group has reacted, leading to $P_A(g - 1)$ or $P_B(f - 1)$ branches.

Therefore: we have, for the number of A and B groups, respectively, at circle 4,

$$\begin{aligned} Y_{4.A} &= qY_2P_B(f - 1) \\ Y_{4.B} &= pY_2P_A(g - 1) \end{aligned} \tag{2a}$$

Continuing in this way, the numbers of A and B groups at circles 6, 8, 10, . . . , are:

$$\begin{aligned} Y_{6.A} &= pY_2P_AP_B(f - 1)(g - 1) \\ Y_{8.A} &= qY_2P_AP_B(f - 1)(g - 1)P_B(f - 1) \\ Y_{10.A} &= pY_2[P_AP_B(f - 1)(g - 1)]^2 \\ &\vdots \\ &\vdots \end{aligned}$$

and

$$\begin{aligned} Y_{6.B} &= qY_2P_AP_B(f - 1)(g - 1) \\ Y_{7.B} &= pY_2P_AP_B(f - 1)(g - 1)P_A(g - 1) \\ Y_{10.B} &= qY_2[P_AP_B(f - 1)(g - 1)]^2 \\ &\vdots \\ &\vdots \end{aligned} \tag{2b}$$

Since

$$Y_i = Y_{i.A} + Y_{i.B} \tag{3}$$

then the numbers of A and B groups at circles 2, 4, 6, . . . , are obtained from eqs. (2) and (3):

$$\begin{aligned} Y_2 &= Y_2 \\ Y_4 &= Y_2Y_0 \\ Y_6 &= Y_2Y_1 \\ Y_8 &= Y_2Y_1Y_0 \\ Y_{10} &= Y_2(Y_1)^2 \\ Y_{12} &= Y_2(Y_1)^2Y_0 \\ &\vdots \\ &\vdots \end{aligned} \tag{4}$$

$$Y_{2(n+1)} = Y_2(Y_1) \left\{ -1 + \sum_0^n 1/2[1 - (-1)^{n+1}] \right\} (Y_0)^{1/2[1 - (-1)^n]} \\ n = 0, 1, 2, \dots$$

where,

$$\begin{aligned} Y_0 &= pP_A(g-1) + qP_B(f-1) \\ Y_1 &= P_AP_B(f-1)(g-1) \end{aligned} \quad (5)$$

Thus, the ratio of the reacting groups at circle $2(n+1)$ to those at circle 2 is generally:

$$Y_{2(n+1)}/Y_2 = Y_1 \left\{ -1 + \sum_0^n 1/2^{[1-(-1)^{n+1}]} \right\} Y_0^{1/2^{[1-(-1)^n]}} \quad (6)$$

Therefore, at the critical point or "gelation point" for the infinite network,

$$Y_1 \left\{ -1 + \sum_0^n 1/2^{[1-(-1)^{n+1}]} \right\} Y_0^{1/2^{[1-(-1)^n]}} = 1 \quad (7)$$

where Y_0 and Y_1 are expressed by eq. (5), and $n = 0, 1, 2, \dots$

Case's⁷ and Kahn's⁸ treatments are the cases of $Y_{6,A}/Y_{2,A}$ and $Y_{6,B}/Y_{2,B}$. Then eqs. (4) and (6) can be rewritten as;

$$\begin{aligned} Y_2/Y_2 &= 1 \\ Y_4/Y_2 &= Y_0 \\ Y_6/Y_2 &= Y_1 \\ Y_8/Y_2 &= (Y_6/Y_2)(Y_4/Y_2) \\ Y_{10}/Y_2 &= (Y_6/Y_2)^2 \\ Y_{12}/Y_2 &= (Y_6/Y_2)^2(Y_4/Y_2) \\ &\vdots \end{aligned} \quad (8)$$

$$Y_{2(n+1)}/Y_2 = (Y_6/Y_2) \left\{ -1 + \sum_0^n 1/2^{[1-(-1)^{n+1}]} \right\} (Y_4/Y_2)^{1/2^{[1-(-1)^n]}}$$

where $n = 0, 1, 2, \dots$. Now, if $Y_6/Y_2 \geq 1$, we have

$$Y_{4n+6}/Y_2 \geq \dots \geq Y_{14}/Y_2 \geq Y_{10}/Y_2 \geq Y_6/Y_2 \geq 1 \quad (9)$$

Equation (9) shows that Case's and Kahn's treatments^{7,8} are suitable for estimating the critical condition for the infinite network in some cases. If $Y_4/Y_2 \geq 1$ and $Y_6/Y_2 \geq 1$, we can have

$$Y_{2(n+1)}/Y_2 \geq \dots \geq Y_6/Y_2 \geq Y_4/Y_2 \geq 1 \quad (10)$$

Equation (10) shows the critical condition for the infinite network

$$Y_4/Y_2 = 1$$

and

$$Y_6/Y_2 = 1 \quad (11)$$

are satisfactory to estimate the gelation point in all cases. When $Y_4/Y_2 = 1$ only, the value of eq. (6) depends on $Y_4/Y_2 - Y_6/Y_2$, or $Y_0 - Y_1$.

Comparison of Y_0 with Y_1

In the case of

$$C_A = rC_B, \quad (12)$$

we can have eqs. (13) and (14):

$$rP_A = P_B \tag{13}$$

$$p = rq \tag{14}$$

Then, eqs. (15) can be derived:

$$p = r/(1 + r)$$

and

$$q = 1/(1 + r) \tag{15}$$

Let $Y_0 - Y_1$ be a function of r, F, G and P_A or P_B , shown by eqs. (16):

$$\phi = \phi(r, F, G, P_A) = Y_0 - Y_1 = Y_4/Y_2 - Y_6/Y_2 \tag{16a}$$

$$= r/(1 + r)P_A\phi'_A \quad \text{when } 0 \leq r \leq 1 \tag{16b}$$

$$= 1/(1 + r)P_B\phi'_B \quad \text{when } r \geq 1 \tag{16c}$$

where

$$F = f - 1$$

and

$$G = g - 1 \tag{17}$$

and ϕ'_A and ϕ'_B are the functions of r, F, G and P_A or P_B , shown by eq. (18).

$$\phi'_A = F + G - (1 + r)FGP_A \quad \text{when } 0 \leq r \leq 1 \tag{18a}$$

$$\phi'_B = F + G - (1 + r)/rFGP_B \quad \text{when } r \geq 1 \tag{18b}$$

Since r, P_A and $P_B \geq 0$, whether ϕ is plus or minus depends on the value of ϕ'_A or ϕ'_B , i.e., r, F , and G . In eq. (18), if

$$0 \leq r \leq (F + G - FG)/FG \leq 1$$

and

$$1 \leq FG/(F + G - FG) \leq r \tag{19}$$

we can obtain $\phi'_A, \phi'_B \geq 0$ at all P_A and P_B . The critical condition of r for

$$\phi'_A = \phi'_B = 0$$

or

$$\phi = 0 \tag{20}$$

can be expressed as

$$r = r(F) = 1/F - (G - 1)/G \quad \text{when } 0 \leq r \leq 1 \tag{21a}$$

$$r = r(F) = FG/(F + G - FG) \quad \text{when } 1 \leq r \tag{21b}$$

where $r(F)$ is a function of F ; if $1 \leq r$ and $1 < G$, eq. (21b) takes the form

$$r = G' - G'^2/(F - G') \tag{21c}$$

where $G' = G/(1 - G)$.

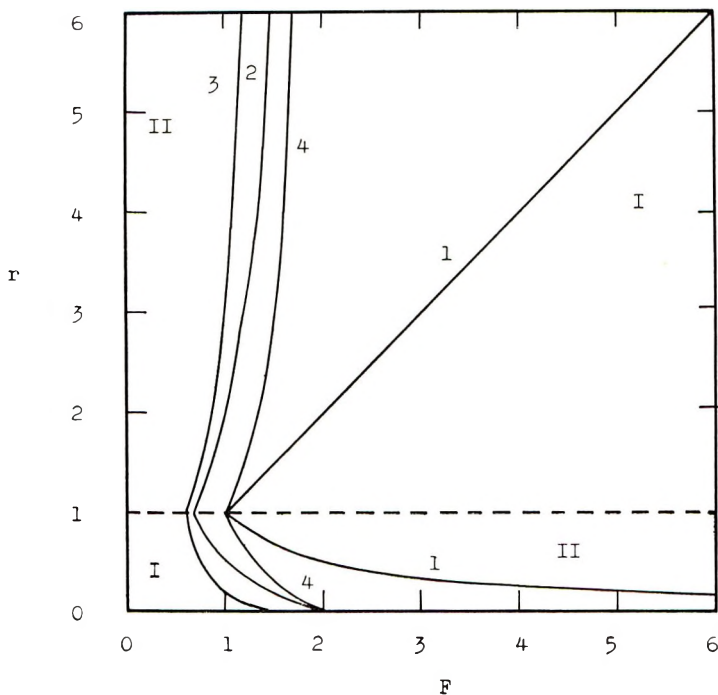


Fig. 2. Critical condition of r for $Y_0 - Y_1 = 0$ at all P_A or P_B [see eq. (21)]: (1) $G = 1$ (2) $G = 2$; (3) $G = 3$; (4) $F = G$.

When $G = 1, 2, 3, \dots$, the function of eq. (21) can be shown in Figure 2. If r is in region I of Figure 2, $\phi'_A \geq 0$ and $\phi'_B \geq 0$, i.e., $\phi \geq 0$, and if r is in region II, $\phi \leq 0$.

Consider the case of $F = G$; then eqs. (18) take the forms

$$\phi'_A = 2F\{1 - (1 + r)/2 \cdot P_A F\}$$

and

$$\phi'_B = 2F\{1 - (1 + r)/2r \cdot P_B F\}$$

If $1 \geq 2/F - 1 \geq r \geq 0$, and $r \geq F/(2 - F) \geq 1$, we have $\phi'_A \geq 0$ and $\phi'_B \geq 0$ at all P_A and P_B . Therefore, if $F = G = 1$, we obtain $\phi'_A \geq 0$ and $\phi'_B \geq 0$ at all P_A and P_B , and if $F = G \geq 2$, we can have $\phi'_A \leq 0$ and $\phi'_B \leq 0$

TABLE I
Comparison of Y_0 with Y_1

Case	r	P_A or P_B	ϕ'
$F = G$ $F = G > 3$	All	All	$\phi' < 0$
$F = G = 2$	"	"	$\phi' \leq 0$
$F = G = 1$	"	"	$\phi' \geq 0$
$FG = F \cong 1$	$r \geq F, r \leq 1/F$	"	$\phi' \geq 0$
$FG > 4$	All	"	$\phi' < 0$

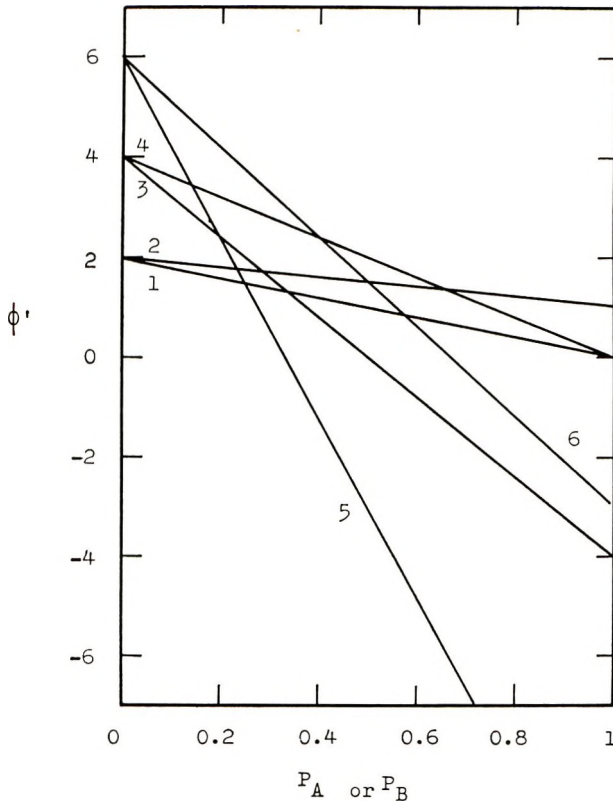


Fig. 3. Dependence of ϕ' on P_A or P_B when $F = G$ and r are constants: (1) $F = 1, r = 1$; (2) $F = 1, r = 0$ or ∞ ; (3) $F = 2, r = 1$; (4) $F = 2, r = 0$ or ∞ ; (5) $F = 3, r = 1$; (6) $F = 3, r = 0$ or ∞ .

at all r and at all P_A or P_B . These results are collected in Table I and the critical condition of r , shown by eq. (21), is shown in Figure 3.

In the case of $FG = F$, eqs. (18) take the forms:

$$\phi'_A = F + 1 - (1 + r)P_A F$$

and

$$\phi'_B = F + 1 - (1 + r)/r \cdot P_B F$$

If $r \leq 1/F$ and $r \geq F$, we can have $\phi'_A \geq 0$ and $\phi'_B \geq 0$ at all P_A and P_B , respectively. These are shown in Table I and in Figure 4, in which ϕ'_A or ϕ'_B is plotted against P_A or P_B in the cases of $FG = F = 2, 3, 4, \dots$

These results show that the relationship of eq. (22) is obtained when the condition of eq. (19) is maintained.

$$Y_4/Y_2 - Y_6/Y_2 \geq 0 \tag{22}$$

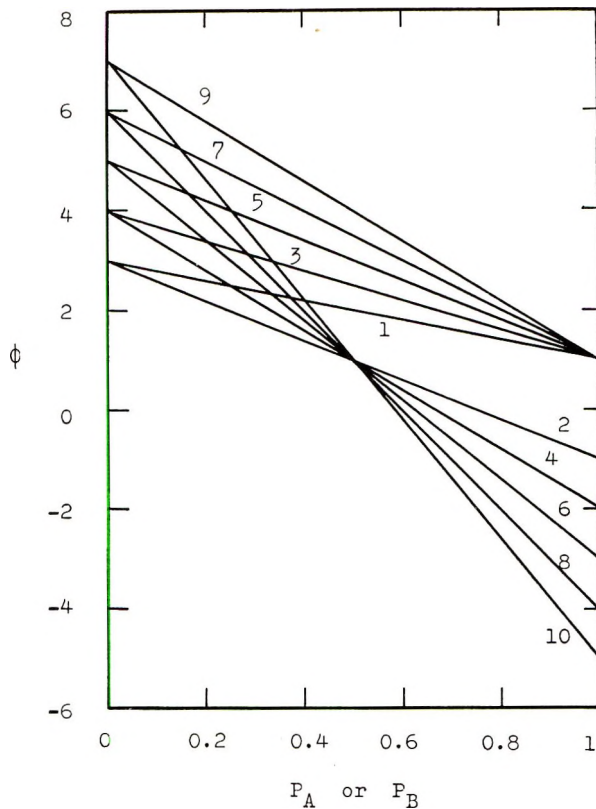


Fig. 4. Dependence of ϕ' on P_A or P_B in the case of $FG = F$ when r and F are constants: (1) $F = 2, r = 0$; (2) $F = 2, r = 1$; (3) $F = 3, r = 0$; (4) $F = 3, r = 1$; (5) $F = 4, r = 0$; (6) $F = 4, r = 1$; (7) $F = 5, r = 0$; (8) $F = 5, r = 1$; (9) $F = 6, r = 0$; (10) $F = 6, r = 1$.

Therefore, if $Y_6/Y_2 \geq 1$ and the condition of eq. (19) is kept, or if $Y_4/Y_2 \geq 1$ and the following relation, eqs. (23), is kept,

$$r \geq (F + G - FG)/FG$$

and

$$r \leq FG/(F + G - FG) \quad (23)$$

we can obtain the following relationship;

$$Y_{2(n+1)}/Y_2 \geq \dots \geq Y_8/Y_2 \geq Y_6/Y_2 \geq Y_4/Y_2 \geq 1 \quad (24)$$

Value of $(Y_0 - Y_1)$

In the case of $F = G$, eqs. (16b) and (16c) take the forms

$$\phi = r/(1+r) \cdot FP_A [2 - (1+r)FP_A] \quad \text{when } 0 \leq r \leq 1 \quad (25a)$$

$$\phi = 1/(1+r) \cdot FP_B [2 - (1+r)/r FP_B] \quad \text{when } 1 \leq r \quad (25b)$$

When r and F are constant, or r and P_A or P_B are constant, eqs. (25a) and (25b) take the forms:

$$\phi = -r(FP_A - 1/(1+r))^2 + r/(1+r)^2 \quad \text{when } 0 \leq r \leq 1 \quad (26a)$$

$$\phi = -1/r \cdot (FP_B - r/(1+r))^2 + r/(1+r)^2 \quad \text{when } 1 \leq r \quad (26b)$$

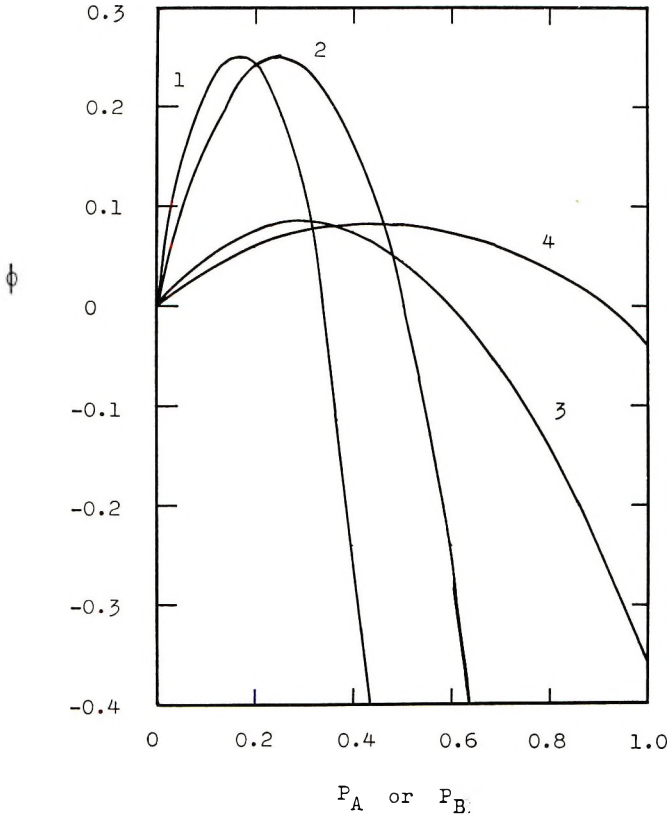


Fig. 5. Dependence of ϕ on P_A or P_B in the case of $F = G$ when F and r are constants [see eq. (26)]: (1) $F = 2, r = 1$; (2) $F = 3, r = 1$; (3) $F = 2, r = 10$ or 0.1 ; (4) $F = 3, r = 10$ or 0.1 .

These are shown in Figures 5 and 6, in the cases of $r = 0.1, 1,$ and $10,$ and P_A or $P_B = 1/2$ and $1.$ If F and P_A or P_B are constant, eqs. (25) can be rewritten as:

$$\phi = -r(FP_A)^2 + 2FP_A - 2FP_A/(1+r) \quad \text{when } 0 \leq r \leq 1 \quad (27a)$$

$$\phi = -(FP_B)^2/r + 2FP_B/(1+r) \quad \text{when } 1 \leq r \quad (27b)$$

Equations (27a) and (27b) are shown in Figure 7, for the case of $F = 2, 3,$ and P_A or $P_B = 1/2$ and $1,$ respectively.

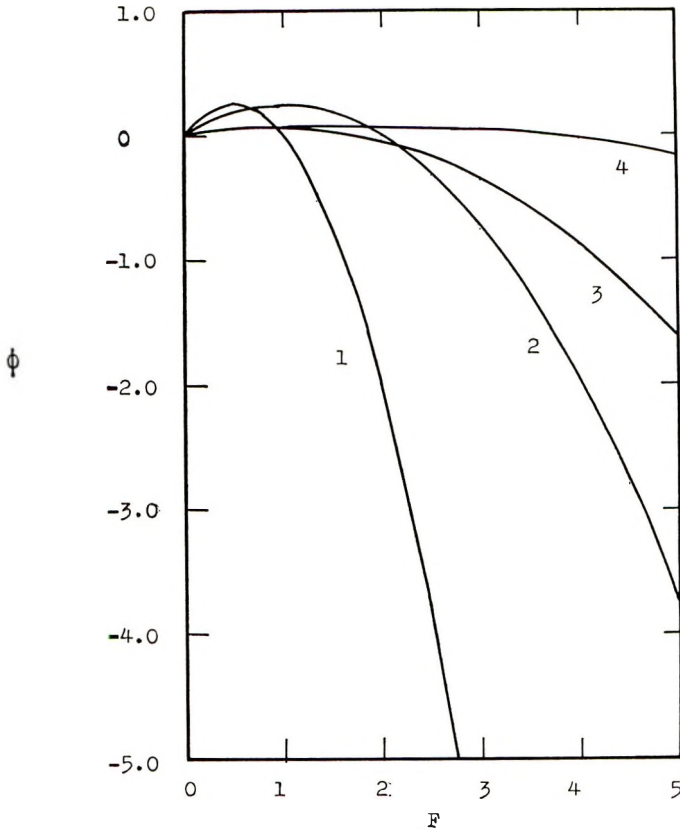


Fig. 6. Dependence of ϕ on F in the case of $F = G$ when P_A or P_B and r are constants [see eq. (26)]: (1) $r = 1, P_A = 1$; (2) $r = 1, P_A = 1/2$; (3) $r = 0.1, P_A = 1$ or $r = 10, P_B = 1$; (4) $r = 0.1, P_A = 1/2$ or $r = 10, P_B = 1/2$.

In the case of $FG = F$, eqs. (16a) and (16b) take the forms:

$$\phi = r/(1+r) \cdot P_A [F + 1 - (1+r)FP_A] \quad \text{when } 0 \leq r \leq 1 \quad (28a)$$

$$\phi = 1/(1+r) \cdot P_B [F + 1 - (1+r)/r \cdot FP_B] \quad \text{when } 1 \leq r \quad (28b)$$

When r and F are constant, we can rewrite eqs. (28) as:

$$\phi = -rF [P_A - (F+1)/2(1+r)F]^2 + (F+1)^2 r / [2(1+r)]^2 F \quad (29a)$$

$$\phi = -F/r \cdot [P_B - (F+1)r/2(1+r)F]^2 + (F+1)^2 r / [2(1+r)]^2 F \quad (29b)$$

Equations (29) are shown in Figure 8 for the cases of $r = 0.1, 1$, and 10 , and $F = 2$ and 3 . If r and P_A or P_B are constant, eqs. (28a) and (28b) can be rewritten as:

$$\phi = rP_A [1 - (1+r)P_A] / (1+r) \cdot F + rP_A / (1+r) \quad (30a)$$

$$\phi = [1 - (1+r)P_B/r] P_B / (1+r) \cdot F + P_B / (1+r) \quad (30b)$$

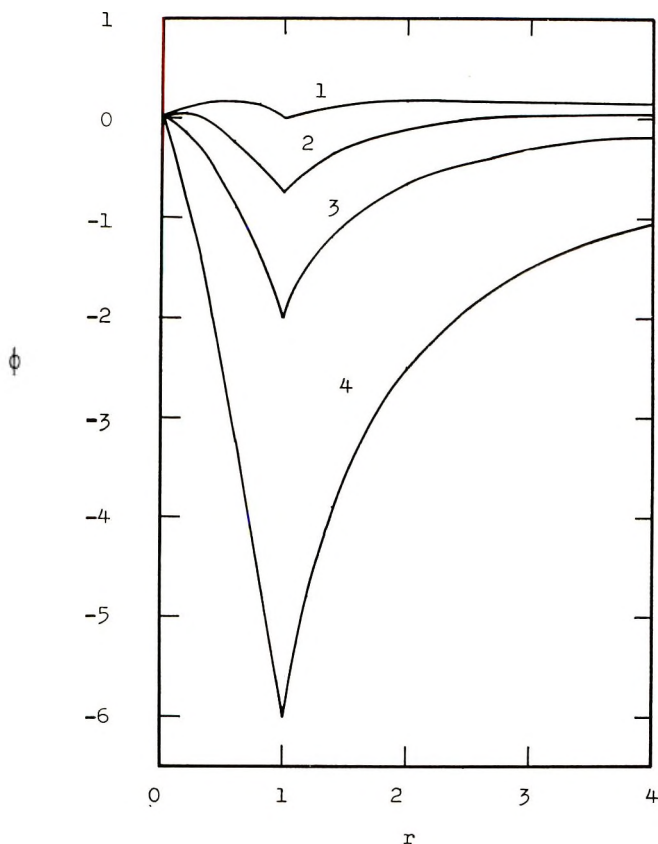


Fig. 7. Dependence of ϕ on r in the case of $F = G$ when F and P_A or P_B are constants [see eq. (27)]: (1) $F = 2$, $P_A = P_B = 1/2$; (2) $F = 3$, $P_A = P_B = 1/2$; (3) $F = 2$, $P_A = P_B = 1$; (4) $F = 3$, $P_A = P_B = 1$.

Equation (30) is shown in Figure 9 for the cases of $r = 0.1$, 1, and 10, and P_A or $P_B = 1/2$ and 1, respectively. When F and P_A or P_B are constant, eq. (28) can be rewritten as;

$$\phi = -P_A^2 F r + P_A(F + 1) - P_A(F + 1)/(1 + r) \quad (31a)$$

$$\phi = -P_B^2 F/r + P_B(F + 1)/(1 + r) \quad (31b)$$

and eqs. (31) are shown in Figure 10, in which the cases of $F = 2$ and 3, and P_A or $P_B = 1/2$ and 1 are treated, respectively.

Extension of Theory for Condensation of Mixtures of A Monomers of Varying Functionality with Mixtures of B Monomers of Varying Functionality

The analysis just presented may be extended to situations in which mixtures of A monomers of varying functionality react with mixtures of B monomers of varying functionality. The general system here treated

is defined by the statement that the original mixture of monomers consists of A_1, A_2, \dots, A_i monomers bearing respectively f_1, f_2, \dots, f_i , functional groups of type A each, mole fractions of which are $\rho_1, \rho_2, \dots, \rho_i$, together with $\sigma_1, \sigma_2, \dots, \sigma_i$, mole fractions of B_1, B_2, \dots, B_i , monomers of functionalities g_1, g_2, \dots, g_i , in groups of type B, where f_i and g_i are i -functional of type A and B, and A groups can react only with B groups and vice versa.

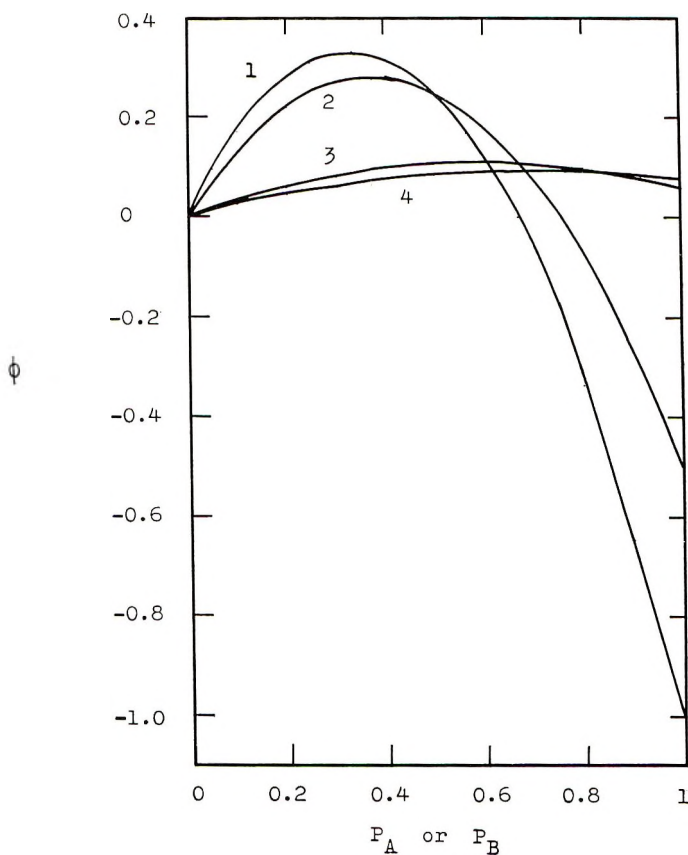


Fig. 8. Dependence of ϕ on P_A or P_B in the case of $FG = F$ when F and r are constants [see eq. (29)]: (1) $r = 1, F = 3$; (2) $r = 1, F = 2$; (3) $r = 10$ or $0.1, F = 3$; (4) $r = 10$ or $0.1, F = 2$.

It is assumed also that all functional groups of a given kind are equally reactive, and that ring formation does not occur in molecular species of finite size.

Referring to Figure 1 again, there are $pY_2(1 - \rho_1)$ of A groups, excepting A_1 , and $qY_2(1 - \sigma_1)$ of B groups, excepting B_1 , at circle 2. Numbers of A groups, except A_1 , that have reacted with B groups, except B_1 , at circle 2 are $pY_2(1 - \rho_1)(1 - \sigma_1)$, and numbers of B groups, except B_1 ,

that have reacted with A groups, except A₁, at circle 2 are $qY_2(1 - \rho_1)$ $(1 - \sigma_1)$, respectively. Equations (32a) and (32b) are defined as:

$$Y'_{2,A} = pY_2(1 - \rho_1)(1 - \sigma_1) \tag{32a}$$

$$Y'_{2,B} = qY_2(1 - \rho_1)(1 - \sigma_1) \tag{32b}$$

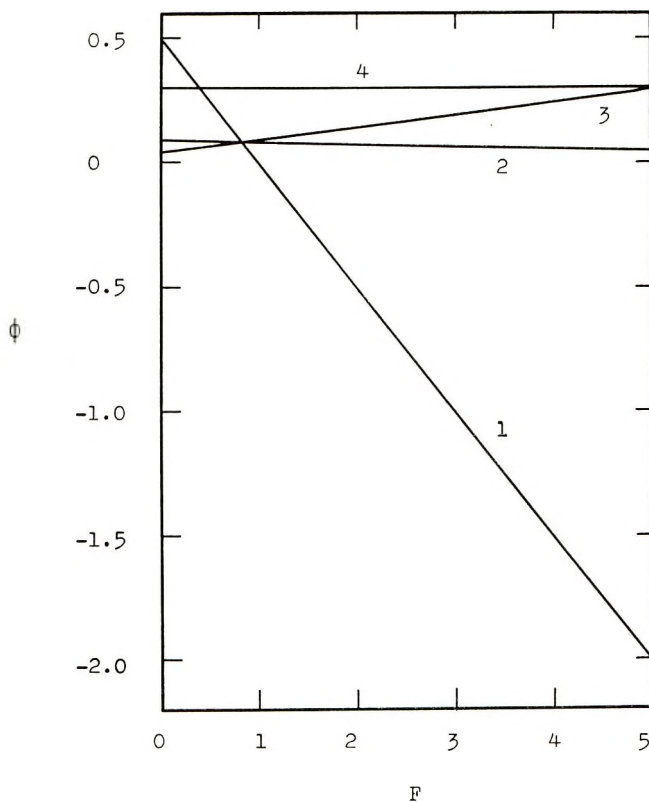


Fig. 9. Dependence of ϕ on F in the case of $FG = F$ when r and P_A or P_B are constants [see eq. (30)]: (1) $P_A = 1, r = 1$; (2) $P_A = 1, r = 0.1$ or $P_B = 1, r = 10$; (3) $P_A = 1/2, r = 1$; (4) $P_A = 1/2, r = 0.1$ or $P_B = 1/2, r = 10$.

With the above mixture of monomers, the numbers of A and B groups, except A₁ and B₁, at circle 4 are obtained as:

$$Y'_{4,A} = qY_2(1 - \rho_1)(1 - \sigma_1)P_B \sum^n \rho_i(f_i - 1) \tag{32c}$$

$$Y'_{4,B} = pY_2(1 - \rho_1)(1 - \sigma_1)P_A \sum^n \sigma_i(g_i - 1)$$

Continuing in this way, the numbers of A and B groups except for each monofunctional monomer, A₁ and B₁, at circles 6, 8, 10, are as follows:

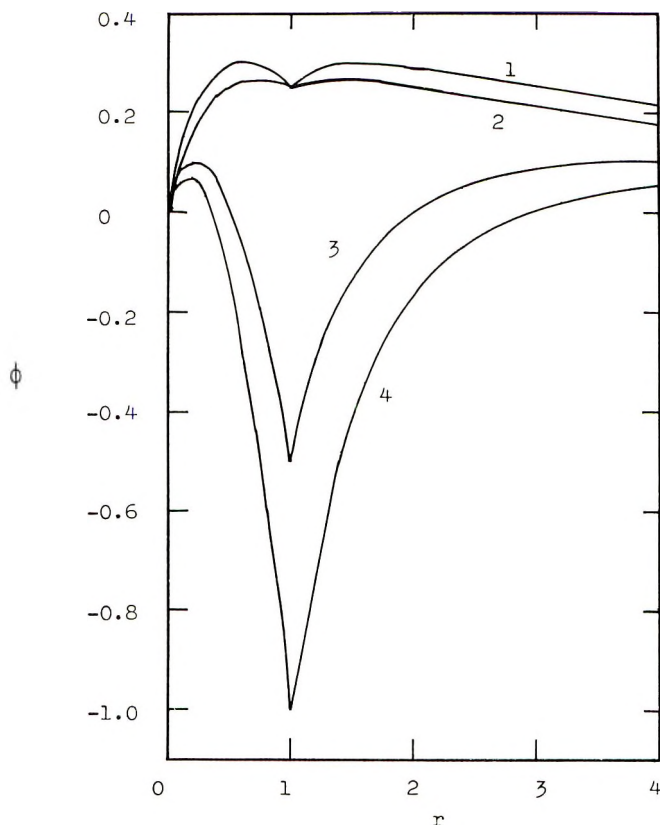


Fig. 10. r -Dependence of ϕ in the case of $FG = F$ when F and P_A or P_B are constants [see eq. (31)]: (1) $F = 3$, $P_A = P_B = 1/2$; (2) $F = 2$, $P_A = P_B = 1/2$; (3) $F = 2$, $P_A = P_B = 1$; (4) $F = 3$, $P_A = P_B = 1$.

$$\begin{aligned}
 Y'_{6,A} &= pY_2(1 - \rho_1)(1 - \sigma_1)P_AP_B \sum^n \rho_i(f_i - 1) \sum^n \sigma_i(g_i - 1) \\
 Y'_{6,B} &= qY_2(1 - \rho_1)(1 - \sigma_1)P_AP_B \sum^n \rho_i(f_i - 1) \sum^n \sigma_i(g_i - 1) \quad (32d) \\
 &\dots \\
 &\dots \\
 &\dots
 \end{aligned}$$

Then, the total number of reactants, except A_1 and B_1 , at circles 2, 4, 6, ... can be expressed from eqs. (33) and (32) as

$$Y'_i = Y'_{i,A} + Y'_{i,B} \quad (33)$$

$$\begin{aligned}
 Y'_2 &= Y_2(1 - \rho_1)(1 - \sigma_1) \\
 Y'_4 &= Y_2Y'_0(1 - \rho_1)(1 - \sigma_1) \\
 Y'_6 &= Y_2Y'_1(1 - \rho_1)(1 - \sigma_1)
 \end{aligned} \quad (34)$$

...

...

...

$$Y'_{2(n+1)} = Y_2 Y'_1 \left\{^{-1 + \sum_0^n 1/2[1 - (-1)^{n+1}]}\right\} Y_0'^{1/2[1 - (-1)^n]} (1 - \rho_1)(1 - \sigma_1)$$

where $n = 0, 1, 2, \dots$, and Y'_0 and Y'_1 are shown by eq. (37).

Therefore, at the critical point or gelation point for the infinite network,

$$Y'_1 \left\{^{-1 + \sum_0^n 1/2[1 - (-1)^{n+1}]}\right\} Y_0'^{1/2[1 - (-1)^n]} (1 - \rho_1)(1 - \sigma_1) = 1 \tag{35}$$

Equation (35) seems to be a modification of eq. (7), and in eq. (35) the chain-stopping effect of monofunctional groups may be taken into account. From this point of view, eq. (8) can be rewritten:

$$\begin{aligned} Y'_2/Y_2 &= (1 - \rho_1)(1 - \sigma_1) \\ Y'_4/Y_2 &= Y'_0(1 - \rho_1)(1 - \sigma_1) \\ Y'_6/Y_2 &= Y'_1(1 - \rho_1)(1 - \sigma_1) \\ Y'_8/Y_2 &= (Y'_6/Y_2)(Y'_4/Y_2)/(1 - \rho_1)(1 - \sigma_1) \\ Y'_{10}/Y_2 &= (Y'_6/Y_2)^2/(1 - \rho_1)(1 - \sigma_1) \\ &\dots \\ &\dots \\ &\dots \end{aligned} \tag{36}$$

where $n = 0, 1, 2, 3, \dots$, and

$$Y'_0 = pP_A \sum^n \rho_i(g_i - 1) + qP_B \sum^n \sigma_i(f_i - 1) \tag{37}$$

$$Y'_1 = P_A P_B \sum^n \rho_i(f_i - 1) \sum^n \sigma_i(g_i - 1)$$

Equation (40b) takes into account the chain-stopping effect of monofunctional groups on the gel formation due to the bifunctional interunit junction and a modification of the equations of Stockmayer² and Kahn.⁸ This disagrees with Yoshida's expression.¹⁰

The function of $Y'_0 - Y'_1$ can be treated in eqs. (16) and (17); we then derive

$$F = \sum^n \rho_i(f_i - 1)$$

and

$$G = \sum^n \sigma_i(g_i - 1) \tag{38}$$

Therefore, if $Y'_6/Y_2 \geq 1$, and the condition of eqs. (19) and (38) is kept, or if $Y'_4/Y_2 \geq 1$, and the condition of eqs. (23) and (38) is kept, we can obtain the following relationship;

$$Y'_{2(n-1)}/Y_2 \geq \dots \geq Y'_8/Y_2 \geq Y'_6/Y_2 \geq Y'_4/Y_2 \geq 1 \tag{39}$$

The simple expression of eq. (35), for the infinite network, is

$$Y'_0(1 - \rho_1)(1 - \sigma_1) = 1 \tag{40a}$$

$$Y'_1(1 - \rho_1)(1 - \sigma_1) = 1 \tag{40b}$$

TABLE II
Gelation Point for Epoxide-Acid Anhydride Systems^a

	Fraction of A (epoxide or alcohol)				Fraction of B (anhydride)				r	$(P_n)_{gel}$		
	ρ_1 Case Alcohols	ρ_2 Mono-epoxide or dihydric alcohol	ρ_3 Glycidol	ρ_4 Epikote 828	ρ_5 Epikote 1001	σ_2 Hexa-hydro-phthalic anhydride	σ_3 Tri-mellitic anhydride	σ_4 Pyro-mellitic dianhydride		Obs.	Calc. [eq. (41a)]	Calc. [eq. (40a)]
I				1.00		1.00			1.00	55.0	50.0	57.7
				1.00		1.00			0.80	50.0	45.0	51.6
				1.00		1.00			1.43	68.0	60.8	69.0
II					1.00				1.35	59.7	40.7	58.1
					1.00				1.35	57.0	40.7	58.1
III		0.156 ^b		0.844		1.00			1.00	63.6	54.4	61.0
		0.153 ^b		0.847		1.00			0.80	57.2	48.8	54.5
		0.275 ^c		0.725		1.00			1.215	72.0	60.4	70.4
		0.275 ^d		0.725		1.00			1.215	70.6	60.4	70.4
		0.275 ^e		0.725		1.00			1.215	71.0	60.4	70.4
		0.275 ^f		0.725		1.00			1.215	70.8	60.4	70.4
		0.275 ^g		0.725		1.00			1.215	72.8	60.4	70.4
		0.275 ^h		0.725		1.00			1.215	71.6	60.4	70.4
IV		0.226 ^b			0.774	1.00			0.864	53.8	43.2	51.0
		0.226 ^c			0.774	1.00			1.00	56.8	46.4	54.9
		0.226 ^d			0.774	1.00			1.00	55.4	46.4	54.9
		0.226 ^e			0.774	1.00			1.00	55.6	46.4	54.9
		0.226 ^f			0.774	1.00			1.00	56.0	46.4	54.9
		0.226 ^g			0.774	1.00			1.00	55.3	46.4	54.9
		0.226 ^h			0.774	1.00			1.00	56.2	46.4	54.9

V	0.126 ^l	0.874	1.00	1.159	68.6	59.6	66.5	68.2	71.0
	0.126 ⁱ	0.874	1.00	1.159	69.0	59.6	66.5	68.2	71.0
	0.126 ^k	0.874	1.00	1.159	63.7	59.6	66.5	68.2	71.0
	0.126 ^j	0.874	1.00	1.159	67.4	59.6	66.5	68.2	71.0
	0.126 ^m	0.874	1.00	1.159	68.0	59.6	66.5	68.2	71.0
VI	0.126 ⁿ	0.874	1.00	1.159	67.5	59.6	66.5	68.2	71.0
	1.00	1.00	1.00	35.0	33.3	33.3			
	1.00	1.00	1.00	30.5	30.0	29.8			
VII	0.20	0.80	0.20	1.00	37.8	36.7	36.6		
	0.20	0.80	0.60	1.00	39.2	38.5	38.5		
	0.20	0.80	0.40	1.00	48.4	45.5	46.3		
	0.20	0.80	0.60	1.00	39.0	37.5	37.4		
	0.20	0.80	0.40	1.20	47.3	45.8	45.8		
VIII	1.00	1.00	1.00	41.1	40.0	40.9			
	1.00	1.00	1.00	36.9	36.0	36.5			
	1.00	1.00	1.00	45.1	44.0	44.7			
IX	0.10	0.90	1.00	1.00	60.4	51.3	58.7		
	0.10	0.90	1.00	0.80	54.1	46.1	52.6		
	0.10	0.90	1.00	1.20	63.7	56.4	64.4		
	0.20	0.80	1.00	1.00	58.0	52.6	59.7		
X	0.10 ^e	0.50	0.40	1.00	56.7	47.6	55.9		
	0.10 ^e	0.50	0.40	0.80	48.3	42.9	50.0		
	0.10 ^e	0.50	0.40	1.20	62.0	52.5	61.2		
XI	0.60	0.40	1.00	1.00	52.6	45.5	54.3		
	0.40	0.60	1.00	1.00	53.8	43.5	52.7		

^a Epoxide and acid anhydride polymerized in the presence of 0.5-1.0 wt.-% of triethanolamine at 70-100°C. Data of Tanaka and Kakiuchi¹¹; ^b octylene oxide; ^c dodecene oxide; ^d allyl glycidyl ether; ^e phenyl glycidyl ether; ^f butyl glycidyl ether; ^g triethylene glycol; ^h ethylene glycol;

ⁱ C₃H₇OH; ^j C₄H₉OCH₂CH₂OH; ^k C₆H₅CH₂OH; ^l (CH₃)₂CHCH₂CH₂OH; ^m  CH₂OH; ⁿ (CH₃)₂C(CH₂OCH₂)OH.

TABLE III
Gelation Point for Polyhydric Alcohol-Carboxylic Acid System^a

Fraction of A (acid)				Fraction of B' (alcohol)				(P _N) gel				
ρ_1	ρ_2	ρ_3	σ_1	σ_2	σ_3	σ_4	r	Obs.	Calc.	Calc.	Calc.	Calc.
Lauric acid	Adipic acid	Trimellitic acid	Oleyl alcohol	Di-ethylene glycol	Tri-methylene propane	Penta-erythritol		[eq.(41a)]	[eq.(41b)]	[eq.(40a)]	[eq.(40b)]	
1.00	1.00		0.05	0.40	0.55		1.00	86.6	81.7	84.2	83.8	
	1.00		0.10	0.30		0.60	1.00	74.2	64.5	71.8	72.8	
	1.00		0.20	0.20	0.30	0.30	1.00	84.3	74.1	92.6	85.8	
0.20	0.80			0.30	0.30	0.40	1.00	84.4	69.0	86.3	86.3	
0.10	0.90		0.10	0.20	0.70		1.00	88.0	80.0	98.7	92.6	
0.10	0.90		0.10	0.20	0.30	0.40	1.00	82.3	69.0	85.2	82.8	
0.10	0.90		0.10	0.33	0.28	0.20	1.00	87.5	75.2	92.9	88.3	
0.10	0.20	0.70	0.10	0.20	0.70		1.00	72.4	62.5	77.2	69.4	
0.10	0.30	0.60 ^b	0.10	0.30	0.60		1.00	79.3	66.6	82.4	74.0	

^a Carboxylic acids and polyhydric alcohols polymerized in the presence of 0.1-0.3 wt.-% *p*-toluenesulfonic acid at 160°C. Data of Yoshida.¹⁰

^b Trimellitic anhydride.

Comparison of Theoretical Values of P_A or P_B with Observed Values

The theoretical values of P_B calculated from eqs. (40) and (41) are compared with observed values¹¹ for the gel formation in epoxide and acid anhydride systems in Table II, where A is epoxide or alcohol, and B is acid or acid anhydride:

$$Y'_0 = 1 \quad (41a)$$

and

$$Y'_1 = 1 \quad (41b)$$

The theoretical values of P_B calculated from the eqs. $Y'_0 = 1$ and $Y'_1 = 1$ are consistent with each other, and agree satisfactorily with the observed values in the cases of VI, VII, and VIII in Table II. In the other cases, I–IV and IX–XI, the calculated value from $Y'_1 = 1$ is more suitable for estimating the gelation point than that from $Y'_0 = 1$. In the presence of monofunctional monomers, the modified eqs. (40) can be more satisfactory to estimate the gelation point than eqs. (41) as shown in case V of Table II.

The experimental results¹⁰ for the condensation reaction of carboxylic acids and polyhydroxyl compounds are compared with the theoretical values calculated from eqs. (40) and (41) in Table III.

Equation (40) is more suitable than eq. (41) for estimating the gel formation for the systems in which monofunctional monomers are contained from the start of the reaction.

References

1. Flory, P. J., (a) *J. Am. Chem. Soc.*, **63**, 3083 (1941); (b) *ibid.*, **63**, 3091 (1941); (c) *ibid.*, **63**, 3091 (1941); (d) *ibid.*, **69**, 30 (1947); (e) *ibid.*, **74**, 2718 (1952); (f) *J. Phys. Chem.*, **46**, 132 (1942).
2. Stockmayer, W. H., (a) *J. Chem. Phys.*, **11**, 45 (1943); (b) *ibid.*, **12**, 125 (1944); (c) *J. Polymer Sci.*, **9**, 69 (1952).
3. Gordon, M., *J. Chem. Phys.*, **22**, 610 (1954).
4. Harris, F. E., *J. Chem. Phys.*, **23**, 1518 (1955).
5. Erlander, S., and D. French, *J. Polymer Sci.*, **20**, 7 (1956).
6. Allen, E. S., *J. Polymer Sci.*, **21**, 349 (1956).
7. Case, L. C., *J. Polymer Sci.*, **26**, 333 (1957).
8. Kahn, A., *J. Polymer Sci.*, **49**, 283 (1961).
9. Brodowsky, H., and S. Prager, *J. Chem. Phys.*, **39**, 1103 (1963).
10. Yoshida, T., private communication.
11. Tanaka, Y., and H. Kakiuchi, *J. Appl. Polymer Sci.*, **7**, 1951 (1963).

Résumé

Les conditions nécessaires à la formation d'un réseau infini due à la jonction bifonctionnelle interunitaire ont été réexaminées et on mentionne la différence entre les théories de Flory, Case ou Kahn. La théorie est étendue à un cas beaucoup plus général que celle de Flory de Case ou de Kahn. On traite également du point critique dans la réaction de condensation entre des mélanges de deux types de groupements fonctionnels contenant une ou plusieurs fonctionnalités. On montre qu'au point critique,

$$P_A P_B (1 - \rho_i)(1 - \sigma_i) \sum_{i=1}^n \rho_i (f_i - 1) \sum_{i=1}^n \sigma_i (g_i - 1) = 1 \text{ et/ou}$$

$$[1/(1 + r)] [r P_A \sum_{i=1}^n \sigma_i (g_i - 1) + P_B \sum_{i=1}^n \rho_i (f_i - 1)] = 1$$

où P_A et P_B sont les probabilités respectives pour qu'un groupe A ou B ait réagi, f_i et g_i sont les fonctionnalités respectives des monomères A_i et B_i , r est le rapport entre les groupes A et B à l'état initial, et ρ_i , σ_i sont les fractions molaires de A_i et B_i , respectivement.

Zusammenfassung

Die notwendigen Voraussetzungen für die Bildung eines unendlichen Netzwerks durch die Verknüpfung bifunktioneller Einheiten wurden neuerlich untersucht, und die Unterschiede zwischen den Theorien von Flory-Case und Kahn wurden festgestellt. Die Theorie wurde auf einen allgemeineren Fall als den von Flory und Case oder Kahn betrachteten ausgedehnt. Weiters wird der kritische Punkt bei der Kondensationsreaktion zwischen Mischungen zweier Typen funktioneller Gruppen mit einer oder mehreren Funktionalitäten behandelt. Es wird gezeigt, dass beim kritischen Punkt

$$P_A P_B (1 - \rho_i) (1 - \sigma_i) \sum_{i=1}^n \rho_i (f_i - 1) \sum_{i=1}^n \sigma_i (g_i - 1) = 1 \text{ und/oder}$$

$$[1/(1 + r)] [r P_A \sum_{i=1}^n \sigma_i (g_i - 1) + P_B \sum_{i=1}^n \rho_i (f_i - 1)] = 1$$

wo P_A und P_B die entsprechende Wahrscheinlichkeit, dass eine A- oder B-Gruppe reagiert hat, f_i und g_i die Funktionalität der Monomeren A_i und B_i , r das Verhältnis von A-Gruppen zu B-Gruppen im Anfangszustand und ρ_i , σ_i die Molenbrüche von A_i bzw. B_i sind.

Received October 23, 1964

Prod. No. 4603A

Anionic Polymerization of ω -Lactam. Part I. Polymerization of ϵ -Caprolactam by Alkaline Catalysts and Ketenimines

TAKAYA YASUMOTO, *Plastics Laboratory, Toyo Rayon Co., Ltd.,
Tokodori, Showaku, Nagoya, Japan*

Synopsis

Ketenimines have been found to be useful cocatalysts for the alkaline polymerization of ϵ -caprolactam. The induction period preceding the start of the reaction is shortened by addition of a ketenimine, and the polymerization rapidly proceeds at low temperature below the melting point of the polymer. A reaction mechanism is proposed for the polymerization of ϵ -caprolactam with alkaline catalyst and ketenimine, which involves a formation of a reactive *N*-imidoyl lactam from ketenimine and lactam, and chain propagation by the stepwise addition of anionic lactam at the end of the molecule leading to the polymer. This mechanism is supported by the experimental fact that imino chloride has the same effect as ketenimine on the alkaline polymerization of ϵ -caprolactam. The conditions for the polymerization have been carefully investigated. Both conversion and relative viscosity of polymer diminish with increasing concentration of ketenimine and also with increasing reaction temperature.

INTRODUCTION

It has been found that the ring-opening polymerization of ω -lactams can be attained in the presence of an alkaline catalyst.¹⁻⁵ Recently it has been also shown that this anionic polymerization of ω -lactams can be accelerated by the addition of certain compounds as cocatalysts. Effective cocatalysts include acylating reagents⁶⁻⁸ such as acid chlorides and anhydrides, and nitrogen-containing compounds⁹⁻¹¹ in which the nitrogen atoms are trivalent and in which at least one nitrogen atom is directly attached to at least two radicals selected from the group consisting of carbonyl, thiocarbonyl, sulfonyl, and nitroso radicals. Furthermore, other cocatalysts are carbon disulfide,¹² carbon monoxide,¹³ isocyanates,¹⁴ carbodiimides,¹⁵ cyanamides,¹⁵ nitriles,⁸ esters,¹⁶ carbonates,¹⁷ urea or thiourea derivatives,¹⁸⁻²⁰ and perhalogenated ketones.²¹

We found that a few ketenimines were useful as cocatalysts to activate the anionic polymerization of ϵ -caprolactam catalyzed with an alkaline catalyst. In this study the conditions of polymerization of ϵ -caprolactam by alkaline catalysts and ketenimines were carefully investigated, and the results are presented and discussed in the present report.

EXPERIMENTAL

Synthesis of Ketenimines

Preparation of Ethylbutylketene *n*-Butylimine. *N*-(*n*-Butyl)- α -ethylcaproamide prepared from α -ethylcaproyl chloride and *n*-butylamine was reacted with phosphorus pentachloride to give *N*-(*n*-butyl)- α -ethylcaproimino chloride. Ethylbutylketene *n*-butylimine was obtained by dehydrochlorination of this imino chloride as shown in eqs. (1) and (2).²²

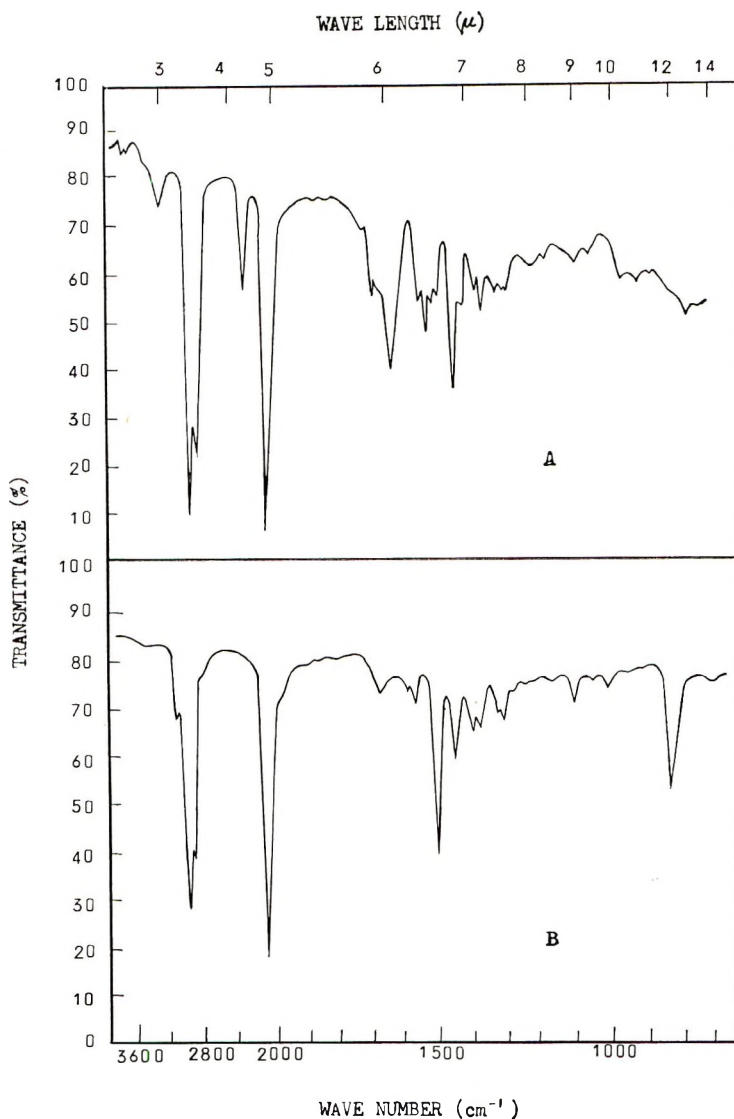
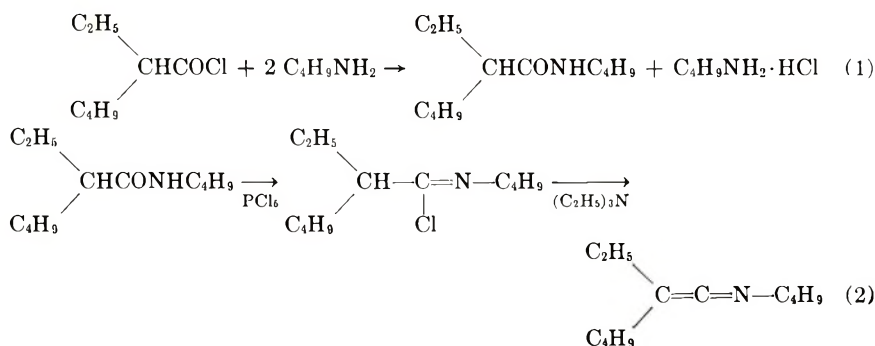


Fig. 1. Infrared spectra of ketenimines: (A) ethylbutylketene *n*-butylimine; (B) ethylbutylketene *p*-tolylimine.



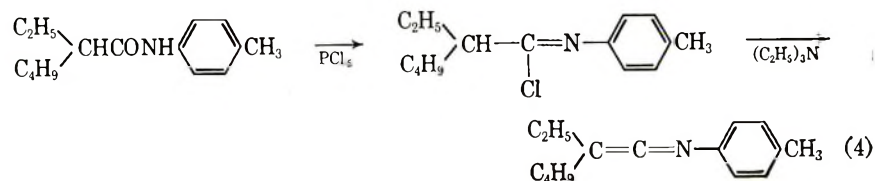
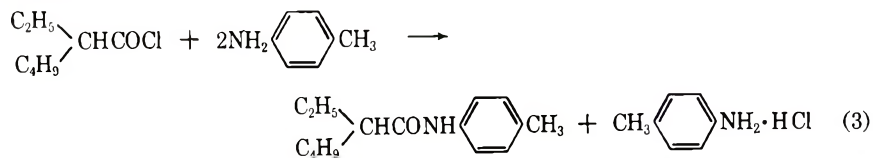
N-(*n*-Butyl)- α -ethylcaproimino chloride (207 g., 0.956 mole) was dissolved in 1200 g. of benzene, and the solution was poured into a 3-liter three-necked round-bottomed flask equipped with a reflux condenser and a stirrer, and 580 g. (5.74 mole) of triethylamine was added to this solution. After stirring for 14 hr. at room temperature, the solution was refluxed under heating for 16 hr. The triethylamine hydrochloride formed was filtered and washed three times with dry benzene. The filtrate and benzene washings were combined, and the solution was concentrated under reduced pressure.

The residue was distilled under vacuum and the fraction boiling at 76°C./3 mm. was collected in 136.3 g. (78.8%) yield. The infrared absorption spectrum of the fraction is shown in Figure 1. A characteristic band corresponding to the twinned double bond (C=C=N) appeared strongly at 2050 cm.⁻¹ (4.88 μ).

ANAL. Calcd. for C₁₂H₂₃N (M.W. 181): C, 79.56%; H, 12.71%; N, 7.73%. Found: C, 79.67%; H, 12.52%; N, 7.57%.

Preparation of Ethylbutylketene *p*-Tolylimine. This ketenimine was prepared by a procedure similar to that used for ethylbutylketene *n*-butylimine.²²

N-(*p*-tolyl)- α -ethylcaproamide prepared from α -ethylcaproyl chloride and *p*-toluidine was reacted with phosphorus pentachloride to give *N*-(*p*-tolyl)- α -ethylcaproimino chloride. As shown in eqs. (3) and (4), ethylbutylketene *p*-tolylimine boiling at 155°C./7 mm. was prepared in 83.3% yield by dehydrochlorination of this imino chloride with triethylamine.



The infrared absorption spectrum of this material is shown in Figure 1. A strong absorption band appeared at 2050 cm.^{-1} ($4.88\ \mu$).

ANAL. Calcd. for $\text{C}_{15}\text{H}_{21}\text{N}$ (M.W. 215): C, 83.72%; H, 9.77%; N, 6.51%. Found: C, 83.65%; H, 9.52%; N, 6.59%.

Polymerization of ϵ -Caprolactam

In order to eliminate the effect of moisture the monomer should be absolutely dry. Thus once-distilled ϵ -caprolactam was stored over P_2O_5 in a desiccator and distilled again under vacuum just before polymerization.

Potassium and sodium metal, ethylmagnesium bromide²³ and lithium aluminum hydride were used as catalysts, and the effect of ketenimines in each polymerization was investigated. ϵ -Caprolactam molten at 90°C . was poured into an ampule equipped with a nitrogen inlet tube, and the desired amount of an alkaline catalyst was added to the lactam under an inert atmosphere. After the catalyst was completely dissolved, the calculated amount of a ketenimine was added and mixed uniformly. The bulk polymerization of the mixture took place at low temperature below melting point of the polyamide. The block polymer formed was shaved thin. About 2 g. of the sample weighed was extracted with hot water for 10 hr. and dried, and then conversion to polymer was calculated.

After the measurement of conversion, 0.250 g. of the dried sample was dissolved in 25.0 ml. of 98% concentrated H_2SO_4 and the relative viscosity (η_r) of the solution was measured by an Ostwald viscometer at $25 \pm 0.05^\circ\text{C}$.

RESULTS

Polymerization with Alkali Metals and Ketanimines

As the mixture of ϵ -caprolactam with an alkali metal and a ketenimine started to polymerize at a low temperature (below melting point of the polymer), its melt viscosity increased, and the mixture became quite viscous as polymerization proceeded. When the ampule was allowed to cool slowly, a transparent liquid remained. This is a supercooled state of the polymer below its melting point. When the ampule was quickly cooled, a solid polymer immediately crystallized out. After further continuous heating of the ampule, a solid polymer was also formed by crystallization. There was a comparatively long induction period in the polymerization with an alkali metal catalyst only, the end of which was indicated by the increase of melt viscosity as the reaction began. The addition of a ketenimine shortened the induction period considerably and made the alkaline polymerization proceed rapidly. This effect of a ketenimine is as remarkable as those of acylating reagents and *N*-acyl lactams which are well known as cocatalysts. The relation between conversion and time in the polymerization at 200°C . with potassium metal and ethyl-

butylketene *n*-butylimine is shown in Figure 2. The polymerization with 1.0 mole-% of both potassium metal and the ketenimine reached an equilibrium after 30 min. heating at 200°C. In the polymerization with 1.0 mole-% of potassium metal only, however, the reaction proceeded slowly and reached an equilibrium after 4 hr. Thus it is evident that an alkaline polymerization of ϵ -caprolactam is promoted by addition of a ketenimine.

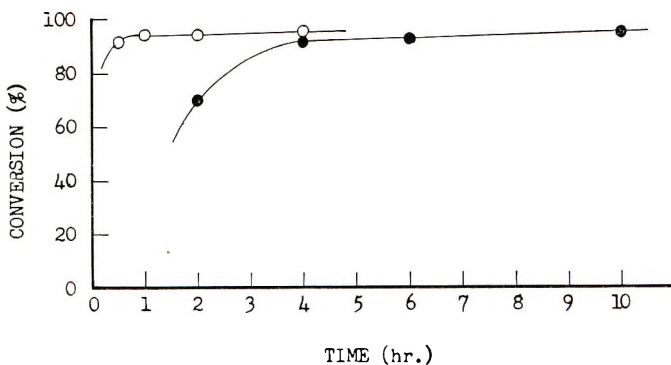


Fig. 2. Relation between conversion and time in the polymerization of ϵ -caprolactam at 200°C. with potassium metal and ethylbutylketene *n*-butylimine: (●) 1.0 mole-% K; (O) 1.0 mole-% K and 1.0 mole-% ketenimine.

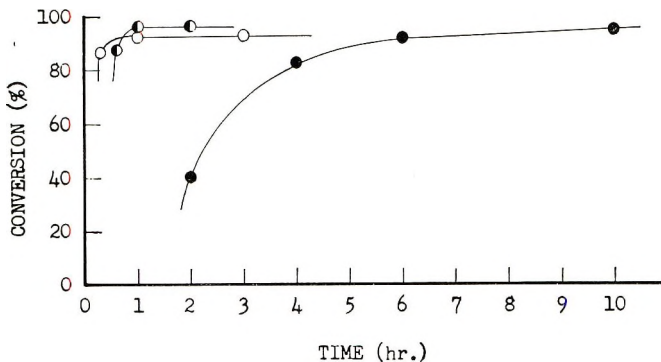


Fig. 3. Comparison between effects of two ketenimines on polymerization of ϵ -caprolactam at 200°C.: (●) 1.0 mole-% Na; (O) 1.0 mole-% Na, and 1.0 mole-% ethylbutylketene *n*-butylimine; (◐) 1.0 mole-% Na and 1.0 mole-% ethylbutylketene *p*-tolyimine.

The effects of ethylbutylketene *n*-butylimine and ethylbutylketene *p*-tolyimine in the polymerization with 1.0 mole-% of sodium metal are compared in Figure 3. With the use of either of the ketenimines, the polymerization reached an equilibrium after 1 hr. heating at 200°C., but in the polymerization with sodium metal only it was necessary to heat over 6 hr. in order to reach an equilibrium. It is found that the ketenimines have a noticeable and almost equal effect in alkaline polymerization.

Polymerization with Grignard's Reagent and Ketenimines

The anionic polymerization with ethylmagnesium bromide²³ as a catalyst is shown in Figure 4. It is obvious that ethylmagnesium bromide is a good catalyst for rapid polymerization. When a ketenimine was added, the polymerization proceeded more rapidly, but the combined effect was not so remarkable as in polymerization with alkali metals. Also conversion in the polymerization with ethylmagnesium bromide was below 85% at an equilibrium and lower than that for polymerization with alkali metals.

Polymerization with Lithium Aluminum Hydride and Ketenimines

The results of the polymerization with 0.5 mole-% of lithium aluminum hydride at 200°C. are shown in Table I. Lithium aluminum hydride was more effective as a catalyst than potassium, sodium, and ethylmagnesium bromide, the polymerization proceeding more rapidly. Perhaps the effect of lithium aluminum hydride should be regarded as a LiH-catalyzed polymerization with AlH_3 as cocatalyst. The conversion reached over 90% at an equilibrium after 30 min. heating at 200°C. As shown in Table I, the rate of polymerization did not change on addition of a ketenimine, and therefore the ketenimines were considered to have no effect.

TABLE I
Relation between Conversion and Time in the Polymerization at 200°C. with Lithium Aluminum Hydride and Ethylbutylketene *n*-Butylimine

Expt. no.	LiAlH_4 concentration, mole-%	Ketenimine concentration, mole-%	Time, hr.	Conversion, %
34	0.5	0	0.5	93.5
35	0.5	0	2	92.6
36	0.5	0	4	93.0
37	0.5	0	8	92.8
38	0.5	1.0	0.5	91.9
39	0.5	1.0	2	90.9
40	0.5	1.0	4	91.6
41	0.5	1.0	8	92.1

Effects of Catalyst and Ketenimine Concentrations

The effect of potassium metal and ethylbutylketene *n*-butylimine concentrations on conversion and relative viscosity (η_r) of polymer obtained in polymerization at 200°C. for 10 hr. are shown in Figures 5 and 6, respectively. Conversion versus potassium metal concentration at various ketenimine concentrations is plotted in Figure 5. It is observed that at a constant concentration below 3.0 mole-% of ketenimine the optimum concentration of potassium metal is 1.0 mole-%, and conversion decreases with increasing concentration of the ketenimine. As shown in Figure 6 relative viscosity of polymer decreases with increasing concentrations of

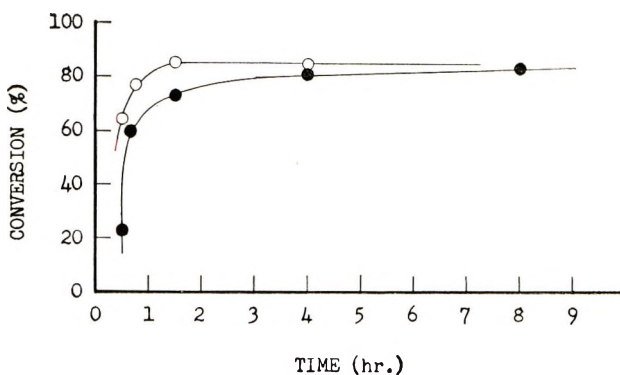


Fig. 4. Relation between conversion and time in the polymerization of ϵ -caprolactam at 200°C. with ethylmagnesium bromide and ethylbutylketene *n*-butylimine: (●) 1.0 mole-% C_2H_5MgBr ; (○) 1.0 mole-% C_2H_5MgBr and 1.0 mole-% ketenimine.

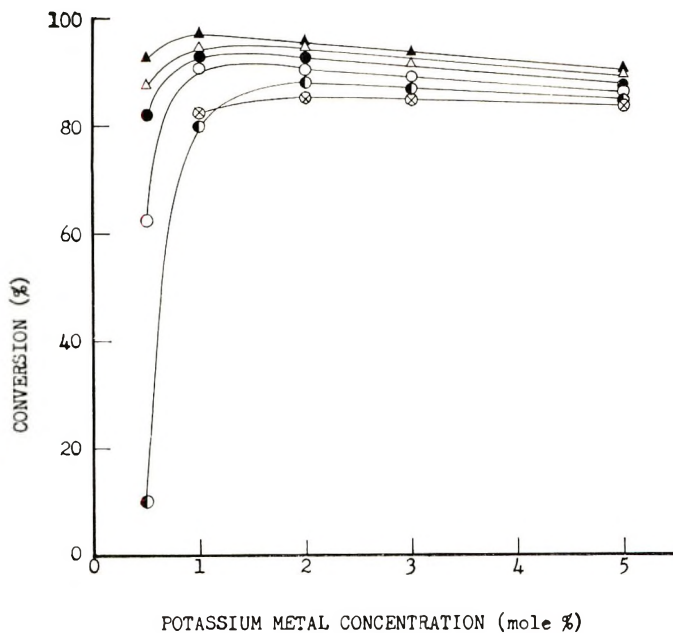


Fig. 5. Relation between potassium metal concentration and conversion in polymerization of ϵ -caprolactam at 200°C. for 10 hr. at various ethylbutylketene *n*-butylimine concentrations: (▲) 0.5 mole-%; (Δ) 1.0 mole-%; (●) 2.0 mole-%; (○) 3.0 mole-%; (●) 4.0 mole-%; (⊗) 5.0 mole-%.

both potassium metal and the ketenimine, and the maximum value was obtained at 0.5 mole-% levels of both.

Effect of Polymerization Temperature

When the relation between conversion and relative viscosity was studied at various reaction temperatures, the experimental results shown in Table

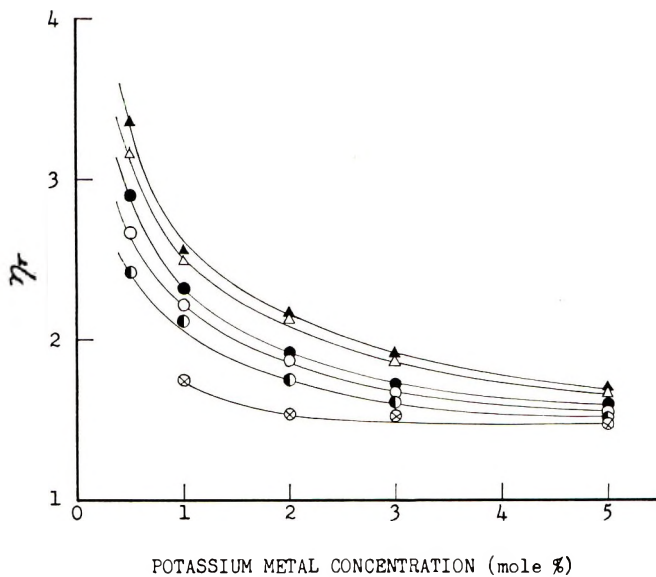


Fig. 6. Relation between potassium metal concentration and relative viscosity with polymerization of ϵ -caprolactam at 200°C. for 10 hr. at various ethylbutylketene *n*-butylimine concentrations: (▲) 0.5 mole-%; (△) 1.0 mole-%; (●) 2.0 mole-%; (○) 3.0 mole-%; (◐) 4.0 mole-%; (⊗) 5.0 mole-%.

II were obtained. These indicate that both conversion and relative viscosity decrease with increasing reaction temperature.

TABLE II

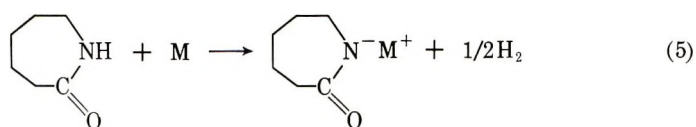
Effect of Reaction Temperature on the Conversion and Relative Viscosity of Polymer

Expt. no.	Potassium metal concentration, mole-%	Ketenimine concentration, mole-% ^a	Temperature, °C.	Time, hr.	Conversion, %	Relative viscosity (η_r)
72	0.5	1.0	150	20	96.9	3.24
73	0.5	1.0	180	5	95.7	3.11
74	0.5	1.0	200	4.5	90.6	3.02
75	0.5	1.0	220	4	84.7	2.71

^a Ethylbutylketene *n*-butylimine.

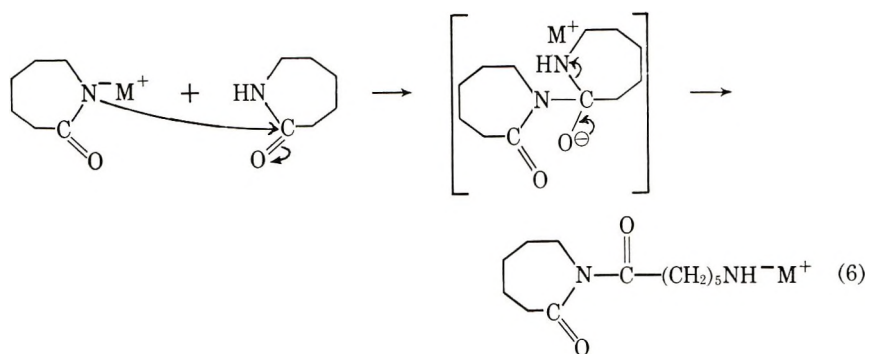
DISCUSSION

The reaction mechanisms are discussed as follows. ϵ -Caprolactam is reacted with an alkali metal, giving an iminium salt of the lactam as shown in eq. (5).



where M is K, Na etc.

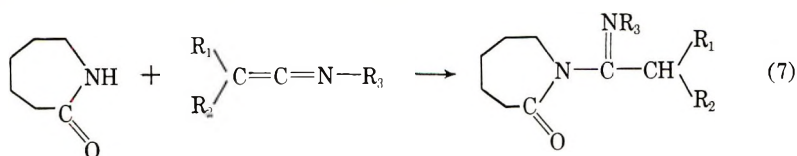
It is known that an iminium salt of the lactam is also formed with a Grignard reagent²³ or lithium aluminum hydride as well as the alkali metals. As shown in eq. (6), it is considered that *N*-acyl lactam²⁴ is formed by the reaction between the iminium salt of lactam and a lactam.



It is reasonable that the group $\text{—NH}^- \text{M}^+$ shown in eq. (6) must disappear and a new iminium salt of the lactam be formed, not only because of the enormous prevalence of amide groups, but also because the —NH^- anion is a much stronger base than the amide of the lactam.^{4,25} The carbonyl group of the *N*-acyl lactam, which is remarkable reactive, is attacked by the lactam anion; this is followed by opening of the *N*-acyl lactam ring, and by the subsequent stepwise addition of the anionic lactam the polymerization proceeds to give a polymer.^{26–29} The formation of this *N*-acyl lactam is the rate-controlling step of the alkaline polymerization of lactam.

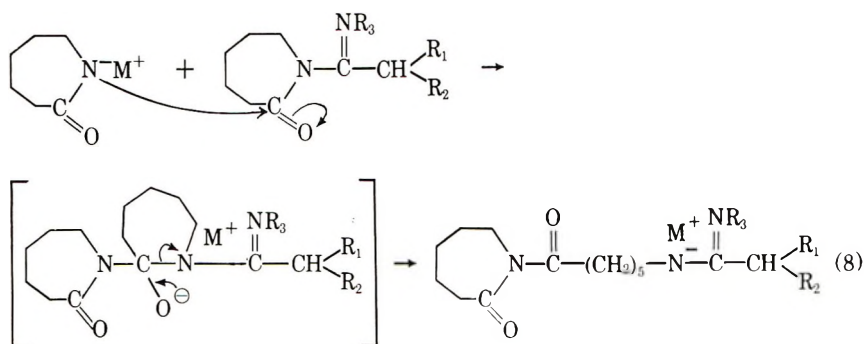
It is generally known that the polymerization is accelerated greatly by the previous addition of a reactive *N*-acyl lactam in the polymerization system.^{9–11}

It is presumed that, as shown in eq. (7), ketenimine reacts with a lactam to form an *N*-imidoyl lactam as a reaction intermediate:



where R_1 , R_2 , and R_3 are hydrocarbon radicals such as alkyl and allyl groups. It is supposed that the carbonyl group of *N*-imidoyl lactam is attacked by a lactam anion in the same mechanism as *N*-acyl lactam,

followed by a ring-opening of the *N*-imidoyl lactam. The effect of ketenimine as cocatalyst for the alkaline polymerization is probably due to the formation of *N*-imidoyl lactam. The mechanism is supported by the experimental fact that in the alkaline polymerization imino chloride is a useful activator and its effects are equal to those of ketenimine. A study of the effects of imino chloride in the alkaline polymerization of ϵ -caprolactam will be reported in a forthcoming paper. As shown in eq. (8), it is presumed that an anionic lactam adds to a reactive *N*-imidoyl lactam (a reaction intermediate from a ketenimine and a lactam), and thus propagation to a polymer proceeds continuously by stepwise addition of the anionic lactam.



It is certain that a metal cation added to polymer transfers to a lactam and a proton is then transferred from lactam to polymer, and a new iminium salt of the lactam thus being formed.

The author takes this opportunity to thank Mr. T. Sakamoto and Mr. S. Wakano for permission to publish this report.

References

1. Hanford, W. E., and R. M. Joyce, *J. Polymer Sci.*, **3**, 167 (1948).
2. Griehl, W., *Faserforsch. Textiltech.*, **6**, 260 (1955); *ibid.*, **7**, 207 (1956).
3. Wichterle, O., *Faserforsch. Textiltech.*, **6**, 237 (1955).
4. Heikens, D., *Makromol. Chem.*, **18**, 62 (1956).
5. Wiloth, F., *Z. Physik. Chem.*, **11**, 78 (1957).
6. Arnold Hoffman & Co., Brit. Pats. 749,332 (1956); 754,944 (1956).
7. Barnes, C. E., W. O. Ney, Jr., and W. R. Nummy, U. S. Pat. 2,809,958 (1957).
8. Badische Anilin u.-Soda Fabrik, Brit. Pat. 868,808 (1961).
9. Mottus, E. H., R. M. Hendrick, and J. M. Butler, U. S. Pat. 3,017,391 (1962); 3,017,392 (1962).
10. Imperial Chemical Industries, Brit. Pat. 908,220 (1962).
11. Wichterle, O., Brit. Pat. 904,229 (1962).
12. Black, W. B., and H. G. Clark, U. S. Pat. 2,912,415 (1959).
13. Lautenschlager, H., H. Friederich, W. Schmidt, and K. Dacks, U. S. Pat. 2,907,755 (1959).
14. Butler, J. M., R. M. Hendrick, and E. H. Mottus, U. S. Pat. 3,015,652 (1962); 3,061,592 (1962).
15. Schnell, H., K. Uerdinger, and G. Fritz, U. S. Pat. 3,015,652 (1962); H. Schnell, K. Uerdinger, and J. Nentwig, U. S. Pat. 3,061,592 (1962).

16. Farbenfabriken, Bayer, Brit. Pat. 934,218 (1963).
17. Imperial Chemical Industries, Brit. Pats. 924,453 (1963); 931,013 (1963); 931,393 (1963); 931,394 (1963).
18. Monsanto Chemical Co., Brit. Pat. 921,047 (1963).
19. Badische Anilin u.-Soda Fabrik, Brit. Pat. 921,278 (1963).
20. Imperial Chemical Industries, Brit. Pat. 944,307 (1963).
21. E. I. du Pont de Nemours & Co., Brit. Pat. 955,917 (1963).
22. Stevens, C. L., and J. C. French, *J. Am. Chem. Soc.*, **75**, 657 (1953); *ibid.*, **76**, 4398 (1954).
23. Monsanto Chemical Co., U. S. Pat. 3,018,273 (1962).
24. Hall, H. K., Jr., *J. Am. Chem. Soc.*, **80**, 6404 (1958).
25. Wichterle, O., J. Šebenda, and J. Kraliček, *Fortschr. Hochpolymer-Forsch.*, **2**, 578 (1961).
26. Murahashi, S., H. Yuki, and H. Sekiguchi, *Ann. Repts. Inst. Fiber Chem. Osaka Univ.*, **10**, 88, 93 (1957).
27. Kurland, J. R., and E. B. Wilson, *J. Chem. Phys.*, **27**, 585 (1957).
28. Šebenda, J., and J. Kraliček. *Coll. Czechoslov. Chem. Commun.*, **33**, 766 (1958).
29. Yoda, N., and A. Miyake, *J. Polymer Sci.*, **43**, 117 (1960).

Résumé

On a trouvé que les cétène-imines préparées sont des co-catalyseurs utiles pour la polymérisation en milieu alcalin de l' ϵ -caprolactame. Par addition d'une cétène-imine, il est possible de réduire la période d'induction avant le début de la polymérisation, et la polymérisation a lieu rapidement à basse température, située en-dessous du point de fusion du polymère. On propose un mécanisme de réaction pour la polymérisation de l' ϵ -caprolactame au moyen de catalyseur alcalin et de cétène-imine. Ce mécanisme implique la formation d'une *N*-imidoyl-lactame réactionnelle à partir de cétène-imine et de lactame et la propagation de la chaîne par addition graduelle de lactame anionique à l'extrémité d'une molécule, ce qui conduit à la formation de polymère. Ce mécanisme est confirmé par le fait expérimental que l'iminochlorure a le même effet que la cétène-imine sur la polymérisation en milieu alcalin de l' ϵ -caprolactame. On a soigneusement étudié les conditions de polymérisation. La conversion et la viscosité relative du polymère diminuent avec l'augmentation de la concentration en cétène-imine et également avec une augmentation de la température de réaction.

Zusammenfassung

Die dargestellten Ketenimine erwiesen sich als brauchbare Kokatalysatoren für die alkalische Polymerisation von ϵ -Kaprolaktam. Durch Zusatz eines Ketenimins kann eine Induktionsperiode vor dem Polymerisationsstart abgekürzt werden, und die Polymerisation verläuft bei niedriger Temperatur unterhalb des Schmelzpunktes rasch. Ein Polymerisationsmechanismus mit Bildung eines reaktionsfähigen *N*-Imidoyllaktams aus dem Ketenimin und Laktam für ϵ -Kaprolaktam mit Alkali als Katalysator und Ketenimin und Kettenwachstum durch schrittweise Addition von anionischem Laktam an das Molekülende wird angenommen. Dieser Mechanismus wird durch die experimentelle Tatsache gestützt, dass Iminochlorid den gleichen Einfluss auf die alkalische Polymerisation von ϵ -Kaprolaktam besitzt wie Ketenimin. Die Bedingungen für die Polymerisation wurden sorgfältig untersucht. Sowohl Umsatz als auch relative Viskosität des Polymeren nehmen mit steigender Keteniminkonzentration und auch mit steigender Reaktionstemperatur ab.

Received October 30, 1964

Revised February 8, 1965

Prod. No. 4665A

Range of Practical Validity of the Debye and the Rayleigh Equations for Determining Molecular Weights from Light Scattering and Methods Allowing a Limited Extension of This Range*

WILFRIED HELLER, *Department of Chemistry, Wayne State University, Detroit, Michigan*

Synopsis

Using the equivalence of the Rayleigh and the Debye equations on light scattering as a basis, the per cent error in molecular weight committed on using the latter is evaluated by comparing results with those derived from the exact Mie scattering functions. The variable is, by necessity, the quantity $M\bar{V}/\lambda^3$ as long as the radiation diagram is symmetrical, where M is the molecular weight, \bar{V} the partial specific volume of the solute, and λ the wave length in the medium. The errors committed are cosequential only if the dissymmetry is finite. A possible method is outlined for correcting M values obtained from the Debye equation outside of its range of practical validity. It may be applied as long as the dissymmetry does not exceed about 30%. The possibility of determining from light scattering the approximate degree of swelling of latex particles and the size of clusters of spheres is discussed briefly.

Introduction

Derivation of the well known Debye equation¹

$$\tau/c = (32\pi^3 n_1^2/3)(dn/dc)^2 M/N_A \lambda_0^4 = HM \quad (1)$$

is based on the assumption that the scattering effect of solutions due to concentration fluctuations is purely dipolar, free from interference effects, and produced by an undistorted primary electromagnetic field, unaffected by the scattered field. The molecular weight M derived from eq. (1) or from the corresponding equation of lateral scattering

$$R_\theta/c = (3H/16\pi)(1 + \cos^2 \theta) M = K(1 + \cos^2 \theta) M \quad (2)$$

can, therefore, be strictly correct only at $c \rightarrow 0$ and if the molecular dimensions are negligibly small relative to the wavelength used. Here, τ/c is the turbidity per unit path length and per unit concentration c (in grams per cubic centimeter); R_θ is the radiant energy scattered, in a direction forming

* This work was supported by the Office of Naval Research. Part of the results was presented at the 11th Canadian High Polymer Forum, Assumption University, Windsor, Ontario, September 7, 1962.

an angle θ with the incident beam, per unit solid angle, unit intensity of the incident beam, and unit volume of the scattering system; dn/dc is the concentration gradient of the difference between the refractive index of the solution, n_{12} , and that of the solvent, n_1 ; λ_0 is the wavelength *in vacuo*; λ is the wavelength in the solvent and N_A is Avogadro's constant.

Finite values of M derived from these equations are therefore affected by an error which is larger, the larger the root-mean-square volume encompassed by a molecule, V . This error should vary also with dn/dc .

The existence of this error is of no consequence as long as it is smaller than the cumulative experimental error inherent in light-scattering experiments. It has not been possible thus far to state at which values of V/λ^3 and dn/dc the theoretical error equals or exceeds the experimental error. Nevertheless, a major misuse of eqs. (1) and (2) was excluded by the common practice of checking, in a given instance, whether the system investigated exhibits dissymmetry, and to abstain from the use of eqs. (1) and (2) if dissymmetry is found. The open question is whether the theoretical error resulting from the use of these equations is in excess of the overall experimental error before a measurable dissymmetry is found or only after a finite dissymmetry has reached a certain "critical" value. The present paper is concerned with this problem, and with related questions.

Remarks on the Rayleigh Equations

In view of arguments to be introduced later, it is necessary to say first a few words about the Rayleigh equation.

The Rayleigh theory of scattering² yields for the turbidity, per unit concentration and path length, of a dispersed system of spheres

$$\begin{aligned} \tau/c &= 24\pi^3 n_1^4 [(m_0^2 - 1)/(m_0^2 + 2)]^2 (\bar{V}_0 V_0 / \lambda_0^4) \\ &= 24\pi^3 [(m_0^2 - 1)/(m_0^2 + 2)]^2 (\bar{V}_0 / \lambda) V_0 / \lambda^3 \end{aligned} \quad (3)$$

Here, V_0 is the volume of an internally homogeneous, isotropic and compact sphere, \bar{V}_0 is its specific volume, and $m_0 = n_2/n_1$ its refractive index relative to that of the medium, n_2 being its absolute refractive index. Just as in the theory from which eq. (1) follows, it is assumed here that the scattering effect is purely dipolar. Since each sphere represents the site of a single representative dipole (or of an assembly of dipoles the oscillations of which are perfectly in phase), the implicit requirement is that V_0 is infinitely small compared to the wavelength. This is equivalent to the assumption underlying eqs. (1) and (2), namely, that the dimensions of alternating volume elements having, at any instant, a positive and negative excess relative to the average concentration, are infinitely small compared to the wavelength. (This, of course, is possible only if the dimensions of the solute itself are sufficiently small.) The conditions of validity of eqs. (3) and (1) are therefore essentially identical. The only difference is the interpretation of the scattering effect.

Although eq. (3) has, in the past, been applied almost exclusively to dispersions or solutions of compact spheres, such a restriction clearly does not exist. The only requirement is that the spheres be internally homogeneous relative to the incident radiation. In other words, a spherically symmetrical random coil is also accessible to treatment by eq. (3) as long as the intersegmental distances are—as is generally the case—very small compared to the wavelength.* If $(m - 1) \rightarrow 0$, it is even unnecessary that the coil be spherically symmetrical. It may have any shape, provided of course that V_0 is small. One may therefore reformulate eq. (3) for the purpose of M determinations of random coils:

$$\tau/c = 24\pi^3 n_1^4 [(m^2 - 1)/(m^2 + 2)]^2 (M \bar{V}^2 / N_A \lambda_0^4) = GM \quad (4)$$

$$R_\theta/c = (3G/16\pi)(1 + \cos^2 \theta)M = J(1 + \cos^2 \theta)M \quad (5)$$

Here, m represents the relative refractive index of the random coil including the contribution, to n_2 , of the occluded solvent, while \bar{V} is the volume occupied by the random coil and the occluded solvent, per unit weight of the coil, excluding the weight of the occluded solvent.

It would be difficult to obtain a definite value for \bar{V} and m (except in presence of dissymmetry). Fortunately, this is not needed. m and \bar{V} may be replaced by the bulk values m_0 and \bar{V}_0 if these values are known, provided interactions between solvent and solute do not complicate matters. In this case, $[(m^2 - 1)/(m^2 + 2)]^2 \bar{V}^2$ should be a constant [see also eq. (6)], so that any expansion of the solute following the process of solution (increase from \bar{V}_0 to \bar{V}) should be compensated by a decrease from m_0 to m . Use of eq. (4) for the proper systems eliminates therefore the need of dn/dc measurements.

Whenever m_0 and \bar{V}_0 can be used, the simultaneous use of eqs. (1) and (3) is of particular interest. The former is then used for determining M , while the latter gives the radius, r_e , of the equivalent compact (hard) sphere. Since there should be a simple relationship between the radius of this equivalent "optical" sphere and the radius R_e of the equivalent "hydrodynamic" sphere,³ a closer theoretical and experimental investigation of this correlation may prove very fruitful.

Principle of the Test of Validity of Equations (1) and (2)

The range of (V_0/λ^3) and m values within which eq. (3) may be used without committing an error of consequence can easily be defined, since the Mie equations for the scattering of spheres,⁴ which is unlimited as to V_0/λ^3 and m , reduce to eq. (3) if $V_0/\lambda^3 \rightarrow 0$. A systematic evaluation of the range of practical validity of eq. (3) has been given recently.⁵ No

* Strictly speaking, these intramolecular discontinuities have a finite effect. This effect is very small, however, and of the same order of magnitude as the effect due to the discontinuities within the medium. The latter are neglected in eqs. (1) and (2). They are, as is well known, the cause of the finite scattering by liquids, treated quantitatively thus far only as the result of thermal fluctuations in density.

similar direct check of the range of validity of eqs. (1) and (2) is possible, since a general theory of scattering due to concentration fluctuations, not restricted to independent very small volume elements, is not available.* One may, however, again use the Mie data, provided it is certain that eqs. (1) and (4), are quantitatively equivalent. If they are, then it is necessary that

$$dn/dc = (3n_1\bar{V}/2)[(m^2 - 1)/(m^2 + 2)] \quad (6)$$

Assuming eq. (6) to be an equality, a new refractive index mixture rule

$$n_2 = n_1^2[1 + 2A (dn/dc)]/[n_1 - A (dn/dc)] \quad (7)$$

where

$$A = 2/3\bar{V}$$

was derived a number of years ago.⁷ More recently, Zimm and Dandliker⁸ developed a general refractive index mixture rule which reduces to eq. (7) if the dimensions of the refracting solute are small compared to the wavelength. This important finding and an additional proof of the unrestricted validity of eq. (7) if $V_0/\lambda^3 \rightarrow 0$ and $c \rightarrow 0$, given elsewhere,^{8a} establishes the full quantitative equivalence of the Debye and Rayleigh equations. Consequently, the Mie data can be used for an indirect quantitative check of the range of validity of eqs. (1) and (2).

Definition of the Quantities Used

The Mie theory considers the quantity α . For compact spheres of radius r , $\alpha = 2\gamma\pi/\lambda$. The quantity corresponding to α in the case of spherically symmetrical random coils is $(6\pi^2M\bar{V}/\lambda^3N_A)^{1/3}$, so that the relationship between α and M is

$$M\bar{V}/\lambda^3 = N_A\alpha^3/6\pi^2 = 1.017385 \times 10^{22}\alpha^3 \quad (8)$$

On using the green Hg line ($\lambda_0 = 5460.73$ A.) as the standard wavelength and water at 25°C. as the solvent ($\lambda = 4093.57$ A.),

$$M\bar{V}_{\text{Hg}} = 6.978978 \times 10^8\alpha^3 \quad (9)$$

The data to be given will be expressed also in terms of the latter quantity.

The relationship between dn/dc and m is implicit in eq. (6). In the limiting case that $(m - 1) \rightarrow 0$, the latter relation simplifies to

$$m = [(dn/dc)/n_1\bar{V}] + 1 \quad (10a)$$

or

$$dn/dc = \bar{V}(n_2 - n_1). \quad (10b)$$

* That such a general theory may be possible, is indicated by Debye's success⁶ in extending the range of validity of Einstein's equation of light scattering due to density fluctuations by introducing the correlation function.

There are two possible types of deviation of data calculated from eqs. (1) or (2) relative to the Mie data: (1) the deviation, at a given $M\bar{V}/\lambda^3$, of τ/c or R_θ/c ; (2) the deviation, at a given τ/c or R_θ/c , of $M\bar{V}/\lambda^3$. Only the latter type of deviation is of interest here. In addition, only those angular scattering data which are pertinent to $\theta = 90^\circ$ will be considered. The per cent deviation in the molecular weight obtained from R_{90}/c on using eq. (2) will be defined by

$$\Delta_M = \left\{ [(M\bar{V}/\lambda^3)_D - (M\bar{V}/\lambda^3)] / (M\bar{V}/\lambda^3) \right\} \times 100 = [(M_D - M) / M] \times 100 \quad (11)$$

where the quantities $(M\bar{V}/\lambda^3)_D$ and M_D are those obtained from the Debye equation and $(M\bar{V}/\lambda^3)$ and M (without subscript) refer to the "true" $(M\bar{V}/\lambda^3)$ and M . The per cent deviation in molecular weight obtained from (τ/c) on using eq. (1) is similarly defined by Δ'_M . The latter is, of course, of interest only if sufficiently long absorption cells are used so as to make (τ/c) a reasonably large quantity.*

The Δ_M and Δ'_M values give immediately the correction factors

$$F = 100 / (\Delta_M + 100) \quad (12)$$

and

$$F' = 100 / (\Delta'_M + 100) \quad (12a)$$

by which M_D (M'_D) has to be multiplied in order to obtain the correct M value.

It should be noted here, that, strictly speaking, Δ_M and Δ'_M represent the percent deviations in the molecular volume, obtained from eqs. (5) and (4), respectively, relative to the Mie values. They represent, however, also the per cent deviations in M in eq. (2) or (1) in view of the interrelation given by eq. (6).

Results

Table I presents the per cent deviations from the true values of molecular weights determined with eq. (2) [or eq. (5)]. The data are given for widely varied values of $M\bar{V}/\lambda^3$ and m . They are illustrated by Figures 1 and 2. An interesting feature is the fact (Fig. 2) that eqs. (2) and (5) perform, at a given M and \bar{V} , better the larger m [or (dn/dc)]. The relationship is linear within the range of m tested. It is more complex at larger m values which are not of interest here.

The results are summarized in Figure 3 which represents an error contour chart, i.e., a topographical map in which elevations are replaced by the per cent deviations in M values obtained from eq. (2) or (5) (solid curves).

Of major practical interest are the 2 and 5% contour lines. The

* Use of very long absorption cells is very uncommon for M determinations, although this method evidently can and has been used.⁹ The advantage is that M data are absolute data since no instrument constant is needed.

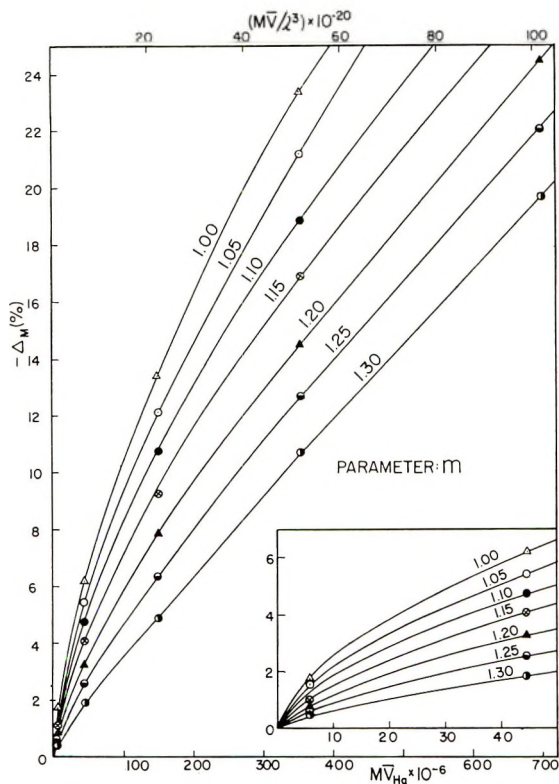


Fig. 1. Variation of the per cent error, Δ_M , in molecular weight as a function of $M \bar{V}/\lambda^3$ or $M \bar{V}_{HR}$. Use of Debye equation in connection with 90° scattering. Parameter m : relative refractive index.

TABLE I
Per Cent Deviation, $-\Delta_M$, of Molecular Weight M Calculated from Equation (2); ($\theta = 90^\circ$)

$M \bar{V}/\lambda^3$ $\times 10^{-20}$	$M \bar{V}_{HR}$ $\times 10^{-6}$	$-\Delta_M, \%$						
		$m = 1.00^a$	$m = 1.05$	$m = 1.10$	$m = 1.15$	$m = 1.20$	$m = 1.25$	$m = 1.30$
0.8139	5.583	1.7	1.60	(0.7)	1.04	0.77	0.62	0.43
6.511	44.67	6.2	5.46	4.74	4.06	3.26	2.58	1.88
21.98	150.7	13.4	12.1	10.7	9.25	7.82	6.40	4.87
52.09	357.3	23.4	21.2	18.9	16.9	14.5	12.7	10.7
101.17	697.9	33.7	31.5	29.2	26.8	24.5	22.1	19.7

^a Extrapolated values.

former line is approximately equal to the average cumulative experimental error involved in careful determinations of M . Any theoretical error within the area encompassed by the 2% line, and the abscissa is therefore practically inconsequential. On the other hand, $(M \bar{V}/\lambda^3)$ - m combinations within the area beyond the 5% line clearly are unsuitable for quantitative

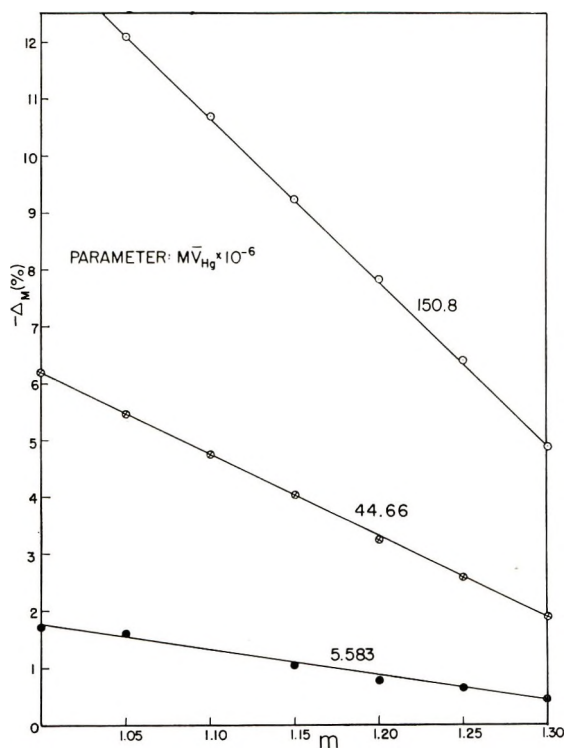


Fig. 2. Variation of the per cent error, Δ_M , in molecular weight as a function of m . Use of Debye equation in connection with 90° scattering. Parameter: $M\bar{V}_{Hg}$.

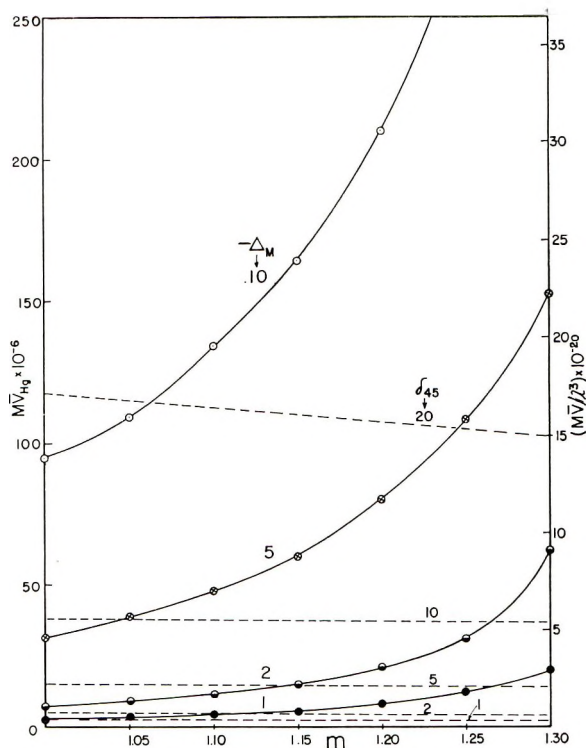
applications of eq. (2) or (5). Table II gives the limiting $M\bar{V}_{Hg}$ values above which Δ_M exceeds the stated percentage values.

Table III gives Δ'_M , i.e., the per cent deviation of M values calculated from (τ/c) according to eq. (1) or (4). Figures 4, 5, and 6 illustrate these data. Table IV, finally, gives the (MV/λ^3) - m combinations at which Δ'_M is 1, 2, 5, and 10%. The differences between Δ_M and Δ'_M are insignificant

TABLE II
 $M\bar{V}_{Hg} \times 10^{-6}$ for Various Per Cent Deviations of Molecular Weights, $-\Delta_M$, Calculated from Equation (2) for $\theta = 90^\circ$ ^a

m	$M\bar{V}_{Hg} \times 10^{-6}$			
	$-\Delta_M = 1.0\%$	$-\Delta_M = 2.0\%$	$-\Delta_M = 5.0\%$	$-\Delta_M = 10.0\%$
1.00	2.5	7.0	31	94
1.05	3.5	9.0	39	109
1.10	4.5	11.5	48	134
1.15	5.5	15.0	60	164
1.20	8.0	21.0	80	210
1.25	12.0	31.0	108	266
1.30	20.0	62.0	152	332

^a Wavelength in solvent = 4093.57 Å.

Fig. 3. Error contour chart for Δ_M (see text).

at low values of (MV/λ^3) and m , but pronounced at large values of MV/λ^3 and m .

TABLE III
Per Cent Deviation from True Value, $-\Delta'_M$, of Molecular Weight Calculated from Equation (1)

$M \bar{V}/\lambda^3$ $\times 10^{-20}$	$M \bar{V}_{HR}$ $\times 10^{-6}$	$-\Delta'_M, \%$						
		$m = 1.00^a$	$m = 1.05$	$m = 1.10$	$m = 1.15$	$m = 1.20$	$m = 1.25$	$m = 1.30$
0.8139	5.583	1.6	1.40	1.18	0.99	0.78	0.60	0.43
6.511	44.67	6.2	5.42	4.69	3.94	3.21	2.51	1.80
21.98	150.7	13.3	11.81	10.35	8.89	7.44	5.99	4.58
52.09	357.3	22.0	19.97	17.89	15.81	13.68	11.55	9.42
101.7	697.9	29	29.36	26.91	24.44	21.94	19.42	16.90

^a Extrapolated values.

Dissymmetry as an Auxiliary Analytical Argument

The results given define completely the range of particle or molecular weights accessible to the equations tested if the particles or molecules are compact and nonswelling so that the specific volume \bar{V} is identical with \bar{V}_0 of the bulk material. If $\bar{V} \neq \bar{V}_0$, it is either necessary to determine \bar{V} or to

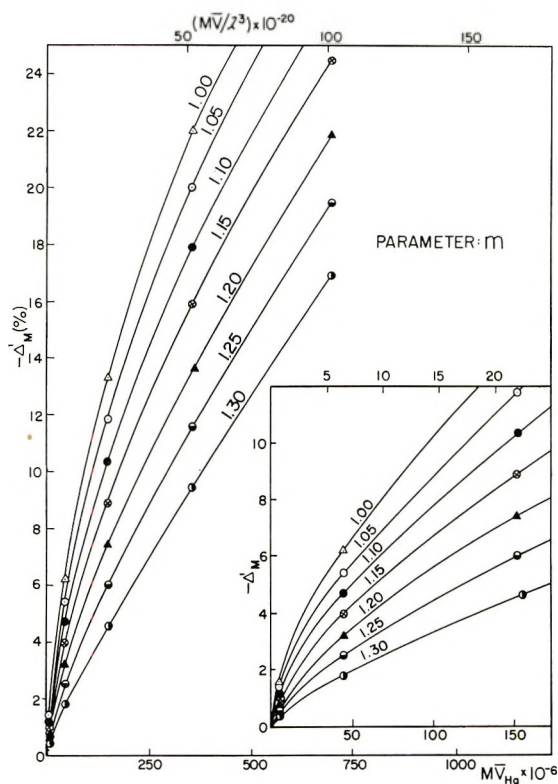


Fig. 4. Variation of the percent error, Δ'_M , in molecular weight as a function of MV/λ^3 or $M\sqrt{V}_{Hg}$ and for various m values. Use of Debye equation in connection with turbidity measurements.

eliminate, by use of a suitable additional argument, the need to know its numerical value if one wishes to take full advantage of the results given. A suitable additional argument is the dissymmetry. As already stated in the introduction, appearance of dissymmetry has always been the qualita-

TABLE IV
 $(M\sqrt{V}/\lambda^3) \times 10^{-20}$ for Various Per Cent Deviations of Molecular Weights, $-\Delta_M$, Calculated from Equation (1) or (4)

m	$(M\sqrt{V}/\lambda^3) \times 10^{-20}$			
	$-\Delta_M = 1.0\%$	$-\Delta_M = 2.0\%$	$-\Delta_M = 5.0\%$	$-\Delta_M = 10.0\%$
1.00 ^a	0.25	1.00	4.50	13.8
1.05	0.35	1.30	5.75	17.3
1.10	0.50	1.75	7.00	21.0
1.15	0.75	2.25	9.00	25.0
1.20	1.30	3.25	12.0	32.5
1.25	1.75	4.75	17.0	42.5
1.30	2.75	7.25	25.0	55.5

^a Extrapolated values.

tive argument of probable invalidity of eqs. (1) and (2). It remained uncertain, however, whether this yardstick is too conservative or too liberal. This question can now be resolved by using, again, data obtained from the Mie theory. Advantage is taken of existing angular scattering functions.¹⁰ Table V, gives the per cent excess, δ_θ , of the intensity of light scattered at the angle θ relative to that at $(180 - \theta)$. The main data (δ_{45}) refer to the conventional angles 45° and 135° , those in parentheses (δ_0) pertain to the

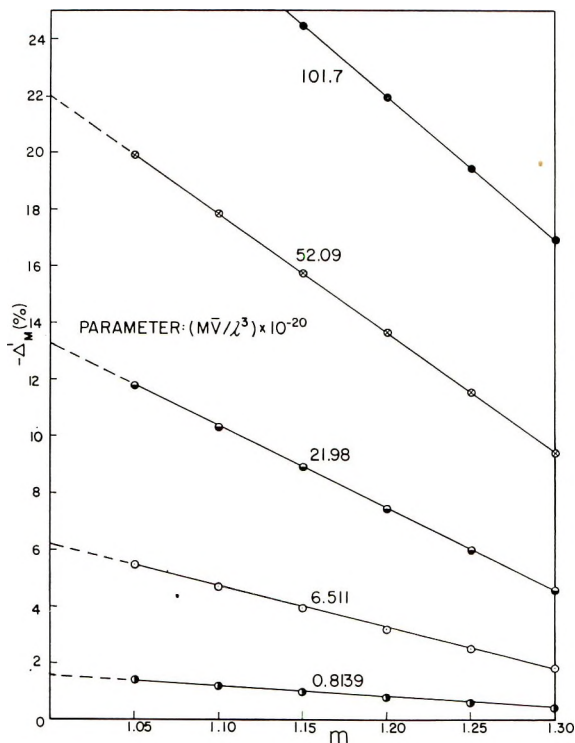


Fig. 5. Variation of the percent error, Δ'_M , in molecular weight as a function of m . Use of Debye equation in connection with turbidity measurements. Parameter: $M\bar{V}/\lambda^3$.

angles 0° and 180° ("extreme" dissymmetry). The data for $m = 1.0$ are the result of secure extrapolation. It follows from Figure 7 and Table V that, to a satisfactory approximation,

$$\log M\bar{V}_{Hg} = 6.26 + 1.39 \log \delta_{45} \quad (13)$$

as long as δ_{45} does not exceed $\sim 45\%$ and $m \leq 1.10$. Interpolations between the data of Table V are therefore relatively easy in these cases.

One derives from these data easily the $M\bar{V}/\lambda^3$ values and associated m values at which δ_{45} reaches value of 1, 2, 5, and 10%, respectively. The dissymmetry contour chart thus obtained is superimposed upon the error contour chart of Figure 3 (dashed lines).

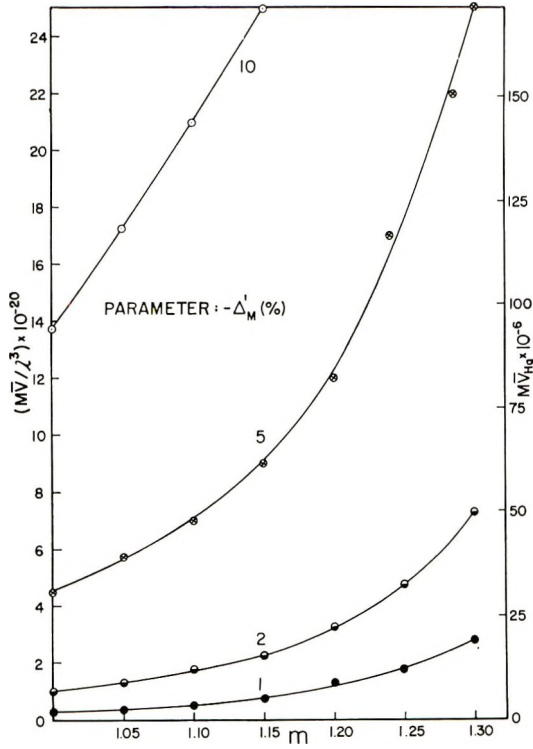


Fig. 6. Error contour chart for Δ'_M (see text).

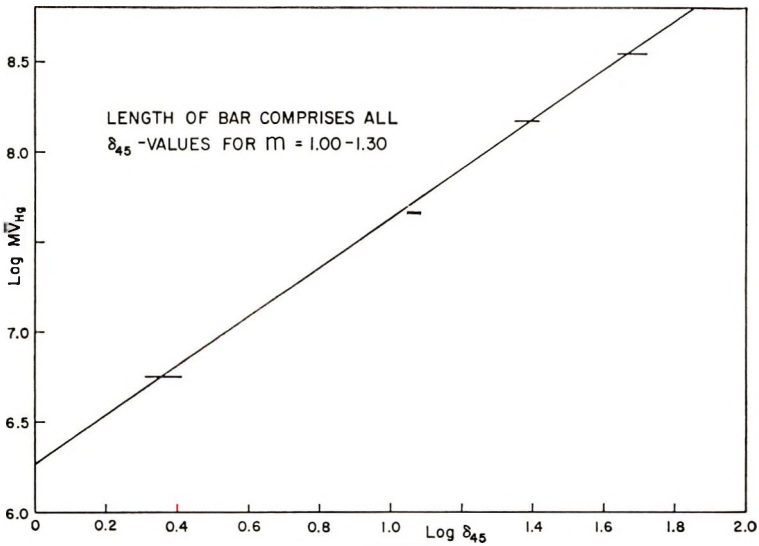


Fig. 7. Variation of Mie dissymmetry with $M\bar{V}_{Hg}$ including test of dissymmetry equation eq. (13).

TABLE V
 Per Cent Excess of R_{45} Relative to R_{135} (δ_{45}) and Per Cent Excess of R_0 Relative to R_{135} (δ_0)

$M\bar{V}/\Lambda^3$ $\times 10^{-20}$	$M\bar{V}_{HK}$ $\times 10^{-6}$	δ_{45} (and δ_0)									
		$m = 1.00$	$m = 1.05$	$m = 1.10$	$m = 1.15$	$m = 1.20$	$m = 1.25$	$m = 1.30$	Eq. (13)		
0.8139	5.583	2.18 (3.15)	2.04 ^a (2.86) ^a	2.32 (3.27)	2.38 (3.31)	2.49 (3.43)	2.49 (3.52)	2.57 (3.52)	2.2		
6.511	44.67	11.0 (13.7)	11.0 (13.8)	11.0 (14.1)	11.0 (14.3)	11.1 (14.6)	11.1 (15.0)	11.1 (15.0)	10		
21.98	150.7	23.0 (34.2)	23.5 (34.6)	24.0 (34.9)	24.4 (35.4)	24.9 (35.8)	25.5 (36.3)	26.0 (36.9)	24		
52.09	357.3	45.0 (70.3)	45.8 (70.0) ^a	47.4 (71.7)	48.2 (72.4)	49.2 (73.2)	50.4 (74.4)	51.6 (75.6)	45		
101.7	697.9	82.3 (134)	84.1 (135.5)	85.9 (137.5)	87.8 (139)	90.0 (141.5)	92.4 (144)	95.2 (147)	72		
175.8	1206.0	144 (255)	148 (259.5)	152.5 (264.5)	157.5 (270)	163 (277)	169.5 (285)	177 (295)	—		

^a Questionable values.

The most important result to follow from this double contour chart is that the largest theoretical error committed on using eq. (2) for $\theta = 90^\circ$ under the most unfavorable condition, i.e., if $(m - 1) \rightarrow 0$, is between 1 and 2% if a well detectable dissymmetry of 2% is used as the limit for application of these equations. For polymer molecules in a poor solvent (tight coiling; low \bar{V}) and, particularly, for polymer molecules dissolved in a highly refracting poor solvent, an even larger dissymmetry is clearly allowed before the theoretical error committed, at a given $M\bar{V}$, becomes important. Thus, $-\Delta_m$ hardly exceeds 2% if $\delta_{45} = 10\%$ provided that $m \sim 1.25$). For the same reasons, the range of permissible practical application of the equation is even larger for globular macromolecules and compact particles. There are, therefore, many instances where one will be able to use safely eqs. (1) and (2) in spite of pronounced dissymmetry.

It is clear from the preceding discussion that not the appearance of dissymmetry, but rather the absolute magnitude of dissymmetry decides the limits for useful practical application of the equations tested. It is informative to define roughly the approximate upper limits of M values obtainable from these equations without consequential error. Polystyrene may be chosen as a typical example. For molecules as tightly packed as they are in the bulk material, one may set $\bar{V}_0 \sim 1.0$ and $m_0 \sim 1.2$. The limiting molecular weight obtained from R_{90}/c with a theoretical error not in excess of 2% would then be 12×10^6 . The dissymmetry, δ_{45} , should then amount to about 4%. This limiting value of M would therefore apply to solutions in a poor solvent where tight segmental packing, roughly comparable to that in bulk, applies. Methyl ethyl ketone may approximate this type of solvent. On the other hand, in dichlorethane, a relatively good solvent, polystyrene is a greatly expanded coil. One calculates in this instance from literature data¹¹ a \bar{V} value such that even at a molecular weight as small as 500,000, $M\bar{V} \geq 30 \times 10^6$. The error in M on using the equations tested should then be nearly 5% since m is, in this case, very close to 1.0. As a rough rule of thumb, one may therefore establish for random coils in good solvents an M value of about 250,000 as the upper safe limit for application of the equations tested without further precautions being necessary. (For macromolecules which are not spherically symmetrical in shape, the limit in M may be much smaller.)

It follows from all this that it is strongly advisable to use for M determinations on randomly coiled macromolecules the poorest possible solvents, which, in addition, have the highest possible refractive index difference relative to the solute (if the objective is merely the determination of molecular weights). The range of M values accessible to eqs. (1) and (2) is then largest. Moreover, the experimental errors are also smallest on account of the maximal scattering intensities achieved under these conditions.

Use of the Debye and Rayleigh Equations outside of Their Range of Practical Validity

If the molecular (particle) dimensions are not small compared to the wavelength, the scattered wavelets emanating from various volume elements of the scattering body are no longer in phase, particularly those originating in the peripheral sections of the body. Quadrupolar and, eventually, multipolar oscillations contribute then to the scattering effect. In addition, the primary field at the site of the now relatively large scattering body becomes distorted, and the scattered field which is now not negligible alters the primary field.

These complications can be avoided except for the attenuating effect of the phase differences, (quadrupolar and multipolar contributions), if $(m - 1) \rightarrow 0$. In this limiting case, the primary field remains homogeneous and the scattered field is too weak to affect the former. One may then still use the Rayleigh or Debye equation on multiplying it by the Rayleigh-Gans attenuation factor $P(\theta)$.^{12,13} Equation (2) must then be written:

$$R_\theta/c = K(1 + \cos^2 \theta)MP(\theta) \quad (14)$$

Similarly eq. (5) becomes

$$R_\theta/c = J(1 + \cos^2 \theta)MP(\theta). \quad (15)$$

Since it is assumed that $(m - 1) \rightarrow 0$

$$[(m^2 - 1)/(m^2 + 2)] \rightarrow (1/3)(m^2 - 1) \quad (16)$$

so that the explicit form of eq. (15) simplifies to

$$R_\theta/c = (M \bar{V}^2 \pi^2 / N_A \lambda^4)(m^2 - 1)^2 [(1 + \cos^2 \theta)/2] P(\theta) \quad (17)$$

Equation (17) is the classical Rayleigh-Gans equation as given by Rayleigh¹² except for the introduction, in the present instance, of M .

Since the phase differences are largest for the peripheral volume elements of a scattering body, the attenuation is smaller and the attenuation factor $P(\theta)$ is larger (closer to 1.0) for spheres of uniform density than for the more voluminous random coils of equal mass (as long as the maximal phase differences $< 1 \lambda$). According to Debye¹⁴

$$P(\theta)_{\text{spheres}} = [(3/x^2)(\sin x - x \cos x)]^2 \quad (18)$$

and

$$P(\theta)_{\text{coils}} = (2/y^2) [e^{-y} - (1 - y)] \quad (19)$$

Here,

$$x = 2\alpha \sin (\theta/2)$$

$$\alpha = 2r \pi/\lambda$$

$$y = (8\pi^2/3\lambda^2) \sin^2 (\theta/2) (\sqrt{r^2})^2$$

r is the radius of the sphere, and $\sqrt{r^2}$ is the root-mean-square end-to-end distance. [Equation (18), formulated differently, had already been given by Gans.¹³]

The determination of M beyond the range of practical validity of eqs. (1)–(5) is therefore more complicated unless one resorts to the ingenious dodge introduced by Zimm¹⁵: in view of the homogeneity of the field, if $(m - 1) \rightarrow 0$, the phase differences are zero at $\theta = 0$ (they are maximal at $\theta = 180^\circ$) so that extrapolation of angular scattering data to the forward direction allows one to use eqs. (1)–(5) in their original form, since $P = 1.0$ as $\theta \rightarrow 0$. The decisive advantage of this method over other possible procedures is that it furnishes also information on the type of the scattering body (compact sphere or random coil), on its characteristic dimensions (radius or gyration radius) and on the degree of polydispersity if the molecular weight is not single-valued. If this additional information is not needed, the far less time-consuming three-point method (a combination of R_{90}/c and δ_{45} measurements), first suggested by Doty and Steiner¹⁶ is preferable. The method of these authors is based upon Rayleigh-Gans data. The availability of the Mie data (Table V) allows one to introduce a related more powerful alternative. One determines first, from a measurement at $\theta = 90^\circ$ and by means of eq. (2), a first approximation value of M . A subsequent measurement of δ_{45} yields $M\bar{V}$ by interpolation from Table V or from Figure 7. As long as $\delta_{45} \leq 30\%$, the *a priori* unknown value of m is clearly immaterial as long as it is ≤ 1.10 . This is unquestionably always the case for random coils in good solvents. Having thus established the value of $M\bar{V}$, one immediately obtains Δ_M [eq. (11), Fig. 1, Table I] and F so that the first approximation value of M can be corrected to the true M value provided one picks the proper m value. Since F is quite sensitive to m , in contradistinction to δ_{45} , one will pick F values applicable to $m = 1.05$ which is intermediate between the probable extremes of m values which may occur for random coils in good solvents (1.00–1.10). Taking for instance a value of δ_{45} of 30%, F results as 0.875, while its true value may be between the extremes 0.86 and 0.89. The residual possible error in M is therefore, in this most unfavorable case, $\leq 3.5\%$. The present method clearly gives not only M , but in addition, V .

The scope of applicability of this method differs, of course, widely for random coils and compact spheres. In the former instance, we can use it only as long as dissymmetries calculated from eq. (19) closely approximate the Mie data in Table V. This applies as long as $\delta_{45} \leq 30\%$. The upper limiting error in M , which can thus be handled is therefore $\sim 20\%$. This corresponds to a limiting $M\bar{V}_{Hg}$ value of $\sim 200 \times 10^6$.

If the scattering bodies are compact homogeneous spheres, the method proposed may be used without any restriction as to the magnitude of δ_{45} (or of m). The situation is particularly simple if $m = m_0$ and $\bar{V} = \bar{V}_0$. Spheres which swell in the liquid in which they are immersed without dissolving (crosslinked polymer spheres) and without losing their optical homogeneity may, however, be handled also, although $m (\neq m_0)$ and \bar{V}

($\neq \bar{V}_0$) are not known. It is then merely necessary to obtain the true values of M , \bar{V} , and m by successive approximation. First, M obtained from eq. (2) is corrected by means of F , the latter having been obtained with the aid of δ_{45} assuming that $m = 1.05$ (or $m = 1.00$); one now inserts the \bar{V} value obtained in eq. (6) or (10) which yields the first approximation value of m . One is now in a position to obtain a second approximation value for F , M , and \bar{V} . It thus appears possible to determine the degree of swelling by a rather simple and accurate optical method. The only complication which arises for an extension of the method to large values of $M\bar{V}/\lambda^3$ is that eqs. (6) and (10) are, in principle, restricted to molecular (particle) dimensions small compared to the wavelength. Correction factors up to $M\bar{V}/\lambda^3 = 3.43 \times 10^{25}$ ($M\bar{V}_{Hg} = 2.36 \times 10^{12}$) are, however, easily derived from tabular data already available.¹⁷ As long as δ_{45} does not exceed 50%, no correction is necessary, since the error in m resulting from the use of eq. (6) is then still less than 2% (if the true m value ≤ 1.30). It may be noted that the method of successive approximation may, in principle, be used also for the correction of M values obtained from eq. (2). However, since the m -dependence of δ_{45} is very small at the low dissymmetry values that may be considered ($\delta_{45} \leq 30\%$), no significant improvement can be expected from successive approximation.

Another case where the method of successive approximation of M , \bar{V} , and m by measurements at $\theta = 45^\circ$, 90° , and 135° may be useful, is that of spherical or nearly spherical aggregates of very small compact spherical particles. As pointed out long ago,¹⁸ the scattering effect produced by clusters of particles is a function of the distances between the individual particles due to the variation of the ("external") interference effect with the magnitude of these distances.

A quantitative investigation of this effect, carried out by Landshoff,¹⁹ following a suggestion to that effect by the writer, lead to an equation equivalent to eq. (18). Unfortunately, the restriction to aggregates where $(m - 1) \rightarrow 0$, which is necessary with this equation, severely limited its potential application, since, generally, far less liquid is occluded within aggregates of compact spheres than within randomly coiled polymer molecules. Application of the method of successive approximation should now make it possible to determine not only the size of such clusters, but also the volume ratio of scattering material and liquid within such a cluster. A simple application will of course be possible only if the clusters in a given scattering system are all of about the same size and if one restricts the analysis to systems exhibiting a dissymmetry, δ_{45} , not in excess of about 50%.

References

1. Debye, P., *J. Appl. Phys.*, **15**, 338 (1944).
2. Rayleigh, J. W. S., *Phil. Mag.*, **12**, 81 (1881), and various other publications.
3. Flory, P. J., *Principles of Polymer Chemistry*, Cornell Univ. Press, Ithaca, N. Y., 1953.
4. Mie, G., *Ann. Physik*, **25**, 377 (1908).
5. Heller, W., *J. Chem. Phys.*, **42**, 1609 (1965).

6. Debye, P., *J. Chem. Phys.*, **31**, 680 (1959).
7. Heller, W., *Phys. Rev.*, **68**, 5 (1945).
8. Zimm, B. H., and W. B. Dandliker, *J. Phys. Chem.*, **58**, 644 (1954).
9. Heller, W., and H. B. Klevens, *Phys. Rev.*, **67**, 61 (1945).
10. Pagonis, W. J., and W. Heller, *Angular Scattering Functions for Spherical Particles*, Wayne State Univ. Press, Detroit, 1960.
11. Outer, P., C. I. Carr, and B. H. Zimm, *J. Chem. Phys.*, **18**, 830 (1950).
12. Rayleigh, J. W. S., *Proc. Roy. Soc. (London)*, **A84**, 25 (1911); *ibid.*, **A90**, 219 (1914).
13. Gans, R., *Ann. Physik*, **76**, 29 (1925).
14. Debye, P., *J. Phys. Colloid Chem.*, **51**, 18 (1947).
15. Zimm, B. H., *J. Chem. Phys.*, **16**, 1093, 1099 (1948).
16. Doty, P., and R. F. Steiner, *J. Chem. Phys.*, **18**, 1211 (1950).
17. Nakagaki, M., and W. Heller, *J. Appl. Phys.*, **27**, 975 (1956), Tables I and III.
18. Heller, W., and G. Quimfe, *J. Phys. Chem.*, **46**, 765 (1942); see particularly footnote 4.
19. Landshoff, R., *J. Phys. Chem.*, **46**, 778 (1942).

Résumé

En employant l'équivalence des équations de Rayleigh et de Debye pour la diffusion lumineuse, on a évalué le pourcentage d'erreur dans la détermination du poids moléculaire en employant cette dernière équation en comparant les résultats avec ceux obtenus à partir des fonctions exactes de la diffusion de Mie. La variable est, par nécessité, la quantité $M \bar{V}/\lambda^3$ aussi longtemps que le diagramme est symétrique (M est le poids moléculaire, \bar{V} le volume partiel spécifique du soluté et λ la longueur d'onde dans le milieu). Les erreurs commises ont lieu seulement si la dissymétrie est finie. On esquisse une méthode possible pour corriger les valeurs de M obtenues à partir de l'équation de Debye en dehors de son domaine de validité pratique. Elle peut être appliquée aussi longtemps que la dissymétrie ne dépasse pas environ 30%. On discute brièvement de la possibilité de déterminer, à partir de la diffusion lumineuse, le degré approximatif de gonflement des particules de latex et la grosseur des agrégats de particules sphériques.

Zusammenfassung

Auf Grundlage der Äquivalenz der Rayleigh- und der Debye-Lichtstreuungsgleichung wurde der prozentuelle Fehler im Molekulargewicht bei Benützung letzterer durch Vergleich der Ergebnisse mit den aus den exakten Mie-Streuungsfunktionen abgeleiteten ermittelt. Die Variable ist, solange das Streudiagramm symmetrisch ist, notwendigerweise die Grösse $M \bar{V}/\lambda^3$. (M ist das Molekulargewicht, \bar{V} das partielle spezifische Volumen des Gelösten und λ die Wellenlänge im Medium.) Die auftretenden Fehler haben nur bei endlicher Dissymmetrie Bedeutung. Eine Methode zur Korrektur der aus der Debye-Gleichung ausserhalb ihres praktischen Geltungsbereiches erhaltenen M -Werte wird angegeben. Sie kann bei Dissymmetrie nicht über 30% angewendet werden. Die Möglichkeit, durch Lichtstreuung den angenäherten Quellungsgrad von Latexteilchen zu bestimmen, wird diskutiert.

Received September 2, 1964

Revised March 8, 1965

Prod. No. 4689A

Energetic and Entropic Components of Tension in Elastomeric Wool Fibers

A. R. HALY, *Division of Textile Physics, C.S.I.R.O. Wool Research Laboratories, Ryde, Sydney, Australia*

Synopsis

Tension against temperature data were obtained for both unreduced wool fibers and fibers in which some of the disulfide bonds had been reduced by a thiol. The measurements were done while the fibers contained a diluent. Coefficients of volume thermal expansion were also measured. From the results the ratio of the energetic component of tension to the total tension (f_e/f) was calculated. Most values of f_e/f were within the range ± 0.20 . In the case of unreduced wool f_e/f changed from negative to positive as the extension increased. With a reduced sample containing 8% of the native disulfide, f_e/f was negative and nearly constant over the range of extension employed. The change for unreduced wool follows from extension-dependent interactions between polypeptide chains. The results indicate that, for unperturbed polypeptide chains from wool taken into solution following disulfide reduction, the end-to-end distance will decrease with increase of temperature, a partially extended form being the lower energy state.

INTRODUCTION

A number of investigators¹⁻⁶ have attributed rubberlike properties to wool or hair keratin. In some cases this has meant only that the material exhibits long-range elasticity, and in other cases that the stress at a fixed extension is chiefly entropic in origin. The extension of wool fibers containing absorbed water is complicated by a concurrent decrease of α -crystallinity and increase of β -crystallinity⁷; furthermore at any instant during extension at convenient rates the number of effective crosslinks between polypeptide chains is very high, and equilibrium tensions are attained extremely slowly. Hence analysis according to theories that have been developed for uniform, relatively lightly crosslinked elastomers is not practical.

However scrutiny of the references cited above indicates that some absorbates are capable of partially or completely destroying the crystallinity of wool, and otherwise greatly reducing the number of effective crosslinks. A diagnostic feature of these changes is an increase in the entropic component of the tension in an extended fiber. Such absorbates can cause unconstrained wool fibers to contract to a length less than their native length. Contraction of this type is frequently termed supercontraction. When lithium bromide solution is the supercontracting reagent the decrease in length proceeds in two distinct stages^{6,8}: the first stage (which

can be reversed by washing out the reagent) is possible at 20°C. in LiBr concentrations in excess of $\sim 6.5M^9$; second-stage supercontraction, which is irreversible, proceeds at higher temperatures. Following a test which indicated the chiefly entropic nature of the tension in wool fibers in LiBr solution,⁶ studies of crosslinking by measurement of equilibrium longitudinal moduli were undertaken.¹⁰

The purpose of this paper is to report a more detailed study of the components of tension in normal and modified wool fibers in aqueous LiBr, making use of some of the considerable advances in the theory of elastomers which have been made in recent years.

The total tension f in a specimen at constant length is the sum of the energetic (f_e) and entropic (f_s) components of the tension. The energetic component is given by

$$f_e/f = -T \left| \frac{\partial (\ln f/T)}{\partial T} \right|_{V,L} \quad (1)$$

where T represents the absolute temperature, and V and L are, respectively, the volume and length of the specimen.

It is often inconvenient to perform experimental work with the specimen maintained at constant volume, and Flory et al.¹¹ have shown that eq. (1), together with the elastic equation of state, yields

$$f_e/f = -T \left| \frac{\partial (\ln f/T)}{\partial T} \right|_{P,L} - [\beta T / (\alpha^3 - 1)] \quad (2)$$

in the extension region in which Gaussian statistics are applicable. Here P represents the pressure, β the volume thermal expansion coefficient of the specimen, and α the strain ratio, i.e., extended length/force-free length. From eq. (2) we find

$$f_e/f = 1 - T/f \left| \frac{\partial f}{\partial T} \right|_{P,L} - [\beta T / (\alpha^3 - 1)] \quad (3)$$

This equation is valid for both unswollen and swollen systems.¹²

In a study¹⁰ of the relative degrees of crosslinking in natural and modified wools, some evidence appeared that the Gaussian approximation did not hold at any attainable extension. When this is the case, Smith et al.¹³ showed that eqs. (2) and (3) should contain another term, but that for many conditions the term is negligible. In the present work the correcting term is approximately $(1/20) [\beta T / (\alpha^3 - 1)]$ and has been neglected.

Accordingly, following measurements of tension as a function of temperature at constant pressure and specimen length, eq. (3) was applied to calculate the energetic component of the tension. Direct evidence of the validity of this approach was provided by Allen et al.,¹⁴ who found satisfactory agreement between determinations of f_e/f from constant pressure and from constant volume measurements on natural rubber.

In the case of wool it was found that f_e/f was usually within the range ± 0.20 , i.e., the entropic component of tension was usually 80–100% of the total tension. For unreduced fibers f_e/f was negative at low extensions, but increased to a positive value as the extension increased. Fibers in which 92% of the disulfide bonds were reduced and alkylated gave negative

values of f_c/f at all extensions. These features are not unique to wool and are explicable in terms of current ideas derived from studies of many polymers in the elastomeric state.

EXPERIMENTAL

Three different wool samples were used, those previously¹⁰ designated samples, 0, 10b, and 14b. Sample 0 is an unreduced Corriedale wool; the other two samples were from the same fleece but had undergone disulfide reduction and alkylation, and will be referred to as S-methyl wools. Their disulfide contents were (10b) 42% and (14b) 8% of the original value.

Measurement of Thermal Expansion

The coefficient of volume thermal expansion β of the wools at swelling equilibrium in 8*M* unbuffered LiBr solution was measured with the aid of a microscope. Ten fiber snippets from each sample were immersed in the solution in a glass cell and irreversibly contracted by heating for 3 hr. at 95–100°C. Their lengths and diameters were then measured at a number of temperatures, by use of an eyepiece micrometer scale. From the result at each temperature the volume swelling above the volume at room temperature ($20 \pm 1^\circ\text{C}$.) was calculated.

Determination of Tension as a Function of Temperature

The method of measuring the tension at various temperatures in a wool fiber immersed in LiBr solution was, in principle, the same as that previously described,¹⁰ being based on the use of a simple, manual extensometer and a Statham force transducer of maximum load 0.15 oz. The test specimen was mounted between two fused quartz hooks, one attached to the transducer and the other to the moving arm of the extensometer. When the extensometer had been adjusted to produce the required fiber length, the movable quartz member was clamped to the base plate carrying the transducer, and disconnected from the lead-screw traveller of the extensometer. Thus the specimen was, in effect, held in a quartz jig, and was unaffected by thermal length changes in the metal body of the extensometer. As before,¹⁰ the LiBr solution was contained in a jacketed glass vessel and controlled in temperature by water circulation through the jacket from a bath with thermostatic control. The temperature was controlled to $\pm 0.1^\circ\text{C}$. In all experiments 8.0*M* LiBr solution was used.

The test specimens were in the form of multiple loops, the number of cross sections supporting the tension being 4, 10, and 20 for samples 0, 10b, and 14b, respectively. Under these circumstances the tension at a given strain was approximately the same in each specimen.¹⁰ Several fibers were tied end-to-end to make the test specimens from the S-methyl wools.

Tension-temperature measurements were made with fibers after both reversible and irreversible thermal treatment in LiBr solution. In both cases the first step in a run was to extend the specimen to the required length and allow it to reach a constant value of tension at the highest temperature to be employed. The time required was about 1 hr. Beyond a certain temperature a very long-term relaxation of the force became apparent,¹⁰ and this fact set the upper limit of temperature; for the wools used here the maximum temperatures for fibers contracted reversibly and irreversibly were approximately 45 and 25°C., respectively. Equilibrium tensions corresponding to lower temperatures were then measured. There was no appreciable stress relaxation during a test.

After measurements on a reversibly contracted specimen, the second stage of supercontraction was induced by heating the fiber in the same solution at 95°C. for approximately 2½ hr. The tension-temperature relationship at various extensions was then determined as before. Because constant length was maintained during each test, there was a small change of α resulting from thermal expansion. This change was neglected, and values of α are based on the force-free length at 25°C.

RESULTS

Volume Swelling

Plots of volume swelling against temperature are shown in Figure 1 for the unreduced sample (0), and the sample containing 8% of the original disulfide (14b). The fibers were irreversibly contracted in 8.0M LiBr

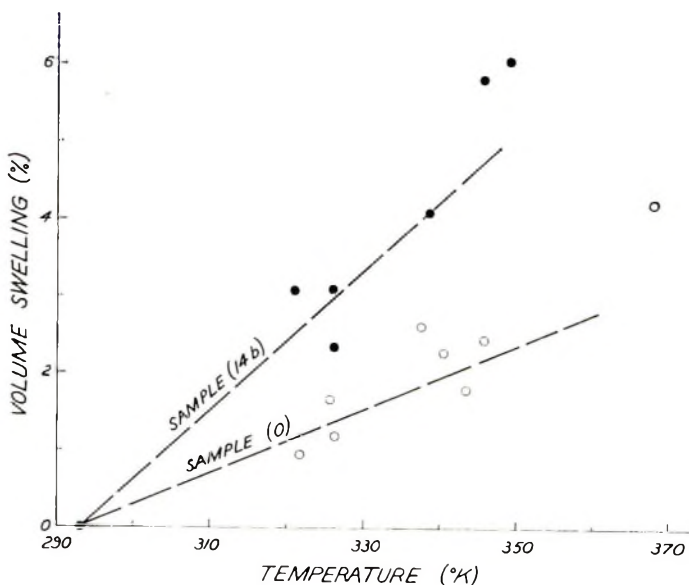


Fig. 1. Volume swelling vs. temperature results for samples 0 and 14b. The straight lines shown are those used in calculating the coefficient of thermal expansion.

solution prior to measurement in the same solution. Because of experimental difficulties no data were obtained at temperatures below ambient, and in order to produce changes large enough for satisfactory measurement it was necessary to raise the temperature to values outside the range used in tension measurements. However, in calculating the thermal expansion coefficient β , the experimental points obtained at the lowest temperatures were favored. The slopes used for calculation of β for samples 0 and 14b are shown in Figure 1. Values found were 4.2×10^{-4} , 5.4×10^{-4} , and 9.4×10^{-4} degrees⁻¹ for samples 0, 10b, and 14, respectively.

No attempt was made to measure β for reversibly contracted samples because the temperatures necessary during the tests would have caused irreversible contraction. For similar reasons it was not possible to determine β as a function of extension; in this case the necessary temperatures would have produced set, i.e., the unconstrained length of a fiber would have changed during a test. Thus the calculated values of $\beta T/(\alpha^3 - 1)$ in the following section are strictly relevant only to zero extension; however, at the extensions involved in this work the resulting error is probably not significant.

Tension-Temperature Data

In Figure 2 tension is plotted against temperature for sample 0 at three different extension ratios. The specimen was irreversibly contracted before these tests. Though plotted on a compressed scale the experimental points illustrate a significant feature that was observed in all cases, viz., at low extensions and low temperatures the curve relating tension and temperature is clearly concave to the temperature axis. This feature is not apparent at higher extensions. It may result from failure to reach equi-

TABLE I
Experimental Data and Calculated Values of f_e/f for Sample 0

α	$\left[1 - \frac{T\partial f}{f\partial T}\right]_{P,L}$ at 25°C.	$\frac{\beta T}{\alpha^3 - 1}$ at 25°C.	$(f_e/f)_{25^\circ C.}$	$(f_e/f)_{10^\circ C.}$	Remarks ^a
1.071	-0.20	—	—	—	Reversibly contracted
1.134	0.09	—	—	—	
1.125	0.27	0.30	-0.03	-0.12	
1.181	0.24	0.19	0.05	0.03	
1.198	0.23	0.18	0.05	-0.02	
1.264	0.20	0.12	0.08	0.05	Irreversibly contracted
1.321	0.17	0.10	0.07	0.06	
1.335	0.12	0.09	0.03	0.04	
1.342	0.16	0.09	0.07	0.08	
1.425	0.17	0.07	0.10	0.14	
1.554	0.20	0.05	0.15	0.17	

^a Amounts of reversible and irreversible contraction were 11.8% and 37.4%, respectively.

librium swelling. Results for sample 10b after reversible supercontraction are shown in Figure 3, and after irreversible supercontraction in Figure 4.

The data for all three samples together with the calculated values of f_e/f at both 25 and 10°C. are presented in Tables I-III. The levels of

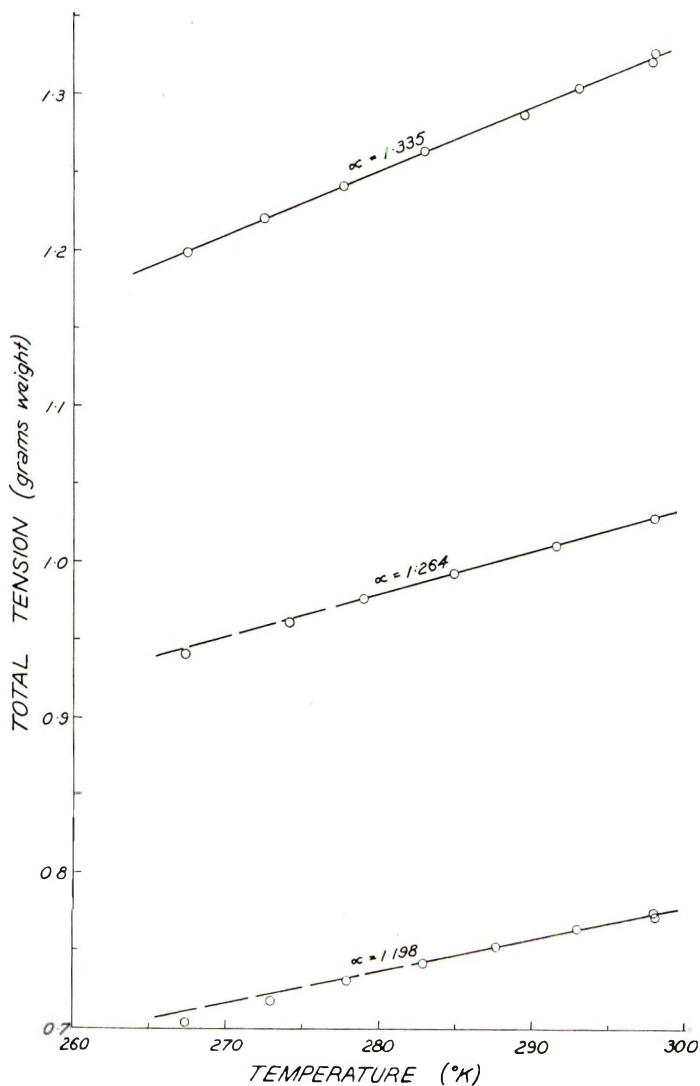


Fig. 2. Tension vs. temperature data at constant length for sample 0 after irreversible supercontraction. The corresponding values of extension ratio α are shown on the graphs.

supercontraction prior to commencement of a series of tension-temperature tests are given in the legends, these values being the reduction in length expressed as a percentage of the native length of a specimen. The

differences between $(f_e/f)_{25^\circ\text{C.}}$ and $(f_e/f)_{10^\circ\text{C.}}$ are usually small, the trend being towards smaller values at 10°C. than at 25°C. , as required by eq. (3). The few cases of large differences arise no doubt from errors in determination of $(\partial f/\partial T)_{P,L}$; these errors are likely to be greatest at low force levels, i.e., at low extension ratios.

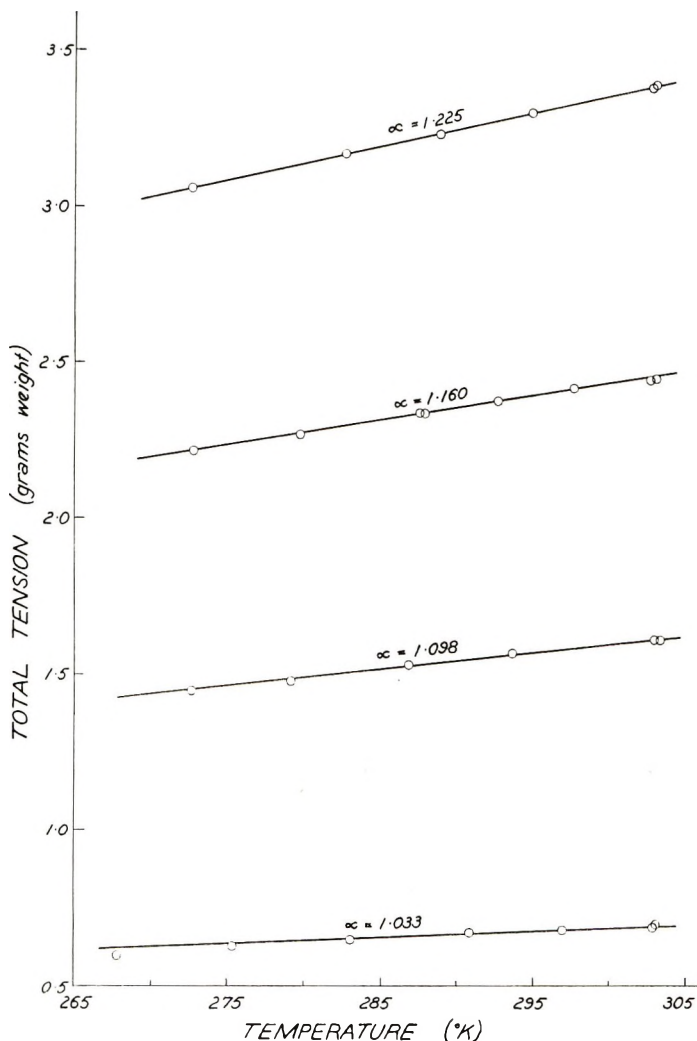


Fig. 3. Tension vs. temperature data at constant length for sample 10b after reversible supercontraction.

To illustrate the results for irreversibly contracted fibers the means of the values of $(f_e/f)_{25^\circ\text{C.}}$ and $(f_e/f)_{10^\circ\text{C.}}$ are plotted in Figure 5 for samples 0 and 14b. Fewer results are available for sample 10b, but there is no evidence that its energetic component of tension becomes significantly negative at any extension ratio within the range examined.

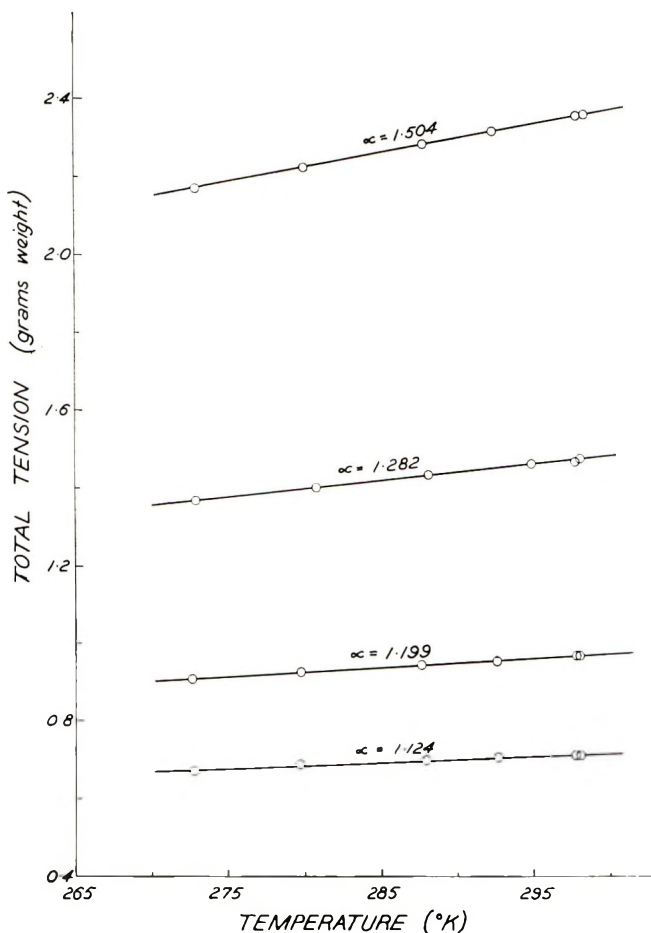


Fig. 4. Tension vs. temperature data at constant length for sample 10b after irreversible supercontraction.

DISCUSSION

Most of the values of f_e/f for wool in LiBr solution (Fig. 5) fall within the range 0 ± 0.20 . The value for an ideal elastomer is zero; values of approximately -0.03 and -0.4 have been found for butyl rubber (290–370°K.) and polyethylene (370–450°K.), respectively, whether swollen or unswollen. Thus wool swollen with LiBr solution has properties which place it well within the range of materials which are referred to as rubbers or elastomers.

Before proceeding to discuss the results in more detail we note that the values of the term $\beta T/(\alpha^3 - 1)$ are large at low extension ratios, and consequently an error in the value of β will be important. At the same time the precision of the determination of $(\partial f/\partial T)_{P,L}$ is also relatively low. For these reasons it is concluded that the downturn in f_e/f at low extension

TABLE II
Experimental Data and Calculated Values of f_e/f for Sample 10b

α	$\left[1 - \frac{T}{f} \frac{\partial f}{\partial T}\right]_{P,L}$ at 25°C.	$\frac{\beta T}{\alpha^3 - 1}$ at 25°C.	$(f_e/f)_{25^\circ\text{C.}}$	$(f_e/f)_{10^\circ\text{C.}}$	Remarks ^a
1.033	0.21	—	—	—	Reversibly contracted
1.098	0.13	—	—	—	
1.160	0.11	—	—	—	
1.225	0.06	—	—	—	
1.102	0.67	0.48	0.19	0.20	Irreversibly contracted
1.124	0.46	0.38	0.08	-0.05	
1.199	0.36	0.22	0.14	0.13	
1.282	0.22	0.15	0.07	-0.01	
1.540	0.13	0.07	0.06	0.02	

^a Amounts of reversible and irreversible contraction were 25.7 and 35.1%, respectively.

TABLE III
Experimental Data and Calculated Values of f_e/f for Sample 14b

α	$\left[1 - \frac{T}{f} \frac{\partial f}{\partial T}\right]_{P,L}$ at 25°C.	$\frac{\beta T}{\alpha^3 - 1}$ at 25°C.	$(f_e/f)_{25^\circ\text{C.}}$	$(f_e/f)_{10^\circ\text{C.}}$	Remarks ^a
1.079	0.21	—	—	—	Reversibly contracted
1.128	0.18	—	—	—	
1.201	0.00	—	—	—	
1.283	-0.04	—	—	—	
1.092	0.78	0.93	-0.15	-0.27	Irreversibly contracted
1.142	0.32	0.57	-0.25	-0.25	
1.157	0.45	0.51	-0.06	-0.17	
1.303	0.10	0.23	-0.13	-0.19	
1.320	0.15	0.22	-0.07	-0.08	
1.338	0.14	0.20	-0.06	-0.07	
1.338	0.11	0.20	-0.09	-0.07	
1.357	0.06	0.19	-0.13	-0.16	
1.461	0.03	0.13	-0.10	-0.13	
1.580	0.01	0.10	-0.09	-0.13	

^a Amounts of reversible and irreversible contraction were 32.0 and 44.3%, respectively.

ratios (Fig. 5) may not be real. Apart from this region it appears that (1) f_e/f increases with increase of α in the case of the unreduced sample 0; (2) f_e/f is constant and negative for sample 14b; (3) f_e/f is probably constant and slightly positive for sample 10b. Mark and Flory¹⁵ published results for polydimethylsiloxane (PDMS) indicating a fall in f_e/f with increase of α , and other cases of variation with α may be found in the literature (for references see Ciferri¹⁶).

Both positive and negative values of f_e/f have been found, and both can be justified theoretically. This problem has been discussed by Ciferri,¹⁶ Ptitsyn,¹⁷ and Flory et al.¹⁸ Ptitsyn¹⁷ showed that, even assuming independent rotations around adjoining bonds, positive or negative values of f_e/f were possible for the PDMS chain because of the sequence of two widely different valency bond angles. A negative value is predicted when, as in polyethylene, the bond angles are equal. Returning to wool, in the case of the polypeptide chain, rotations are permitted about the N to α -carbon bond and about the α -carbon to β -carbon bond (assuming as usual that the peptide group is planar), and analogously to the PDMS chain either positive or negative values of f_e/f should be possible.

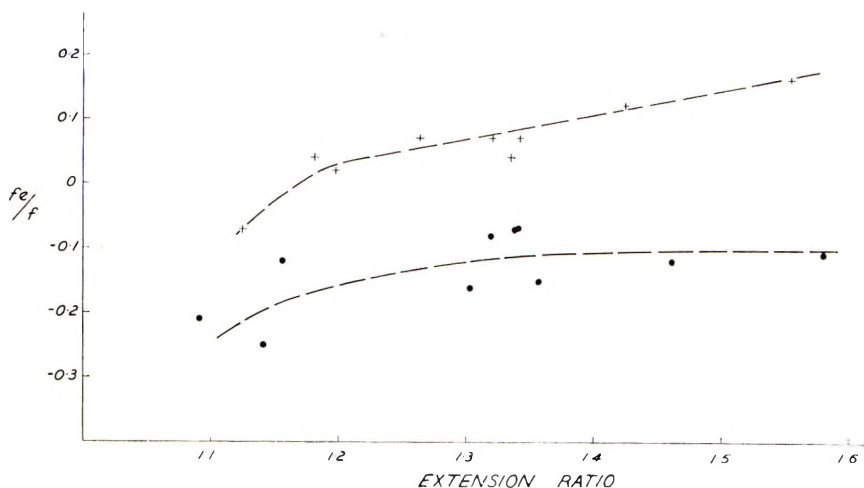


Fig. 5. Ratio of the energetic component of tension to the total tension (f_e/f) plotted against extension ratio: (+) sample 0; (O) sample 14b. Values of f_e/f are means of results at 10 and 25°C.

However, the fact that f_e/f for sample 14b is negative and approximately constant at all extensions suggests that the change from positive to negative in the case of sample 0 is not a consequence of intrachain properties. The result for sample 14b is in accord with the theory of rubber elasticity, the derivation of which requires that interactions between chains, if any, should not change with extension.¹² It is unlikely that a full explanation of the data for sample 0 will be found without reference to interactions between the polypeptide chains; unreduced wool as in sample 0 is a highly crosslinked material, the disulfide content being sufficient to provide approximately one covalent crosslink for every ten monomer units; furthermore these coexist with large numbers of bulky and reactive side chains. Thus the presence of extension-dependent interactions between chains seems feasible, and an interpretation of the increasing value of f_e/f with increase of α , for sample 0, is that it arises from changes in such inter-

actions. On this basis the results for samples 10b and 14b would be explained in terms of the loss of extension-dependent interactions as the disulfide content was decreased.

A previous observation is of interest in this connection. It was found¹⁰ that when the calculated number of crosslinks in wool (calculated from the longitudinal modulus of irreversibly contracted fibers in LiBr solution) was plotted against disulfide content, the graph was approximately linear over a considerable range, but sharply increased in slope at high disulfide content. As above, the result could be explained by supposing that at high disulfide content the reduction of these bonds is accompanied by a consequent loss of other interactions between chains.

Subject to the conditions imposed by its derivation from the elastic equation of state for simple elongation a relationship holds between the relative value of the energetic component of tension and the chain dimensions. The relationship is $f_e/f = Td(\ln \bar{r}^2)/dT$. Here \bar{r}^2 is the mean square distance between the ends of the free polymer chain, unperturbed by external constraints arising from, for instance, specific solvent effects or interaction with other chains. The present data suggest that $d(\ln \bar{r}^2)/dT$ will be negative for polypeptide chains from wool, taken into dilute solution (in a suitable medium) following complete disulfide reduction. This means that the unperturbed dimensions of the chains will decrease with increase of temperature, a more extended form being the lower energy state. It is encouraging to note that good agreement has been obtained^{12,15} between values of $d(\ln \bar{r}^2)/dT$ obtained from studies of bulk polymers and of the same polymers in solution, but there are as yet no data from wool peptides in solution with which to compare the above result.

References

1. Bull, H. B., and M. Gutmann, *J. Am. Chem. Soc.*, **67**, 533 (1945).
2. Woods, H. J., *Nature*, **157**, 229 (1946); *J. Colloid Sci.*, **1**, 407 (1946).
3. Jordon-Lloyd, D., and M. Garrod, *Fibrous Proteins Symposium*, Society of Dyers and Colourists, Leeds, 1946, p. 24.
4. Meyer, K. H., and C. Haselbach, *Nature*, **164**, 33 (1949).
5. Elod, E., and H. Zahn, *Melliand Textilber.*, **30**, 17 (1949).
6. Haly, A. R., and M. Feughelman, *Textile Res. J.*, **27**, 919 (1957).
7. Bendit, E. G., *Textile Res. J.*, **30**, 547 (1960).
8. Haly, A. R., and J. C. Griffith, *Textile Res. J.*, **28**, 32 (1958).
9. Haly, A. R., and J. W. Snaith, *Biochim. Biophys. Acta*, **44**, 180 (1960).
10. Haly, A. R., *Kolloid-Z.*, **191**, 105 (1963).
11. Flory, P. J., A. Ciferri, and C. A. J. Hoeve, *J. Polymer Sci.*, **45**, 235 (1960).
12. Ciferri, A., C. A. J. Hoeve, and P. J. Flory, *J. Am. Chem. Soc.*, **83**, 1015 (1961).
13. Smith, K. J., A. Greene, and A. Ciferri, *Kolloid Z.*, **194**, 49 (1964).
14. Allen, G., U. Bianchi, and C. Price, *Trans. Faraday Soc.*, **59**, 2493 (1963).
15. Mark, J. E., and P. J. Flory, *J. Am. Chem. Soc.*, **86**, 138 (1964).
16. Ciferri, A., *J. Polymer Sci.*, **45**, 528 (1960).
17. Ptitsyn, O. B., *Vysokomol. Soedin.*, **5**, 1219 (1963).
18. Flory, P. J., V. Crescenzi, and J. E. Mark, *J. Am. Chem. Soc.*, **86**, 146 (1964).

Résumé

Des résultats de la tension en fonction de la température ont été obtenus pour des fibres de laine non réduite et pour des fibres dans lesquelles certains liens disulfures ont été réduits par un thiol, les mesures ayant été effectuées alors que les fibres contenaient un diluant. On a également mesuré les coefficients de dilatation thermique en volume. À partir des résultats, on a calculé le rapport entre la composante ϵ énergétique de la tension et la tension totale (f_e/f). La plupart des valeurs de f_e/f se situent dans le domaine de $\pm 0,20$. Dans le cas de la laine non réduite f_e/f change depuis une valeur négative jusqu'à une valeur positive lorsque l'allongement augmente. Avec un échantillon réduit contenant 8% de disulfure à l'état natif f_e/f est négatif et presque constant dans le domaine d'allongement utilisé. Le changement pour la laine non réduite dépend des interactions entre les chaînes de polypeptide qui dépendent de l'allongement. Les résultats montrent que pour les chaînes de polypeptide perturbées provenant de la laine prise dans la solution après la réduction au disulfure, la distance entre extrémités de chaîne diminue avec une augmentation de la température, une forme partiellement étendue formant l'état énergétique plus bas.

Zusammenfassung

Spannungs-Temperaturdaten wurden für unreduzierte Wollfasern und Fasern, bei welchen einige Disulfidbindungen mit einem Thiol reduziert worden waren, erhalten. Die Messungen wurden an verdünnungsmittelhaltigen Fasern durchgeführt. Weiters wurde der Koeffizient der thermischen Volumexpansion gemessen. Aus den Ergebnissen wurde das Verhältnis der energetischen Spannungskomponente zur totalen Spannung (f_e/f) berechnet. Die Werte für f_e/f lagen meist in einem Bereich von $\pm 0,20$. Bei unreduzierter Wolle ändert sich f_e/f mit steigender Dehnung von negativen zu positiven Werten. Bei einer reduzierten Probe, die noch 8% der nativen Disulfidgruppen enthält, war f_e/f negativ und über den angewendeten Dehnungsbereich nahezu konstant. Die Änderung bei unreduzierter Wolle ist eine Folge der dehnungsabhängigen Wechselwirkung zwischen Polypeptidketten. Die Ergebnisse zeigen, dass beim Einbringen von ungestörten Polypeptidketten aus Wolle in Lösung nach der Disulfidreaktion der End-zu-End-Abstand mit steigender Temperatur abnimmt, wobei eine partiell gestreckte Form den niedrigeren Energiezustand bildet.

Received February 10, 1965

Prod. No. 4695A

Inorganic Polymers. Part I. A Solid Inorganic Foam

R. A. SHAW and TAKESHI OGAWA, *Department of Chemistry, Birkbeck College, University of London, London, England*

Synopsis

The preparation of a solid inorganic foam is reported. Hexaaminocyclotriphosphazatriene, $N_3P_3(NH_2)_6$, used either without purification, or when recrystallized from water, gives phospham as a dense powder. If, however, the starting material is precipitated from its aqueous solution by suitable organic solvents, a foamed material results. Possible reasons for this divergence in behavior are discussed. The ammonia evolved on thermal decomposition acts as a built-in foaming agent.

INTRODUCTION

This paper is the first of a series devoted to inorganic polymers. The monomer and polymer described in this study are wholly inorganic. In later papers, organic substituents and/or linking groups will play some part. We shall for convenience define as "inorganic polymers" those macromolecules where elements other than carbon play a significant part in the polymer framework. The choice of what constitutes a "significant part" is obviously a personal one, and as such will of necessity be somewhat arbitrary. A perusal of the work presented at the International Symposium on Inorganic Polymers at Nottingham in 1961,¹ will give an idea of the current arbitrariness of definition of what constitutes an inorganic polymer, both with regard to molecular size and molecular constitution.

Earlier we have reported^{2,3} the syntheses of different phosphams, $(NPNH)_n$, derived from hexaaminocyclotriphosphazatriene, $N_3P_3(NH_2)_6$, and octaaminocyclotetraphosphazetraene, $N_4P_4(NH_2)_8$, respectively. (For earlier work on phosphams see Shaw et al.^{4,5})

Thus hexaaminocyclotriphosphazatriene (HACTP), recrystallized from water or used without purification, forms a phospham with the elimination of ammonia on heating to temperatures $>250^\circ C$.² The phospham thus obtained is a white to grey powder ($d \simeq 2.2$ g./cc.).² It possesses a highly crosslinked, three-dimensional structure and thus is insoluble in all solvents which do not decompose it.

Recrystallization of HACTP from water, however, decreases the yield considerably, as some hydrolysis takes place. The aqueous mother liquor still contains a considerable proportion of starting material and its hydrolysis products, as their solubilities in water are quite high. These can be

recovered before much hydrolysis has occurred, by means of rapid precipitation with a water-miscible organic solvent such as ethanol, acetone, etc.

Precipitated HACTP forms a foam on rapid heating to a temperature $>250^{\circ}\text{C}$., conveniently achieved by placing the sample into a furnace preheated to the required temperature. The foam thus obtained is a white, very light, porous material ($d \simeq 0.03\text{--}0.05$ g./cc.).⁶

We have investigated the divergence of behavior between recrystallized and precipitated HACTP.

EXPERIMENTAL

Hexaaminocyclotriphosphazatriene (HACTP)

HACTP is prepared by the reaction of hexachlorocyclotriphosphazatriene with liquid ammonia.



A large excess of liquid ammonia (200 ml.) was collected in a three-necked, 1-liter flask fitted with a stirrer. A light petroleum (b.p. $60\text{--}80^{\circ}\text{C}$.) solution (500 ml.) containing hexachlorocyclotriphosphazatriene (50 g.), was added dropwise with stirring to the liquid ammonia at $\sim -35^{\circ}\text{C}$. After several hours the temperature was slowly brought to room temperature, and the reaction mixture was left to stand overnight. The precipitate obtained was filtered off, washed with light petroleum, and dried under vacuum. The white precipitate was then refluxed with dry diethylamine and chloroform for 8–10 hr. to remove the ammonium chloride by converting it to the chloroform-soluble diethylammonium chloride.⁷

The residue of crude HACTP was washed with warm chloroform and dried under vacuum at room temperature. It could be used *per se*, or further purified.

Pure HACTP is obtained by recrystallization from a small quantity of warm water by saturating it at $45\text{--}50^{\circ}\text{C}$. with the crude HACTP, filtering off any sparingly soluble material, and allowing to stand at room temperature for 24 hr.

ANAL. Calc. for $\text{H}_{12}\text{N}_9\text{P}_3$: N, 54.5%; P, 40.3%; H, 5.2%; Found: N, 54.3%; P, 40.0%; H, 5.4%.

To obtain foam-producing HACTP, crude HACTP was dissolved in a small amount of water and rapidly precipitated with various water-miscible organic solvents, the ratio of precipitating solvent to aqueous solution being approximately 10:1 by volume. Alcohols such as methanol, ethanol, *n*-propanol, isopropanol, and *n*-butanol, ketones such as acetone and methyl ethyl ketone, and ethers such as diethyl ether, tetrahydrofuran, and dioxane, were employed.

Phospham

Pure phospham is obtained by the thermal condensation polymerization of HACTP at temperatures higher than 250°C. under an atmosphere of dry oxygen-free nitrogen. Oxidation and/or hydrolysis takes place when the reaction is carried out under ordinary atmospheric conditions, especially at higher temperatures and during extended reaction times, giving a grey colored phospham of inferior hydrolytic stability. In the present work, the foaming was carried out in a furnace preheated to the required temperature in an atmosphere of dry nitrogen.

X-Ray Powder Photography

The x-ray photographs of ground powders of HACTP's were taken in Lindemann tubes of 0.3 mm. diameter. The copper $K\alpha$ radiation of $\lambda = 1.542$ A. was used as the x-ray source with a nickel filter. A JIC-Walker recording microdensitometer, Model D31, was used to obtain the intensity- 2θ graphs.

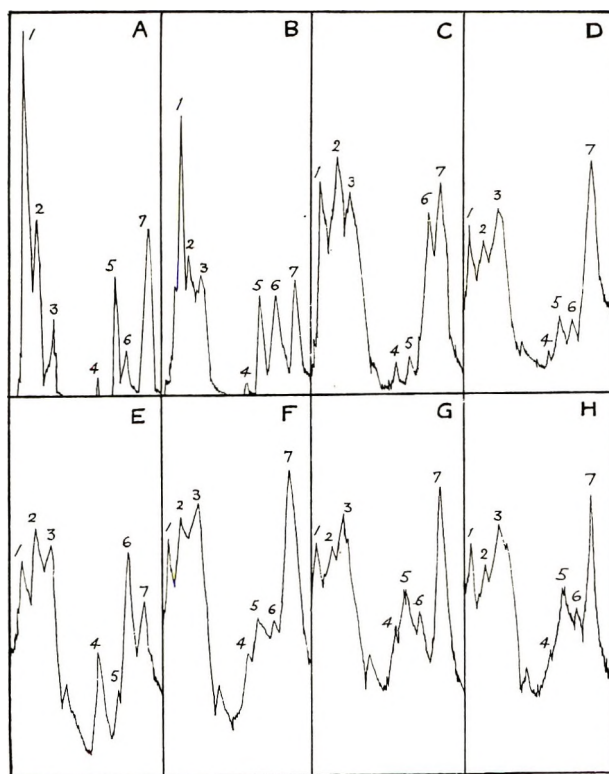


Fig. 1. Intensity- 2θ diagrams of HACTP's precipitated with various solvents: (A) pure, recrystallized; (B) methanol-precipitated; (C) ethanol-precipitated; (D) *n*-propanol-precipitated; (E) *n*-butanol-precipitated; (F) acetone-precipitated; (G) tetrahydrofuran-precipitated; (H) dioxane-precipitated.

Large numbers of lines appeared in the HACTP patterns. Only those covering 2θ values between 6 and 30° , where the main differences in the patterns appear, are shown in Figure 1.

RESULTS AND DISCUSSION

Pure, recrystallized HACTP undergoes thermal bulk condensation polymerization without prior melting, to form a phospham at temperatures $>250^\circ\text{C}$. The ammonia gas liberated within the crystals of HACTP shatters these with considerable force. When these were viewed on the heating stage of a Reichert-Kofler microscope, violent movement of the crystals was observed at the decomposition temperature. By contrast, HACTP precipitated from its aqueous solution by suitable organic solvents, melts, when rapidly heated, and yields a foam by the simultaneous, vigorous evolution of ammonia. The foam thus obtained is very light and mechanically fairly fragile. It is indefinitely stable at room temperature to atmospheric moisture, does not burn, and is insoluble in all solvents which do not decompose it. The density of the foam is of the order of 10^{-2} g./cc. and depends on the foaming ability of the precipitated HACTP's. The infrared spectrum of the foamed material shows only very broad peaks and is indistinguishable from that of phospham powder obtained from pure, recrystallized HACTP.

The melting point of the precipitated HACTP is indistinct. When heated slowly, decomposition starts at about $80\text{--}100^\circ\text{C}$., no melting or foaming occurs at higher temperatures, and the phospham obtained is the usual dense powder.

In order to form a foam, the monomer should melt (or at least have its lattice forces considerably reduced) prior to decomposition. Possible reasons why precipitated HACTP should melt before decomposition while pure, recrystallized HACTP decomposes without melting include different arrangements of the molecules in the crystal,⁸⁻¹⁰ presence of impurities, clathrate formation, etc.

Numerous experiments were carried out to discover the cause of the foaming, and to test the reproducibility of the results.

TABLE I
Foaming Ability of HACTP's Precipitated with Various Solvents

Solvent	Foaming	Appearance of the foam
MeOH	None	
EtOH	Poor	Homogeneous fine pores
<i>n</i> -PrOH	Good	Homogeneous coarse pores
<i>n</i> -BuOH	Good	Pores of various sizes
Acetone	Very good	" " " "
Methyl ethyl ketone	Very good	" " " "
Tetrahydrofuran	Very good	" " " "
Diethyl ether	Poor	" " " "
Dioxane	Good	" " " "

Effect of the Nature of the Precipitating Solvent on the Foaming Ability of HACTP

Table I shows the foaming ability of HACTP's precipitated with various solvents. The results are the mean obtained from several different HACTP preparations. With ethanol as the precipitating solvent some differences in the foaming ability of different samples were observed, but with all other solvents good reproducibility was obtained. No foam was ever obtained from HACTP's precipitated by methanol. Samples precipitated by ketones always showed good foaming abilities. It is clear that the precipitating solvents play a significant part in the foaming ability of HACTP.

Carbon and hydrogen determinations carried out on some of the precipitated HACTP's are shown in Table II.

TABLE II
Typical Carbon and Hydrogen Analyses of Precipitated HACTP's

Precipitating solvent	Carbon, %	Hydrogen, %
MeOH	0.95	5.14
EtOH	0.49	5.74
<i>n</i> -BuOH	0.66	5.01
Acetone	0.61	5.28

It can be seen that approximately 1% (by weight) of precipitators seemed to be retained in the HACTP's after vacuum drying for several hours at room temperature. The carbon values are small, and there are no grounds for assuming that the foaming is due to clathrate formation of HACTP with the organic solvent; in particular, as if anything, more methanol, which does not cause foaming, than any of the other solvents is retained.

Effect of Drying

Precipitated HACTP's, left wet with the solvents, decomposed on heating to give hard brown residues. Wet HACTP's were extremely unstable and changed on several days standing at room temperature to a viscous mass. Precipitates sufficiently dry to give powders were relatively stable and formed foams on heating; further drying under vacuum did not alter their foaming ability.

Effect of Impurities

Pure recrystallized HACTP, when dissolved in water and precipitated at once by organic solvents, possesses no foaming ability. Hence foaming must be due to a coprecipitated impurity, and not just to precipitation producing a more random and more readily meltable form of HACTP.

Crude HACTP as obtained from the synthesis (cf. experimental) does not foam. Hence foam-causing impurities are either formed in contact with the water during the solution-precipitation stage, or, if present prior to this, are

for some reason unable to lower the melting point of HACTP, and hence permit foaming.

Possible impurities contained in the precipitated HACTP are, partially hydrolyzed phosphazenes, incompletely ammonolyzed chlorophosphazenes, aminophosphazene hydrochloride, ammonium chloride, diethylamine hydrochloride, etc. To ascertain which of these impurities, if any, cause the foaming, the following experiments were carried out.

Pure recrystallized HACTP was dissolved in a small amount of water, and small amounts of ammonium chloride or diethylamine hydrochloride were added, followed by a large amount of organic solvent. The dried precipitates did not show any tendency to melt or foam.

Hexachlorocyclotriphosphazatriene was heated with water for several hours, and then concentrated ammonia solution was added to obtain water-soluble, partially hydrolyzed aminochlorophosphazenes. After a few days at room temperature and filtering, pure, recrystallized HACTP was dissolved in a small amount of the filtrate, and a large amount of acetone added. The dried precipitates yielded a foam on heating.

Pure recrystallized HACTP was ground to a fine powder, moistened with concentrated hydrochloric acid or sulfuric acid, and immediately placed in a hot furnace. No foam was obtained. Hence foaming is not due to general acid catalysis. Powdered HACTP was mixed with other phosphazene derivatives possessing lower melting points, such as hexamethoxycyclotriphosphazatriene and 2, 2-diphenyldichlorodiaminocyclotriphosphazatriene, and the mixed powders were heated, but again no foaming was observed. Hence foam-causing impurities possess either specific structural features, or require coprecipitation to become effective.

Hydrolysis of HACTP

The elementary analysis of a typical, precipitated HACTP and of a foam derived from it are shown in Table III. It can be seen that the percentage of phosphorus in the precipitated HACTP is considerably lower than the calculated value required for $N_3P_3(NH_2)_6$, while the P/N ratio has however not been appreciably altered. This is probably due to the extremely hygroscopic nature of the precipitated HACTP and/or concomitant hydrolysis, e.g., $P-NH_2$ being replaced by $P-O^{\ominus}NH_4^{\oplus}$.

TABLE III
Comparison of Analytical Results of Acetone-Precipitated HACTP and of a Solid Foam Derived from It with Pure HACTP and Phospham

	C, %	H, %	N, %	P, %	Composition
Acetone-precipitated HACTP	0.30	5.55	46.24	35.93	$H_{14.37}N_{8.65}P_3O_{1.83}^a$
Pure HACTP	0	5.20	54.54	40.36	$N_{12}N_9P_3$
Foam	0.66	3.78	42.22	42.91	$H_{2.72}N_{2.17}PO_{0.47}^a$
Phospham	0	1.66	46.66	51.66	HN_2P

^a C was neglected in calculation of empirical formulae; oxygen by difference.

When methanol was used as a precipitant, the amounts precipitated were smaller than those when the other organic solvents were used, and the precipitates did not foam, suggesting that foamable precipitates are mixtures of pure HACTP and partially hydrolyzed products, which are probably too soluble in methanol to be precipitated. These hydrolysis products are probably less soluble in the other organic solvents, such as acetone, and therefore are precipitated together with the HACTP, thus giving the foam-producing mixtures.

Some hydrolysis products may have been formed by traces of moisture during the early purification stages, i.e., during refluxing of the HACTP with diethylamine to remove ammonium chloride. Pyrolysis at this stage does not, however, produce a foam. As pure recrystallized HACTP on dissolution in and immediate reprecipitation from water does not foam, this suggests that some impurities present in the crude HACTP catalyze its hydrolysis when dissolved in water.

The structure of the foamed material is difficult to elucidate from the analytical data, since the extent of reaction is not known, as foaming (which makes the reaction unsuitable for thermogravimetric analysis) is usually complete in a few minutes. The completion of ordinary phospham formation usually requires somewhat higher temperatures and longer reaction times.² It is possible that the phosphazene rings which are believed to be retained in ordinary phospham² are at least partially destroyed in the foamed material.

X-Ray Powder Photographs

X-ray powder photographs taken of a series of precipitated HACTP's, are shown in Figure 1. Numerical values of 2θ for corresponding peaks are given in Table IV.

It is interesting to note from Figure 1 that the peaks of the alcohol-precipitated HACTP's shift towards smaller values of θ as the size of the alkyl group becomes larger, and the foaming ability increases. With *n*-

TABLE IV
Relationship between the Precipitants Used and the Values of 2θ of Corresponding Peaks^a

Peak num- bers	2θ							
	Recrys- tallized	MeOH ppt.	EtOH ppt.	<i>n</i> -PrOH ppt.	<i>n</i> -BuOH ppt.	Acetone ppt.	THF ppt.	Dioxane ppt.
1	12.68	12.68	11.42	10.64	11.62	10.68	10.48	10.68
2	13.84	13.84	13.54	12.64	13.74	12.50	12.78	12.88
3	15.92	15.82	15.26	14.78	15.74	14.88	14.30	14.50
4	21.46	21.40	21.30	21.26	21.64	21.16	20.98	21.46
5	23.82	23.80	23.10	22.60	23.14	22.70	22.20	22.88
6	25.18	25.60	25.80	24.50	25.56	25.00	24.10	24.80
7	28.14	28.00	27.20	26.70	27.66	27.20	27.00	26.72

^a See Fig. 1.

butanol, which is not very miscible with water, the speed of the precipitation of the HACTP is governed to some extent by the absorption of the water into the butanol and appeared to be less rapid. This may be the reason why the peaks in this case did not shift towards smaller values of θ .

With acetone and ethers, the patterns are similar to each other, showing more diffuse structures than those obtained with alcohols and smaller values of θ . The foaming abilities of ketone- and ether-precipitated HACTP's were always better than those precipitated by other organic solvents. These results suggest that the smaller the values of θ , the greater the foaming ability of HACTP.

From the experimental results discussed above, it seems most likely that impurities such as partially hydrolyzed HACTP are the cause of the foaming. Impurities such as ammonium chloride, on the other hand, have no effect on melting or foaming, either because they are too soluble in the aqueous-organic phase, or, if coprecipitated, they lack the ability to depress the melting point of HACTP.

CONCLUSIONS

Pure, recrystallized hexaaminocyclotriphosphazatriene (HACTP) undergoes thermal bulk condensation polymerization with the liberation of ammonia to give phospham as a dense powder. The reaction proceeds in the solid phase, as the compound decomposes before its melting point. If suitable impurities are present, however, the HACTP melts on sudden heating to temperatures higher than 250°C., and the simultaneous, vigorous elimination of ammonia causes the formation of a foamed material. The ammonia acts as a built-in frothing agent, a rather novel way of producing a solid foam. The impurities which seem to be the most effective are compounds having structures similar to that of HACTP.

The mechanism by which the effective foam producing impurities depress the melting point of HACTP is not quite clear. The evidence from the x-ray powder photographs, together with what little there is known about the probable structures of the impurities favors a depression of melting point of HACTP through solid solution rather than eutectic formation.

The exact nature of the solvent used in the precipitation is only of major importance in the foam formation insofar as it determines the solubility of the impurity and HACTP in a mixture of water and the organic solvent. The differences in solubility will probably give differences in the crystal lattice dimensions of the precipitated HACTP, and the greater the lattice distances, the less energy would be required for the melting process.

It is noteworthy that so far no foaming has been observed with octaaminocyclotetraphosphazetetraene, $N_4P_4(NH_2)_8$.

References

1. *International Symposium on Inorganic Polymers, Nottingham*, Chemical Society Special Publication, London, **15**, 1961.
2. Miller, M. C., and R. A. Shaw, *J. Chem. Soc.*, **1964**, 3233.

3. Miller, M. C., D. W. Rhys, and R. A. Shaw, *Ind. Chemist*, **40**, 183 (1964).
4. Shaw, R. A., *J. Polymer Sci.*, **50**, 21 (1961).
5. Shaw, R. A., B. W. Fitzsimmons, and B. C. Smith, *Chem. Rev.*, **62**, 247 (1962).
6. Phillips, L. N., personal communication.
7. Klement, R., and O. Koch, *Chem. Ber.*, **87**, 333 (1954).
8. Shaw, R. A., and C. Stratton, *J. Chem. Soc.*, **1962**, 5004.
9. Bullen, G. J., R. A. Shaw, and C. Stratton, unpublished results.
10. Becke-Goehring, M., and K. John, *Z. Anorg. Chem.*, **304**, 126 (1960).

Résumé

On décrit la préparation d'une mousse solide inorganique. L'hexaaminocyclotriphosphazotriène, $N_3P_3(NH_2)_6$, employé soit sans purification, soit après recristallisation dans l'eau, donne une phosphane sous forme d'une poudre épaisse. Cependant, si on précipite le corps de départ de sa solution aqueuse par un solvant organique convenable, on obtient une mousse. On discute les différentes raisons de ces divers comportements. L'ammoniac qui se dégage par décomposition thermique, joue le rôle d'agent promoteur de la mousse.

Zusammenfassung

Über die Darstellung eines festen anorganischen Schaumstoffes wird berichtet. Hexaaminozyklotriphosphazatrien, $N_3P_3(NH_2)_6$, liefert sowohl ohne Reinigung als auch bei Umkristallisation aus Wasser Phospham als ein dichtes Pulver. Wenn jedoch das Ausgangsmaterial aus seiner wässrigen Lösung durch geeignete organische Lösungsmittel gefällt wird, entsteht ein Schaumstoff. Die möglichen Ursachen für dieses unterschiedliche Verhalten werden diskutiert. Das bei der thermischen Zersetzung entwickelte Ammoniak wirkt als eingebautes Schäumungsmittel.

Received December 24, 1964

Revised March 9, 1965

Prod. No. 4707A

NOTES

Free Radicals in Popcorn Polymers

Popcorn polymerization is recognized as a free-radical mechanism that results in a polymer that is insoluble due to extensive crosslinking.^{1,2} Once an insoluble nucleus is formed, the polymer propagates itself at a logarithmic rate when placed in the presence of additional monomer.³ The growing chains which result have restricted mobility and hence no rapid termination rate. Evidence for the existence of these nonterminated, growing chain ends was obtained in this work by subjecting the polymer samples to electron spin resonance measurements.

A sample of fresh butadiene popcorn polymer was removed from the tube in which it was grown, ground, and immediately resealed under vacuum in a 7 mm. Pyrex tube. Using a Varian ESR instrument a total spin concentration of 10^{16} /g. was detected. Heating of a similar sample in air at 140°C. for 1.5 hr. lowered the spin concentration to one-fourth of the unheated value.

Additional samples and the results obtained are tabulated in Table I.

TABLE I

Sample	Wt. used, g.	Approx. line width, gauss	Relative spin conc. per g.
Butadiene popcorn	0.123	10	1
Butadiene popcorn, heated 48 hr., 125°C. in vacuum	0.0118	10	0.2
Butadiene popcorn, heated 94 hr., 125°C. in air	0.0114	5	0.4
Butadiene popcorn, exposed to air, 96 hr., room temp.	0.0121	10	0.3
Methyl(methacrylate)-on-butadiene popcorn	0.0123	10	0.1
Styrene-on-butadiene popcorn	0.0156	—	Not detectable

A sample of methyl(methacrylate) popcorn seed that was grown on butadiene popcorn⁴ showed only 10% of the free radical concentration found for the pure butadiene popcorn. Styrene-on-butadiene popcorn seed showed no detectable spin concentration. This is in agreement with the author's previous findings that once styrene-on-butadiene popcorn polymer is removed from the tube in which it was grown, i.e., exposed to air, the loss of activity for continued growth is extremely rapid.⁵

Heating of butadiene popcorn seed in vacuum produced a significant lowering of the radical concentration. This can be explained by the increased mobility of the chains at the higher temperature and hence the greater probability of chain termination.

One of the most interesting observations was the change in the nature of the free radicals when the butadiene popcorn is heated in the presence of air. The decrease from 10 to 5 gauss for the approximate line width obtained indicated a free radical of a different species. It is evident that the oxidation of the polymer results in the formation of the

hydroperoxide groups in the carbon atoms alpha to the double bonds. These peroxide radicals are not those responsible for the propagation of the polymer, however, even though they may be present in sizeable amounts.⁶

We wish to thank Mr. J. L. Holcomb of Varian Associates for his cooperation in obtaining these analyses and the Petroleum Research Fund of the American Chemical Society for their financial assistance.

References

1. Miller, G. H., R. L. Alumbaugh, and R. J. Brotherton, *J. Polymer Sci.*, **9**, 453 (1952).
2. Immergut, E. H., *Makromol. Chem.*, **10**, 93 (1953).
3. Bamford, C. H., W. G. Barb, A. D. Jenkins, and P. F. Onyon, *The Kinetics of Vinyl Polymerization by Radical Mechanisms*, Butterworths, London, 1958.
4. Miller, G. H., and A. K. Bakhtiar, *Can. J. Chem.*, **35**, 584 (1957).
5. Miller, G. H., and C. F. Perizzolo, *J. Polymer Sci.*, **18**, 411 (1955).
6. Miller, G. H., *J. Polymer Sci.*, **11**, 269 (1953).

GLENN H. MILLER
DAVID CHOCK
ERNEST P. CHOCK

Chemistry Department
University of California
Santa Barbara, California

Received January 6, 1965
Revised April 8, 1965

**Preparation of Titanium Dichloride Dipropionate
and Polypropylene with High Amorphous Content**

INTRODUCTION

The high degree of stereoregularity found in the isotactic polypropylene prepared by Natta¹ emphasizes a unique property of the catalytic system. We find that a small modification of the catalyst causes a substantial loss of steric control over the product. Amorphous polypropylene has been recovered from polymerization products by Natta, and has been reported in a fluid-bed process with Ziegler-type catalysts.² The use of titanium dichloride dipropionate as the transition metal in combination with aluminum triisobutyl gives a product which is highly atactic.

Amorphous Polypropylene

Polymerizations. These polymerization studies were undertaken to test the catalyst, titanium dichloride dipropionate in combination with aluminum alkyl, and to characterize any unique properties this system might exhibit. The actual experiments were carried out in peroxide bottles, shielded with a brass cage, and thermostated at 50°C. in a tumbling polymerization bath.

The results obtained have been summarized in Table I.

TABLE I
Results from the Propylene Polymerization

Propyl- ene, g.	Titanium dichloride dipropion- ate, g.	Aluminum isobutyl, g.	$\frac{\text{Al}}{\text{Ti}}$	Time, hr.	Yield, %	$[\eta]$, 150°C. decalin	% extracted by hot isooctane
6	0.286	1.6	7.5	41	16	1.9	
31	0.393	1.6	5.4	41	16	5.2	93
17	0.297	1.6	7.2	144	49	3.2	
24	0.445	1.6	4.8	144	65	4.7	91
30	0.949	2.4	3.4	137	50	2.7	
28	0.449	1.6	4.8	137	64	2.5	
20	0.414	1.6	5.2	137	47	2.7	
26	0.346	1.6	6.2	117	53	3.3	88
22	0.246	1.6	8.7	117	38	3.7	
28	0.273	1.6	7.8	117	40		
26	0.262	1.6	8.2	117	50	3.1	
25	0.213	1.6	10.1	117	28	4.2	
21	0.387	1.6	5.5	117	57	3.9	
26	0.319	1.6	6.7	117	42	3.1	
26	0.592	1.6	3.6	117	68	2.4	

One large scale run was carried out in a 4-liter autoclave. (By D. E. Winkler of the Organic Chemistry Department.) A charge of 500 g. followed by 245 g. of propylene on the second day resulted in 100 g. of polymer or a 13% yield. The polymer had an $[\eta]$ of 2.7 at 150°C. in decalin.

Summary of Physical Properties

Direct current resistivity 5.4 × 10 ¹⁶ ohm/cm.	ASTM D 257-54T
Dielectric constant 1.89 at 1000 cycle/sec. 2.04 at 2 Mc/sec.	ASTM D 150-54T
Power factor 0.00084 at 100 cycle/sec. 0.00042 at 2 Mc/sec.	ASTM D 150-54T
Arc resistance melts away	ASTM D 495-56T
Tensile properties 165 psi at break, 985% elongation no characteristic yield point	ASTM D 638-56T
Brittle Point -6°C.	ASTM D 746-55T
Softening point 147°C.; Flowpoint 200°C.	
Density 0.876 g./ml. by gradient method on film at 25°C.	
Birefringence of oriented polymer was too low to measure, less than 0.001	
Light scattering inconclusive, requires high temperature methods	
Melt index 0.20, 6 min. at 190°C.	ASTM D 1238-52T

Miscellaneous Results

One radiation experiment was attempted and this resulted in extensive degradation. An amorphous polymer with an intrinsic viscosity of 2.7 was dosed with 50 Mrad. of 3 Mev electrons. The degraded product had an intrinsic viscosity of 0.50.

Exploratory Tests with Other Monomers

3-Methylbutene-1 (Isopropyl Ethylene). This monomer did not polymerize in the system tested.

Butene-1. Butene-1 was relatively unreactive with titanium dichloride dipropionate catalyst. Five per cent yield of polymer was formed in 9 days.

4-Methylpentene-1 (Isobutyl Ethylene). Films pressed from polyisobutyl ethylene prepared by the use of titanium tetrachloride and aluminum isobutyl were found to crack when folded. Films prepared by polymerizing with titanium dichloride dipropionate and aluminum isobutyl did not crack when folded and appeared to have a superior clarity. A 10% yield of polymer was formed in 10 days.

Catalysts

Titanium Dichloride Dipropionate. During a study of a system involving titanium tetrachloride dissolved in propionic acid, it was discovered that the addition of a hydrocarbon, e.g., Skellysolve-B, causes a crystalline compound to separate. This product is highly deliquescent and on exposure to the atmosphere, evolves hydrogen chloride gas.

The analytical results obtained for titanium, chlorine, carbon, and hydrogen best fits the empirical formula TiCl₂C₆H₁₁O₄. A similar reaction has been described with titanium tetrachloride and acetic acid.³

Exploratory Experiments with Vanadium Tetrachloride

Experiments to test the generality of the effect of substitution on transition metal were attempted. Vanadium tetrachloride appears to give the same type of reaction with propionic acid. This derivative appeared crystalline, but proved to be difficult to isolate. Qualitative experiments with the crude salt (no analysis) and aluminum isobutyl indicated that propylene would slowly polymerize at 50°C. and ~8 atm. propylene pressure. The intrinsic viscosities observed were 4.0 and 6.0.

EXPERIMENTAL

Peroxide Bottle Runs

The solvent, *n*-heptane, 100 ml., was first syringed into the bottle under nitrogen. The solid catalyst was dropped into the bottle using a dry bag. The weight of catalyst used was determined by difference on the catalyst container. Aluminum isobutyl, 2.0 ml. was syringed in; the mixture was stirred and the solid catalyst crushed with a stirring rod until a uniform black dispersion resulted.

Propylene was passed through a purifying train (this train was constructed by D. O. Collamer) which consisted of a Drierite tower followed by a cetane bubbling tower containing aluminum isobutyl, and loaded into a peroxide bottle at -40°C. The bottle was capped with a Hycar gasket and placed in the 50°C. tumbling polybath.

Upon removal from the polybath, the excess propylene was bled off by inserting a needle through the cap and regulating the flow with a finger. The polymer was removed from the bottle with the aid of some 10% conc. HCl in IPA (isopropyl alcohol) and placed in a beaker with ~200 ml. of HCl-IPA. The coagulate was removed and ground in a Waring blender with fresh methanol with some added HCl-IPA. The polymer was ground three more times with pure methanol, with a trace of Ionol in the last wash, and dried in a vacuum oven.

A 5-fold scale up of the bottle runs with titanium dichloride dipropionate has been completed. Titanium dichloride dipropionate (1.48 g.) was dropped into 500 ml. of dry heptane in a 1-quart ginger ale bottle. Aluminum isobutyl (10 ml.) was added, and the bottle charged with 138 g. of propylene. The bottle was placed in the 50°C. polybath and allowed to react for 13 days. An 83% yield of amorphous polypropylene was obtained. This material had an intrinsic viscosity of 3.1.

Four-Liter Autoclave

Premixed catalyst was prepared in a 1-liter bottle under dry nitrogen. Titanium dichloride dipropionate, 8.2 g., was placed in approximately 1 liter of dry *n*-heptane. Aluminum isobutyl, 35 ml., was syringed in and the catalyst ground with a stirring rod. This was charged with 3 l. of heptane followed by 500 g. of polypropylene into the autoclave. The polymer was worked up with IPA and methanol.

Dry Bag Technique

A 3-way stopcock is fitted to a 3 mil 24" × 48" polyethylene bag by inserting the single end into a hole in the corner of the closed end and wrapping it with a rubber band. Nitrogen is attached to one side and a vacuum line to the other. The materials are placed inside, and the open end rolled up, and fastened with clothespins. The bag is filled and evacuated three times. This gives a simple anhydrous system. The manipulations are carried out by grasping through the bag from the outside.

MATERIALS

Titanium Dichloride Dipropionate

Titanium tetrachloride (30 ml. 54 g., .27M) is dissolved in 200 ml. of propionic acid, under a nitrogen blanket, and allowed to stand overnight. The addition is accompanied by a vigorous evolution of HCl. The crystals of dichloride dipropionate are precipitated by the addition of 270 ml. of petroleum ether. The supernatant liquid is decanted

off using a dry bag. The precipitate is washed four times with petroleum ether and finally filtered with a sintered glass funnel. The filter cake is dried by allowing dry nitrogen to pass through it. The material obtained weighed 12.3 g. representing a 16% yield. The analysis obtained was the following:

Calc. for $\text{TiCl}_2\text{C}_6\text{H}_{11}\text{O}_4$: Ti, 18.1%; Cl, 26.7%; C, 27.2%; H, 3.8%. Found: Ti, 18.8%; Cl, 25.4%; C, 27.5%; H, 4.2%.

Aluminum Isobutyl

The material used in these experiments was purchased from Hercules Powder Company and used without further purification.

Propylene

The propylene used was Phillips Pure Grade. This was further purified by passing it through towers of Drierite and aluminum isobutyl in cetane. The propylene used in the large scale autoclave was not treated.

Amorphous Polypropylene

Table I summarizes the results obtained using peroxide bottles with 100 ml. of *n*-heptane as a solvent, in a 50°C. tumbling polybath. This polymer has a melting range of 160–240°C., and a brittle point of –6°C. (ASTM D 746-55T; G. Natta¹ reported the second-order transition point for atactic polypropylene to be –35°C.)

DISCUSSION

An interesting feature of the titanium dichloride dipropionate with aluminum-isobutyl system is that the overall rate of polymerization, as compared to the usual titanium tetrachloride-aluminum alkyl systems, is much slower. We can expect the slower rate process to be more selective and give the thermodynamically more stable product. This implies that the amorphous form of polypropylene is actually a lower energy form.

The fact that a definite compound, titanium dichloride dipropionate, can be isolated from a solution in propionic acid is difficult to rationalize. If one clings to the notion that transition metals, in general, derive a special stability in octahedral complexes, then one must postulate that the carboxyl group functions as a bidentate ligand.

References

1. Natta, G., *Chim. Ind.*, **38**, 751 (1956).
2. Gaylord, N. G., and H. F. Mark, *Linear and Stereoregular Addition Polymers*, (Polymer Reviews, Vol. 2), Interscience, New York, 1959, p. 127.
3. Pande, K. C., and R. C. Mehrotra, *J. Prakt. Chem.*, **5**, 101 (1957); R. N. Kapoor, K. C. Pande, and R. C. Mehrotra, *J. Indian Chem. Soc.*, **35**, 157 (1958).

J. KUMAMOTO*

Shell Development Company
Emeryville, California

Received February 16, 1965

* Present address: IBM San Jose Research Laboratory, San Jose, California.

BOOK REVIEWS

N. G. GAYLORD, Editor

Stability Constants. I. Inorganic Ligands; II. Organic Ligands, L. G. SILLÉN, AND A. E. MARTELL, *Chemical Society, London*, 1964. xviii + 754 pp., \$23.00.

This is the second edition of a compilation that originally appeared in 1957 and 1958 as two volumes under the auspices of the International Union of Pure and Applied Chemistry and is now issued in revised and updated form by The Chemical Society. Section I, which deals with inorganic ligands, was compiled by Lars Gunnar Sillén; section II, organic ligands, was contributed by Arthur E. Martell. A lengthy section gives details on how to use the tables. An index of ligands and metals is a helpful aid for locating pertinent material.

Fundamental Phenomena in the Material Sciences, Vol. 1, Sintering and Plastic Deformation, L. J. BONIS and H. H. HAUSNER, Editors, Plenum Press, New York, 1964. ix + 134 pp., \$9.50.

Consists of six chapters discussing the sintering and plastic deformation of metals, ceramics, and polymers. An appendix contains a selected annotated bibliography with more than a hundred recent references.

Das Diisocyanat-Polyadditionsverfahren, O. BAYER, Carl Hanser Verlag, München, 1963. 48 pp., DM 6.80.

This booklet presents a history of the discovery and development of the isocyanate addition reactions based on the personal recollection of the foremost investigator in this field. Included are fibers and films from linear polyurethanes, polyurethane lacquers, urethane molding compounds, adhesives, foams, polyureas, elastomers, etc.

Mechanochemistry of Polymers, N. K. BARAMBOIM, trans. R. J. MOSELEY and W. F. WATSON, Editors, Macleren & Sons, Ltd., London, 1964. 261 pp., \$7.00.

An English translation of an account of Russian work in this field carried out up to 1959. Discusses the physical-mechanical properties of high polymers, mechanical degradation, mechanochemical synthesis of copolymers, alteration in macrostructure, in surface properties, and in molecular configuration, and the equipment for carrying out mechanical-chemical processes. Has 262 references but no index.

High Polymers, M. GORDON, Addison-Wesley, Reading, Massachusetts, 1964. 158 yp., \$6.75.

This book is concerned with the structure and physical properties of high polymers rather than with methods of synthesis. Includes the theories of molecular packing and relaxation, chemical bonding, states of aggregation, coiling and uncoiling, crystallinity, diffusion, and solubility.

ERRATA

Cyclic Distribution in Dimethylsiloxanes

(article in *J. Polymer Sci.*, **A3**, 971-984, 1965)

By JACK B. CARMICHAEL and ROBERT WINGER

Dow Corning Corporation, Midland, Michigan

On page 973, the equation at the bottom of Table II should read:

$$\left(\frac{\text{Area of } n}{\text{Wt.-% of } n} \right) = \left(\frac{\text{Area of } 5-}{\text{Wt.-% of } 5-} \right) \times R$$

Infrared Spectra of Polybutadienes

(article in *J. Polymer Sci.*, **A3**, 1587-1599, 1965)

By JOHN L. BINDER

Central Research Laboratories The Firestone Tire Company, Akron, Ohio

The full captions for the figures in this article are:

Fig. 1. Solid line (—) observed spectrum. Circles (O) spectrum calculated from band envelopes shown, in part, by dotted lines (- -).

Fig. 2. Dotted lines (- -) spectra calculated from band envelopes shown by solid lines (—).

Fig. 3. Upper curve, observed spectrum of high *cis*-1,4- polybutadiene. Circles (O) give spectrum calculated from band envelopes shown in lower part.

Fig. 4. Specific absorbances of bands shown in Figure 3 versus time of isomerization.

Fig. 5. Rate curve of specific absorbance of 740 cm.^{-1} band.

Fig. 6. Upper curve, observed spectrum of a high *cis*-1,4 polybutadiene. Circles (O) spectrum calculated from band envelopes shown in lower part.

Fig. 7. Upper curve, observed spectrum of an isomerized *cis*-1,4- polybutadiene. Circles (O) spectrum calculated from band envelopes shown, in part, by dotted lines (- -).

Fig. 8. Rate curves of specific absorbances of bands in 10-11 μ region.